

ANNALES
UNIVERSITATIS SCIENTIARUM
BUDAPESTINENSIS
DE ROLANDO EÖTVÖS NOMINATAE

SECTIO GEOLOGICA

TOMUS XXIV.

1982

REDIGUNT

B. GÉCZY

J. KISS

L. STEGENA

M. MONOSTORI



BUDAPEST

1984

ANNALES

UNIVERSITATIS SCIENTIARUM BUDAPESTINENSIS DE ROLANDO EÖTVÖS NOMINATAE

SECTIO BIOLOGICA

inceptit anno MCMLVII

SECTIO CHIMICA

inceptit anno MCMLIX

SECTIO CLASSICA

inceptit anno MCMLXXIV

SECTIO GEOGRAPHICA

inceptit anno MCMLXVI

SECTIO GEOLOGICA

inceptit anno MCMLVII

SECTIO HISTORICA

inceptit anno MCMLVII

SECTIO IURIDICA

inceptit anno MCMLIX

SECTIO LINGUISTICA

inceptit anno MCMLXX

SECTIO MATHEMATICA

inceptit anno MCMLVIII

SECTIO PAEDAGOGICA ET PSYCHOLOGICA

inceptit anno MCMLXX

SECTIO PHILOLOGICA HUNGARICA

inceptit anno MCMLXX

SECTIO PHILOLOGICA MODERNA

inceptit anno MCMLXX

SECTIO PHILOSOPHICA ET SOCIOLOGICA

inceptit anno MCMLXII

GEOCHEMISCHE UNTERSUCHUNGEN EINIGER EOZÄNER UND OLIGOZÄNER KALKSTEINE AUS DEM SIEBENBÜRGISCHEN BECKEN (RUMÄNIEN)

von

J. IMREH, N. MÉSZÁROS, S. MIHÁLKA, ZS. BERNER

Universität „Babes-Bolyai“, Lehrstuhl für Geologie und Mineralogie, Cluj-Napoca, Rumänien

SUMMARY

The paper reports a geochemical investigation, carried out on 99 samples of limestones stemming from four occurrences (Rohia, Poiana Blenchii, Piatra and Glod) located in the northern part of the Transylvania Basin. The samples were chemically assayed for the major elements (Table 1) and the minor elements were determined by spectrometric methods (Table 2). The occurrences were designated in tables and graphs by the following abbreviations: Gd = GLOD Pr = PIATRA; Pb = POIANA BLENCHII, Rh = ROHIA. An arabic numeral accompanying these symbols indicates the horizons (levels). The chemical analysis data was used for obtaining histograms of the content frequencies, which led to some conclusions concerning the specific features of each occurrence. Since the samples were collected along a vertical from different horizons — the superior one being labelled 1 in each occurrence — we obtained diagrams enabling us to establish the correlations between different elements, based on their distributions.

The last part of the paper is devoted to the results of the dichotomic (Cluster) analysis, and the factorial analysis. The matrices of the empirical coefficients of linear correlations are presented in tables 4, 5, 6, 7, 8. They were used for plotting a dendrogram (fig. 14). Table 10 displays the results of the factorial analysis. They led to the determination of different groups of positively or negatively correlated elements. In turn, the correlations were used for assigning the various elements to either the carbonate or the silicate phases or to the HCl-insoluble residue. Another result of these studies was the ascertaining of the different migration stages of the elements in the di- and the epigenesis processes, respectively the mobilization, redistribution and concentration of some elements in these processes.

* * *

Das untersuchte Gebiet befindet sich im Norden Siebenbürgens in der Preluca-Zone, von den Flüssen Someş und Lăpuş begrenzt.

Die hierbefindlichen Kalksteinlager wurden vom geologischen Standpunkte bereits von FR. HAUER und G. STACHE (1863), K. HOFMANN (1879, 1883, 1891), A. KOCH (1894) untersucht. Ab 1957 wurden hier erneut Untersuchungen von G. RĂILEANU und E. SAULEA (1956), I. DUMITRESCU (1957), N. MÉSZÁROS (1957, 1965, 1967, 1980), G. BOMBIŢĂ (1972), V. LĂZĂRESCU (1966) und A. RUSU (1977) durchgeführt.

In den letzten zehn Jahren wurden mehrere geochemische Studien dieser Kalksteinablagerungen von J. IMREH, N. MÉSZÁROS und Mitarbeitern (1979, 1980, 1981, 1982) veröffentlicht. Die vorliegende Arbeit ist als Vergleichsstudie von Ablagerungen aus vier verschiedenen Aufschlüssen zu betrachten, die den obereozänen (Priabon) und teilweise oligozänen (Stampien) s.g. „Culmea Cozlei“-Kalken angehören.

Die „Culmea Cozlei“-Kalke

Die „Culmea Cozlei“-Kalke bilden eine Schichtenfolge der die Klausenburger Schichten (oberen Grob-Kalke), Brebi-Ablagerungen (*Nummulites fabiani* und Bryozoenmergel) und Hoia-Schichten angehören.

Dieser etwa 50–70 m dicke, aus organogenen Kalksteinen aufgebaute Schichtenkomplex besteht hauptsächlich aus Bioakkumulaten, welche je nach den am häufigsten anzutreffenden Arten: Milioliden-, Nummuliten-, Korallen-, Muschel-, Algen- oder meistens gemischte Kalksteine sind und sich in Form von Schichten verschiedener Dicke (von ein paar dm bis etliche m) überlagern.

Die Nummuliten sind überall zu finden, massenhaft kommen sie jedoch nur in drei verschiedenen Horizonten vor. Dasselbe gilt auch für die Algenkalke, welche aber hauptsächlich im obersten Drittel der Folge anzutreffen sind. Auch die Riffkorallenhorizonte lagern im oberen Teil dieser Schichtenfolge, deren unteren Teil die „*Vulsella dubia transsilvanica*“-Kalke bilden.

Bei Rohia sind in den oberen Schichten auch Seeigel-Reste häufig.

Die „Cuciulat“-Schichten

Im unteren Teil dieser Schichten befinden sich Mergel und Kalkmergel, welche ab und zu Kohleneinlagerungen, Süß-, Brackwassermuscheln und Schnecken bergen. An manchen Stellen (Glod und Piatra) trifft man Kalksteinbänke an, die einst von Algen und Nummuliten aufgebaut wurden.

Diese Schichten wurden, von Westen nach Osten, an vier verschiedenen Orten: Glod, Piatra, Poiana Blenchii und Rohia, untersucht, überall wurden den aufeinanderfolgenden Schichten Proben entnommen, aus 22 Horizonten in Glod, 24 in Piatra, 41 in Poiana Blenchii und 12 in Rohia. Die Proben wurden, wie folgt numeriert: die Zahl eins (1) gibt den obersten Horizont an, die grösste Zahl entspricht dem tiefsten. Die danebenstehende Buchstaben geben den Ort, von welchen die Proben stammen, an, Gd = Glod, Pr = Piatra, Pb = Poiana Blenchii, Rh = Rohia.

Nach demselben Verfahren untersuchten wir bereits früher, auch die übrigen tertiären Ablagerungen des Siebenbürger Beckens (IMREH J. et JAKAB E., 1965; IMREH J. et I. BEDELEAN 1967; IMREH J. et ST. MIHÁLKA 1970; IMREH J. et IMREH G. 1971; IMREH J. und IMREH G. 1972).

Die Nützlichkeit eines solchen Verfahrens ist leicht verständlich, da man dadurch:

a) eine klare Übersicht über die chemische Beschaffenheit der Bänke hat,

b) aus der Verteilung der Elemente in den verschiedenen Horizonten die Wanderung derselben während der Dia- und Epigenese verfolgen kann,

c) eine Übersicht über die Wechselbeziehungen zwischen den Elementen, aus denen die Lagerung besteht, gewinnt,

d) die Mineralphase, in welcher die verschiedenen Elemente vorkommen, definieren kann.

Diese Arbeit erschien uns, nach dem Ergebnisse der vorangegangenen Studien, als nötig, da wir bemerkten, dass eine Kalkablagerung die makroskopisch homogen zu sein scheint, sich von chemischem Standpunkt aus (vor allem was die Elemente betrifft, die in äusserst geringer Menge vorkommen) aber als recht heterogen erweist. Eine Kalkbank entsteht in einer Zeitspanne in welcher die Bedingungen nicht unbedingt immer die gleichen bleiben müssen.

In einigen Fällen, so z.B. im „Baci-Grobkalk“ bei Klausenburg, kommen sogar Dolomithorizonte vor (IMREH J. u IMREH G. 1972), obwohl man, makroskopisch betrachtet, geneigt wäre, ihn als homogen zu deuten.

In den an 99 Proben durchgeführten chemischen Untersuchungen forschten wir nach folgenden Hauptelementen: Si, Al, Fe, Ca und Mg. Die Spektralanalyse galt dem Nachweis der Spurenelemente.

Chemische Analysen

In Tabelle 1 sind die Ergebnisse der chemischen Analysen zusammengefasst. Die beiden letzten Spalten entsprechen dem freien Kalzit und dem errechneten Dolomitgehaltswert.

Die Daten aus Tabelle 1 halfen zur Aufstellung der Histogramme für die verschiedenen Aufschlüsse.

Der SiO_2 -Gehalt

Abb. 1 zeigt, dass im Histogramm die meisten Werte der Klasse 2–4% in Poiana Blenchii (N=17), 3–4% in Glod (N=6), 1–2% in Piatra (N=8), und 4–3% in Rohia (N=3) angehören. Das Aussehen der Frequenzschaubilder verrät eine Ähnlichkeit zwischen Glod und Piatra, die in einem geringeren Masse auch für Poiana Blenchii und Rohia zutrifft. Es sei bemerkt, dass Glod und Piatra zwei benachbarte Aufschlüsse aus dem westlichen Teil des untersuchten Gebietes sind, Poiana Blenchii und Rohia befinden sich im östlichen Teil desselben.

Fe_2O_3 -Gehalt

Die Histogramme von Abb. 2 zeigen, dass die Höchsthäufigkeit (N=7) für Glod der Klasse 0,2–0,4%, für Piatra (N=8) der Klasse 0–0,2%, für Poiana Blenchii (N=12) der Klasse 0,4–0,6% und für Rohia (N=4) der Klasse 0,8–1% entspricht. Interessant ist die Feststellung, dass sich die Frequenzschaubilder der beiden extremen Aufschlüsse (Glod im Westen und Rohia im Osten) stark ähneln und dass sogar den beiden anderen, im Inneren der untersuchten Zone befindlichen Aufschlüssen, eine gewisse Ähnlichkeit nicht abzusprechen ist.

Al_2O_3 -Gehalt

Aus Abb. 3 sieht man, dass sich für Glod und Piatra die Höchsthäufigkeiten (N=4) in mehreren Klassen gruppieren. Für Poiana Blenchii

Tabelle 1.

Chemische Analysen der Proben

Probe		SiO ₂ %	Al ₂ O ₃ %	Fe ₂ O ₃ %	Kalzit %	Dolomit %
1	1 Gd	3,25	1,12	1,12	91,61	2,29
2	2 Gd	3,87	1,04	0,83	92,85	0,67
3	3 Gd	8,17	1,73	0,78	85,92	1,34
4	4 Gd	1,49	0,82	1,43	92,89	2,27
5	5 Gd	4,34	1,83	2,87	88,69	1,81
6	6 Gd	1,77	0,48	0,40	95,09	1,81
7	7 Gd	4,60	0,97	0,64	91,77	1,81
8	8 Gd	3,47	0,65	0,41	94,28	1,34
9	9 Gd	5,38	0,94	0,56	90,12	2,86
10	10 Gd	6,90	1,22	0,67	89,40	1,34
11	11 Gd	7,64	1,39	0,77	88,46	0,89
12	12 Gd	3,71	0,54	0,34	93,94	1,34
13	13 Gd	2,84	0,61	0,24	94,63	1,00
14	14 Gd	3,53	0,49	0,22	94,64	0,67
15	15 Gd	2,30	0,25	0,15	96,19	0,89
16	16 Gd	7,96	1,09	0,51	88,11	1,50
17	17 Gd	1,88	0,30	0,18	96,14	1,56
18	19 Gd	8,99	2,51	1,02	80,52	5,13
19	19 Gd	5,26	0,81	0,65	91,95	1,34
20	20 Gd	2,84	0,45	0,29	94,76	1,13
21	21 Gd	2,90	0,34	0,31	94,69	0,80
22	22 Gd	1,54	0,30	0,23	97,89	0,76
23	1 Pr	1,92	1,58	0,49	95,16	0,45
24	2 Pr	9,56	3,56	2,47	79,20	3,10
25	3 Pr	6,53	1,93	1,36	85,12	2,64
26	4 Pr	0,90	0,22	0,19	97,93	0,91
27	5 Pr	4,54	1,20	0,36	92,39	0,67
28	6 Pr	1,47	0,54	0,27	97,22	0,45
29	7 Pr	4,96	1,18	0,52	90,56	1,55
30	8 Pr	10,06	2,67	0,99	83,70	1,77
31	9 Pr	1,49	0,36	0,16	97,22	0,45
32	10 Pr	1,26	0,18	0,11	98,09	0,45
33	11 Pr	1,94	0,35	0,16	96,99	0,21
34	12 Pr	0,84	0,13	0,09	98,85	0,21
35	13 Pr	6,90	1,21	0,54	87,69	1,09
36	14 Pr	1,90	0,38	0,17	96,61	0,45
37	15 Pr	2,43	0,49	0,23	92,91	0,89
38	16 Pr	3,79	0,79	0,36	92,82	1,31
39	17 Pr	0,82	0,31	0,15	98,22	0,45
40	18 Pr	0,86	0,17	0,13	98,22	0,54
41	19 Pr	1,78	0,46	0,27	95,42	1,26
42	20 Pr	5,07	1,72	0,65	89,90	1,13
43	21 Pr	1,74	0,60	0,22	96,39	0,59
44	22 Pr	2,75	0,89	0,32	93,03	1,26
45	23 Pr	9,08	3,67	1,08	82,53	2,05
46	24 Pr	4,81	1,35	0,56	90,04	2,14
47	1 Pb	8,38	2,79	1,22	80,37	6,47
48	2 Pb	4,85	3,59	1,39	82,08	4,61
49	3 Pb	78,87	8,31	3,63	2,87	1,33
50	4 Pb	77,84	9,26	4,14	4,74	2,05

Probe	SiO ₂ %	Al ₂ O ₃ %	Fe ₂ O ₃ %	Kalzit %	Dolomit %	
51	5 Pb	81,61	9,29	3,06	0,48	1,77
52	6 Pb	2,66	1,22	1,52	88,44	6,65
53	7 Pb	3,47	0,66	0,59	89,20	6,86
54	8 Pb	3,84	1,08	0,60	85,78	9,29
55	9 Pb	2,31	0,81	0,61	89,25	7,20
56	10 Pb	3,45	0,93	0,81	90,19	4,13
57	11 Pb	7,92	2,45	0,75	84,45	4,30
58	12 Pb	1,59	0,85	0,53	88,41	9,11
59	13 Pb	2,11	0,96	0,26	94,92	2,16
60	14 Pb	8,70	1,34	0,76	82,39	6,58
61	15 Pb	3,29	1,23	0,59	91,65	3,19
62	16 Pb	2,59	0,63	0,30	67,17	28,05
63	17 Pb	2,70	0,82	0,49	82,68	13,64
64	18 Pb	2,74	1,08	0,40	88,76	7,36
65	19 Pb	2,32	0,92	0,54	94,17	0,61
66	20 Pb	3,71	1,12	0,68	91,72	2,25
67	21 Pb	2,67	0,76	0,33	94,27	2,16
68	22 Pb	3,03	1,19	0,57	86,84	8,79
69	23 Pb	5,87	1,59	0,60	87,77	4,61
70	24 Pb	1,29	0,77	0,21	92,31	5,07
71	25 Pb	7,41	0,77	0,31	81,31	7,04
72	26 Pb	8,14	1,49	0,48	85,56	4,48
73	27 Pb	6,65	1,35	0,53	89,83	2,03
74	28 Pb	32,16	3,46	1,18	57,81	3,12
75	29 Pb	5,23	1,39	0,71	88,49	4,57
76	30 Pb	4,54	1,76	0,59	88,95	4,54
77	31 Pb	5,49	1,21	0,69	89,94	2,25
78	32 Pb	2,71	0,85	0,36	90,99	5,77
79	33 Pb	5,91	1,77	0,78	88,33	0,61
80	34 Pb	9,48	2,49	1,77	80,50	3,17
81	35 Pb	11,46	4,29	1,49	76,91	3,67
82	36 Pb	4,22	1,67	1,00	86,53	6,93
83	37 Pb	10,06	3,52	1,58	78,57	3,43
84	38 Pb	13,94	5,74	2,07	66,98	9,11
85	39 Pb	6,47	3,21	1,20	81,89	6,95
86	40 Pb	3,53	1,09	0,72	90,32	4,15
87	41 Pb	3,56	1,50	0,49	92,09	2,20
88	1 Rh	6,29	2,00	1,84	87,60	0,67
89	2 Rh	3,87	1,41	0,87	91,10	1,59
90	3 Rh	4,58	1,65	0,87	90,99	1,34
91	4 Rh	4,52	0,78	0,61	92,47	1,13
92	5 Rh	6,38	0,97	0,89	89,60	0,67
93	6 Rh	1,81	0,23	0,30	97,22	0,21
94	7 Rh	5,78	1,47	0,94	89,28	1,34
95	8 Rh	2,76	0,53	0,36	94,74	1,13
96	9 Rh	2,83	0,66	0,49	94,26	1,31
97	10 Rh	3,03	0,67	0,37	94,51	1,00
98	11 Rh	4,18	0,87	0,56	93,44	0,67
99	12 Rh	5,53	1,20	0,79	89,39	1,72

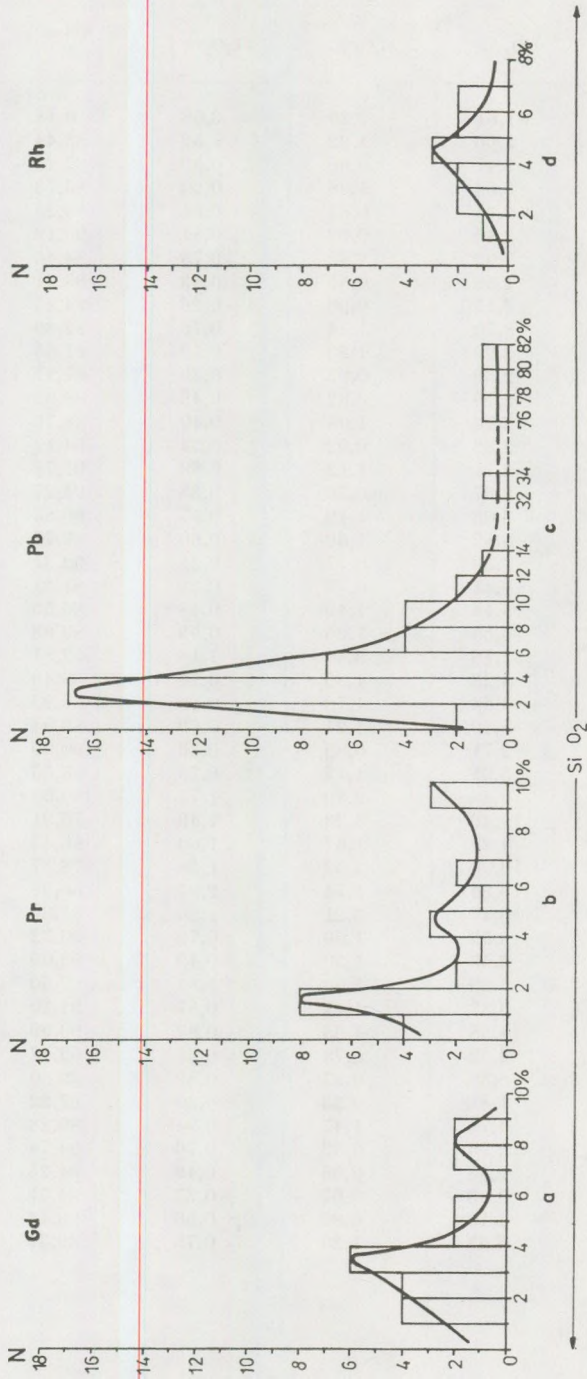


Abb. 1.

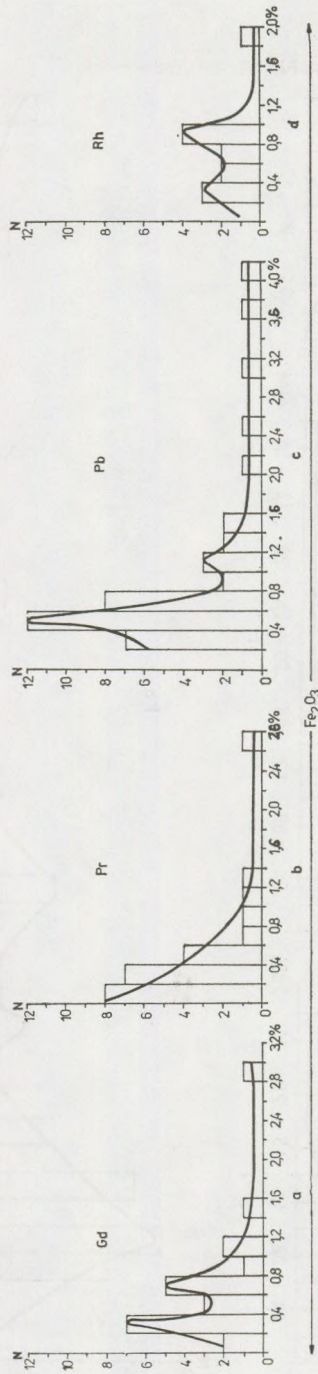


Abb. 2.

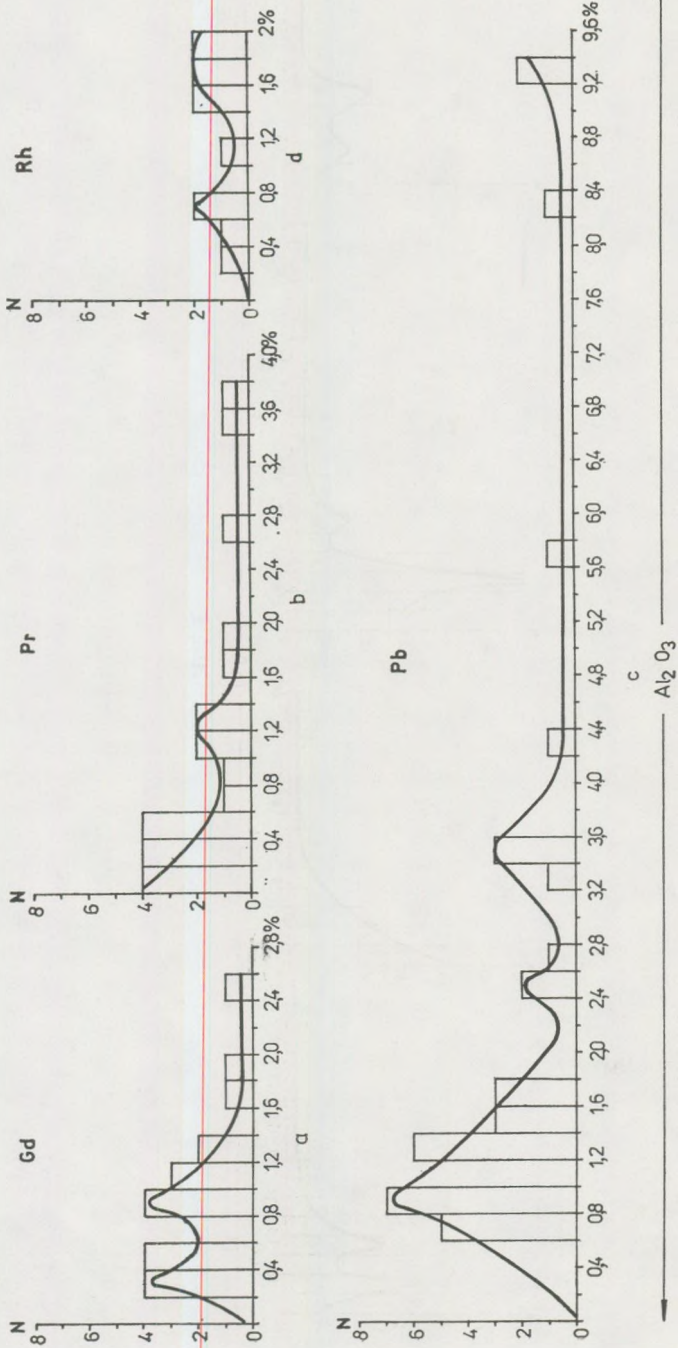


Abb. 3.

ist die Höchsthäufigkeit ($N=7$) für die Klasse 0,8–1%, für Rohia, in Klassen 1,4–2%, wobei jedoch auch eine Gruppierung mit erhöhten Al_2O_3 ersichtlich ist. Die Häufigkeitsdiagramme unterscheiden sich weitgehend voneinander, die Häufigkeitsverteilung ist polymodal.

Vergleicht man die Häufigkeitshöchstwerte der Aufschlüsse, so merkt man, dass sich der Rohia-Kalk, dessen Höchsthäufigkeiten für SiO_2 , Al_2O_3 und Fe_2O_3 sich in Klassen mit grösseren Gehalt befinden, wesentlich von den anderen Kalksteinen unterscheidet.

Freies $CaCO_3$

Ausser den Poiana Blenchii-Kalken, wo die Höchsthäufigkeit ($N=23$) der Klasse 80–90% angehört, erschienen die Höchstwerte der übrigen Aufschlüsse in der Klasse 90–100%. Die Häufigkeitsdiagramme ähneln einander.

Errechneter $CaMg(CO_3)_2$ -Gehalt

Abb. 5 zeigt für den Aufschluss Rohia die Höchsthäufigkeitswerte ($N=5$) in Klasse 1–1,5%, für Glod ($N=7$) in Klasse 0,5–1% und 1–1,5%, für Piatra ($N=8$) in Klasse 0–0,5% und für Poiana Blenchii ($N=12$) in Klasse 2–4%.

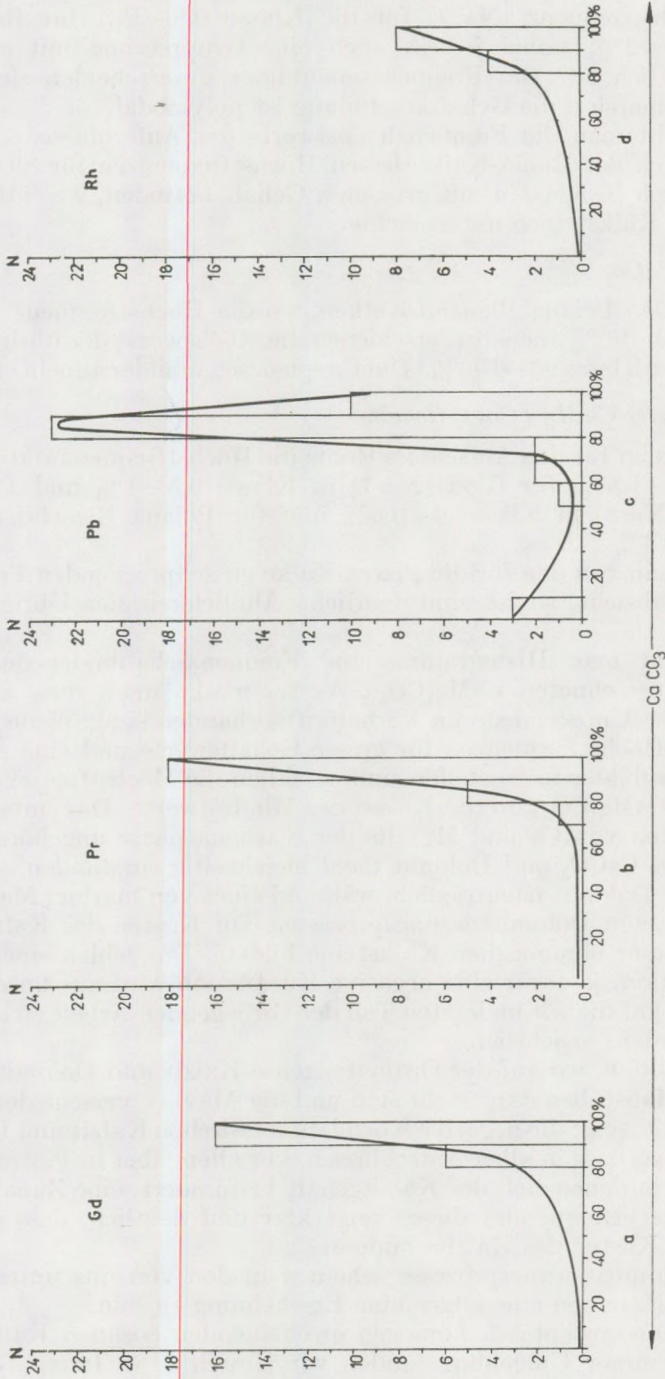
Wenn man von den für die Piatra-Kalke entsprechenden Häufigkeitsdiagramme absieht, so ist eine deutliche Ähnlichkeit der Übrigen festzustellen.

Vergleicht man Histogramme und Häufigkeitsdiagramme der freien $CaCO_3$ und errechneten $CaMg(CO_3)_2$ -Werte, merkt man, dass zwischen diesen gewisse Unterschiede im Verhalten vorhanden sind. Wenn für das freie $CaCO_3$ Höchsthäufigkeiten für grosse Gehaltswerte und eine Ähnlichkeit der Diagramme festzustellen sind, so fallen die Höchsthäufigkeiten des errechneten $CaMg(CO_3)_2$ in die Klasse der Mindestwerte. Das unterschiedliche Verhalten von Ca und Mg, die der Karbonatphase angehören, zeigt deutlich, dass $CaCO_3$ und Dolomit nicht gleichzeitig entstanden, sondern, dass sich der Dolomit nachträglich, während eines von mariner Metasomatose eingeleiteten Dolomitierungsprozesses, auf Kosten des Kalzits und Aragonits dieser organogenen Kalksteine bildete. Das Fehlen einer positiven Korrelation, ja sogar eine negative Korrelation wird aus unseren Berechnungen, auf die wir im letzten Teil der vorliegenden Arbeit zu sprechen kommen werden, ersichtlich.

Auch Abb. 6, wo auf der Ordinatenachse Kalzit und Dolomit in verschiedenen Maßstäben dargestellt sind und die Abszisse verschiedene Horizonte darstellt, zeigt die negative Korrelation zwischen Kalzit und Dolomit. Man stellt fest, dass in allen Aufschlüssen, vor allem aber in Piatra, in den Horizonten, in denen sich der Kalzitgehalt vermindert, eine Zunahme der Dolomitwerte erfolgte und dieses zeigt klar und deutlich, dass sich der Dolomit auf Kosten des Kalzits bildete.

Die Dolomitierungsprozesse scheinen in den von uns untersuchten tertiären Kalksteinen eine allgemeine Erscheinung zu sein.

In den makroskopisch homogen erscheinenden eozänen Kalksteinen der Klausenburger Umgebung fanden wir (Imreh J. u. Imreh G., 1972)



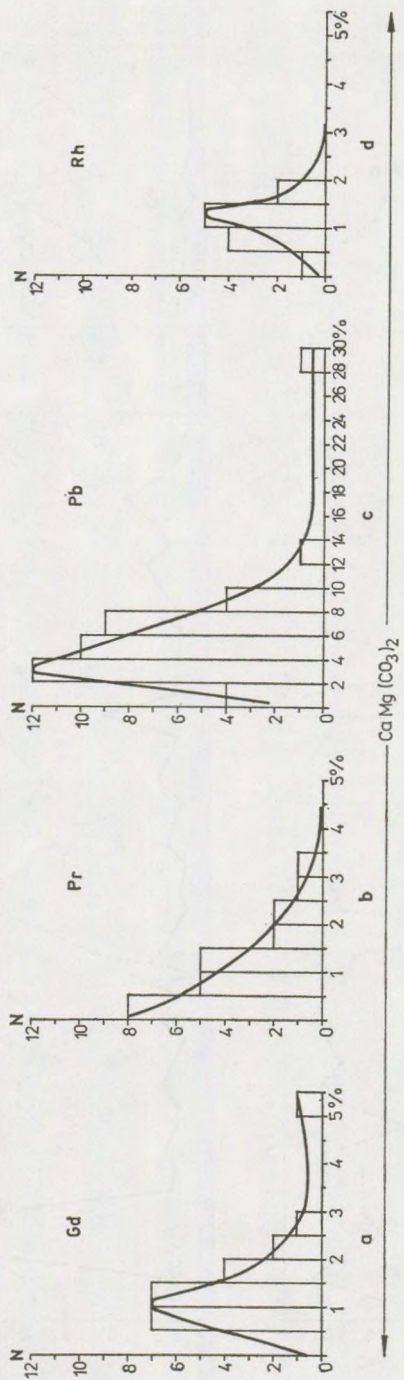


Abb. 5.

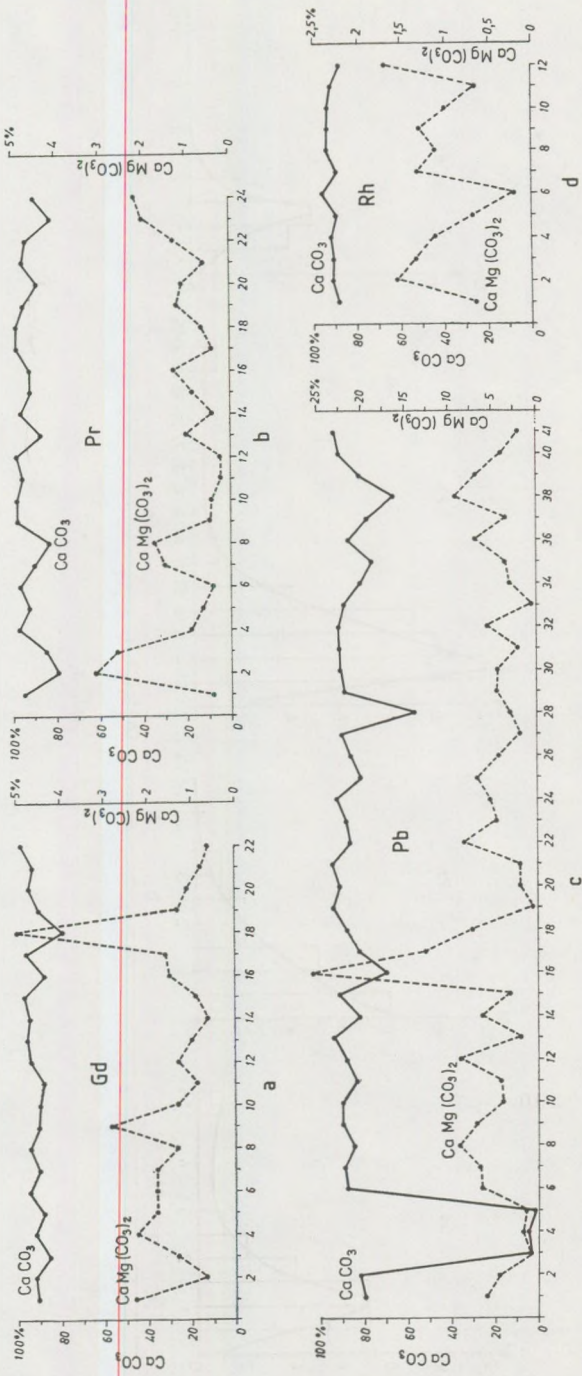


Abb. 6.

einen Horizont mit einem Dolomitgehalt von 74,63%, welcher ein von den übrigen Horizonten stark abweichender Wert ist. Aus der gegensätzlichen Verteilung vom Kalzit und Dolomit in den Horizonten lässt sich die Intensität und die Zeitspanne, in der der Dolomitierungsprozess stattfand, feststellen.

Abb. 6 z.B. zeigt eine stark unterschiedliche Verteilung von CaCO_3 und $\text{CaMg}(\text{CO}_3)_2$ im 16-ten Horizont (Probe 16 Pb) des Poiana Blonchii-Kalkes. Diese 16-te Probe gehört altersmässig dem Unteroligozän an, folglich spielte sich der Dolomitierungsprozess in jenem erdgeschichtlichen Zeitabschnitt ab. Dieselben Prozesse spielten sich, bei geringerer Intensität, auch in anderen Horizonten (8 Unteroligozän, 22 und 38 Ober-eozän) ab.

Abb. 6 zeigt dasselbe für Glod (Horizont 18), oder Piatra in den Horizonten 2, 6, 8, 13 und 14.

Bemerkenswert ist die Feststellung von Essam El Hinawi (1971), dass in den mitteleozänen Kalksteinen des Gebel Mokkatam und östlich von Helwan (neben Kairo) kein Dolomitierungsprozess stattfand, die ober-eozänen Kalksteine derselben Aufschlüsse jedoch eine gewisse Dolomitierungsprozess aufweisen. Nach El Hinawi fanden diese Prozesse während des Kontaktes von Meerwasser und Kalkablagerung, also im frühdiagenetischen Stadium (Anadiagenese) statt.

Zeichnet man die entsprechenden Schaubilder für die SiO_2 , Al_2O_3 und Fe_2O_3 Werte, so fällt die parallele Verteilung von Si, Al und Fe, die als unlöslicher Rückstand der Kalksteine in HCl zurückbleiben auf. In Abb. 7 ist so deutlich, dass die positive Korrelation zwischen diesen drei Elementen keine zusätzliche Erklärung benötigt.

Spektralanalyse

Die Spektralanalyse wurde mit Hilfe eines PGS-2, K. Zeiss-Spektrographen, bei einer Dispersion von $7,2 \text{ \AA}/\text{mm}$ im ersten Spektralorden, durchgeführt. Es wurde im Intervall $2000 - 3700 \text{ \AA}$ gearbeitet. Zur Auswertung und Interpretation der Spektren benützten wir ein MF-2 Mikrofotometer (K. Zeiss, Jena). Folgende Elemente wurden nachgewiesen: Ti, Mn, Cr, Ni, Co, V, Mo, W, Sn, Be, Sr, Ba (Tabelle 2).

Tabelle 2 zeigt, dass die bedeutendsten Elemente Sr und Ba sind, da sie die grössten Gehaltswerte zeigen. Die Bedeutung des Sr für die von M. FORNASERI und L. GANDI (1963, 1968) untersuchten italienischen Kalksteine wurde bereits unterstrichen, dasselbe tun wir für jene des Siebenbürger Beckens.

Abb. 8 zeigt, dass die häufigsten Sr-Gehaltswerte der Klasse $0,05 - 0,1\%$ (mit Ausnahme der Poiana Blonchii-Kalke, für welche diese in Klasse $0,3 - 0,35\%$ enthalten sind) angehören.

Interessant ist die Feststellung, dass im Falle des Ba der Poiana Blonchii-Kalk ein, dem Sr gegenüber, verschiedenes Verhalten aufweist.

Die Frequenzmaxima der Ba-Gehaltswerte fallen für alle vier Aufschlüsse in die Klasse $0 - 0,5\%$ (Abb. 9).

Tabelle 2.

Spektralanalysen der Proben
(g/t)

Probe	Sr	Ba	Ti	Ni	Cr	Mn	Co	V	Mo	W	Sn	Be	
1	1 Gd	1 000	3 000	170	10	100	150	—	—	—	—	—	
2	2 Gd	500	64	180	—	—	360	—	—	—	—	—	
3	3 Gd	100	200	160	10	180	410	—	—	—	—	—	
4	4 Gd	1 000	200	80	10	—	660	—	—	—	—	—	
5	5 Gd	300	560	210	—	100	240	—	—	—	—	—	
6	6 Gd	1 000	200	30	10	—	160	—	—	—	—	—	
7	7 Gd	700	76	115	—	160	200	—	—	—	—	—	
8	8 Gd	3 000	240	90	—	30	320	—	—	—	—	—	
9	9 Gd	3 000	400	90	—	100	200	—	—	—	—	—	
10	10 Gd	1 000	310	160	10	160	50	—	—	—	—	—	
11	11 Gd	700	120	270	10	180	250	—	—	—	—	—	
12	12 Gd	1 000	310	80	—	—	100	—	—	—	—	—	
13	13 Gd	1 000	310	30	—	—	140	—	—	—	—	—	
14	14 Gd	1 000	350	280	—	—	170	—	—	—	—	—	
15	15 Gd	1 000	125	30	—	—	160	—	—	—	—	—	
16	16 Gd	700	560	500	10	160	100	—	—	—	—	—	
17	17 Gd	700	190	145	—	—	200	—	—	—	—	—	
18	18 Gd	300	125	260	10	190	180	—	—	—	—	—	
19	19 Gd	700	170	30	—	—	150	—	—	—	—	—	
20	20 Gd	700	34	80	—	—	210	—	—	—	—	—	
21	21 Gd	700	210	80	—	—	290	—	—	—	—	—	
22	22 Gd	1 000	250	—	—	—	250	—	—	—	—	—	
23	1 Pr	720	10 000	350	—	—	700	70	—	—	—	—	
24	2 Pr	1 100	9 100	1 200	10	10	700	10	300	—	—	—	
25	3 Pr	4 700	6 100	450	10	—	1 000	10	20	—	—	—	
26	4 Pr	1 800	10 000	200	10	10	200	—	60	—	—	—	
27	5 Pr	1 400	2 000	500	10	10	10	—	200	—	—	—	
28	6 Pr	1 900	1 200	400	20	—	10	—	70	—	—	—	
29	7 Pr	1 600	760	400	30	30	10	10	15	—	—	—	
30	8 Pr	1 700	1 300	800	10	100	40	10	300	—	—	—	
31	9 Pr	880	850	100	10	10	10	—	90	—	—	—	
32	10 Pr	640	760	100	—	—	10	—	100	—	—	—	
33	11 Pr	940	1 300	10	—	—	10	—	100	—	—	—	
34	12 Pr	1 100	730	300	—	10	100	—	200	—	—	—	
35	13 Pr	1 000	700	570	—	100	100	10	330	—	—	—	
36	14 Pr	880	700	300	10	—	—	—	90	—	—	—	
37	15 Pr	880	300	250	—	—	100	—	200	—	—	—	
38	16 Pr	540	100	400	—	100	—	10	300	—	—	—	
39	17 Pr	880	500	400	—	—	—	—	90	—	—	—	
40	18 Pr	720	130	300	—	—	—	—	60	—	—	—	
41	19 Pr	840	30	400	—	—	90	—	60	—	—	—	
42	20 Pr	700	50	450	—	10	300	20	150	—	—	—	
43	21 Pr	420	30	300	10	—	—	—	50	—	—	—	
44	22 Pr	720	30	300	10	—	—	—	50	—	—	—	
45	23 Pr	740	100	400	35	200	200	20	100	—	—	—	
46	24 Pr	660	30	250	10	200	300	10	250	—	—	—	
47	1 Pb	4 200	1 800	430	35	76	340	3	10	—	—	—	
48	2 Pb	4 570	3 000	540	30	30	230	—	10	—	—	—	
49	3 Pb	20	30	1 000	115	165	290	3	100	10	100	10	3

Probe	Sr	Ba	Ti	Ni	Cr	Mn	Co	V	Mo	W	Sn	Be *	
50	4 Pb	20	30	1 000	80	130	260	3	86	10	—	10	3
51	5 Pb	100	78	1 000	76	110	230	3	96	10	—	10	3
52	6 Pb	4 300	900	720	29	—	1 000	3	30	—	—	—	—
53	7 Pb	4 370	70	300	10	—	340	—	30	—	—	—	—
54	8 Pb	3 020	130	200	10	—	260	—	30	—	—	—	—
55	9 Pb	3 100	46	210	10	—	195	—	30	—	—	—	—
56	10 Pb	3 800	88	78	10	—	210	—	30	—	—	—	—
57	11 Pb	3 630	300	180	40	78	300	3	43	—	—	—	—
58	12 Pb	3 150	230	42	10	—	780	—	37	—	—	—	—
59	13 Pb	3 410	143	37	10	—	420	—	34	—	—	—	—
60	14 Pb	3 100	105	115	10	105	410	3	46	—	100	10	—
61	15 Pb	3 480	52	52	10	30	140	—	10	—	—	10	—
62	16 Pb	3 370	50	30	10	30	140	—	10	—	—	10	—
63	17 Pb	3 395	84	31	10	30	200	—	10	—	—	10	—
64	18 Pb	3 210	68	32	10	30	145	—	10	—	—	10	—
65	19 Pb	4 600	58	39	37	30	110	—	10	10	—	10	—
66	20 Pb	3 740	90	62	10	—	320	—	10	10	—	10	—
67	21 Pb	3 510	40	46	10	30	230	—	10	—	—	10	—
68	22 Pb	3 020	105	64	46	30	120	—	48	10	—	10	—
69	23 Pb	3 230	45	120	46	30	62	3	72	10	100	10	—
70	24 Pb	3 470	32	52	10	—	80	—	27	—	—	10	—
71	25 Pb	3 100	26	47	10	—	74	—	10	—	—	—	—
72	26 Pb	3 270	70	300	10	82	220	3	42	—	100	—	—
73	27 Pb	3 410	50	94	10	74	165	3	39	—	—	—	—
74	28 Pb	3 000	210	1 000	70	165	360	20	165	10	100	10	—
75	29 Pb	3 350	70	42	10	30	62	3	10	—	—	—	—
76	30 Pb	3 270	84	210	27	30	185	—	33	—	—	—	—
77	31 Pb	3 200	52	42	10	30	92	3	10	—	—	—	—
78	32 Pb	3 300	40	66	10	—	270	—	20	—	—	—	—
79	33 Pb	3 250	56	38	10	30	62	3	10	—	—	—	—
80	34 Pb	3 050	700	200	38	86	290	3	30	10	—	10	—
81	35 Pb	3 100	105	150	10	100	140	3	30	—	—	10	—
82	36 Pb	3 230	58	115	38	30	210	3	30	10	—	—	—
83	37 Pb	3 310	200	290	54	120	450	15	30	—	100	10	—
84	38 Pb	3 150	270	320	68	220	250	20	96	10	100	10	—
85	39 Pb	3 400	60	86	10	74	56	3	10	—	—	—	—
86	40 Pb	3 420	45	80	47	30	150	3	10	10	—	—	—
87	41 Pb	4 010	60	68	49	30	170	3	10	10	—	—	—
88	1 Rh	720	150	170	10	100	180	—	—	—	—	—	—
89	2 Rh	1 000	3 000	170	10	100	180	—	—	—	—	—	—
90	3 Rh	700	360	230	10	—	100	—	—	—	—	—	—
91	4 Rh	3 000	560	130	10	160	190	—	—	—	—	—	—
92	5 Rh	700	250	170	10	180	100	—	—	—	—	—	—
93	6 Rh	1 000	150	120	—	—	50	—	—	—	—	—	—
94	7 Rh	800	490	280	—	160	50	—	—	—	—	—	—
95	8 Rh	3 000	380	90	—	—	80	—	—	—	—	—	—
96	9 Rh	700	380	10	—	—	50	—	—	—	—	—	—
97	10 Rh	1 000	200	60	—	—	200	—	—	—	—	—	—
98	11 Rh	1 000	185	240	10	30	30	—	—	—	—	—	—
99	12 Rh	700	200	210	10	200	100	—	—	—	—	—	—

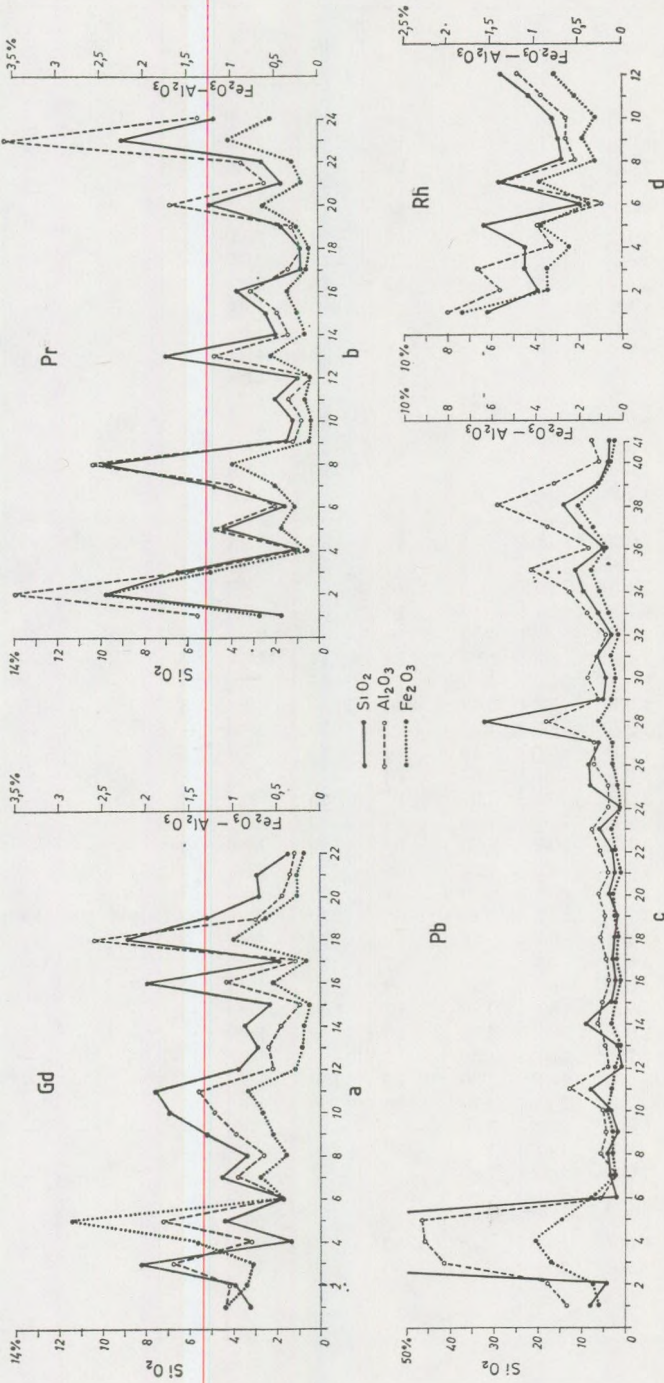
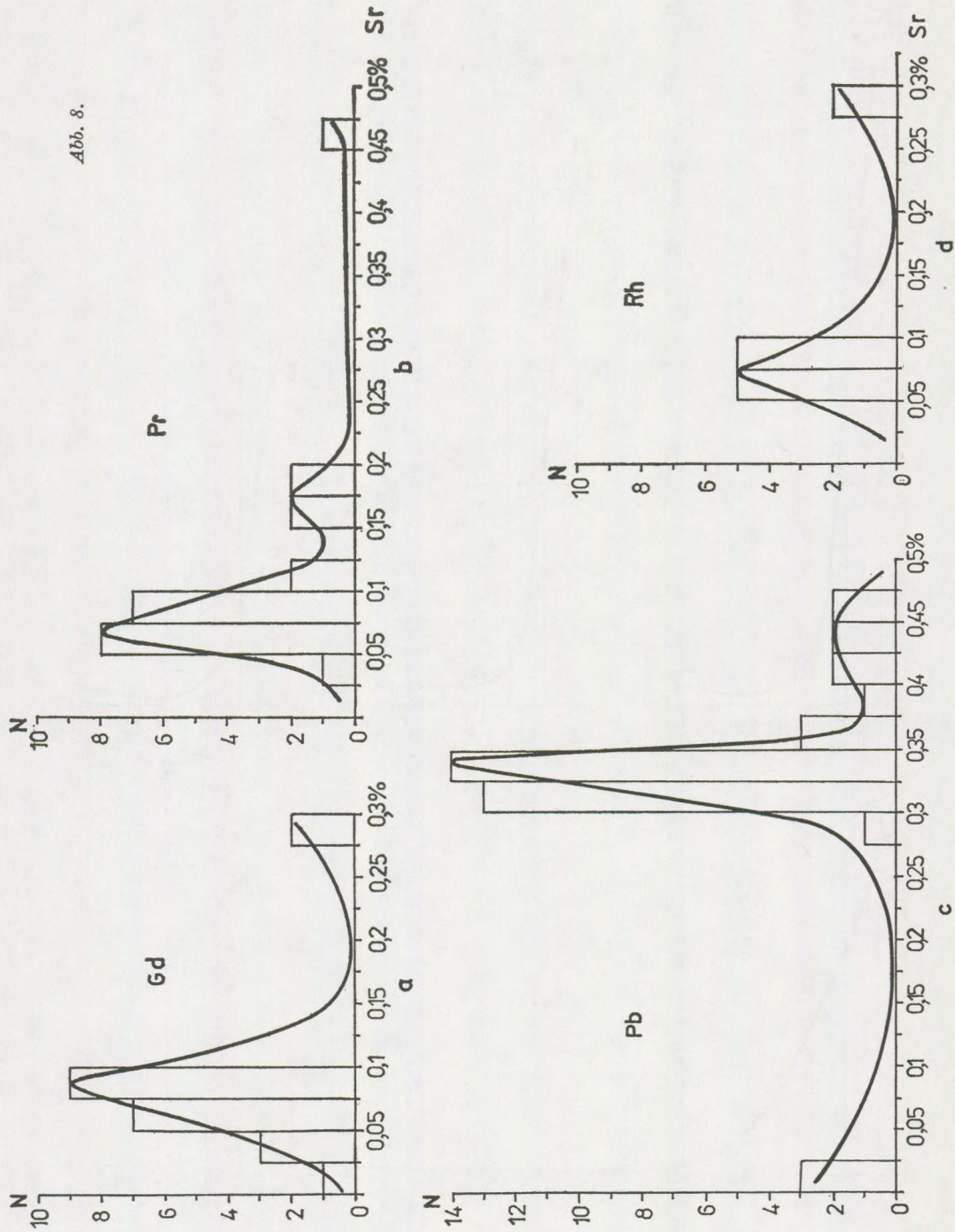


Abb. 7.

Abb. 8.



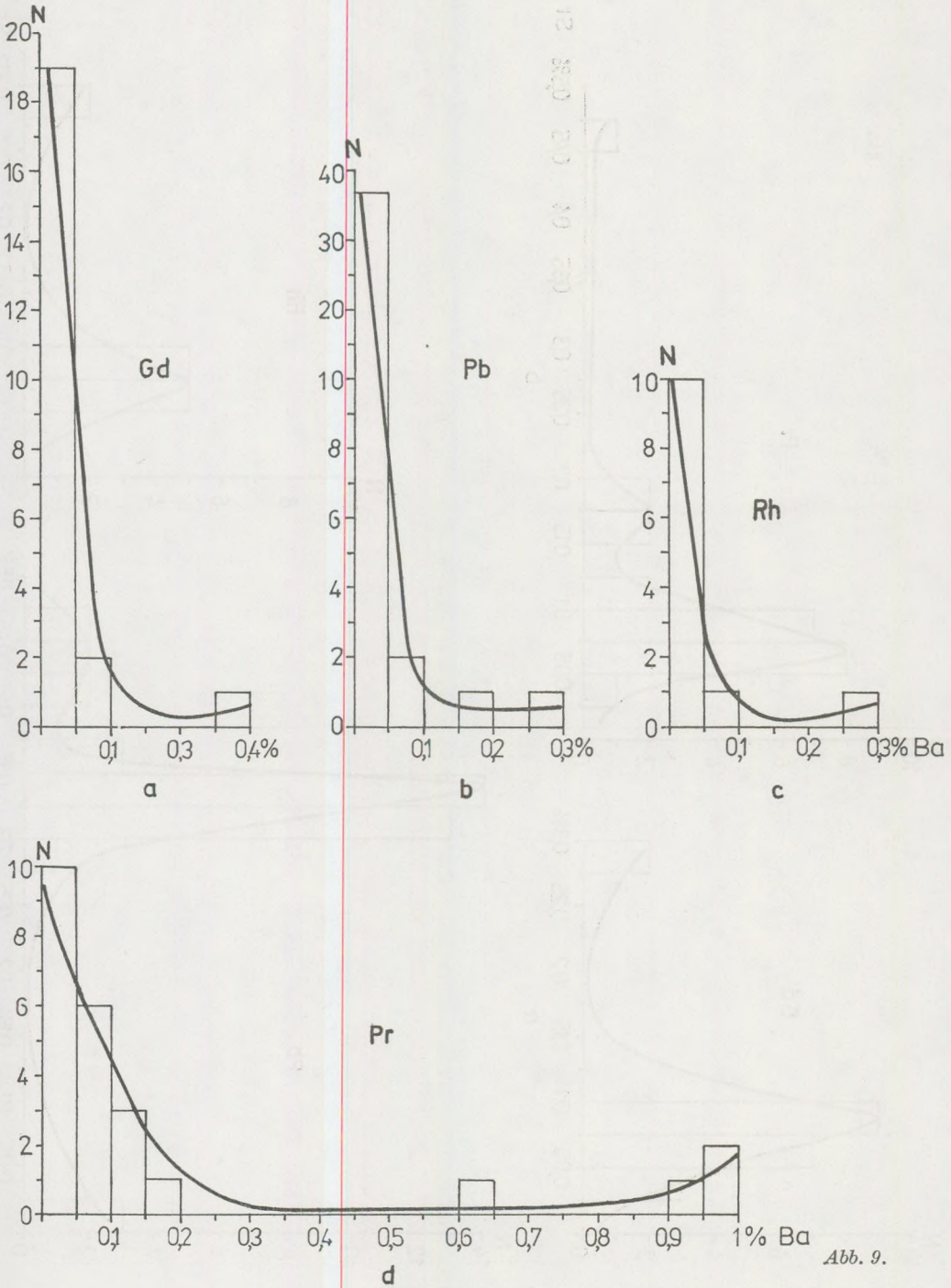


Abb. 9.

Untersucht man die parallele Verteilung von Sr und Ba in den verschiedenen Horizonten (Abb. 10), so entdeckt man, dass diese nicht nur im Siebenbürger Becken anzutreffen ist, sondern auch von W. KÜHN (1976) für einige Horizonte des Triaskalksteines aus dem Thüringer Becken festgestellt wurde. Bei uns sind es aber einige Horizonte in denen die Verteilung der Elemente beinahe entgegengesetzt ist. Für Rohia und Poiana Blenchii z.B. trifft man eine parallele Verteilung in den oberen Horizonten an, während die Piatra-Kalksteine in den oberen Horizonten eine entgegengesetzte Verteilung aufweisen. Die parallele Verteilung von Sr und Ba wird bei diesen in einigen unteren Horizonten sichtbar.

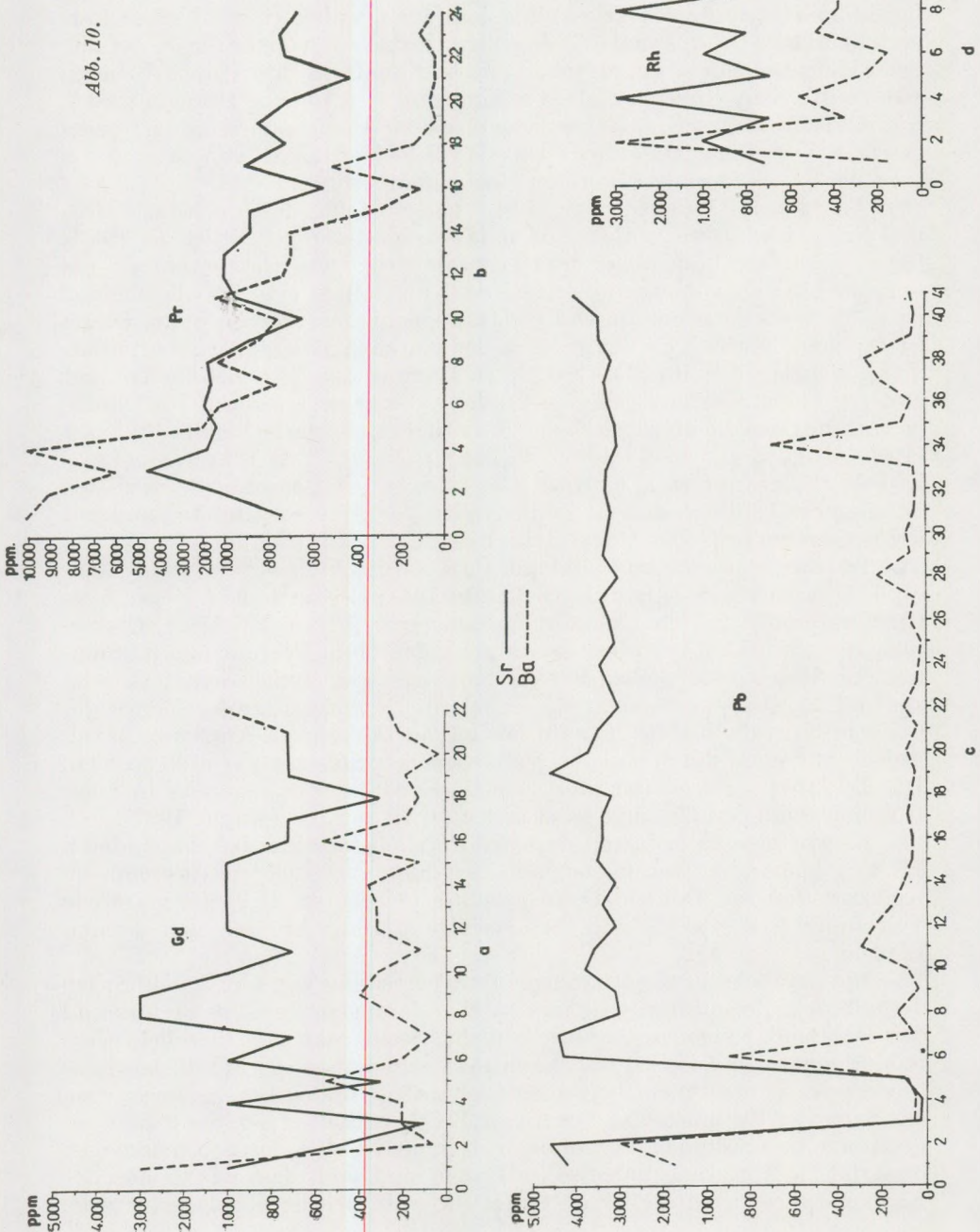
Aus diemem Vergleich der Abb. 6 und 10 folgt, dass auch für CaCO_3 und Sr beziehungsweise Ba keine parallele Verteilung deutlich ist (bloss für verschiedene Fundstellen und hier nur in einigen Horizonten) obwohl bei den übrigen von uns untersuchten Kalksteinen eine im allgemeinen parallele Verteilung von Sr und CaCO_3 angenommen werden kann. Dieses ist durchaus normal, da das Sr auch der Karbonatphase angehört und als SrCO_3 abgelagert wird. Das SrCO_3 entstammt den Muschelschalen und anderen Skeletresten, welche zur Bildung dieser organogenen Kalksteine beitragen. Dass die Muschelschalen Sr enthalten, bemerkt bereits BØGGILD (1930), J. L. KULP et al. (1952), J. IMREH (1959), R. WASKOWIAK (1962) und M. BARBIERI et al. (1976). Ebenfalls war es BØGGILD, der auf den höheren Sr-Gehalt in den Aragonitschalen der Art *Crassatellites* und auf der geringeren Sr-Gehalt der Kalzitschalen der Art *Pecten* hinwies.

In einer obereozänen Kalkbank im Bett des Flusses Someş bei Klausenburg fanden wir (J. IMREH, G. IMREH 1961) ein durchaus reiches Cölestin-Vorkommen in den Hohlräumen einiger Steinkerne der Arten: *Crassatella* sp., *Corbis subpectulus*, *Cerithium giganteum*, *Pectunculus pulvinatus*. Als Skelettreste blieben nur die Kalzitgehäuse zweier Arten: *Vulsella* sp. und *Echinolampas giganteus*, erhalten. Die relativ grosse Menge der Cölestin-Kristalle bildete sich auf kosten der zahlreichen Aragonitschalen, welche nur noch durch die übriggebliebenen Steinkerne verraten werden. Die Bildungsmöglichkeiten der Cölestin-Kristalle wurde bereits in einer früheren Studie erklärt und beschrieben (J. IMREH, G. IMREH, 1961).

Es war also zu erwarten dass der Parallelismus, der bei den anderen Kalken bemerkbar wurde, auch in den hier untersuchten Aufschlüssen nachzuweisen sei. Der einzige Aufschluss jedoch, wo sich eine parallele Verteilung von CaCO_3 und Sr verfolgen lässt, ist der von Poiana Blenchii.

Die parallele, bzw. entgegengesetzte Verteilung von CaCO_3 und Sr ist deshalb von Bedeutung, weil sie den Wanderungsprozess des Sr während der Dia- und Epigenese veranschaulicht. Stellt man eine parallele Verteilung von Sr und CaCO_3 fest, kann man sagen, dass der Mobilisierungsprozess des Sr noch nicht begonnen oder stattgefunden hat, sondern, dass das Sr in der Kalkmasse in Form von SrCO_3 enthalten ist. Stellt man jedoch eine gegensätzlich Verteilung von Sr und CaCO_3 fest, so heisst das, dass die Mobilisierungsprozesse im Gange sind und, dass das Sr aus der Karbonatphase nachträglich als Sulfat (Cölestin) wieder abgelagert wurde.

Abb. 10.



Dadurch geht das Sr aus der Karbonatphase in den in HCl unlöslichen Rückstand über.

In Tabelle 3 sind die Ergebnisse der prozentuellen, beziehungsweise atomare Verhältnisse von Sr und Ca zu sehen. Die Werte schwanken zwischen 13,92 (6,32) und 0,28 (0,13) und mit Hilfe der in Tabelle 3 enthaltenen Werte wurden die Histogramme aus Abb. 11, 12, 13 zusammengestellt.

Die häufigsten $\frac{\%Sr}{\%Ca} \cdot 1000$ -Werte fallen in Klasse 2–3‰, (N=24) und in den benachbarten Klassen auch beinahe so häufig. Hier fällt noch eine Frequenzgruppe in den Klasse: 8–9‰ und 10–11‰ (N=8), bzw. 9–10‰

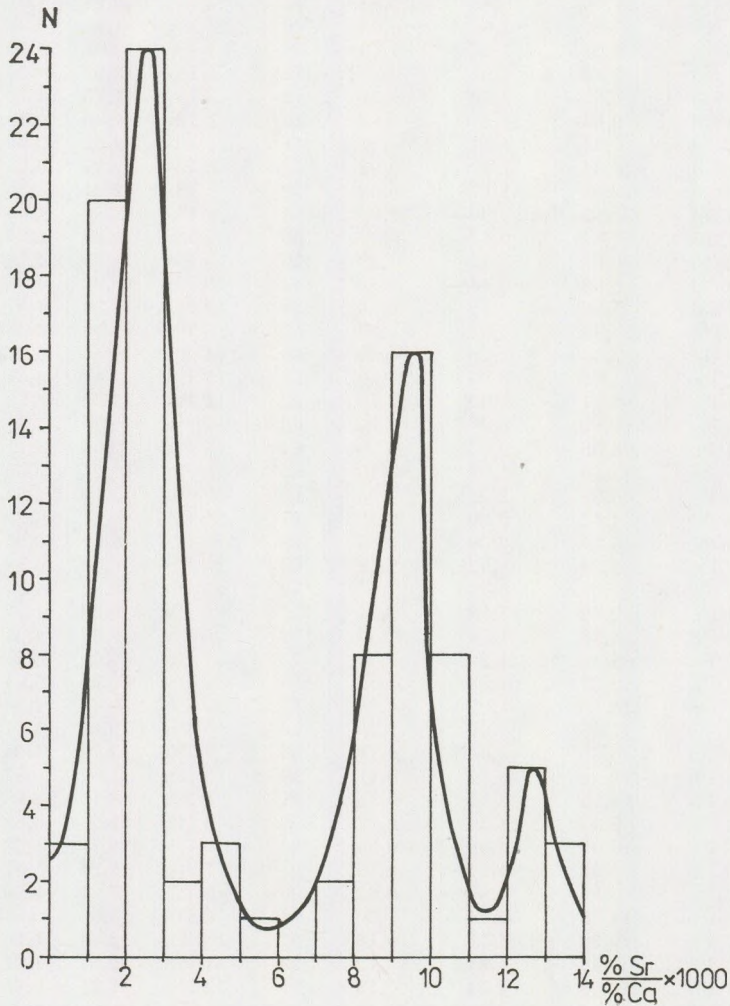


Abb. 11.

Tabelle 3.

Procentuelle und atomare Verhältnisse von Sr, Ba und Ca

Probe		$\frac{\%Sr}{\%Ca} \cdot 10^3$	$\frac{Sr}{Ca} \cdot 10^3$	$\frac{\%Ba}{\%Ca} \cdot 10^3$	Probe	$\frac{\%Sr}{\%Ca} \cdot 10^3$	$\frac{Sr}{Ca} \cdot 10^3$	$\frac{\%Ba}{\%Ca} \cdot 10^3$	
1	1 Gd	2,72	1,24	8,18	39	17 Pr	2,24	1,01	1,27
2	2 Gd	1,34	0,61	0,17	40	18 Pr	1,83	0,83	0,33
3	3 Gd	0,28	0,13	0,57	41	19 Pr	2,20	1,00	0,07
4	4 Gd	2,69	1,22	0,53	42	20 Pr	1,94	0,88	0,13
5	5 Gd	0,84	0,38	1,57	43	21 Pr	1,08	0,49	0,07
6	6 Gd	2,62	1,19	0,52	44	22 Pr	1,93	0,87	0,08
7	7 Gd	1,90	0,86	0,20	45	23 Pr	2,24	1,01	0,30
8	8 Gd	7,95	3,61	0,63	46	24 Pr	1,83	0,83	0,08
9	9 Gd	8,32	3,78	1,10	47	1 Pb	13,06	5,93	5,60
10	10 Gd	2,79	1,27	0,86	48	2 Pb	13,92	6,32	9,13
11	11 Gd	1,97	0,89	0,33	49	3 Pb	1,73	0,79	2,60
12	12 Gd	2,66	1,21	0,82	50	4 Pb	1,05	0,48	1,58
13	13 Gd	2,64	1,20	0,81	51	5 Pb	52,62	23,92	41,05
14	14 Gd	2,64	1,20	0,92	52	6 Pb	12,15	5,52	2,54
15	15 Gd	2,59	1,17	0,32	53	7 Pb	12,24	5,56	0,19
16	16 Gd	1,98	0,90	1,58	54	8 Pb	8,80	4,00	0,37
17	17 Gd	1,82	0,82	0,49	55	9 Pb	8,68	3,94	0,12
18	18 Gd	0,93	0,42	0,38	56	10 Pb	10,53	4,78	0,24
19	19 Gd	1,90	0,86	0,46	57	11 Pb	10,74	4,88	0,88
20	20 Gd	1,84	0,83	0,09	58	12 Pb	8,90	4,07	0,65
21	21 Gd	1,84	0,83	0,55	59	13 Pb	8,98	4,08	0,37
22	22 Gd	2,55	1,16	0,63	60	14 Pb	9,41	4,27	0,31
23	1 Pr	1,89	0,85	26,20	61	15 Pb	9,49	4,31	0,14
24	2 Pr	3,47	1,52	28,70	62	16 Pb	12,54	5,70	0,18
25	3 Pr	13,80	6,27	17,90	63	17 Pb	10,26	4,66	0,25
26	4 Pr	4,59	2,02	25,50	64	18 Pb	9,04	4,11	0,19
27	5 Pr	3,79	1,72	5,40	65	19 Pb	12,21	5,55	0,15
28	6 Pr	4,88	2,22	3,08	66	20 Pb	10,19	4,63	0,24
29	7 Pr	4,42	2,00	2,09	67	21 Pb	9,31	4,23	0,10
30	8 Pr	5,07	2,30	3,88	68	22 Pb	8,69	3,95	0,30
31	9 Pr	2,26	1,02	2,18	69	23 Pb	9,20	4,18	0,12
32	10 Pr	1,63	0,74	1,93	70	24 Pb	9,39	4,27	0,08
33	11 Pr	2,42	1,10	3,35	71	25 Pb	9,53	4,33	0,07
34	12 Pr	2,78	1,26	1,84	72	26 Pb	9,55	4,34	0,20
35	13 Pr	2,85	1,29	1,99	73	27 Pb	9,49	4,31	0,13
36	14 Pr	2,27	1,03	1,81	74	28 Pb	12,97	5,89	0,90
37	15 Pr	2,36	1,07	0,80	75	29 Pb	9,46	4,30	0,19
38	16 Pr	1,45	0,66	0,26	76	30 Pb	9,19	4,17	0,23
77	31 Pb	8,89	4,04	0,14	89	2 Rh	2,74	1,24	8,23
78	32 Pb	9,06	4,12	0,11	90	3 Rh	1,92	0,87	0,98
79	33 Pb	9,14	4,15	0,15	91	4 Rh	8,11	3,68	1,51
80	34 Pb	9,47	4,30	2,17	92	5 Rh	1,95	0,88	0,69
81	35 Pb	10,07	4,58	0,34	93	6 Rh	2,71	1,23	0,40
82	36 Pb	9,33	4,24	0,16	94	7 Rh	2,24	1,01	1,37
83	37 Pb	10,56	4,80	0,63	95	8 Rh	7,91	3,59	1,00
84	38 Pb	11,75	5,34	1,00	96	9 Rh	1,85	0,84	1,00
85	39 Pb	10,38	4,71	0,18	97	10 Rh	2,64	1,20	0,52
86	40 Pb	9,46	4,30	0,12	98	11 Rh	2,67	1,21	0,49
87	41 Pb	10,88	4,94	0,16	99	12 Rh	1,95	0,89	0,55
88	1 Rh	2,05	0,93	0,42					

($N=16$), welche den Frequenzschaubildern ein bimodales Aussehen verleihen auf.

Vergleicht man die von M. FORNASERI und L. GRANDI (1968) für die italienischen Kalksteine aufgestellten Histogramme mit unseren Ergebnissen (op. cit. S. 751, Abb. 5, 6), so werden zwei benachbarte Höchstfrequenzen in der 2-ten und 3-ten Klasse, ähnlich den Ergebnissen unserer Untersuchungen, feststellbar. Der einzige Unterschied besteht bloss darin, dass diese Frequenzen für die italienischen Kalkstein in die Klassen: 0,25 – 0,5% und 0,5 – 0,75%, unsere Ergebnisse aber in die Klassen: 1 – 2% und 2 – 3%, fallen.

Die von uns erhaltenen grösseren Gehaltswerte der 2-ten und 3-ten Klasse sind durch das erdgeschichtliche Alter (Eozän – Oligozän) unseren Proben erklärlich. Untersucht man aber die chemischen Analysen der italienischen Kalksteine (M. FORNASERI, L. GRANDI, 1963), wir können feststellen, dass die Sr-Werte der eozän – oligozänen Kalksteine viel grösser sind, als die der älteren Kalksteine. Die zweite Frequenzgruppe im Falle unserer Kalksteine, ist von den äusserst grossen Sr-Werten der Poiana Blenchii-Kalke verursacht.

Zeichnet man die Schaubilder für die verschiedenen Aufschlüsse, so ist diese klar ersichtlich (Abb. 12) und man kann das unterschiedliche Verhalten der Poiana Blenchii-Kalke gut verfolgen. Der Durchschnittswert des $\frac{\%Sr}{\%Ca} \cdot 1000$ – ohne den Poiana Blenchii-Kalk in betracht zu ziehen – ist beinahe doppelt so gross, als der von M. FORNASERI und L. GRANDI (1963, 1968) für die italienischen Kalksteine errechnete. Untersucht man nur die italienischen Kalksteine eozänen und oligozänen Alters, so findet man einen Mittelwert von 2,52 (op. cit. Tab. X.), der mit dem von uns berechneten fast übereinstimmt.

Die Poiana Blenchii-Kalke fallen durch ein, was die Sr-Werte betrifft, besonderes Verhalten auf; in den Pietra-Kalken lassen sich grosse Ba-Werte (10 000 ppm) und ein relativ grosser Sr-Gehalt (4700 ppm) in den oberen Horizonten nachweisen.

Trotzdem lässt sich, bei einem Vergleich der Histogramme für die Ba- und $\frac{\%Ba}{\%Ca} \cdot 1000$ -Frequenz, eine Ähnlichkeit der Schaubilder erkennen. Das heisst, dass sich die Ba-Verteilung denselben Regeln in allen vier Aufschlüssen unterwirft.

M. FORNASERI und L. GRANDI (1968) untersuchten die Wechselbeziehungen zwischen Sr, $MgCO_3$, unlöslichen Rückstand und $CaCO_3$ in 21 Dolomitproben und fanden für die empirischen linearen Korrelationskoeffizienten (r) folgende Werte:

	Sr	$MgCO_3$	Unl. Rückst.	$CaCO_3$
$CaCO_3$	0,175	–0,416	–0,83	1,0
Unl. R.	0,008	–0,161	1,0	–0,83
$MgCO_3$	–0,323	1,0	–0,161	–0,416
Sr	1,0	–0,323	–0,008	0,175

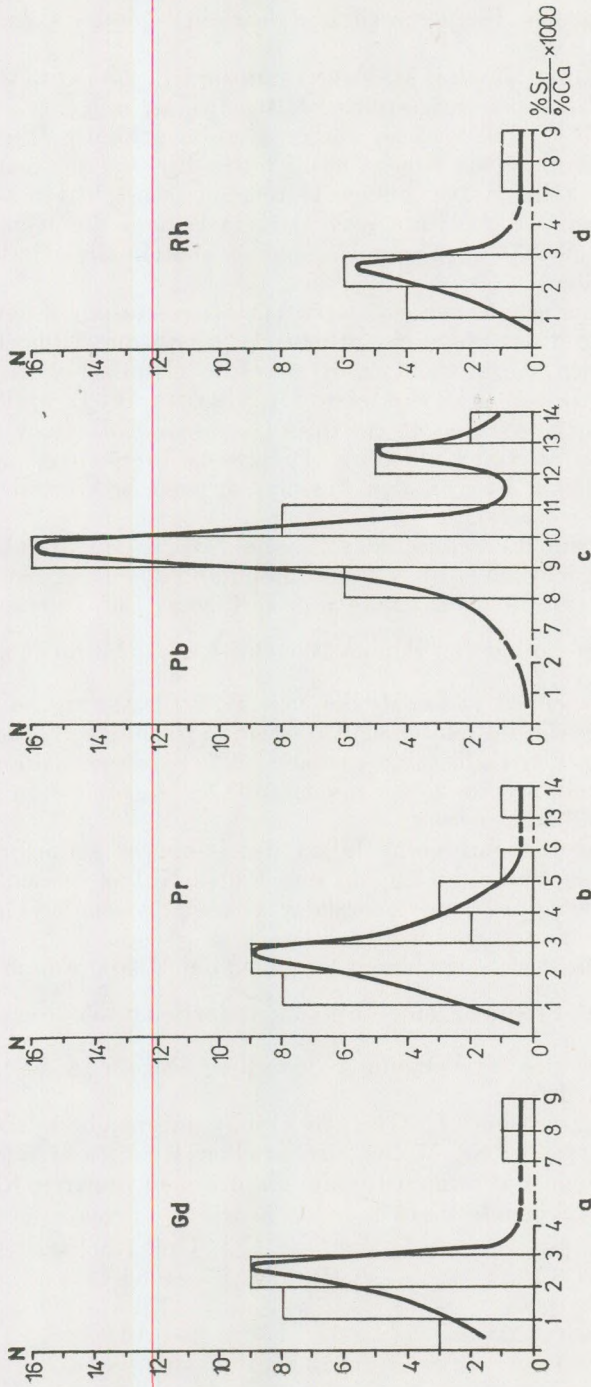


Abb. 12.

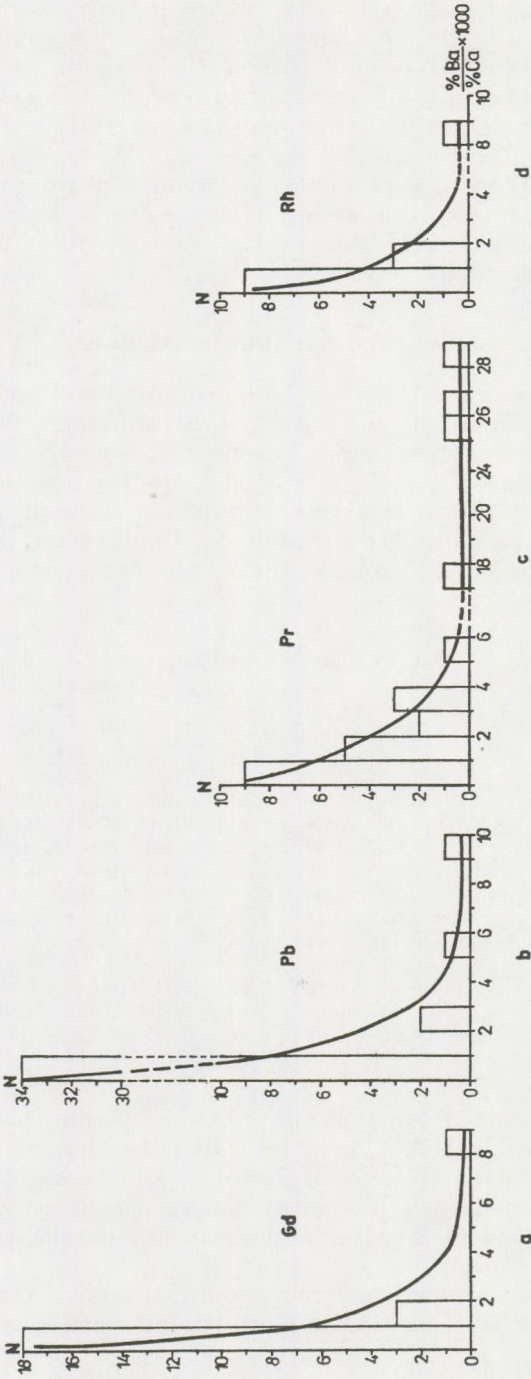


Abb. 13.

$\frac{\% \text{Ba}}{\% \text{Ca}} \times 1000$

Das Beispiel zeigt klar, dass der einzige positive Korrelationswert zwischen Sr und Ca durch den kleinen Wert 0,175 ausgezeichnet ist, die übrigen sind mit Ausnahme des unlöslichen Rückstandes, wo die Korrelation Null ist, durch negative Werte ausgezeichnet.

Erklärt werden kann dieses dadurch, dass ein Teil des Sr in kleinen Mengen im unlöslichen Rückstand – (wie der r -Werte aussagen) – in Form von SrSO_4 (Cölestin) vorkommt, der grösste Teil jedoch in der Karbonatphase enthalten ist. Der kleine Wert des Korrelationskoeffizient r von Ca–Sr im Falle der italienischen Kalksteine, wird dadurch erklärt, dass diese Dolomiten sind.

Dichotomische Analyse (Cluster Analysis)

Zu diesem Zwecke berechneten wir die empirischen linearen Korrelationskoeffizienten, die in Tab. 4, 5, 6, 7 für jeden einzelnen, und in Tab. 8 für alle Aufschlüsse angegeben sind. Tabelle 4, 5, 6 und 7 zeigt, dass die Korrelation zwischen Sr und Ca positiv und nur für Piatra negativ ist, während in Tab. 8 – wo alle vier Aufschlüsse zusammen betrachtet werden –, die Sr–Ca Korrelation negativ ist. Daraus folgt, dass das Korrelationsstudium für jeden einzelnen Aufschluss separat, vorteilhafter ist.

Tabelle 4.

Matrix der „ r^2 “-Werten (Gold)

	Si	Fe	Al	Kt	Do	Ti	Mn	Cr	Ni	Ba	Sr
Si	1,00	0,20	0,79	-0,90	0,39	0,64	-0,21	0,86	0,49	-0,06	-0,20
Fe	0,20	1,00	0,65	-0,49	0,34	0,24	0,30	0,34	0,22	0,25	-0,26
Al	0,79	0,65	1,00	-0,95	0,64	0,51	0,06	0,80	0,53	0,11	-0,32
Kt	-0,90	-0,49	-0,95	1,00	-0,68	-0,59	0,03	-0,85	-0,58	-0,06	0,25
Do	0,39	0,34	0,64	-0,68	1,00	0,18	0,01	0,46	0,40	0,16	0,05
Ti	0,64	0,24	0,51	-0,59	0,18	1,00	-0,15	0,60	0,43	0,15	-0,26
Mn	-0,21	0,30	0,06	0,03	0,01	-0,15	1,00	-0,14	0,11	-0,18	-0,01
Cr	0,86	0,34	0,80	-0,85	0,46	0,60	-0,14	1,00	0,60	0,14	-0,17
Ni	0,49	0,22	0,53	-0,58	0,40	0,43	0,11	0,60	1,00	0,29	-0,25
Ba	-0,06	0,25	0,11	-0,06	0,16	0,15	-0,18	0,14	0,29	1,00	0,06
Sr	-0,20	-0,26	-0,32	0,25	0,05	-0,26	-0,01	-0,17	-0,25	0,06	1,00

Dieselben Tabellen zeigen auch für Si, Al und Fe eine positive Korrelation – was auch aus Abb. 7, in welcher die Verteilung des SiO_2 , Al_2O_3 und Fe_2O_3 in den Horizonten angegeben wird – zu sehen ist.

Die geochemischen Besonderheiten der verschiedenen einzelnen Elemente eines jeden Gebietes wurden durch die dichotomische Analyse untersucht und hervorgehoben.

Die Veränderlichen werden durch die stufenförmige Verschmelzung, bei dem Niveau der Höchstwerte der Korrelationskoeffizienten der Matrix erzielt.

Tabelle 5.

Matrix der „r“-Werten (Piatra)

	Si	Fe	Al	Kt	Do	Ti	Mn	Cr	Ni	Co	V	Ba	Sr
Si	1,00	0,83	0,92	-0,98	0,81	0,74	0,40	0,58	0,41	0,79	0,52	0,12	0,26
Fe	0,83	1,00	0,88	-0,89	0,87	0,83	0,70	0,24	0,30	0,60	0,35	0,47	0,35
Al	0,92	0,88	1,00	-0,93	0,79	0,72	0,54	0,51	0,48	0,75	0,34	0,29	0,19
Kt	-0,98	-0,89	-0,93	1,00	-0,89	-0,75	-0,52	-0,52	-0,40	-0,78	-0,46	-0,20	-0,30
Do	0,81	0,87	0,79	-0,89	1,00	0,66	0,61	0,46	0,39	0,68	0,30	0,27	0,40
Ti	0,74	0,83	0,72	-0,75	0,66	1,00	0,40	0,14	0,15	0,44	0,53	0,32	0,18
Mn	0,40	0,70	0,54	-0,52	0,61	0,40	1,00	-0,01	0,01	0,34	-0,01	0,71	0,56
Cr	0,58	0,24	0,51	-0,52	0,46	0,14	-0,01	1,00	0,39	0,65	0,48	-0,23	-0,15
Ni	0,41	0,30	0,48	-0,40	0,39	0,15	0,01	0,39	1,00	0,38	-0,26	-0,01	0,23
Co	0,79	0,60	0,75	-0,78	0,68	0,44	0,34	0,65	0,38	1,00	0,35	-0,06	0,12
V	0,52	0,35	0,34	-0,46	0,30	0,53	-0,01	0,48	-0,26	0,35	1,00	-0,06	-0,21
Ba	0,12	0,47	0,29	-0,20	0,27	0,32	0,71	-0,23	-0,01	-0,06	-0,06	1,00	0,38
Sr	0,26	0,35	0,19	-0,30	0,40	0,18	0,56	-0,15	0,23	0,12	-0,21	0,38	1,00

Tabelle 6.

Matrix der „r^c“-Werten (Poiana Blenchi)

	Si	Fe	Al	Kt	Do	Ti	Mn	Cr	Ni	Co	V	Mo	W	Sn	Ba	Sr
Si	1,00	0,89	0,91	-0,97	-0,26	0,83	0,03	0,61	0,76	0,22	0,67	0,46	0,25	0,34	-0,08	-0,90
Fe	0,89	1,00	0,95	-0,90	-0,24	0,82	0,16	0,67	0,78	0,33	0,57	0,44	0,26	0,30	0,12	-0,76
Al	0,91	0,95	1,00	-0,92	-0,26	0,79	0,02	0,75	0,78	0,38	0,63	0,45	0,29	0,34	0,10	-0,79
Kt	-0,97	-0,90	-0,92	1,00	0,07	-0,82	-0,03	-0,63	-0,75	-0,24	-0,65	-0,43	-0,26	-0,38	0,03	0,89
Do	-0,26	-0,24	-0,26	0,07	1,00	-0,21	0,03	-0,14	-0,24	-0,10	-0,16	-0,23	-0,07	0,07	-0,01	0,14
Ti	0,83	0,82	0,79	-0,82	-0,21	1,00	0,34	0,58	0,74	0,39	0,73	0,36	0,33	0,19	0,26	-0,60
Mn	0,03	0,16	0,02	-0,03	0,03	0,34	1,00	0,01	0,09	0,14	0,18	-0,10	0,11	-0,11	0,24	0,06
Cr	0,61	0,67	0,75	-0,63	-0,14	0,58	0,01	1,00	0,69	0,76	0,70	0,39	0,65	0,44	0,01	-0,50
Ni	0,76	0,78	0,78	-0,75	-0,24	0,74	0,09	0,69	1,00	0,50	0,70	0,73	0,45	0,35	0,06	-0,61
Co	0,22	0,33	0,38	-0,24	-0,10	0,39	0,14	0,76	0,50	1,00	0,63	0,32	0,66	0,25	-0,01	-0,11
V	0,67	0,57	0,63	-0,65	-0,16	0,73	0,18	0,70	0,70	0,63	1,00	0,50	0,61	0,36	-0,12	-0,58
Mo	0,46	0,44	0,45	-0,43	-0,23	0,36	-0,10	0,39	0,73	0,32	0,50	1,00	0,24	0,41	-0,13	-0,38
W	0,25	0,26	0,29	-0,26	-0,07	0,33	0,11	0,65	0,45	0,66	0,61	0,24	1,00	0,35	-0,08	-0,22
Sn	0,34	0,30	0,34	-0,38	0,07	0,19	-0,11	0,44	0,35	0,25	0,36	0,41	0,35	1,00	-0,19	-0,35
Ba	-0,08	0,12	0,10	0,03	-0,01	0,26	0,24	0,01	0,06	-0,01	-0,12	-0,13	-0,08	-0,19	1,00	0,31
Sr	-0,90	-0,76	-0,79	0,89	0,14	-0,60	0,06	-0,50	-0,61	-0,11	-0,58	-0,38	-0,22	-0,35	0,31	1,00

Tabelle 7.

Matrix der „r“-Werten (Rohia)

	Si	Fe	Al	Kt	Do	Ti	Mn	Cr	Ni	Ba	Sr
Si	1,00	0,78	0,75	-0,95	0,18	0,64	0,18	0,78	0,62	-0,08	-0,29
Fe	0,78	1,00	0,90	-0,87	0,04	0,44	0,33	0,45	0,53	0,07	-0,36
Al	0,75	0,90	1,00	-0,89	0,35	0,61	0,30	0,38	0,55	0,22	-0,41
Kt	-0,95	-0,87	-0,89	1,00	-0,36	-0,60	-0,27	-0,73	-0,60	-0,11	0,34
Do	0,18	0,04	0,35	-0,36	1,00	0,13	0,18	0,29	0,13	0,45	0,02
Ti	0,64	0,44	0,61	-0,60	0,13	1,00	-0,21	0,48	0,50	0,05	-0,29
Mn	0,18	0,33	0,30	-0,27	0,18	-0,21	1,00	0,21	0,33	0,36	0,21
Cr	0,78	0,45	0,38	-0,73	0,29	0,48	0,21	1,00	0,49	0,12	-0,04
Ni	0,62	0,53	0,55	-0,60	0,13	0,50	0,33	0,49	1,00	0,23	-0,11
Ba	-0,08	0,07	0,22	-0,11	0,45	0,05	0,36	0,12	0,23	1,00	0,02
Sr	-0,29	-0,36	-0,41	0,34	0,02	-0,29	0,21	-0,04	-0,11	0,02	1,00

Tabelle 8.

Matrix der „r“-Werten (Alle vier Aufschlüsse)

	Si	Fe	Al	Kt	Do	Ti	Mn	Cr	Ni	Ba	Sr	Sr/Ca
Si	1,00	0,47	0,70	-0,80	0,07	0,51	0,15	0,59	0,55	-0,01	0,13	0,26
Fe	0,47	1,00	0,74	-0,56	0,12	0,40	0,44	0,40	0,38	0,21	0,14	0,20
Al	0,70	0,74	1,00	-0,77	0,19	0,46	0,27	0,52	0,64	0,15	0,26	0,37
Kt	-0,80	-0,56	-0,77	1,00	-0,61	-0,38	-0,26	-0,48	-0,60	0,01	-0,38	-0,50
Do	0,07	0,12	0,19	-0,61	1,00	-0,10	0,17	0,01	0,27	-0,11	0,50	0,53
Ti	0,51	0,40	0,46	-0,38	-0,10	1,00	0,26	0,20	0,22	0,40	-0,09	-0,05
Mn	0,15	0,44	0,27	-0,26	0,17	0,26	1,00	-0,02	0,14	0,39	0,29	0,25
Cr	0,59	0,40	0,52	-0,48	0,01	0,20	-0,02	1,00	0,28	-0,11	-0,14	-0,06
Ni	0,55	0,38	0,64	-0,60	0,27	0,22	0,14	0,28	1,00	-0,06	0,51	0,54
Ba	-0,01	0,21	0,15	0,01	-0,11	0,40	0,39	-0,11	-0,06	1,00	-0,04	-0,05
Sr	0,13	0,14	0,26	-0,38	0,50	-0,09	0,29	-0,14	0,51	-0,04	1,00	0,88
Sr												
Ca	0,26	0,20	0,37	-0,50	0,53	-0,05	0,25	-0,06	0,54	-0,05	0,88	1,00

Die Zusammenhänge zwischen den verschiedenen Komponenten zeigen die Dendrogramme (Abb. 14), wo der Kalzit mit Kt und der Dolomit mit Do bezeichnet wird.

In Abhängigkeit von den verschiedenen Verschmelzungskriterien der Veränderlichen kennt man mehrere Verfahren. Wir benützten das aus der Literatur als „Single Linkage“ bekannte Verfahren. Die Berechnungen wurden auf Grund des von J. DAVIS veröffentlichten (1972) Cluster-Programms durchgeführt. Es wird jedoch darauf hingewiesen, dass wenn man die Proben auf die verschiedenen Horizonte verteilt, ihre Zahl merklich fällt. Als Vergleich zur Faktorialmethode sei gesagt, dass eben durch die Eigenartigkeit dieser Methode die Komponenten, die sich in verkehrter Korrelation befinden, als selbständige Gruppen hervortreten. Gegenätzliche Kausalbeziehungen zwischen ihnen können nur nach einer ge-

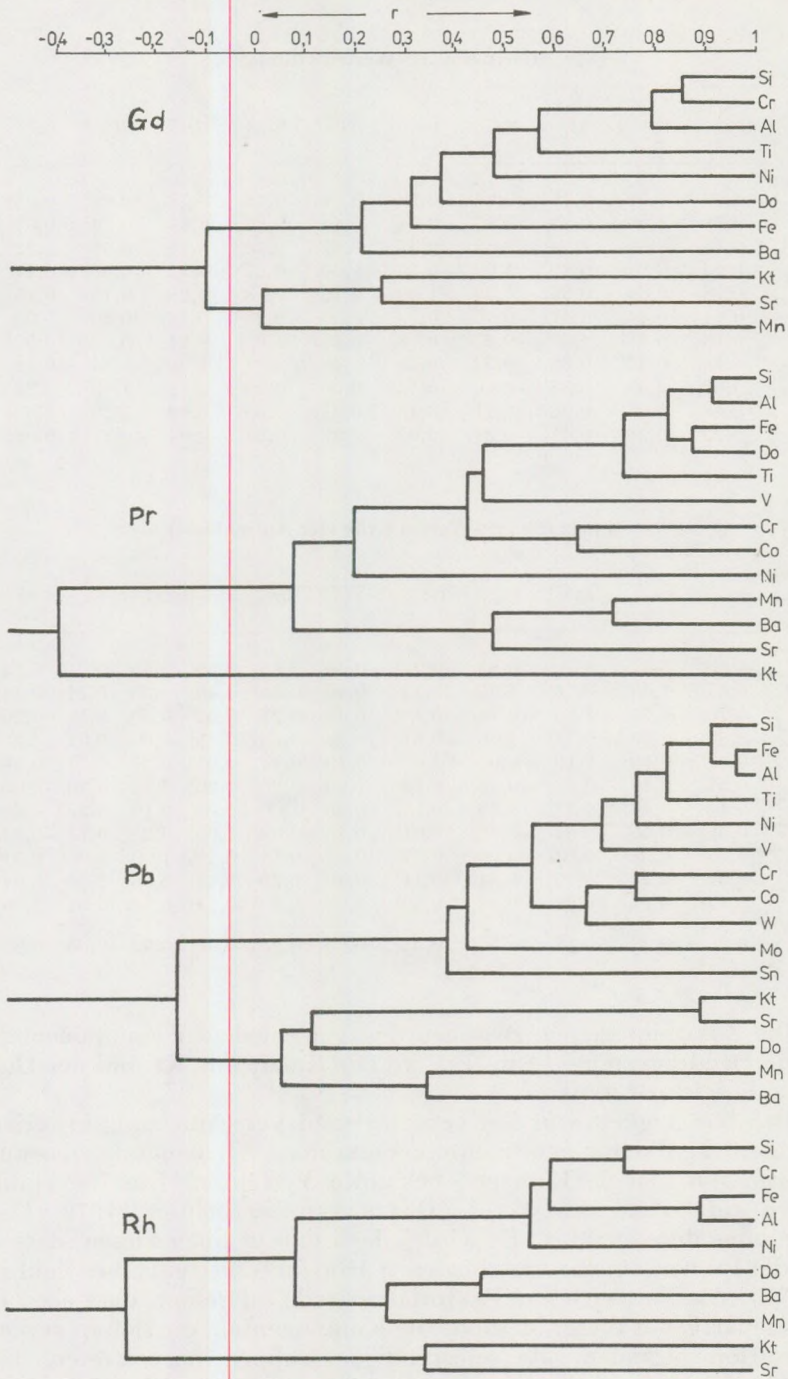


Abb. 14.

nauen zusätzlichen Analyse der Korrelationsmatrix festgestellt werden. Im Allgemeinen kann man sagen, dass in allen vier Aufschlüssen drei Verzweigungen, also drei Gruppen unterschieden werden können: *a*) die Elemente aus dem in HCl unlöslichen Rückstand, *b*) die der Karbonatphase angehörigen Elemente, *c*) die übrigen Elemente, welche abhängig von den Bedingungen, mal in der Karbonatphase, mal im unlöslichen Rückstand auftreten.

Im Aufschluss von Glod erschienen in der I-ten Gruppe Si, Cr, Al, Ti, Ni, Co, Fe, Ba in der II-ten Gruppe Ca und Sr, in der III-ten Gruppe Mn. Bemerkenswert ist die Anwesenheit des Dolomits in der Gruppe der Leitelemente des unlöslichen Rückstandes.

Für den Aufschluss Piatra ist eine Differenzierung innerhalb der zwei grossen Gruppen – unlöslicher Rückstand und Karbonatphase –, im Sinne einer Unterteilung des unlöslichen Rückstandes in Untergruppen, festgestellt worden. 1. Si, Al, 2. Fe, Mg (Do), 3. Ti, V, 4. Cr, Co, Ni.

Für die Karbonatphase fanden wir eine aus Mn, Ba und Sr, und eine aus Ca bestehende Untergruppe.

Die Elemente des unlöslichen Rückstandes der Poiana Blenchii-Kalke lassen sich in folgende Untergruppen einteilen: 1. Si, Al, Fe, 2. Ti, Ni, V, 3. Cr, Co, W, 4. Mo, Sn. Der Karbonatphase gehören die Untergruppen: 1. Ca (Kt), Sr, 2. Mn, Ba, 3. Mg (Do).

Im unlöslichen Rückstand des Rohia-Kalkes unterscheidet man folgende Untergruppen: 1. Si, Cr, 2. Fe, Al, 3. Ni. Für die Karbonatphase fanden wir zwei Untergruppen: 1. Mg (Do), Ba, Mn, 2. Ca (Kt), Sr.

Es ist leicht festzustellen dass die im unlöslichen Rückstand befindlichen Elemente immer zusammen erscheinen.

Was die Elemente der Karbonatphase betrifft, so können manche Elemente mit Elementen, die dem unlöslichen Rückstand angehören, auftreten. So z.B. erscheint der Dolomit (Mg) in Glod und Piatra-welche zwei benachbarte Aufschlüsse sind – zusammen mit Si, Al, Ti und Ni, während er in Poiana Blenchii und Rohia zusammen mit Ca und Sr vorkommt. Wenn man die ganze Zone untersucht und die Tabellen mit der Korrelationsmatrix aller Proben (Tab. 8) vergleicht stellt man dasselbe fest, dass in allen vier Aufschlüssen drei Hauptgruppen – allerdings mit einigen Unterscheiden was die Verteilung der Elemente in diesen Gruppen betrifft – unterschieden werden können.

Die erste Gruppe stellt der unlöslichen, siliziumhaltigen Rückstand der Kalksteine, welcher von verschiedenen spezifischen Komponenten kommt, dar: SiO_2 , Al_2O_3 , Fe_2O_3 , TiO_2 . Die Elemente Cr, Co, Ni und V haben, vielleicht weil sie in geringen Mengen vorkommen, eine weniger definierbare Stellung innerhalb der Gruppe. Obzwar Co und V nicht in derselben Untergruppe vorkommen, sind sie doch zusammen in den Aufschlüssen von Piatra und Poiana Blenchii ($r=0,35$ bzw. $0,63$) anzutreffen.

Eine andere Gruppe wird von den Elementen Sn, Mo, W, welche nur in Poiana Blenchii, vorkommen, gebildet. Ihre Anwesenheit wird durch das Anhäufen, Anschwemmen verschiedener Zersetzungsprodukte pegmatitischen Ursprungs, die im Rahmen der Zone vorkommen, erklärt.

Der Dolomit hat innerhalb der Gruppe zonenmässig ein unterschiedliches Verhalten. Die beste Korrelation ist mit der Silikatgruppe der Zone Piatra, $r > 0,8$ für Si, Fe, Al, bzw. $r > 0,6$ für Ti, Mn, Co, welches eine Gruppe von Elementen ist, gegenüber die Verbindungen in den Zonen Glod ($r = 0,34 - 0,64$, für Si, Al, Cr, Ni) und Rohia immer schwächer werden. In Poiana Blenchii erscheinen sie (obzwar die Korrelationskoeffizienten fast gleich Null sind) im negativen Bereich, eine schwache negative Korrelation andeutend, etwa $- 0,25$ für Si, Fe, Al, Ti und Ni.

Auf die gleiche Art fällt die Intensität der negative Korrelation mit dem Kalzit zusammen.

Die zweite Gruppe enthält praktisch eine einzige Komponente, CaCO_3 , der sich manchmal Sr oder Ba anschliessen. Es kann ein Paralellismus in der Beziehung CaCO_3 -Sr festgestellt werden. Die Intensität der positiven Korrelation zwischen CaCO_3 -Sr wächst von Zone und Zone parallel mit dem Wachsen der Korrelation Dolomit-Kalzit (Tab. 9).

Tabelle 9.

Die Korrelation zwischen verschiedene Phase

Phase	Korrelationskoeffizienten „r“			
	Piatra	Glod	Rohia	Poiana Blenchii
Silikat - Dolomit	0,79 - 0,87 ←	0,34 - 0,64	0,04 - 0,35	(-0,25) - (-0,26)
Kalzit - Dolomit	-0,89	-0,68	-0,36	0,07 →
Kalzit - Strontium	-0,30	0,25	0,34	0,89 →

Der parallele, aber entgegengesetzte Verlauf (Tab. 9) der Wechselbeziehung zwischen der Silikatphase und Dolomit, bzw. Kalzit-Dolomit war zu erwarten und widerspiegelt eine natürliche negative Korrelation zwischen der Karbonatphase und Silikatphase also des unlöslichen Rückstandes. Dieses war auch aus den grössten negativen Werten von r zu erwarten.

Die dritte Gruppe umfasst die Vergesellschaftung von Ba-Mn, obzwar die Wechselbeziehungen in verschiedenen Zonen für diese beiden Elemente relativ klein sind. In Piatra schliesst sich dieser Gruppe auch Sr an und weist eine relativ starke Korrelation mit Mn ($r = 0,56$), und eine schwächere mit Ba ($r = 0,38$) auf.

Faktorialanalyse

Um zusätzliche allgemeine geochemische Daten, die die Wanderung und Verteilung der Elemente über die ganze Verbreitzungszone der untersuchten Kalkgebilde beeinflussten und steuerten, zu erhalten, gruppieren wir die chemischen Daten und interpretierten sie mit Hilfe der Faktorialanalyse. Es wurde die Methode der Hauptkomponenten gewählt und die Matrix durch die Methode VARIMAX rotiert. Die Rechnungen wurden aufgrund der Programmpackete der statistischen Bibliothek des Rechners Felix C-256, durchgeführt.

Die Faktorialanalyse begann von der Matrix der Koeffizienten der Linearkorrelation. Die Bedeutung dieser Zusammenhänge wurden in der rotierten Matrix, die in Tab. 10 zu sehen ist zusammenfasst, aus der, um einen Prozentsatz von 72,8% aus der Gesamtveränderung auszudrücken, drei Faktoren genügen.

Tabelle 10

Die Ergebnisse der Faktorialanalyse

	Faktor 1	Faktor 2	Faktor 3
Si	-0,88521	0,10918	0,04307
Fe	0,66135	0,11597	0,43858
Al	0,84380	0,25356	0,25392
Kt	-0,79370	-0,48763	-0,07428
Do	0,09710	0,73220	0,07196
Ti	0,52596	-0,20591	0,55438
Mn	0,08551	0,28904	0,74319
Cr	0,79066	-0,18849	-0,21282
Ni	0,58776	0,52684	-0,00272
Ba	-0,04898	-0,13424	0,83680
Sr	0,01009	0,91800	0,09003
Sr/Ca	0,13379	0,91608	0,08084
	39,77%	59,25%	72,80%

Kt = Kalzit

Do = Dolomit

Faktor 1. Zeichnet sich durch grosse positive faktorielle Anteile für Si, Fe, Al, Cr, Ni, Ti und einen negativen Anteil für CaCO_3 aus. Lithogenetisch betrachtet, entspricht dieses zum Nachteil der Ausfällung des CaCO_3 , einer Zufuhr silikatischen Materials. Die Anwesenheit von Cr, Ni und Ti und ihr Anschluss zu diesem Faktor (der Silikatphase), also dem unlöslichen Rückstand, deutet auf eine Zufuhr basischen Materials (basischen Magmangesteine) während der Bildungszeit dieser Kalksteine, hin.

Faktor 2 vereint durch grosse faktorielle Anteile, Dolomit, Sr und das $\frac{\text{Sr}}{\text{Ca}}$ - Verhältnis und könnte als ein frühzeitiger diagenetischer Faktor,

durch den auch der Dolomitierungsprozess des Kalkschlammes stattfindet, gedeutet werden. Gleichzeitig findet auch eine Neuverteilung und Konzentrierung des Sr statt. Der hohe Faktoranteil des $\frac{\text{Sr}}{\text{Ca}}$ – Verhältnisses und dasselbe Vorzeichen wie für das Sr, zeigt, dass die Bereicherung an Sr des Kalksteines zeitlich von der Ausfällung des kalkigen Materials verschoben ist und erst während der Diagenese, parallel mit dem Dolomitierungsprozess, stattfand. Daraus folgt dass, obzwar das im Meerwasser enthaltene Sr von den aus Aragonit aufgebauten Skeletteilen der Organismen festgehalten wird, seine Verteilung, bzw. Anreicherung im Kalkstein erst während der Diagenese stattfindet und zeitlich mit dem Dolomitierungsprozess übereinstimmt. Die positive Korrelation zwischen Ca (Kalzit) und Mg (Dolomit) ist dadurch erklärlich, dass die Schalenteile der Organismen, wie bereits BARBIERI, M. et al. (1976) zeigte, auch eine beträchtliche Menge Mg enthalten. Man weiss heute, dass der Kalzitteil der Schalen, im Gegensatz zum aragonitischen Perlmutterteil, ziemlich viel Mg enthält.

Im der bereits erwähnten Studie zeigt Barbieri eine Tabelle (Tab. 3, S. 24 op. cit.), in der das Verhältnis Kalzit/Aragonit des jetztlebigen *Mytilus galloprovincialis* und des fossilen *Mytilus edule* ersichtlich ist.

Berechnet man die Mittelwerte aus dieser Tabelle, so stellt man fest, dass die rezenten Schalen zu 53,5% aus Kalzit und zu 46,47% aus Aragonit bestehen. Dieses entspricht einer Kalzit/Aragonit – Verhältnis von 1,15 für die heutigen und 0,69 für die fossilen Schalen. Betrachtet man Tabelle 4 (S. 25. op. cit.) aus derselben Arbeit, so merkt man, dass bei rezenten Gehäusen das Atomverhältnis $\frac{\text{Sr}}{\text{Ca}}$ 1000 den Wert 1,1 und im Falle der fossilen Schalen einen Wert von 1,2 hat.

Der Magnesiumgehalt ist 1321 g/t für rezente und 973 für fossile Schalen. Berechnet man die Differenz der Kalzitwerte der fossile und rezenten Schalen so ist ein Überschuss von 12,7% Kalzit zu Gunsten der rezenten Gehäuse ersichtlich.

Aus ähnlichen Berechnungen findet man einen Überschuss von 12,7% Aragonit in Falle der fossilen Schalenteile. Die genaue Übereinstimmung der beiden Werte wird als zufällig betrachtet.

Wenn man nun alle Dinge kennt, so ist die kleinere Mg-Gehalt der fossilen Schalen, der den rezenten Schalen gegenüber einen Defizit von 26,35% aufweist, leicht erklärlich. Dieser Unterschied zwischen den Mg-Gehaltswerten rezenter und fossiler Schalen ist nicht dem „Arten-Effekt“ zuzuschreiben, sondern, ist der Fortspülung des Mg während der Prozesse, die sich nach der Ausfällung des Kalkmaterials abspielen, zu verdanken. Man stellt also fest, dass bei Kalken, die aus Kalzit – und Aragonitresten aufgebaut wurden, die Mobilität des Mg viel grösser als jene des Ca ist, und folglich eine grosse Rolle im Dolomitierungsprozess spielen kann. Man kann also, ohne die Rolle des im klassischen Sinne verstandene Dolomitierungsprozess zu leugnen und zu übersehen, sagen, dass die Mg – Sr Korrelation nicht ausschliesslich auf diese Art, sondern auch auf Kosten

des in den Aragonit- und Kalzitskelettenteilen der Meerestiere enthaltenen Mg und Sr, stattgefunden hat.

Faktor 3 umfasst mit grossen Faktorialteilen das Ba und Mn, welches die späte hypergene Konzentration (Anreicherung) dieser beiden Elemente durch ihre geochemische Frischverteilung in untersuchten Gesteinprofil widerspiegelt. Diese Hypothese stützt sich jedoch auf die relativ kleine Korrelation ($r = 0,39$) dieser beide Elemente und fordert deshalb Vorsicht bei der Interpretation.

LITERATUR

- BARBIERI, M., CORTESI, C., PENTA, A., TOLOMEI, L. (1976): Stronzio e magnesio in conchiglie di lamellibranchiati pleistocenici ed attuali del Lazio. — *Periodico di Mineralogia*, 55, 1-2-3, Roma.
- BØGGILD, O. B. (1930): Shell structure of molluscs (Cit. J. L. Kulp).
- BOMBIȚA, G. (1972): Studii geologice in Munții Lapusului. — *An. Inst. Geol.* 39., Bucuresti.
- DUMITRESCU, I. (1957): Asupra faciesurilor și orizontarii Cretacicului superior și Paleogenului din Bazinul Lapusului. — *Lucr. Inst. Petrol și Gaze*, 3, Bucuresti.
- EL-HINAWI, E. ESSAM (1971): Petrography and Chemistry of some Egyptian Carbonate Rocks. — *N. Jb. Geol.-Paläont., Abh.* 138, 3.
- FORNASERI, M., GRANDI, L. (1963): Contenuto in stronzio di serie calcaree italiane. — *Giorn. Geol. Ann. Mus. Geol. Bologna*, 2, 31.
- FORNASERI, M., GRANDI, L. (1968): Nuovi dati sul contenuto in stronzio di serie calcaree italiane. — *Periodico di Mineralogia*, 37.
- HAUER, F., STACHE, G. (1863): Geologie Siebenbürgens. — *Verl. Braunmüller, Wien.*
- HOFMANN, K. (1879): Bericht über die im östlichen Theile des Szilágyer Comitates während der Sommercampagne 1878 vollführten geologischen Specialaufnahmen. — *Földt. Közl.* 9., 5-6., Budapest.
- HOFMANN, K. (1883): Bericht über die im Sommer im süd-östlichen Theile des Szatmárer Comitates ausgeführten geologischen Specialaufnahmen. — *Földt. Közl.* 13, 1-3, Budapest.
- HOFMANN, K. (1891): Geologische Übersichtskarte, 1 : 75 000 „Gaura und Galgó“.
- IMREH, J. (1959): Cölestin-Kristalle in Eozän-Versteinerungen. — *N. Jb. Geol. Paläont. Mh.* 11.
- IMREH, J., IMREH, G. (1961): Contribuții la studiul genezei colestinei sedimentare. — *Stud. Cerc. Geol.* 6, 2, Bucuresti.
- IMREH, J., JAKAB, E. (1965): Étude géochimique de quelques calcaires éocènes du Bassin Transylvain (Roumanie). — *Bull. Serv. Carte géol. Als. Lorr.* 18, 4.
- IMREH, J., BEDELEAN, I. (1967): Étude géochimique des calcaires tortoniens de la bordure occidentale du Bassin Transylvain (Roumanie). — *Bull. Serv. Carte géol. Als. Lorr.* 20, 4.
- IMREH, J., MIHÁLKA, ST. (1970): Étude géochimique de quelques calcaires éocènes de la partie Nord-Ouest du Bassin Transylvain (Roumanie). — *Bull. Serv. Carte géol. Als. Lorr.* 23, 3-4.
- IMREH, J., IMREH, G. (1971): Contenuto in stronzio e bario dei calcari eocenici e tortoniani della parte ovest e nord-ovest del Bacino Transilvanico (Romania). — *Periodico di Mineralogia*, 40, 3.
- IMREH, J., IMREH, G. (1972): Geochemische Bedeutung des Sr und Ba beim Studium tertiärer Kalksteine, TMPM 17.
- IMREH, J., IMREH, G. (1972): Studiul geochimic al unor calcare de la Baciu. — *Studia Univ. Babes-Bolyai, ser. Geol.-Min. f. 1.*
- IMREH, J., MÉSZÁROS, N., MIHÁLKA, ST. (1979): Studi geochimici sulle serie calcaree terziarie del Bacino Transilvanico (Romania). — *Periodico di Mineralogia*, 48, 1-2-3.
- IMREH, J., MÉSZÁROS, N., CIURILEANU, I. (1980): Studiul geochimic al calcarelor de la Rohia (Jud. Maramures). — *Studia Univ. Babes-Bolyai, Geol.-Geogr.* 25, 1.
- IMREH, J., MÉSZÁROS, N., MIHÁLKA, ST. (1981): Studiul geochimic al calcarelor terziare din nord-vestul Bazinului Transilvaniei. — *Studia Univ. Babes-Bolyai, Geol.-Geogr.* 26, 2.
- IMREH, J., MÉSZÁROS, N., CIURILEANU, I. (1980): Geochemische Untersuchungen über die Kalksteine aus dem Siebenbürgischen Becken (Rumänien). — *Ann. Univ. Budapestinensis.*
- KOCH, A. (1894): Die Tertiärbildungen des Beckens der Siebenbürgischen Landestheile, Paläocen. — *Földtani Int. Évkönyve.*
- KULP, J. L., TURKIAN, K., BOYD, D. W. (1952): Strontium content of limestones and fossils. — *Bull. Geol. Soc. of America*, 63.
- KÜHN, W. (1976): Buntmetallführende Karbonatbänke der höheren Trias in Thüringer Becken. — *Chem. Erde*, 35, 76.
- MÉSZÁROS, N. (1957): Fauna de moluste a depozitelor paleogene din NV Transilvaniei. — *Ed. Acad. Bucuresti.*
- MÉSZÁROS, N., GHURCA, V. (1965): Paleogenul dintre masivele Ticau și Preluca. — *Studia Univ. Babes-Bolyai, Geol.-Geogr.* 2.
- MÉSZÁROS, N., GEORGESCU, C., ROIBAN, M. (1967): Eocenul și baza oligocenului in regiunea Ileanda Mare-Poiana Blenchi. — *Studia Univ. Babes-Bolyai, Geol.-Geogr.* 1.
- MÉSZÁROS, M. (1980): Az eocen-oligocen határ kérdése az Erdélyi Medencében. — *Őslénytani Viták*, 25, Budapest.
- RAILEANU, GR., SAULEA, E. (1966): Paleogenul din regiunea Cluj și Sibou (NW Bazinului Transilvaniei). — *An. Com. Geol.* 29, Bucuresti.
- RUSU, A. (1977): Stratigrafia depozitelor oligocene din NV Transilvaniei (regiunea Treznea-Hida-Poiana Blenchi). — *An. Inst. Geol.-Geofiz.* 51, Bucuresti.
- WASKOWIAK, B. (1962): Geochemische Untersuchungen an rezenten Molluskenschalen mariner Herkunft. — *Freiberger Forschungshefte* 136.

CONTRIBUTION TO THE PROBLEM OF WEATHERING OF DIASPORITES

by

A. MINDSZENTY

Mineralogical Department of the L. Eötvös University, Budapest

J. BÉRCI

Training Reactor of Technical University – Budapest

(Received: 15th September, 1982)

Introduction

The weathering of diasporites on exposure is a widely known phenomenon and has been investigated by several authors (BÁRDOSSY, 1977; GLADKOVSKI, GUTKIN, 1960; MINDSZENTY, 1976). Relatively little attention was paid, however, to the textural changes occurring during the weathering process on the one hand, and to the trace element content of the weathering product vs. fresh rock on the other.

In the field seasons of 1974 and 1975 one of the senior authors had the opportunity to study this problem in Lang Son North Vietnam, where the weathering of diasporites is a process going on today. Micropetrographic and geochemical conclusions of the microscopic investigations and laboratory tests carried out on the Vietnamese samples are presented here.

Previous work

It was Russian authors (SHAROVA and GLAZUNOVA, 1966) who first mentioned the phenomenon of weathering in connection with the Vietnamese bauxites. On the basis of chemical and mineralogical analyses they concluded that the weathering process was essentially a desilification, proceeding with or without deferrification. They assumed that chlorites would begin to decompose first, and as destruction advances silica is gradually carried away while the neosynthesis of hydrohematite, gibbsite and partly diaspore would set in in the residual material. The presence of diaspore, gibbsite and hydrohematite was recorded by the conventional mineralogical means in the weathering product. As to chemistry, an increase of ferric at the expense of ferrous iron and in most of the cases also a slight relative enrichment of alumina was said to be a characteristic phenomenon.

Present work

Megascopic and microscopic study of about 150 samples, supplemented by limited amounts of X-ray diffraction and DT analyses, together with the standard five-component wet-chemical analyses served as a basis for the petrographic statements outlined below.

The weathering of the grey diasporites is essentially an oxidation caused by high-oxygen surface waters. It begins with the destruction of chamosite which is characterized by a finely dispersed phase of amorphous ferric-hydroxide turning up first along cracks, fissures and grain boundaries. (see Fig. 1.) As oxidation advances ferrioxide gradually impregnates the whole material giving rise to a secondary texture consisting essentially of hydrohematite and limonite, with diaspore as the only recognizable primary mineral. At places also well-developed crystallites of gibbsite and fine-grained kaolinite were observed both in the form of pore-space fillings (Figs. 2, 3.)

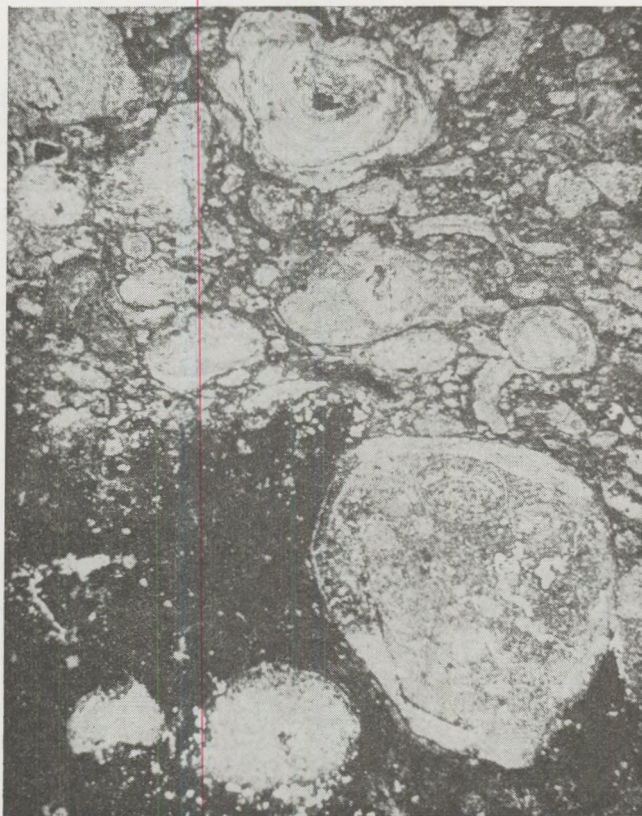


Fig. 1. Weathered oolitic diasporite impregnated by finely dispersed (black) ferric hydroxide formed during decomposition of chamosite
M = 12,5x nicols parallel

The mechanism of the above described phenomenon can tentatively be outlined as follows:

Due to high-oxygen surface waters the octahedral ferrous ions of chamosite become oxidized and therefore released from the structure in

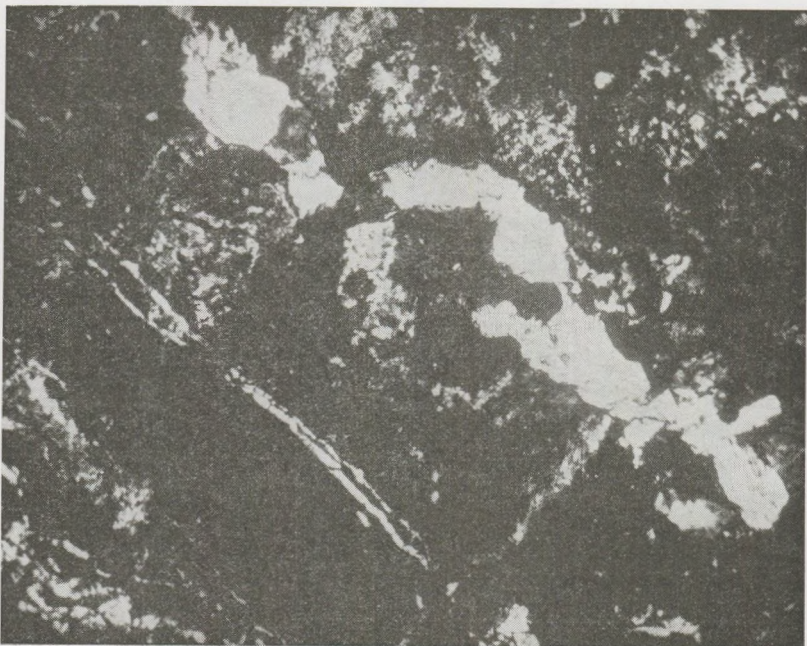


Fig. 2. Pore-space filling secondary gibbsite (white)
in oxidized diasporite
M = 50x, nicols crossed

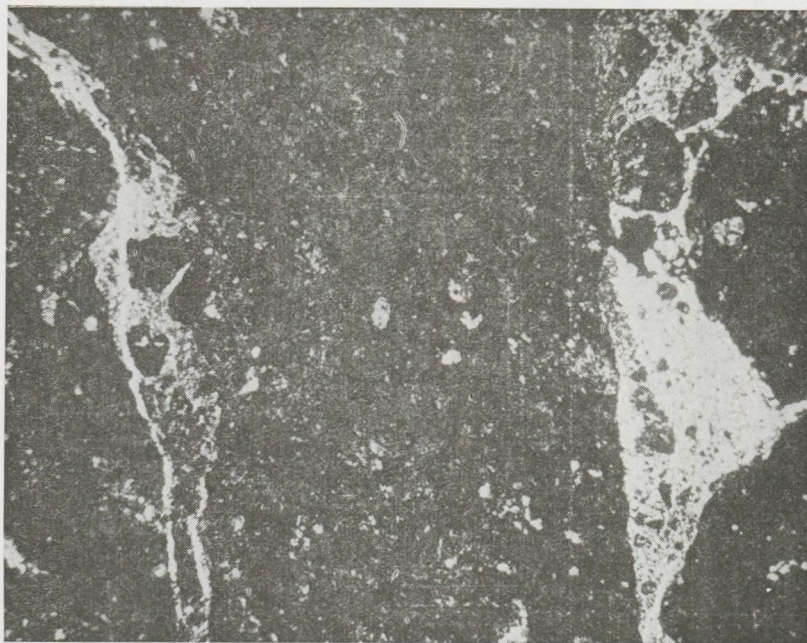


Fig. 3. Fine-grained kaolinite filling the cracks
of a weathered diasporite specimen
M = 50x, nicols crossed

the form of hydrated ferric ions. Electrostatically unbalanced, the structure necessarily disintegrates. The relatively weak bond between the octahedral Al^{3+} ions and the $(Al_2Si_2O_{10})$ -sheets results in the tearing off of Al^{3+} by water dipoles and in the neosynthesis of gibbsite.

Carried away by percolating water, the remaining $(Al_2Si_2O_{10})$ -units may form space-filling kaolinite elsewhere in the bauxite body.

The neosynthesis of diasporé — mentioned by SHAROVA and GLAZUNOVA — could not be detected either by microscopic or by X-ray diffraction methods. The apparent increase of the diasporé content of the weathered samples is most probably due to relative enrichment.

Trace element content

Five pairs of oxidized and fresh-rock specimens were selected for trace-element analysis. Sc, V, Cr, Co, Ni, Lu, Ce, Yb, La, Th were all determined by the activation method. Irradiation and measurements were

Standard Wet-chemical analyses

N ^o -of sample	Description	Al ₂ O ₃	SiO ₂	Fe ₂ O ₃	FeO
B1-33	Fresh bauxite (grey)	51.28	20.45	7.78	3.67
B1-33	Weathered bauxite (yellow)	39.47	40.53	4.19	0.84
Tmk-4/3	Fresh bauxite (grey)	54.60	8.70	6.35	13.50
Tmk-4/3	Weathered bauxite (red)	56.10	2.90	22.31	1.17
Bx-23	Fresh bauxite (grey)	56.16	11.43	6.19	9.23
Bx-23	Weathered bauxite (green)	55.5	7.97	9.55	10.24
Kpf-46	Fresh bauxite (green)	52.50	8.46	13.69	8.27
Kpf-46	Weathered bauxite (yellow)	49.97	2.98	27.29	1.29
K-276/7	Fresh bauxite (grey)	58.16	8.62	3.89	11.99
K-276/7	Weathered bauxite (yellow)	59.41	0.73	18.18	0.72

Mineralogical composition Bauxite samples (in percentages). (Based

N ^o -of sample	Description	Diasporé	Boehmite	Gibbsite	Goethite	Hematite	Siderite
B1-33	Fresh bauxite (grey)	0.4	37.9	1.3	2.5		
B1-33	Weathered bauxite (yellow)	3.9	0.4	2.8		0.9	0.4
Tmk-4/3	Fresh bauxite (grey)						
Tmk-4/3	Weathered bauxite (red)	54.5	—	—	5.2	6.0	
		63.3	—	—	4.0	19.0	1.2
BX-23	Fresh bauxite (grey)	38.8	15.4		—		
BX-23	Weathered (green)	52.9	—		10		

carried out in the Training Reactor of the Technical University, Budapest. The results are summarized in Table No 3. Although not at the first glance, it can be seen that there are two elements that show a clear tendency of enrichment or decrease during the weathering process, namely V which increases and La the amount of which markedly decreases in the oxidized samples as compared to the fresh ones.

Since the investigation of the trace-element content of bauxites is yet far from complete in a world-wide scale, we do not attempt to find any precise explanation to the above distribution of trace elements. The results are to be accepted rather just as a contribution to the problem of trace-elements in bauxites in general.

Acknowledgements

The authors wish to express their thanks to the Laboratories of the Bauxite Prospecting Co., Balatonalmádi, for preparing the thin sections

Table 1

of 5 Fresh/Weathered pairs of bauxites

TiO ₂	CaO	MnO	MgO	K ₂ O	Na ₂ O	-H ₂ O	+H ₂ O	CO ₂	P ₂ O ₅	S _{tot}
2.58	0.20	tr	0.56	0.38	0.17	0.46	12.85	0.09	0.03	
0.46	0.18	0.01	tr	0.70	0.19	0.28	13.63	0.13	0.04	
2.60	0.11	0.02	0.08	0.90	0.10	L.O.I.:	11.40	0.03	0.01	0.11
3.20	0.08	0.02	0.04	0.50	0.06	L.O.I.:	12.70	∅	tr	0.06
3.46	tr	0.04	tr	0.11	0.10	0.24	13.09	tr	0.04	
3.56	tr	tr	0.32	0.03	0.09	0.23	12.83	0.07	0.04	
3.70	tr	0.04	0.43	0.05	0.11	0.18	12.88	0.07	0.03	
4.01	tr	0.02	tr	0.09	0.20	0.28	13.47	0.09	0.09	0.08
2.89	0.36	0.05	tr	0.04	0.04	0.11	12.87	0.63	∅	0.09
3.17	1.06	0.09	tr	0.01	0.01	0.45	14.92	0.84	0.22	0.04

Table 2.

of three Fresh/Weathered pairs of
on quantitative X-ray diffracton analyses)

Calcite	Rodochrosite Olygonite Chlorite	Chamosite	Kaolinite	Phyllo- silicate	Quartz	Anatase	Rutile	Others	H ₂ O	Isomorphous Al subst. in goethite	Isomorphous Al subst. in hematite
1.6	5.7	23.1 9.1	26.0 60.4	4.7 8.3	0.5	2.3 tr	0.3 tr	0.5 5.5	0.5 1.1	5 -	- ∅
1.0		24.4 1.8	5.0 1.0	- 3.8	1.0 0.4	2.3 2.8	0.3 0.4	0.5 0.5	0.8 0.8	∅ 1	1 1
-		27.5	10.5		1.0	3.1	0.4	0.5	0.6	1	-
1.5		26.8	3.5		0.5	2.0	0.5	0.5	0.8	∅	-

Trace element content of five Fresh/Weathered method. (The percentages represent the

N°-of sample	Note	Ce g/t	Lu g/t	Th g/t
B1 - 33	Fresh	88.4 6.5%	0.2 34.6%	52.2 5%
B1 - 33	Weathered	16.6 21.7%	0.5 6.8%	13.3 11.2
Tmk - 4/3	Fresh	88.0 6.6%	0.7 4.2%	74.3 4%
Tmk - 4/3	Weathered	144.2 4.9%	0.7 5.3%	76.0 4.1%
Bx - 23	Fresh	140.0 4.8%	1.2 7.1%	67.0 4.3%
Bx - 23	Weathered	140.8 4.8%	1.5 7.7%	66.1 4.4%
Kpf - 46	Fresh	116.0 5.6%	3.2	66.4 4.5%
Kpf - 46	Weathered	133.0 5.1%	1.0	70.1 4.4%
K - 276/7	Fresh	101.2 5.9%	0.6 11.6%	56.9 4.6%
K - 276/7	Weathered	111.3 5.4%	0.5 11.9%	63.6 4.4%
Clarke (lithosphere/g/t) Goldschmidt (1954)		41.6	0.75	11.5

Table 3.

bauxite pairs analysed by neutron activation
 nuclear error of the measurement)

Cr g/t	Yb g/t	Sc g/t	Co g/t	La g/t	V g/t	Ni g/t
634 7.5%	4,4 6.7%	46,4 2.7%	31,1 33.4%	54,9 17.7%	106 14.7%	125 12.5%
164 17.8%	—	21.4 4.0%	46.6 9.8%	—	47 37.8%	173 30.9%
992 5.6%	4.5 7%	64.8 2.3%	42.1 10.7%	104.2 11.7%	96 15.7%	98 2.5%
129.8 4.8%	5.6 5.9%	74.3 2.1%	— —	42.8 20.9%	282 8.5%	95 6.9%
896 5.8%	4.4 7.0%	56.4 2.4%	94.3 14.7%	90.2 12.6%	84 22.8%	268 6.7%
983 5.4%	4.5 7.0%	24.7 2.4%	109.8 12.7%	78.6 13.6%	156 10.9%	298 7.1%
120.4 4.8%	5.2 6.3%	60.7 2.3%	79.3 16.9%	62.3 17.3%	215 6.1%	129
131.7 4.6%	6.2 5.5%	61.0 2.3%	42.0 27.9%	62.3 16.5%	219 5.9%	133
905 5.4%	3.5 7.6%	50.3 2.5%	44.4 25.6%	32.6 26.6%	126 13.0%	269 17.7%
730 6.6%	3.9 7.3%	51.8 5.2%	—	12.9 59.5%	169 15.3%	398 72%
200	2.66	5.0	40	18.3	150	100

and carrying out the chemical analyses; and to the Research Institute of the Hungarian Aluminium Corporation for the X-ray diffraction analyses.

REFERENCES

- BÁRDOSY, GY (1977): Karsztbauxitok. Akad. Kiadó, Budapest (in Hungarian).
- GLADKOVSKI, A. K., GUTKIN, E. S. (1960): O mineralah obrazovavsihsia pri vivetrivanii boksitov Severouralskovo basseina. Trudi Sverdlov. gor. inst.-ta, vipusk 35, (in Russian).
- KOMLÓSSY, GY. (1976): Mineralogie, geochemie et genétique des bauxites du Vietnam du Nord. Acta Geol. Acad. Hung., 20.
- MINDSZENTY, A. (1976): On the structure and texture of some diasporites. Travaux de l'ICSOPA, No 13.
- MINDSZENTY, A. (1979): Contribution to mineralogy of the Lang Son bauxites (North Vietnam). General Geol. Review, No 13. (in Hungarian, English abstr.).
- SHAROVA, A. K., GLAZUNOVA, Z. F. (1966): Mineralogiceski sostav triasovih boksitov Vietnama. Genezis Boksitov. Izd. vo Nauka, USSR. (in Russian)
- TSHEBOTARIEV, M. B., BUI PHU MINH (1961): Severo Vietnamski boksitonosni raion. Sovjetskaia Geologia, No 6. (in Russian)

ON THE CRYSTAL STRUCTURE OF MÁTRAIT

by

T. WEISZBURG, GY. A. LOVAS

Department of Mineralogy, Eötvös Loránd University

(Received: 15th March, 1982)

SUMMARY

A new natural ZnS modification, named mátrait, different from sphalerite and wurtzite was described by S. KOCH (1958). On the basis of X-ray oscillation photographs K. SASVÁRI (1958) suggested that its structure is similar to that of the known synthetic 3R modification. The results of the present study, carried out on the original material, indicate that the mátrait has an orthorhombic structure with space group Pbcn and cell dimensions of $a_0 = 1.814$ nm, $b_0 = 1.756$ nm, $c_0 = 0.514$ nm, $Z = 40$. Since there are strong indications of fairly frequent presence of lattice defects in mátrait, more complete structural data can be expected from future TEM examinations.

Introduction

In the course of a systematic mineralogical study of a hydrothermal Pb—Zn ore deposit in Gyöngyösoroszi (MÁTRA Mts., N-Hungary), S. KOCH (1958) found a new ZnS mineral which proved to be different from sphalerite and wurtzite both in morphology and optical properties. This new mineral was named after the mountain where the mine of the occurrence was located. X-ray single crystal photographs of the material were taken by K. SASVÁRI (1958) using a 114.6 mm oscillation camera. On the basis of these patterns he identified its structure with that of a synthetic ZnS modification described by BUCK and STROCK (1955). As the experimental techniques have become more sophisticated since the time of this early study, a re-examination of the mátrait structure was undertaken. The original material was kindly provided by Prof. S. KOCH.

Experimental

Using S. KOCH's (1958) photographs, mátrait crystals could be readily identified in the original material which is in fact a mixture of sphalerite, wurtzite and mátrait. A stereo—microscope was used for selecting mátrait for further examinations. None of the examined mátrait crystallites in the grain size range optimum for X-ray single crystal measurements proved to be true single crystals. They are crystal clusters of two or more members. The best available choice was a crystal of $0.2 \times 0.2 \times 0.8$ mm in size on which curved crystal faces parallel to the direction of its elongation were recog-

nizable. Later it turned out that the elongated form was a result of an oriented clustering of three or four smaller crystal lamellae.

The density of mátrait was determined by the floatation method using a mixture of thallium phormiate and malonate and water. Because of the very small grain size and the relatively viscous liquid only limited precision could be expected, $d_0 = 3.97(2) \text{ gcm}^{-3}$.

The X-ray oscillation photographs (Fig. 1.) were taken around the axis of elongation using $3 \pm 10^\circ$ oscillation range, by a STOE Weissenberg camera. The Ni-filtered Cu $K_\alpha/\lambda = 0.15418 \text{ nm}$ radiation used for the measurements was provided by a SIEMENS K4 generator. The oscillation pattern showed that the directions of elongation is a true crystallographic direction with length of 0.514 nm. The minor-symmetric spot pattern indicated that this axis is orthogonal. It was labelled as c^* axis.

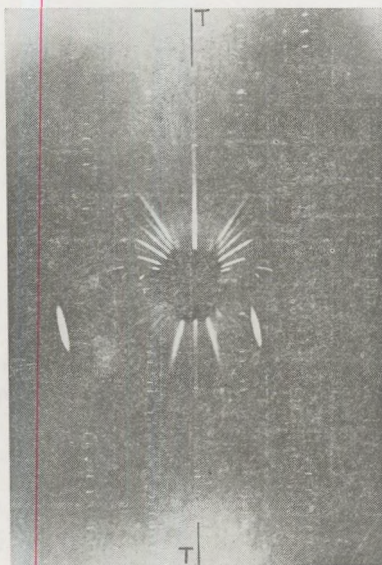


Fig. 1.

On the zero-layer ($hk0$) Weissenberg photograph (Fig. 2) the T_1 and T_2 axes' choice is quite obvious, their angular distance is 90° . From the analysis of extinctions on upper-layer Weissenberg photographs it turned out that every second axial spot is in extinction on the zero-layer. So, using the $T_1 = a^*$ and $T_2 = b^*$ labelling, the axial systematic absences are: $h00h = 2n+1$, $0k0k = 2n+1$. Since the a^* and b^* axes proved to be orthogonal, the structure is orthorhombic with unit cell dimensions of $a_0 = 1.814 \text{ nm}$, $b_0 = 1.756 \text{ nm}$, $c_0 = 0.514 \text{ nm}$.

Among the non-axial reflections further systematic absences could be recognized. On the first layer ($hk1$) Weissenberg photograph (Fig. 3.) the $h01$ reflections are totally absent and there is a $k = 2n+1$ absence in the

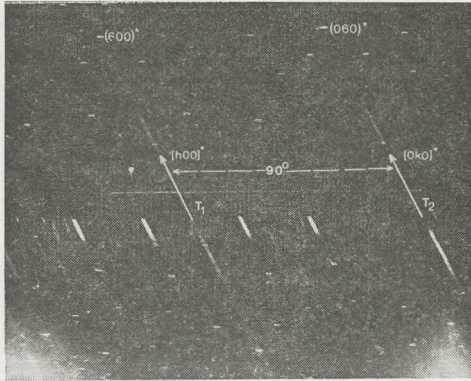


Fig. 2.

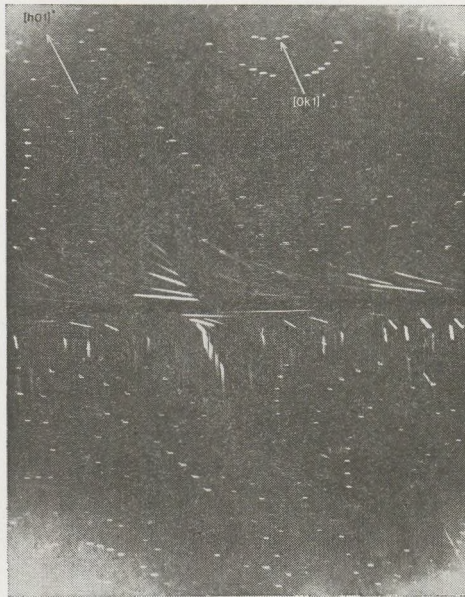
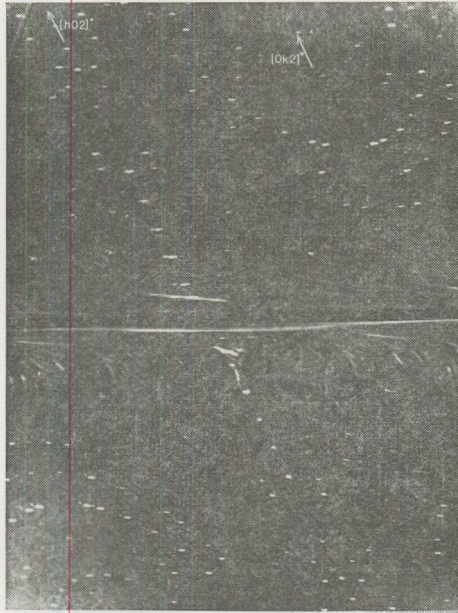
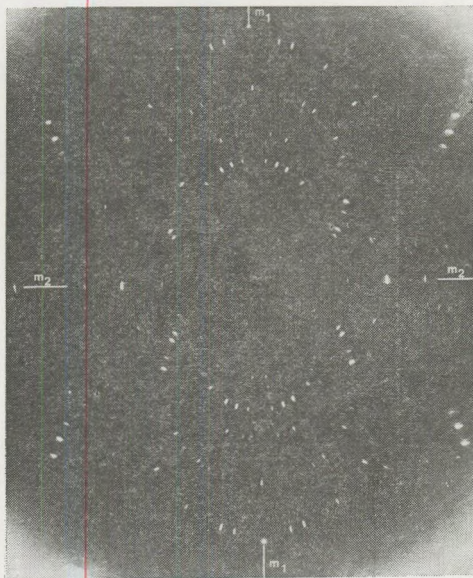


Fig. 3.

$0k1$ reflections. On the second $(hk2)$ layer (Fig. 4.) only a $k = 2n + 1$ extinction could be recognized in the $0k2$ reflections. No systematic absences could be observed in the general (hkl) reflections, which indicates a primitive unit cell.

For further study the crystal was transferred to a HUEBER precession camera, retaining the same rotation orientation that was used for oscillation and Weissenberg examinations and setting b^* as precession axis.

*Fig. 4.**Fig. 5.*

On the Laue photograph along the b^* axis (Fig. 5.) two two-fold symmetries perpendicular to each other are shown. On the $h01$ precession photograph (Fig. 6.) two systematic extinctions could be recognized; in $h00$ the $h = 2n+1$ while in $h01$ the $l = 2n+1$. In addition to these a $h = 2n+1$ systematic weakening is characteristic for the whole $h01$ reflection set.

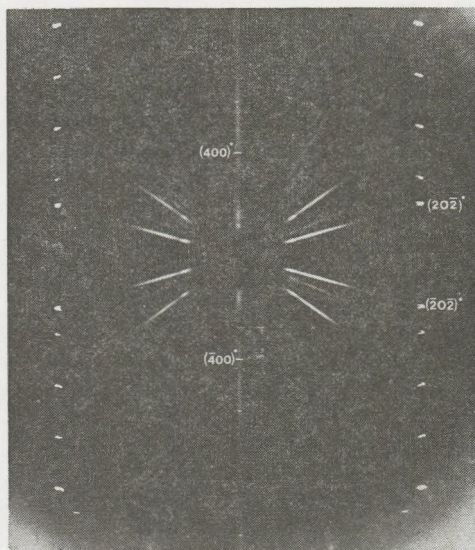


Fig. 6.

Discussion

An orthogonal unit cell with dimensions of $a_0 = 1.814$ nm, $b_0 = 1.756$ nm, $c_0 = 0.514$ nm is the simplest that could be chosen from the measured reflection set. It is not equivalent to any of the ZnS modifications known to us, and it does not seem to be a transformation of any of the known basic structures. The generalized systematic absences clearly indicate that the space group is $Pbcn$ (No. 60). For calculation of the unit cell content a chemical analysis was made by É. KLIVÁNYI which showed besides Zn and S no other substitution but some 5% Fe. Since the difference between the molecular weight calculated from the chemical analysis (96.89) and that of pure ZnS (97.43) is negligible, the latter one was used for further purposes. Using the measured unit cell volume, d_0 and Mw, the unit cell content is $Z = 40$ formula weight. Though it was impossible to collect a reliable data set for complete structure determination because of the poor quality of the crystal, there are some indications of the atomic arrangement. The crystal data indicate 5 formula weight in the asymmetric unit. The systematic weakening of $h = 2n+1$ in $h01$ however suggests that there might be some atoms in special positions as well.

Conclusions

The results of the present study on the crystal structure of mátrait described by Koch (1958) does not support the earlier crystallographic classification of mátrait as $\text{ZnS} - 3\text{R}$.

An orthorhombic unit cell was determined with dimensions of $a_0 = 1.814$ nm, $b_0 = 1.756$ nm, $c_0 = 514$ nm. According to the systematic absences its space group is Pbcn (No. 60). The measured density is $d_0 = 3.97(2)$ g/cm³ and the unit cell content is $Z = 40$.

The special irregularities on the single crystal diffraction patterns and some preliminary TEM examinations indicate that the mátrait has characteristic real structural features. The complex description of the mátrait structure can be expected only from a detailed TEM study in the near future.

Acknowledgement

The authors are grateful for the possibility of using the original material collected by Professor S. KOCH. Special thanks are due to Professor J. KISS for initiating this study and for his continuous interest.

REFERENCES

- BUCK, C. C. and STROCK, L. W. (1955): Trimorphism of zincsulfide. *Amer. Min.* 40. p. 192.
KOCH, S. (1958): The associated occurrence of three ZnS modifications in Gyöngyösorszi. *Acta Min. Petr. Tom. XI.* p. 11-22.
SASVÁRI, K. (1958): ZnS mineral with ZnS - 3R Crystal Structure. *Acta Min. Petr. Tom. XI.* p. 23.

THE STRUCTURE OF A "WAD" SAMPLE FROM DOGNACEA (RUMANIA)

by

I. DÓDONY and T. WEISZBURG

Department of Mineralogy Eötvös L. University

H-1088 Budapest, Múzeum krt. 4/a. Hungary

(Received: 15th March, 1982)

ABSTRACT

The definition of the mineralogical and crystallographic data of fine-grained Mn-O-OH-R (R=Ba, K H₂O, etc.) minerals are uncertain in many cases (as it seems e.g. from the confusion in the names of these minerals).

A "wad" from Dognacea (Rumania) was examined by X-ray and electron diffraction and direct lattice imaging techniques (4.6 Å point-to-point resolution).

The structural data of BURSILL et al. (1979) gave a good starting point.

In the "wad's" powder diffraction pattern there were only a small number of reflections, all of which were broad. They agreed best with the data of todorokite.

In the low magnification (25-50 000 \times) electron micrographs platy and elongated grains of μm size can be seen, where the planes are perpendicular to (010) pyrolusite.

On the selected-area electron diffraction patterns of the plates continuous diffraction lines were found superimposed on the h0l spot patterns.

Some grains showed continuous diffraction in only one direction [100]*, however the rest diffracted continuously in 2 or 3 directions, in accordance with the equivalent directions [101]*, at an angle of cca. 60°.

The interpretation of these streaks was possible only by the analysis of the direct lattice images.

The grains showing continuous diffraction in the a^* direction are of a random "mixture" of pyrolusite, ramsdellite, hollandite, psilomelane and other unnamed structures. The "mixture" is meant on the unit cell level.

The grains showing continuous diffraction in more than one direction are, to our present knowledge, of a new structural form. The random mixture (by a_0) in the sample investigated shows a "sagenite"-type network on the unit cell level.

Introduction

Recent studies of certain members of Mn-oxide minerals by electron diffraction and high resolution electron microscopy have confirmed that this group is an isostructural series (WADSLEY 1964, BURSILL 1979/a). The general formula is $A_{2-y}B_{8-z}X_{16}$ (BYSTRÖM & BYSTRÖM 1950), where $A = \text{Ba}^{2+}, \text{Pb}^{2+}, \text{K}^+, \text{Cs}^+, \text{Rb}^+, \text{NH}_4^+$, $B = \text{Mn}^{2+}, \text{Mn}^{4+}, \text{Fe}^{3+}$, $X = \text{O}^{2-}, (\text{OH})$. The interrelations of these crystal structural types have been discussed theoretically, too (BURSILL 1979/b). Experimental growth of these crystals under hydrothermal conditions was carried out by GIOVANNOLI and STÄHLI (1970). Both X-ray and transmission electron microscopy (TEM) investigations have been made mainly from high-temperature synthesized phases.

The present paper is part of a systematic mineralogical study of Mn-oxides of the Carpathian Basin. Structural details, new structural forms and twinings are described here all on the unit cell level. The methods used in completing this work were the following: X-ray powder diffraction, TEM, selected area electron diffraction (SAED), energy dispersive X-ray spectrometry (EDS).

Material and Techniques

The sample originated from Dognacea, Rumania (Collection of Mineralogical Dept. of Eötvös L. University, Budapest). Its chemical composition was proved to be homogeneous by microprobe and EDS analyses made by JEOL JSM-35 scanning electron microscope combined with a LINK spectrometer.

X-ray powder diffraction analysis was carried out by using a SIEMENS D-500 diffractometer.

Of all the methods used it was the TEM that proved to be the most effective. The observations were made by a JEM-100CX type microscope equipped with a tilt ($\pm 60^\circ$)-rotation side-entry goniometer stage, and by a JEOL JEM-100 U microscope, using an accelerating voltage of 100 KV. The highest electron optical magnification was 250.000 x. The best point - to - point resolution of the 100CX microscope was 4.6 Å.

The sample was gently ground under aethyl-alcohol in an agate mortar, and it was set on a holey carbon supporting film. The thin crystal flakes overlapping the holes were tilted mainly into the [010] projection (all crystallographical directions and planes are related to pyrolusite). The micrographs were taken using the axial illumination and the 2.7 Å⁻¹ objective aperture. The high resolution images were interpreted intuitively. A SAED pattern was made to each measured crystal.

Results

The X-ray powder diffraction pattern of the sample is shown by Fig. 1. The $d_{(hkl)}$ set and the distribution of the intensities on the pattern resemble strongly that of todorokite. The broadening of the peaks and the comparatively high baseline indicate very small coherently diffracting volumes caused by either small grain size or structural disorder, may be both. This question could be answered by interpreting the electron micrographs.

The chemical constituents of a crystal shown by Fig. 2/a were assayed semi-quantitatively by the EDS spectrum (Fig. 2/b). Ca, Zn, Cu are considered to be unusual "A"-type cations of the structure. In addition there are also Ba, Sr and K in this position. Ti is a replacement of Mn.

On the low magnification TEM micrographs the sample appears as thin laths and plates parallel to (010) and usually elongated along the c axis up to some μm .

When the [010] direction of the elongated crystals was oriented parallel to the electron beam, a SAED pattern like shown by Fig. 3. was pro-

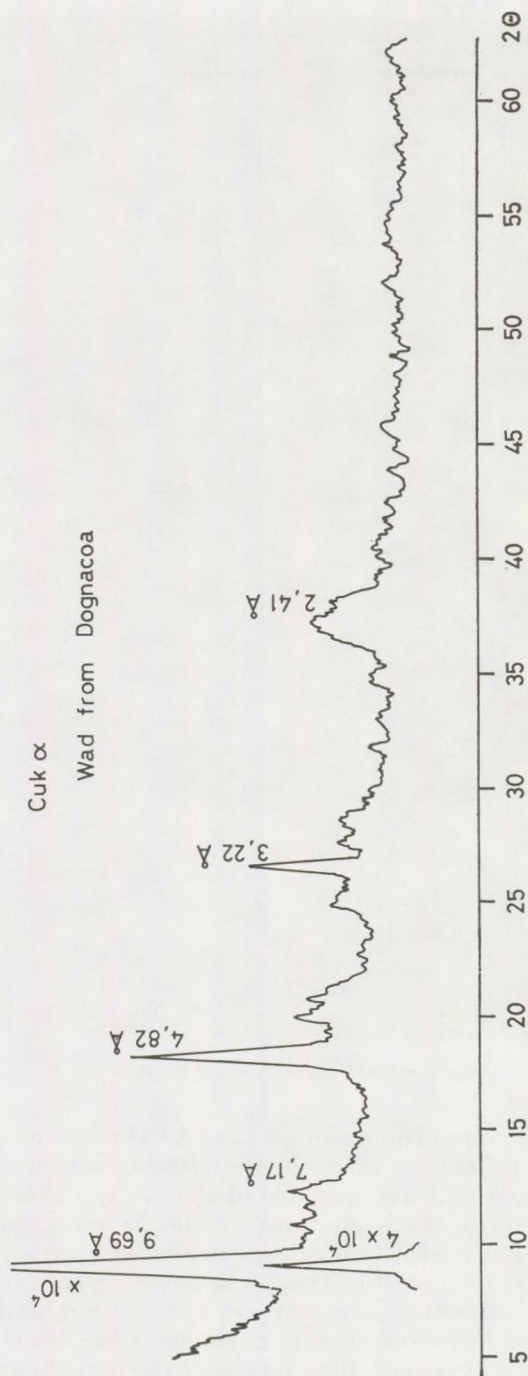


Fig. 1. X-ray powder diffraction pattern of the sample



Fig. 2/a. SEM picture of the sample

duced. There is a common feature in all the SAED patterns of the lath-form crystals: the diffraction effect in the $[100]$ direction is continuous. This fact corresponds with the features of the X-ray diffraction pattern. The interpretation of these streaks is rather easy by using the high resolution micrographs. Each lath-form crystal exhibited a structural disorder of the kind depicted by Fig. 3/b. This phenomenon gives important clues to the relationship between the structures of pyrolusite-rams dellite-hollandite-psilomelane and other (unnamed) members of the Mn-O-(OH) group. The distances between two dark lines represent the periodicity of the high-

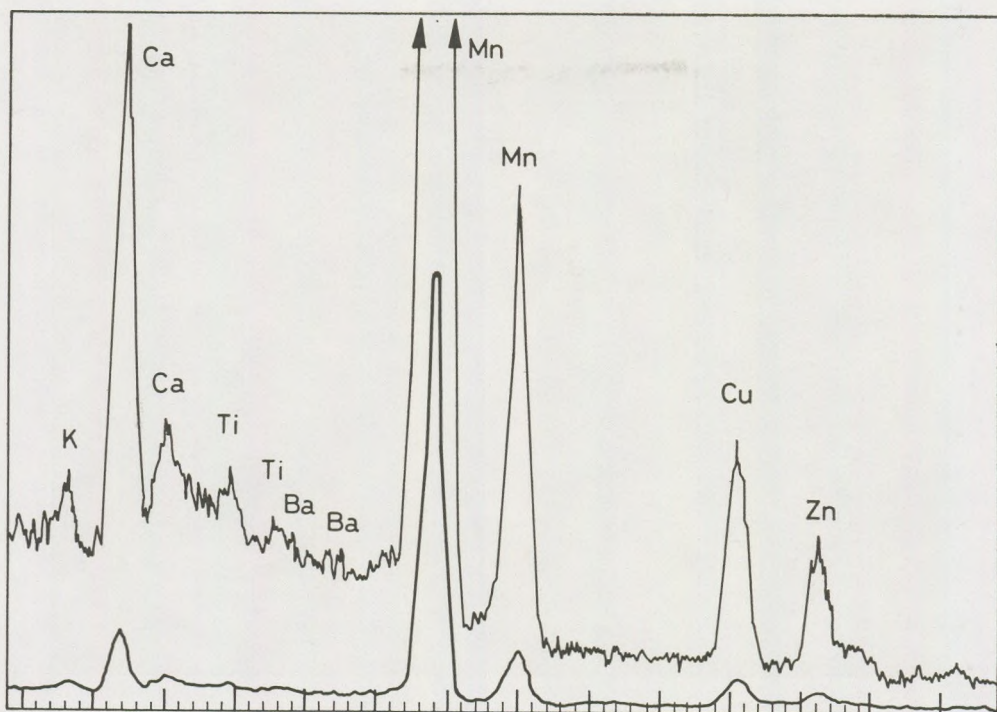


Fig. 2/b. EDS spectrum of the crystals shown on Fig. 2/a.
(The two curves were registered at different sensitivities)

density lattice planes of the above structures as follows: $(020)_{\text{ramsdellite}}$, $(200) (100)_{\text{hollandite}}$, $(100) (001)_{\text{psilomelane}}$. The $d_{(200)}$ of pyrolusite is invisible because this distance is smaller than even the highest resolution of our microscopes. Within a few nm-es of the image the distributions and periodicity of the above lattice planes can be visually examined. It can be seen that all the lathy crystals consist of a random mixture of unit-cell-wide Mn-oxide lamellae. Those regions which show a lattice plane distance greater than 13.5 \AA (001) psilomelane have not yet been identified crystallographically and are mostly unnamed. The connections between the crystallographic directions within these laths are as follows: $[100]_{\text{pyrolusite}}$ parallel to $[010]_{\text{ramsdellite}}$, $[110]_{\text{hollandite}}$, $[100] [001]_{\text{psilomelane}}$, and $[001] [001]_{\text{pyrolusite}}$ parallel to $[001]_{\text{ramsdellite}}$, $[001]_{\text{hollandite}}$ and $[010]_{\text{psilomelane}}$.

Besides the lathy grains about a third of the crystals have the platy habit. Basically they have the same $(h0l)$ SAED patterns, but the streaks run in the three crystallographically near equivalent directions at an angle of 60° . These are $[100]$, $[101]$ $[101]$.

A typical SAED pattern is shown in Fig. 4. The strong reflections in the pattern correspond to the pyrolusite structure, but between these

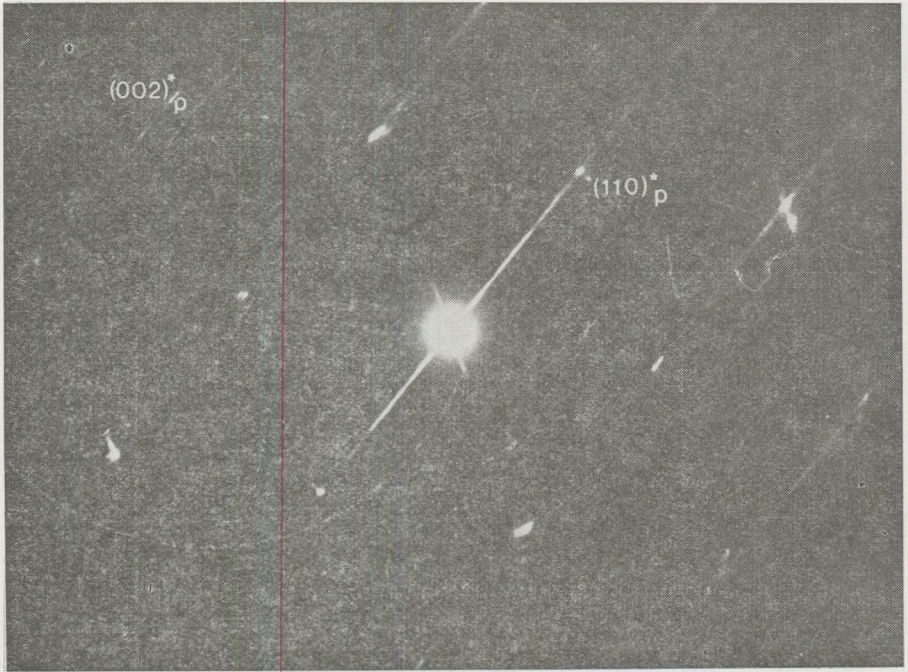


Fig. 3/a. SAED pattern of wad in [010] projection

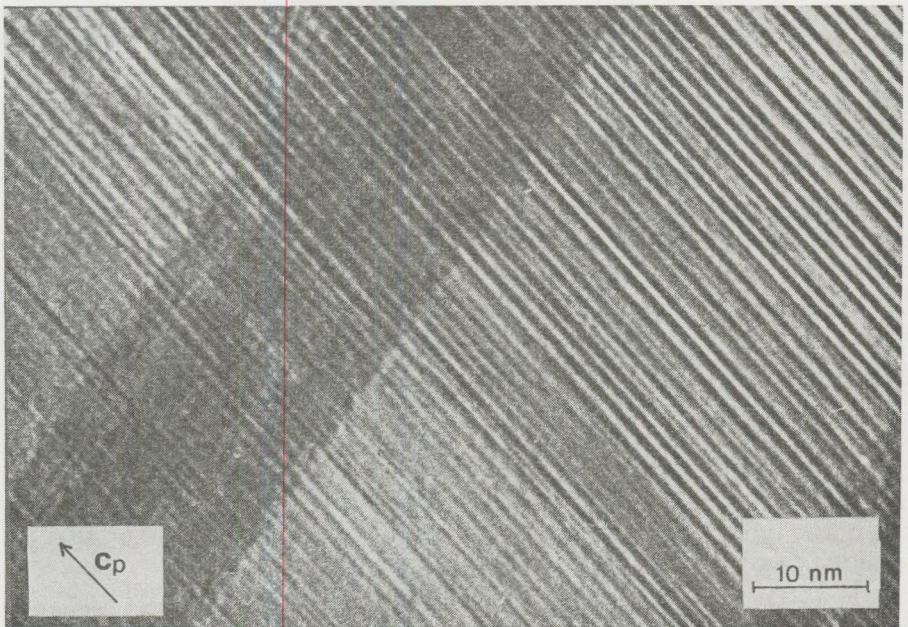


Fig. 3/b. HRTEM image of wad in [010] projection. Diam. of obj. ap. 0.27 nm^{-1}

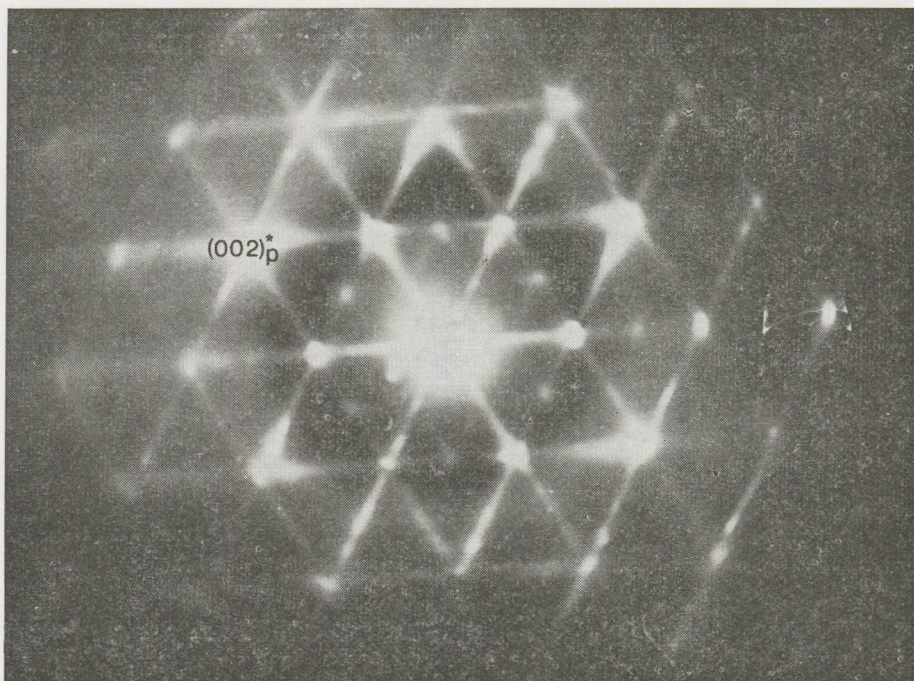


Fig. 4. SAED pattern. A continuous scattering is superimposed on the basic spot pattern in three crystallographic directions
(See extra reflections indicating superstructure)

there are several sets of superstructure reflections. One of these sets consists of the streaks mentioned above.

Another set of superstructure reflections is marked by weak spots. These reflections are characterized by fraction indices.

On this discussed real structure of the lath-shaped grains an additional feature of disorder is superimposed. It is a twinning on the unit cell level, characterized in our projection by sagenite-law. It is shown at low magnification by Fig. 5. that the elements of sagenite-network are in the nm range.

The structural tunnels between the high-density planes (filled by A-type cations) appear in two forms. One is a parallel system within the " a_0 " thickness and the successive " a_0 " layers are rotated around the $[100]$ axis by 60° . This means essentially a twin connection, between the consecutive layers where the intergrowing plane is (100) and the twin axis is $[100]$ (Fig. 6.)

The other form is where the tunnels are in different (by 60°) orientations with in the same " a_0 " thickness. In this case these channels form two-dimensional continuous sheet system. This is represented by Fig. 7. and Fig. 8.

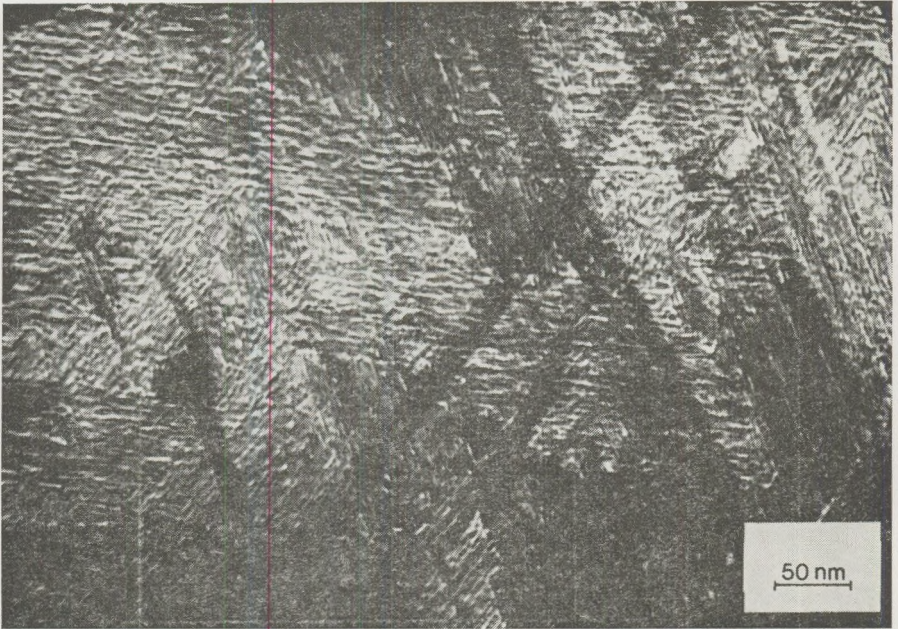


Fig. 5. Low magnification picture of a sagenite type network with size in the nm range

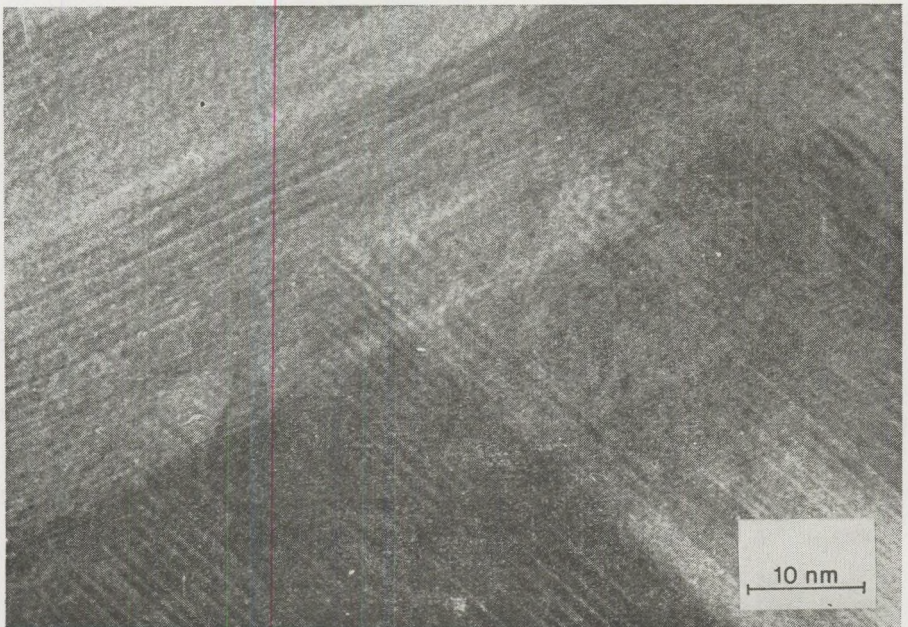


Fig. 6. HRTEM image showing a (100) twin connection between adjacent layers

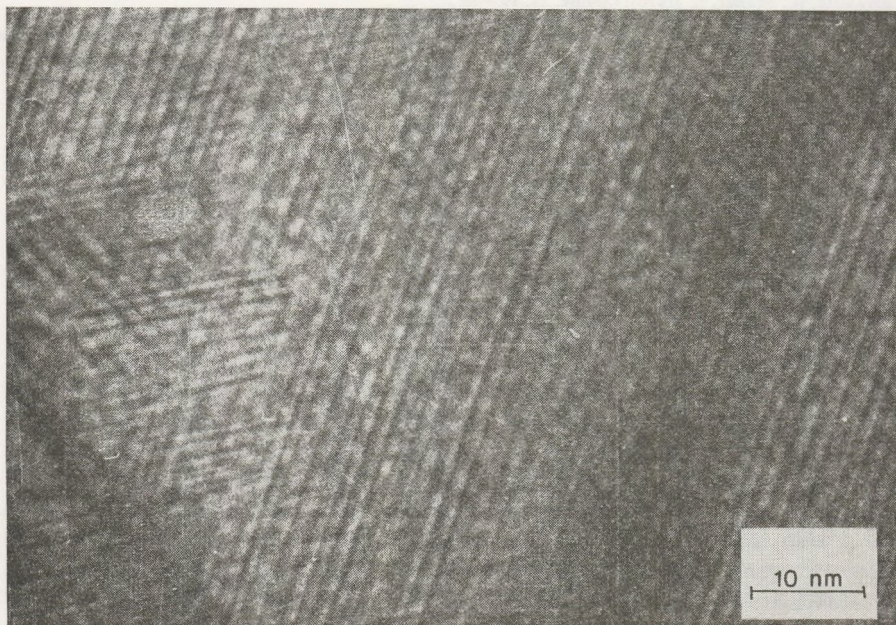
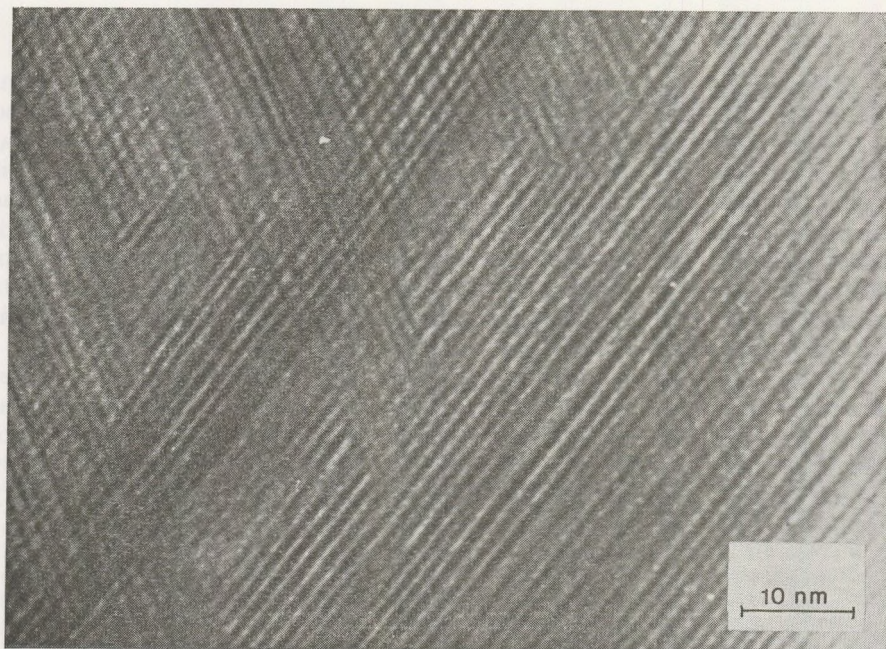


Fig. 7-8. HRTEM images showing special structural patterns where channels in the structure form a two-dimensional continuous network within a single unit-cell thickness

Conclusions

The "wad" can be described neither as a single mineral nor as a composition of minerals in the traditional sense. As a result it cannot be studied by conventional mineralogical methods. Only the HRTEM technique, capable of imaging the unit cells of simultaneously present minerals and their various twinning structures, can give a lead to its determination. The diffraction phenomena found in was are not unique. The todorokite, described in considerable quantities from deep-sea nodules, looks very similar in TEM and its electron diffraction pattern is also alike. (STRACZEK et al. 1960. Since we had no material to compare the "wad" with, it is only a hypothesis that the features of todorokite are the ones mentioned above.

It can be pointed out that minerals with todorokite-like powder patterns, regardless whether they are of hydrothermal or other continental origin or come from deep-sea nodules, always contain a considerable amount of Cu, Zn (Co, Ni etc.). It may be that the described structural model provides special possibilities for these metals to build into it. To verify these theories, further investigations are necessary.

REFERENCES

- BURSILL, L. A. (1979a): *Acta Cryst.* A35, 449-458.
BURSILL, L. A. (1979b): *Acta Cryst.* B35, 530-538.
BYSTRÖM, A., BYSTRÖM, M. A. (1950): *Acta Cryst.* 3, 146-154.
GIOVANOLI, R., STÄHLI, E. (1970): *Chimia*, 24, 49-88.
STRACZEK, J. A., HOREN, A., ROSS, M., WARSHAW, Ch. M. (1960): *Amer. Min.* 45, 1174-1184.
WADSLLEY, A. D. (1964): *Non-Stoichiometric Compounds*. Edited by L. Mendelsohn, p. 111. Academic Press, New York.

MINERALOGICAL STUDY ON VATERITE AND OTHER RELATED MINERALS OF THERMAL WATER ORIGIN

by

I. DÓDONY* and A. BALOG**

*Dept. of Mineralogy; **Dept. of Petrology and Geochemistry, Eötvös L. Univ. Budapest, Hungary

(Received: 25th September, 1982)

SUMMARY

Mineralogical study was conducted on a scale sample from the tubing of the thermal water well of Táska (S. W. Hungary). Simultaneous occurrence of different CaCO_3 polymorphs was recognized. Optical-microscopical and X-ray diffraction studies indicated the presence of calcite and aragonite. The reason for an unusual calcite/aragonite shift was suggested to be a change in the concentration of minor chemical constituents (like Sr and Ba) during precipitation. Elektron-microscopical investigations were initiated to find structural explanation for this phenomenon. Besides calcite and aragonite the TEM study revealed the presence of vaterite too. As a result of careful interpretation of the micrographs, a new mineral $(\text{Ca}_3\text{Sr}/\text{CO}_3)_6$ was also recognized. It has a vaterite-like structure and can be regarded as a member of a suggested new mineral series of CaCO_3 - SrCO_3 .

Introduction

The frequent occurrence of thermal waters in Hungary is connected with two different sedimentary rock formations; the porous neogenic and the cracked, fissured mezozoic carbonates. In about 10 percent of the wells solid precipitations in the upper region of the tubing cause serious problems. The main reasons for scale precipitations are: change in pressure, gas-water interactions, changes in temperature and chemistry of the water. It is likely that scale formation is affected also by the total amount of dissolved salts. Scales from thermal well tubings show great variability and have often different morphology depending upon the site of precipitation (e.g. inside the tubing, at the outlet or some distance away from there.). Scales from inside the tubing are usually compact, hard and durable while those from other places have often loose and porous texture. The rate of scale precipitation varies in a wide range. There are wells where the daily precipitation is 1.2 mm in thickness while in other wells such an accumulation takes several months. Skeleton-crystals indicating fast crystallisation are abundant in these scales. Chemical analyses show that they consist of pure monophase CaCO_3 in almost every case. As regards structure, however, they are far from being homogeneous: several polymorphic modifications of CaCO_3 can be recognized in them.

The crystallographic study of the polymorphs of CaCO_3 started as early as the beginnings of X-ray crystallography, with the structure determination of Calcite (W. L. BRAGG, 1914). The structure of Vaterite, the

third polymorph of CaCO_3 , was determined by WYCKOFF and MERWIN (1951) and later refined by McCONNELL and LONG (1959) and KOMHI (1963). Vaterite is hexagonal with unit cell dimensions of

$$\begin{aligned} a &= 7.135 \text{ \AA} & c &= 8.524 \text{ \AA} \\ Z &= 6 \\ \text{pseudo cell} \\ a' &= a/3 & c' &= c \\ Z' &= 2 \\ \text{Int. max. } h-k &= 3n \end{aligned}$$

These data were confirmed by electron-diffraction studies as well. On the basis of cell dimensions and optical properties Vaterite was classified as a member of the Bastnäsité-Synchisite series. There are also a number of CaCO_3 modifications, called Vaterite, but having a structure more or less different from what was cited above. The details of the structure of these modifications, however, are not yet known.

In 1962 the Japanese hydrologist Y. Kitano published a study on the formation of different polymorphic modifications of CaCO_3 . He has pointed out that there is no Vaterite in springwater precipitations because even if it did form it would transform immediately into Calcite or Aragonite. He explains it with the ample supply of CO_2 available in these solutions, and with the presence of ions inhibiting the formation of Vaterite.

The abundance of CaCO_3 both in the regional sense and in various geological formations gives the reason for its more detailed crystallographic and mineralogical study. The present study was carried out on solid precipitations from a thermal water well in Táska, Somogy county, (SW-Hungary).

Geological and hydrogeological description of the Táska – 1 well

The borehole Táska – 1 was drilled as part of an exploration programme for new hydrocarbon resources. It was located onto an upthrown-block of mezozoic paleozoic formations. This block belongs to a relatively uplifted zone striking S of the Tab – Karád – Nikla – Iharosberény line. Towards S the mezozoic-paleozoic complex is faulted down to greater depths (Fig. 1.) The hole turned out to be unproductive for hydrocarbons but has been producing thermal water of 80°C at a rate of 1400 l/min ever since (the water contains NaCl and HCO_3^-). The scale precipitation in this well is not too heavy and has a high organic matter content.

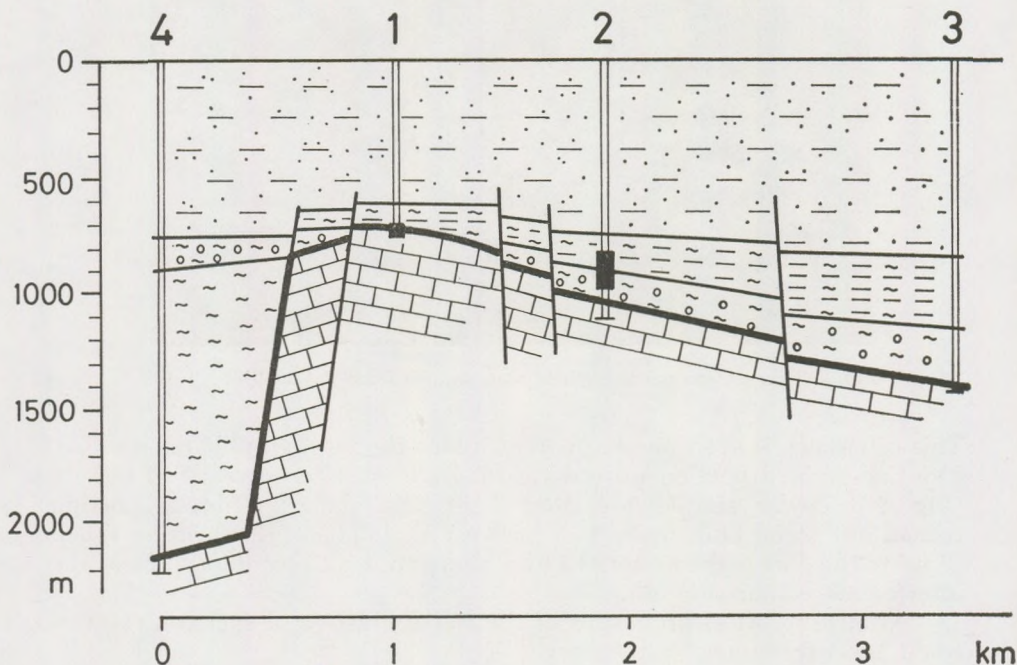
Visual and optical-microscopic study

Scale precipitations from the tubing have a conspicuously compact texture as compared to the loose, porous samples collected from other locations. Two different zones can be distinguished in the compact sample even by visual examination. The upper thinner layer has a finer grain size. The zone beneath is thicker and has fibrous structure with a silky lustre.

É

TÁSKA

D



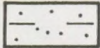
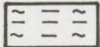
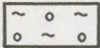
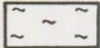
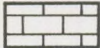

-  U. Pannonian sánd, sandstone, clay, claymarl
-  L. Pannonian claymarl, marl
-  Miocene conglomerate, marl, limestone
-  Oligocene claymarl
-  Triassic limestone
-  fault

Fig. 1. Geological surrounding of borehole Táaska

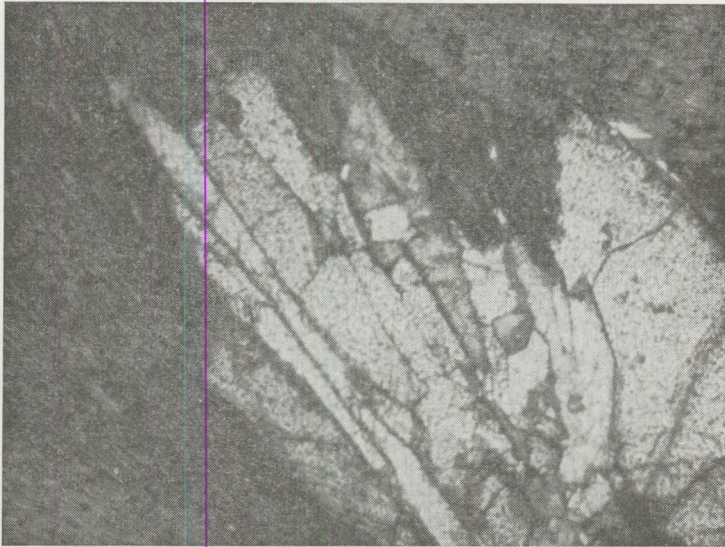


Fig. 2. Thin section micrograph of scale sample from Táska + N, N=40x

This difference is even more apparent under the petrographic-microscope. The fine-grained portion proved to consist of skeleton-crystals of Calcite (Fig. 2.). Under simple polarised light the radially fibrous portion turned out to be built up of rust-brown radial spherulitic clusters. When crossing the Nicols the material's own very intensive colour suppresses the interference colour (Fig. 2.).

No other optical properties of the radial clusters of skeleton-crystals could be determined.

Chemical analysis

The chemical analysis was carried out in the Chemical Laboratory of the Hungarian Geological Institute (MÁFI).

insoluble part	0.02%
TiO ₂	—
Al ₂ O ₃	0.07%
Fe ₂ O ₃	0.02%
FeO	0.19%
MgO	0.91%
CaO	54.24%
Na ₂ O	0.28%
K ₂ O	0.02%
—H ₂ O	0.04%
L.O.I.	43.54%
P ₂ O ₅	0.02%

The spectroscopic analysis of the sample was undertaken in the Laboratories of the Department of Petrology and Geochemistry of the L. Eötvös University.

Ni	20 g/t
Mn	600 g/t
Cu	16 g/t
Be	8 g/t
Pb	10 g/t

The Sr and Ba contents of different parts of the sample were determined by flame-photometric method at the same Department. The percentage of Sr in sample T/a is 1.9 while Ba amounts to 0.4%. In the case of sample T/b the Sr content is 2.5%, and that of Ba is 0.1%. The relatively high Sr and Ba content seems to be characteristic for this material. It is 2 to 3 times (in some instances 10-to 20 times) higher than the average Sr and Ba content of carbonatic rocks (Wedepohl). However, the Ca/Sr ratio hardly exceeds the value of 25 whereas the average ratio for carbonatic rocks is 56.

X-ray diffraction and thermal analysis

Sample T/a was identified as Calcite, and sample T/b as Aragonite by X-ray powder diffraction method. Since there were no indications of the presence of any unique Sr or Ba mineral, it is likely that Sr and Ba are involved mainly in cation substitutions.

The DTA curve of sample T/b showed the endothermic reaction at 400–440 °C characteristic of the calcite-aragonite transition. Unlike published studies of similar materials, however, this sample produced a 1 percent weight loss simultaneously with the said phase transition.

Results presented so far indicate that during the process of scale formation after some time and seemingly without any obvious reason the precipitation of calcite was replaced by the formation of aragonite. As there could not be any major change in circumstances during scale formation, a change in concentration of minor chemical constituents is suspected as responsible for this phenomenon.

Chemical analyses indicated that the Sr/Ba ratio is considerably higher in sample T/b than in T/a. Trying to find explanation for this, laser-spectroscopic and electron diffraction studies were initiated.

Laser-spectroscopic study

Interpretation of the spectra proved that the amount of Sr in the calcite bands is considerably smaller than in the aragonite portions. A limit-concentration of Sr can be selected, above which only aragonite, and below which only calcite forms. In the intermediate zone the two may be coexistent. (Fig. 3.)

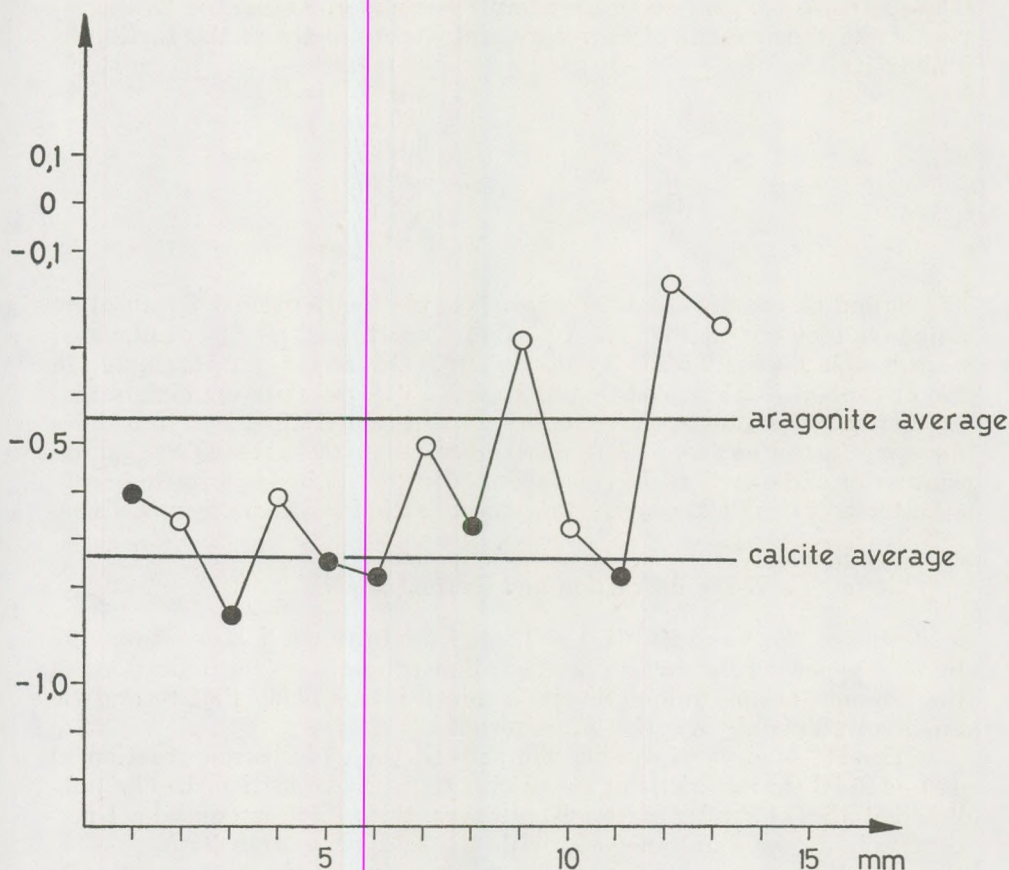


Fig. 3. Laser-spectroscopic Sr/Ca concentrations of the sample from Táska

Electron-microscopic study

The joint occurrence of different modifications of CaCO_3 in the scales was confirmed by TEM methods. The study was carried out with a JEOL JEM 100CX electron-microscope equipped with a side-entry tilt-rotating stage and with a JEM 100U electron-microscope. The sample was ground in an agate mortar under ethanol then thin flakes of it were deposited on a holey carbon supporting film.

The SAED picture of vaterite in $[\bar{1}2\bar{1}0]$ projection is shown on Fig. 4. Its symmetry agrees well with the space group determined for vaterite by KAMHI (1963). The SAED pattern of an unknown mineral (Fig. 5.) shows distinct similarities with those of CaCO_3 polymorphs. As this pattern was taken on the JEM-100U and this microscope has no goniometer stage, only Laue-zone picture could be registered. Comparing the crystallographic



Fig. 4. SAED pattern of vaterite in (1210) projection

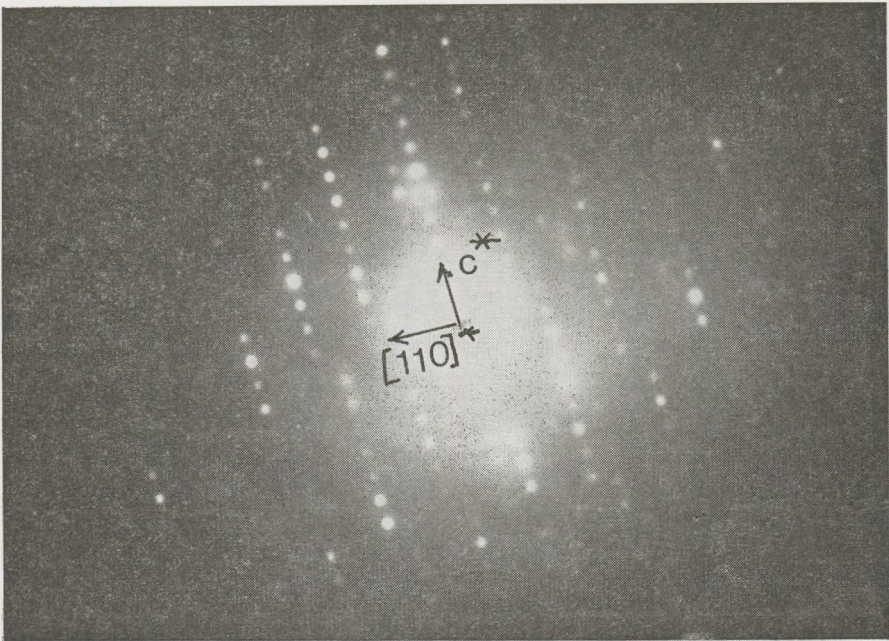


Fig. 5. SAED pattern of the new carbonate phase

parameters of this phase with those of CaCO_3 with space group Pbnm , its unit-cell dimensions can be expressed as:

$$\begin{aligned} a &= 2 \times a_0 \\ b &= b_0 \\ c &= 3/2 c_0 \end{aligned}$$

The (110) and (001) directions of this crystal-grain are almost perpendicular to the direction of the electron-beam. An image of the (001) lattice-planes of the same crystal can be seen on Fig. 6., which indicates that this grain has a faultless single-crystal structure.

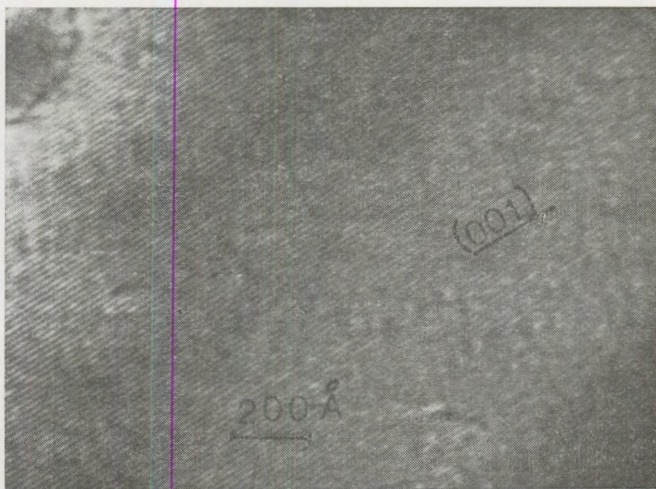


Fig. 6. Lattice image of (001) planes of the same crystal that can be seen on Fig. 4

From the interpretation of the electron-diffraction patterns it turned out that besides the known vaterite a new carbonate structure can be recognized (Figs. 5 and 6.). As its periodicity in "a" and "c" direction can be expressed as multiples of the same periodicities of vaterite (Sg: Pbnm), their structural relation is strongly indicated. The Ca atoms in the orthorhombic vaterite form pseudo-hexagonal planes perpendicular to the c-axis at $z = 0$ and $z = 1/2$. In this new mineral every third of these planes are identical, while within each layer the translations of the Ca atoms are $2 \times a_0$. This alteration in the translational values can be assigned to the Ca/Sr substitution. If 1/6 of the cations in the orthorhombic vaterite structure is substituted, one of their possible orderings can produce a SAED pattern like the one shown on Fig. 5. Since the amount of different substituting cations in the basic vaterite structure may vary and so may their ordering, the existence of several new vaterite-related minerals can be supposed. The new phase ($\text{Ca}_5\text{Sr}/\text{CO}_3/6$) recognized in a scale sample

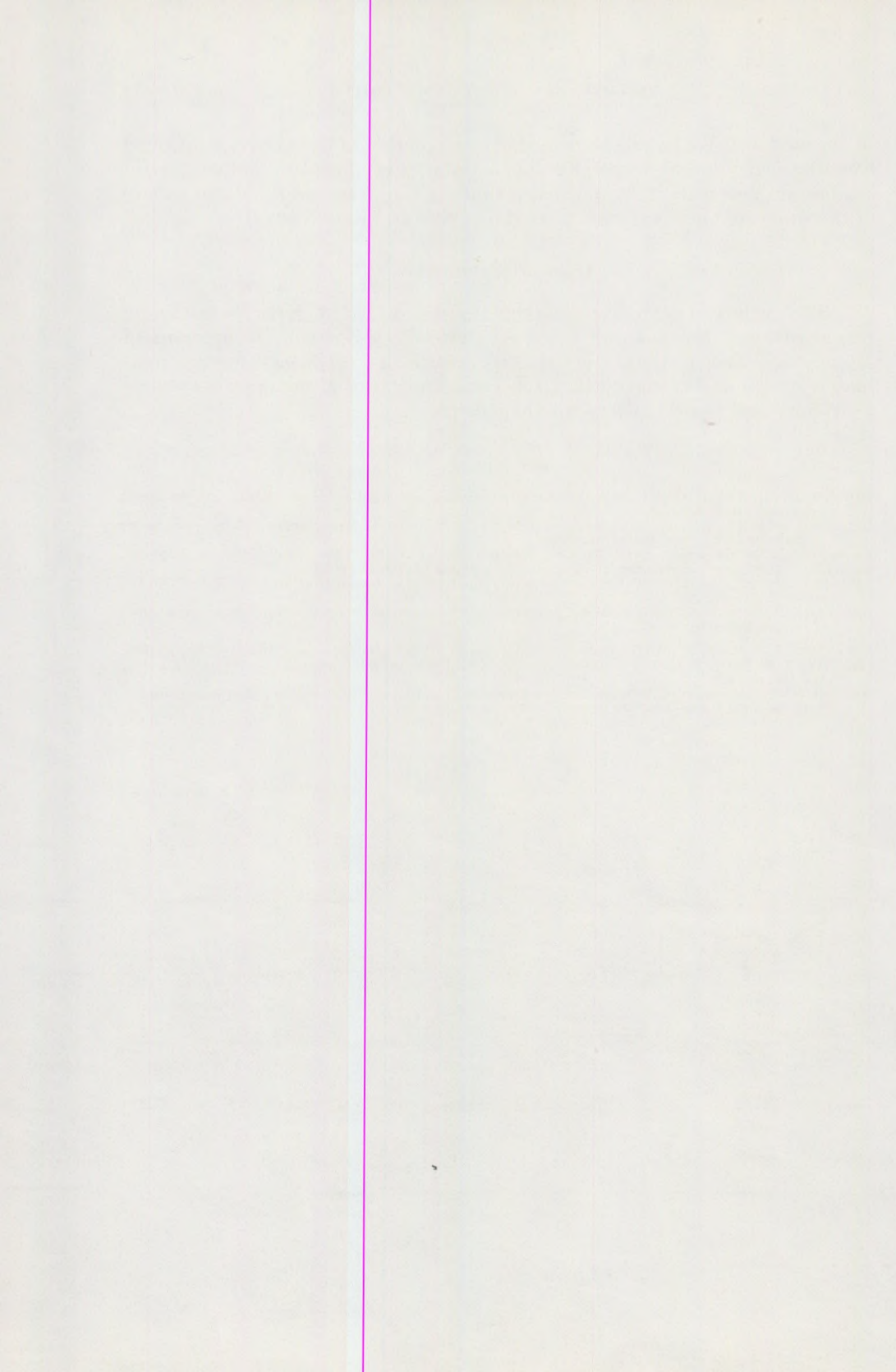
of thermal well Táska can be regarded as a member of the above-mentioned hypothetical mineral series. Further crystallographical and mineralogical studies are necessary to gain a more thorough understanding of the nature of the suggested new vaterite-related (Ca, Sr)CO₂ mineral serial.

Acknowledgements

The authors wish to express their thanks to Prof. J. KISS for initiating this study and the possibility to use the facilities of the Department of Mineralogy. Special thanks are due to Prof. K. I. SZTRÓKAY for his invaluable advice and to the staff of the Departments of Mineralogy as well as Petrology and Geochemistry for their help.

REFERENCES

- BALOG, A. (1978): A hazai termálvizek kicsapódási termékeinek mineralógiai-geokémiai vizsgálata — Budapest, manuscript, in Hungarian.
- BALOG, A. (1982): Néhány magyarországi hévíz szilárd kiválási termékeinek ásványtani és geokémiai vizsgálata. — Hidrológiai Közöny. 62., in Hungarian.
- BRAGG, W. L.: The analysis of crystals by X-ray spectrometer. — Proc. Roy. Soc. London, Vol. 89, A, p. 468.
- KAMHI, S. R. (1963): On the Structure of Vaterite, CaCO₃. — Acta Chryst. 16., p. 770.
- KITANO, Y., HOOD, D. W. (1962): Pure Aragonite Synthesis — Journal of Geophysical Research Vol. 67, No 12., pp. 4873.
- BISCHOFF, J. L., FYFE, W. S. (1968): Catalysis, Inhibition, and the calcite-aragonite problem — American Journal of Science Vol. 266., pp. 65.
- MCCONNELL, J. D. C. (1959): Vaterite from Ballycraigy Lerne, Northern Ireland — Min. Mag. Vol. 32., pp. 535.
- SZTRÓKAY, K. I., NAGY, B. (1968): Natürliches Vaterit-Vorkommen im Budaer-Gebirge — Földtani Közöny, Vol. 98., pp. 423.
- NAGY, B. (1979): Mineralogical, petrographic, geochemical and genetic investigations of pulverulent dolomites from the Buda Hills. — Földtani Közöny, Vol. 109, pp. 46–74.



FORMULAS FOR THE DETERMINATION OF EULER ANGLES OF PLAGIOCLASES

by

L. ÖRKÉNYI-BONDOR

MÁFI, Budapest XIV, Népstádion út 14

(Received: 25th October, 1982)

SUMMARY

The anortite-content of plagioclases is determined by the position of crystallographical and optical main vibration directions related to each other, by using an U-stage. Besides the evaluation made with the aid of stereographical projection of migration curves introduced by E. Fedorov and improved by W. Nikitin, M. Reinhard and recently by C. Burri, there is a possibility to determine the anortite-content without representation, too. Using the vector-geometrical evaluation of measurements made by U-stage and with the application of formulas given in this paper, we can obtain the Euler-angles.

Euler angles can be determined not only by stereographic projection reading the Wulf net but also by calculating without drawing. In the following we give the formulas for the determination of the Euler angles type I, II, III, pointing out that using these formulas values shown in the table in the book "Die optische Orientierung der Plagioklase" by C. BURRI, R. PARKER, E. WENK will be obtained.

As far as we know Euler-angle values for low-and high-level plagioclase-members with different anortite content can be found only in this above mentioned book. The practical aim of the formulas given by us is to determine the An% percentage with the help of the table at our disposal or to eliminate the uncertainty in determining the twinning law removing difficulties arising from pseudosymmetry.

The designation in the formulas is as follows:

The axes of the XYZ system of co-ordinates are by order of succession the twin axes of the Roc Tourne, Albite and Carlsbad twin laws.

The axes of the X'Y'Z' system of co-ordinates are by order of succession the a_0 , b_0 and c_0 vectors i.e. the unit vectors of the n_x , n_β , n_γ optical main vibration directions.

Calculation of Euler angles type I

$$\Theta = \arccos(a_0 \cdot Z_0)$$

$$\Psi = \arccos(b_0 \cdot T_0)$$

$$T_0 = \cos(\arccos a_{0x} + 90^\circ) i + \sin(\arccos a_{0x} + 90^\circ) j$$

$$\Phi = \arccos(T_0 \cdot X_0) = 270^\circ - \arccos a_{0x}$$

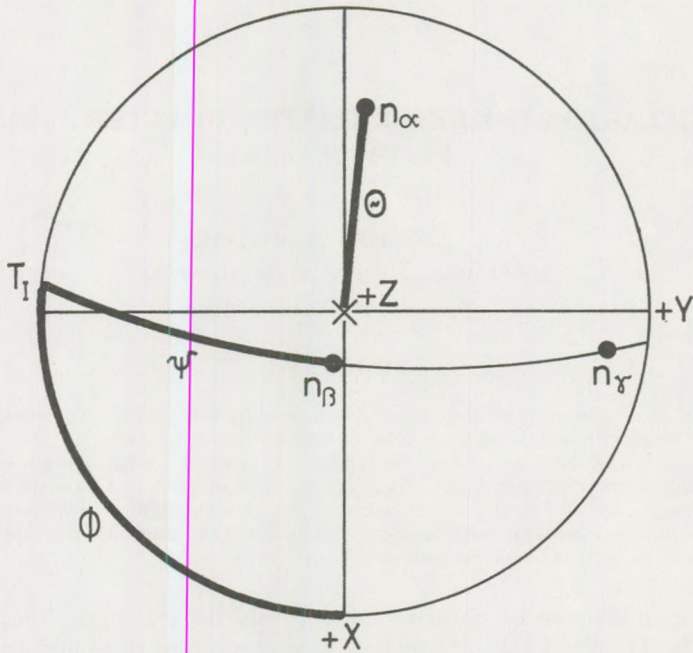


Fig. 1a. Euler angles type I.
An₁₅ High temperature

These formulas are valid without any limitation. As in the case of plagioclases n_x is always in the 3rd quadrant (taking into consideration space above XY plane) these formulas can be used without limitation.

Euler angles type II

$$T = \arccos(b_0 \cdot Z_0)$$

$$L_x = \arccos(a_0 \cdot T_{11_0})$$

$$T_{11_0} = \cos(\arccos b_{0_x} - 90^\circ) i + \sin(\arccos b_{0_x} - 90^\circ) j$$

The last formula is valid only with limitation. If the value of $\arccos b_{0_x}$ is smaller than 90° and larger than 270° , this formula can be used, however if the value of $\arccos b_{0_x}$ is between $90^\circ - 270^\circ$, the following relationship is prevalent.

$$T_{11_0} = \cos(\arccos b_{0_x} - 90^\circ) i + \sin(\arccos b_{0_x} + 90^\circ) j$$

$$R = \arccos(T_{11_0} \cdot X_0)$$

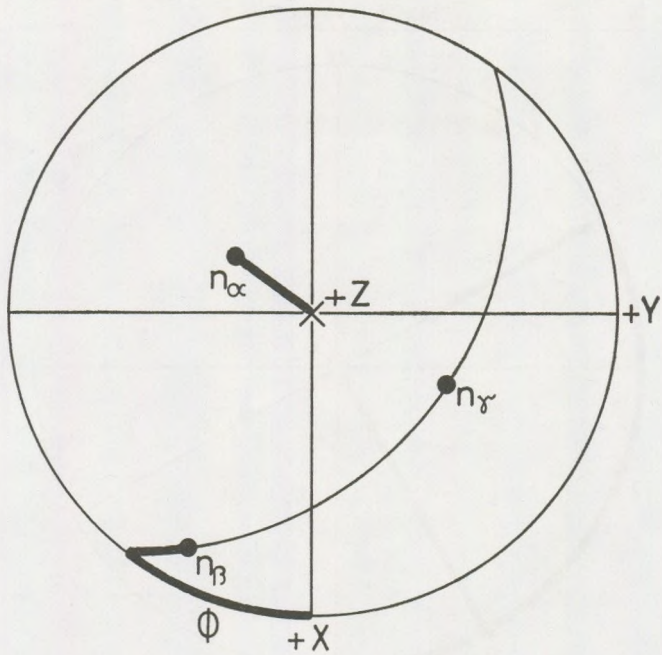


Fig. 1b. Euler angles type II.
 An_{75} High temperature

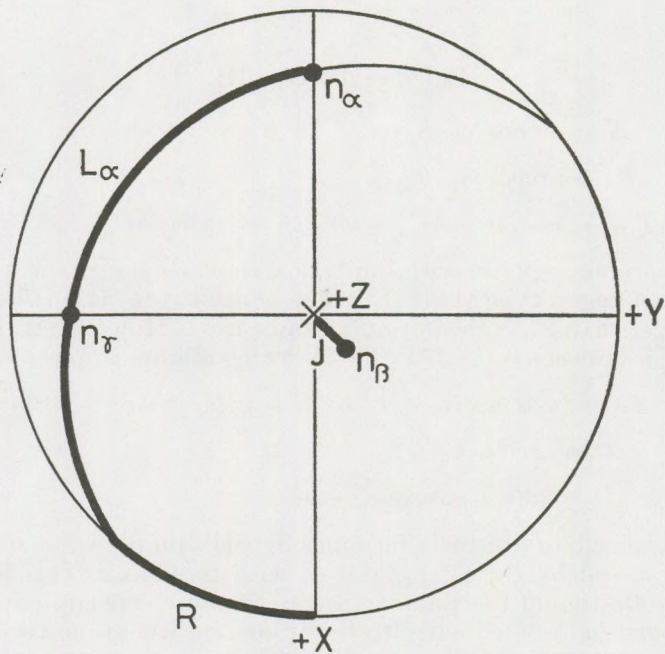


Fig. 2a. Eulerian angles type II.
 An_{10} Low temperature

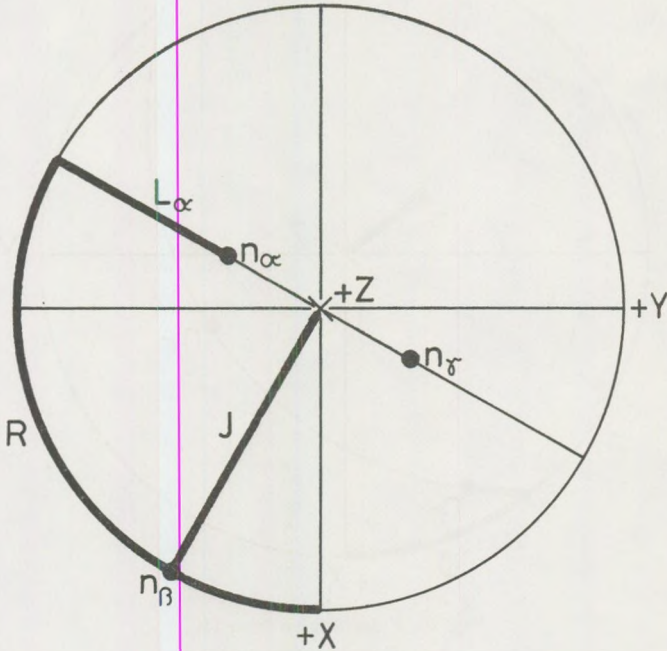


Fig. 2b. Eulerian angles type II.
An₈₀ High temperature

Euler angles type III

$$N = \arccos(c_0 \cdot Z_0)$$

$$K_\alpha = \arccos(a_0 \cdot T_{III_0})$$

$$T_{III_0} = \cos(\arccos C_{0x} - 90^\circ) i + \sin(\arccos C_{0x} - 90^\circ) j$$

This formula is valid with limitation similarly as it is in the case of the Eulerian angles type II. If the value of arc cos b_{0x} is smaller than 90° , or it is larger than 270° , this formula can be used. However, if the value of arc cos b_{0x} is between $90^\circ - 270^\circ$, the following relationship is prevalent.

$$T_{III_0} = \cos(\arccos c_{0x} + 90^\circ) i + \sin(\arccos c_{0x} + 90^\circ) j$$

$$D = \arccos X_0 \cdot T_{III_0}$$

$$D = 360^\circ - (\arccos c_{0x} - 90^\circ)$$

The applicability of these formulas depends on the value of the angles which are closed by the n_α , n_β , and n_γ with the X axis. This fact follows from the definition of the Eulerian angles, because it is laid down that the rotation must be carried out into that direction where the two axes come into congruent rotating by the smaller angle around the rotation axis.

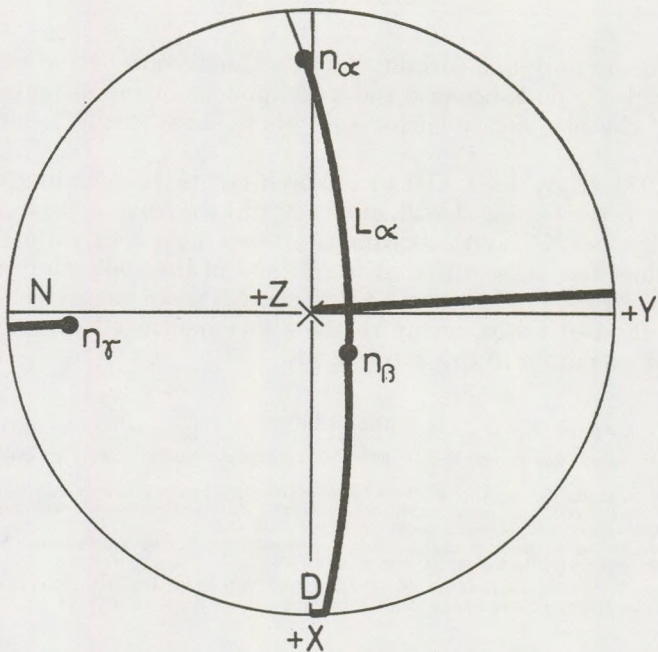


Fig. 3a. Eulerian angles type III.
 An_{10} Low temperature

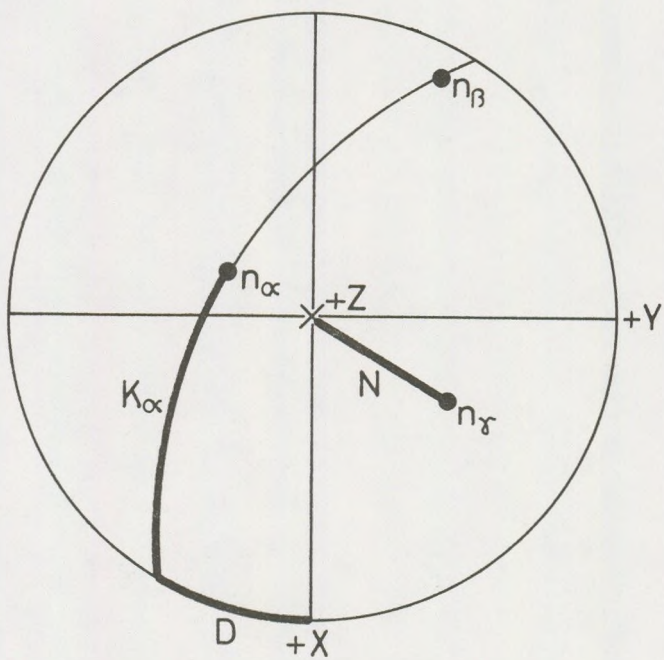


Fig. 3b. Eulerian angles type III.
 An_{90} High temperature

We can see only one formula for the calculation of the value of the Eulerian angles type I, because the x component of the n_x main vibration direction of the plagioclase encloses an angle between $270^\circ - 90^\circ$ with the X axis.

In a 1974 study by C. BURRI (Vereinfachte Berechnung der Euler-Winkel Charakterisierung der Plagioklasoptik) rotation of crystallographic coordinate system XYZ into coordinate system n_x, n_β, n_γ , a different method was used, thus here signs different from those in the 1967 study may appear. In spite of this, the last idea of C. BURRI is more closely related to the original method of Euler, owing to the abovementioned practical reasons we made an exception to this latter study.

REFERENCES

- BURRI, C. (1974): Vereinfachte Berechnung der Euler-Winkel Charakterisierung der Plagioklasoptik. — SMPM 54, 33–38.
- BURRI, C., PARKER, R. L., WENK, E. (1967): Die optische Orientierung der Plagioklase. — Basel, Birkhäuser
- BURRI, C., ÖRKÉNYI-BONDOR, L., VINCZE-SZEBERÉNYI, H. (1976): Rechnerische Auswertung von U-Tischoperationen durch elementare Vektormethoden. — SMPM 56, 1–38.
- ÖRKÉNYI-BONDOR, L. (1978): Eulerian angles and the pseudosymmetry of the plagioclase. — Ann. Univ. Sc. Budapestinensis Sectio Geologica, 20, 143–154.
- ÖRKÉNYI-BONDOR, L., VINCZE-SZEBERÉNYI, H. (1974): (110) , $(\bar{1}\bar{1}0)$, (130) and $(\bar{1}\bar{3}0)$ plagioclase twinning in andesite from Hungary. — Acta Geol. Acad. Scientiarum Hungaricae, 18, 99–138.

KINEMATICS OF TECTONIC MOVEMENTS AND VOLCANISM OF THE MEDITERRANEAN GEOSYNCLINAL BELT AND ITS "FRAME" AT THE OROGENIC PERIOD OF THE ALPINE "CYCLE"

by

YE. YE. MILANOVSKY

Department of Historical and Regional Geology Moscow State University, USSR

(Received: 15th March, 1982)

The Late Cenozoic orogenic period of the Mediterranean geosynclinal belt development was marked by exceptionally intensive and diverse tectonic deformations. The latter led to formation of its contemporary folded-nappe structure and contrasting relief. At the same time powerful and numerous volcanic outbursts are noted within the limits of this belt and some areas framing it.

We call the late concluding period of the geosynclinal belt development "cycle" following the geosynclinal period proper — the orogenic one. This is in accordance with the precise meaning of the term "orogenesis" (i.e. mountain building). At this period the part of ascending movements within geosynclinal troughs increases on the whole. The troughs die off, become subjected to folded upthrust and nappe deformations (in the beginning of the stage) and transformed into folded-block structures with mountain relief (at the end of the stage). Parallel to this margin foredeeps and inner (intermontane) depressions are set up. They widen and deepen being filled in with elastic material (molasse formations). Fast non-compensated submersion of some of them leads to the occurrence of deep depressions of inland seas.

Transition from the geosynclinal period proper to the orogenic one is manifested by dying off of the last geosynclinal troughs, occurrence of epigeosynclinal folded structures and initial stage of foredeep subsidence between them and the platform "frame". This transition is not quite simultaneous in different parts of the Mediterranean belt. It "glides" from the boundary of the Middle-Late Eocene till the Early Miocene-i.e. between 40 and 25 mln years ago. Two stages can be distinguished at the orogenic period: a longer early one (15–30 mln years) and a shorter (5–10 mln years) late one still in effect. They clearly differ in the style of tectonic movements and deformations, velocity, value and predominant directions of their horizontal and vertical components, type of relief, scale and peculiarities of volcanic activity and volcanic products. The second one should be more correctly called a mature stage taking into account that the orogenic period is far from being completed. These stages change nearly simultaneously all over the Mediterranean belt—in the Late Miocene

(before the Late Sarmatian in the Caucasus) or at the boundary of Miocene and Pliocene, i.e. between 10 and 5 mln years ago.

The aim of this communication is to give a brief analysis of tectonic conditions under which volcanic eruptions took place at the orogenic period. It is to clear up the structural position of volcanic areas and regions, to ascertain kinematics of movements and geodynamic situation at certain stages and phases of orogenesis and to reveal peculiarities of geotectonic regime and deep structure of volcanic areas throwing light on deep processes that controlled tectonic deformations and magmatism in the Mediterranean belt and its "frame" during the Late Cenozoic. These problems arouse keen interest and draw attention of a wide circle of researchers. To analyze them we have at our disposal voluminous though not equal for different areas geological and geophysical material. At the same time we are still far from their complete and single-valued solution. Moreover, different researchers have put forward different almost contradictory ideas on geodynamic conditions under which deep magmatic chambers were formed and orogenic volcanism was manifested.

According to considerations based on plate tectonics conception, essentially andesite volcanism, typical for the orogenic period, is identified with that of "island arcs" and is generically associated with processes of plate collision and subduction in the hypothetic Benioff zones possibly existed in different parts of the Mediterranean belt, where lithospheric plates and micro-plates approached each other. Areas of volcanism of some epoch can be considered as a surface projection of the supposed Benioff paleo-zones — along which the collision and subduction of some lithospheric plates and microplates under the other one took place. Intensification of volcanism at some epochs is considered an indication of activation of these processes. In other words it is regarded as evidence of horizontal contraction of some regions of the Mediterranean belt or its general compression at such epoch.

On the contrary, other researchers believe that intensification of volcanic activity in certain regions of the Mediterranean belt indicates that at certain moments of tectonic development of this belt these regions were subjected not to compression but to some extension (MILANOVSKY, KORONOVSKY, 1973).

Late Geosynclinal Stage (Paleocene-Eocene).

Before analyzing tectonic conditions of volcanism at different orogenic stages, let us briefly dwell upon the conditions maintained in the Mediterranean belt at the latest stage of the geosynclinal period proper — Paleocene-Eocene. By the end of Mesozoic as a result of intensive horizontal compression of the Middle and Late Cretaceous the ophiolite "trenches" of the Mediterranean belt were completely "closed". At the place of a number of geosynclinal troughs in its inner parts zones of folded or folded-nappe structure appeared, sometimes with a wide development of strongly deformed ophiolite complexes, mélangé, etc. in them. Volcanic activity attenuated, but in some regions Laramian intrusive massifs were formed

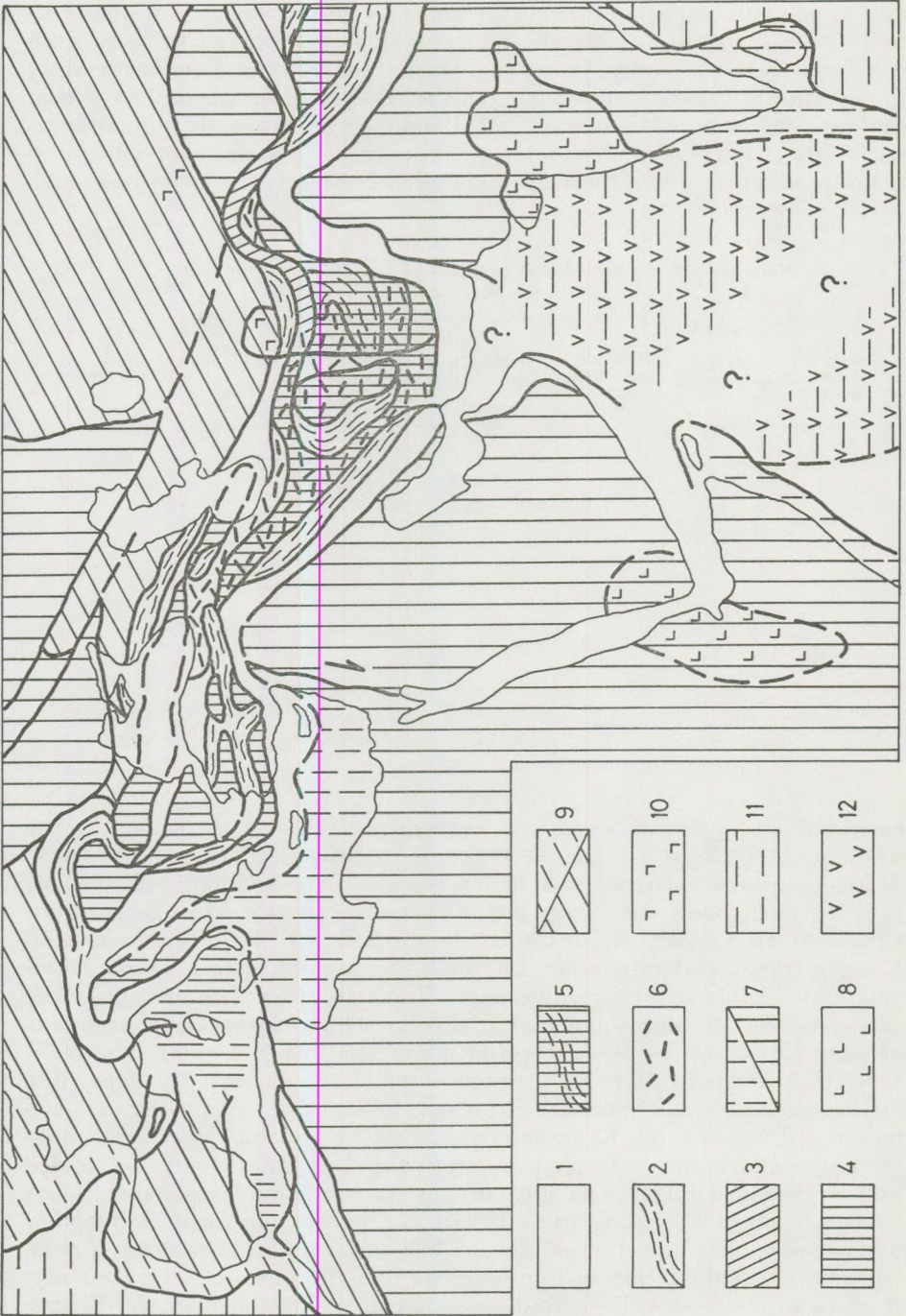
(the zone of Bulgarian Srednegorye, Pontides and others). Only some troughs with carbonate or flysch sedimentation still existed or were even somewhat activated in the Paleocene. During the Eocene, however (mainly in the Middle Eocene) the eastern half of the Mediterranean belt—from eastern Turkey to Afghanistan and Pamirs—was covered by enormous outbursts of extreme andesite volcanism (Fig. 1). By its scope (the volume of products — more than 200.000 km³, see table 1) the latter one much

Table I.

Volumes of Cenozoic volcanic products in the Mediterranean belt
(thousand km³)

Periods of tectonic development	Stages of development	Absolute age, mill. y.	Western part	Trans-caucasian transversal zone	Eastern part	Belt on the whole	
Orogenic	Late (mature) orogenic end of N ₁ —Q	5—10	30—35	37	5—10	80	120—125
	early orogenic p ₂ ³ —N ₁		38—43	~1	~1	40—45	
geosynclinal proper	late geosynclinal p ₂ ¹⁻²	55	~1	~200		~200	

exceeded all preceding ones and subsequent volcanic eruptions in the whole Mediterranean belt. (MILANOVSKY, KORONOVSKY, 1973; KORONOVSKY, 1979). Eruptions occurred both under sea and onground under most different tectonic conditions. These include some geosynclinal troughs, yet not subjected to folding (for instance, depressions of Minor Caucasus and Eastern Iran); median massifs (Lut and other massifs of Iran); some Mesozoic folded zones and even some parts of epihercynian Turanian plate adjacent to the Mediterranean belt (Badhyz). Thus, Eocene volcanism was of areal superimposed character and manifested over an enormous territory. Only its petrochemical character could somewhat vary depending on the peculiarities of structure and development of certain tectonic elements. All this testifies to enormous dimensions and very deep occurrence of magmatic chambers feeding Eocene volcanoes. The absence of folded and upthrust deformations and of olistostrom complexes synchronous to volcanism in the whole eastern half of the Mediterranean belt testify against possible connection of Eocene volcanism with phenomena of compression and subduction in hypothetical Benioff zones. On the contrary, it gives grounds to believe that this vast area developed in the Eocene



- 1 [Empty box]
- 2 [Wavy lines]
- 3 [Diagonal lines (top-left to bottom-right)]
- 4 [Vertical lines]
- 5 [Horizontal lines]
- 6 [Dashed lines]
- 7 [Diagonal lines (top-right to bottom-left)]
- 8 [L-shaped symbols]
- 9 [X-shaped lines]
- 10 [L-shaped symbols]
- 11 [Horizontal lines]
- 12 [V-shaped symbols]

under conditions of some horizontal extension. The eastern half of the Mediterranean belt in its turn was the northern part of gigantic planetary area of Paleocene-Eocene volcanism and horizontal expansion covering the Northwestern part of the Indian ocean jointly with the adjacent regions of the Indian and Afro-Arabian platform and the Middle East (MILANOVSKY, 1974). It must be noted that the western boundary of the vast Mid-eastern area of Eocene volcanism coincides with the West-Arabian deep fracture zone. This makes it possible to assume not left-but right-shifting wrench displacements to have taken place along this zone during the Eocene contrary to those of subsequent times. These shifts led to a relative displacement of the Arabian block southward and contributed to the widening of the eastern half of the Mediterranean belt.

Early Orogenic stage (Late Eocene-Miocene).

During the Early Orogenic stage folded and folded-nappe structures are formed at the place of geosynclinal troughs and geoanticlinal uplifts. They are subjected to strong compression and differential uplift usually of moderate intensity. The foredeeps and some inner depressions occur at their periphery. The troughs are first sometimes non-compensated, but later they are filled in with mainly fine-grained molassic material. This indicates the absence of the high mountain relief. In some foredeeps only (for instance, Pre-Carpathian, Pre-Alpine) fine clastic sediments alternate with the coarser ones. Occurrence of folded structures is sometimes accompanied by granitoid batholiths (the Alps, Dinarids, Eastern Pontides, Minor Caucasus, etc.) and regional metamorphism in their central zones. In a number of regions of the Mediterranean belt — on median massifs and inner zones of some folded structures — during the Early Orogenic stage subaerial, less often submarine volcanism with prevalence of explosive formations of acid and intermediate composition is manifested. Their total volume was estimated as 40–45,000 km³ (MILANOVSKY, KORONOVSKY, 1976).

With Early Orogenic stage are associated linear-folded deformations most intensive and widespread over the area of the Mediterranean belt. In most epigeosynclinal folded systems they were accompanied by the development of gently dipping upthrusts and tectonic nappes with the amplitude of up to some dozen and even hundred km. The summary value of horizontal contraction of individual folded systems is estimated as being from several tens to 100 and even 300 km (Alps, by TRÜMPY, 1973). Fold

←

Fig. 1. Distribution of early paleogene volcanism in the structure of Mediterranean belt and its "frame". Compiled by E. E. MILANOVSKY, 1980. 1–6 — Mediterranean geosynclinal belt:

1 — late geosynclinal troughs; 2 — Mesozoic folded zones; 3 — Hercynian folded zones; 4 — median massifs; 5 — Mesozoic folded zones on the median massifs; 6 — Early-Middle-Eocene mainly andesitic volcanism in the Mediterranean belt; 7 — precambrian platforms and their submarine continuation; 8 — Paleocene-Eocene mainly basaltic volcanism on the platforms; 9 — regions of Paleozoic folding; 10 — Eocene volcanism in their limits; 11 — oceanic basins; 12 — Paleocene-Eocene basaltic volcanism on the oceanic floor

vergence and nappe movements nearly always (with the exception of Great Caucasus) are directed towards the northern or southern platform "frame" of the belt and away from the median massifs located in the "rear" of folded structures. Therefore their greater part is of monovergent structure. Owing to different orientation and arc-like bends of many of them (Carpathians, Hellenides, Taurides, Betides, Rif and oth.) the mass horizontal movement took very different directions. Only rare folded structures, suppressed from two sides between platform blocks or platform and peripheral rigid massif (Pyrenées, partly, Alps and Great Caucasus), are of fan-like antivergent character.

In the eastern half of the belt covering the Caucasus—Iran—Afghanistan, intensity of compressional deformations falls down on the whole in comparison with the western (Mediterranean proper) half and some of the structures that occurred here at the Early Orogenic stage are of relatively simple folded structure. During this stage a number of rather short phases is distinguished when fold- and nappe-forming deformations were strongly intensified. They are as follows: Pre-Late Eocene (Adigeny), Pre-Oligocene (Pyrenean), Late-Oligocene-Early Miocene (Savian), Middle Miocene (Styrian), Late Miocene (Attic). The relative role of these phases in the development of individual epigeosynclinal folded structures of the belt was different. In each of them, however, several (not less than two) phases are manifested. The wave of compressional deformations was always displaced from inner zones (rear in monovergent structures and central in the fan-like ones) towards the outer ones, and then involved the inner zones of foredeeps as well.

Roughly in the Early Orogenic stage we may distinguish two main substages corresponding to Late Eocene-Oligocene (Fig. 2A) and Miocene (Fig. 2B) respectively. Since the boundary of the Middle-Late Eocene till the end of the Oligocene, geosynclinal troughs of Pyrenées, Balkan, Pontides, Minor Caucasus are completely "closed" and transformed into folded structures. Folded, upthrust and nappe deformations cover inner zones of the Alps, Dinarides, Hellenides, Taurides, Zagros, Elburz Apennines, Tell, Rif, Betides, southern slope of the Great Caucasus, etc, gradually spreading towards the foreland of these geosynclinal systems. The inner zones of Alps, Pyrenées and others are subjected to regional metamorphism simultaneously with main compressive deformations and directly after them (in the Oligocene). The Oligocene is characterized by the initial stage of the first foredeeps formation (Fore-Pyrenean, Fore-Alpine). Outer zones of many geosynclinal systems or even some geosynclinal troughs on the whole (the Carpathian flysch trough), however, exist till the end of the Oligocene.

During the Miocene all these troughs or their outer zones die off, flysch Carpathians, Kopet-Dag, the outermost zones of the Alps, Hellenides, Taurides, Apennines, Atlasides, Betides and oth., are successively covered by folded or nappe deformations and move upon their foreland. Foredeeps appear or deepen and widen in direction to the platform in front of them. By the end of the Miocene their inner zones are also subjected to compressional deformations.

Median massifs located between the main branches of folded structures of the Mediterranean belt in contrast to them were not subjected to compression during the Early Orogenic stage. Just the opposite they somewhat widened their area. They were dissected by diversely oriented, sometimes intersecting normal faults and gaping faults and were transformed into mosaic systems of horsts and grabens and sometimes of narrow troughs with the crust of suboceanic type. Rising mantle diapirs manifested by intensive regional isostatic gravity maxima (ARTEMYEV, 1971) and vast fields of anomalously high heat flow (ČERMAK, RYBACH, 1979) are closely connected with these massifs. Heating of the continental crust within the limits of these areas led sometimes to formation of paligenetic magmatic chambers and eruptions of volcanic rocks of mainly acid and intermediate composition. All these phenomena were rather poorly expressed in the inner zones of the eastern half of the belt but very strongly manifested in its western, Mediterranean proper one. This allows to speak about close structural and genetic connection between the deep mantle diapir uplift and diversely directed horizontal expansion of the crustal upper part in intermountain areas, on the one hand, and the compressional deformations and centrifugal (relative to intermountain areas) displacements (as if "wringing out") of crustal upper parts in the alpine epigeosynclinal folded zones framing the former on the other hand (MILANOVSKY, 1968; MILANOVSKY, KORONOVSKY, 1973). The process of mantle diapir rise in the areas of different median massifs began, evidently, not quite simultaneously, proceeded with different intensity and stopped at different stages. Early stages of this process — general elevation and surface fracturing with a formation of a number of shallow depressions — were "imprinted" in the Rodopian and Anatolian massifs. In the Pannonian massif horizontal expansion at the Early Orogenic stage (in Miocene) was more significant: here a denser network of deep volcano-active grabens appeared, and at the end of the Miocene general subsidence of the Pannonian basin started. Lastly, in the Western Mediterranean area vast and deep volcano-active grabens (Campidano in Sardinia and, probably, a number of others) originated already in the Oligocene, and in the Miocene strong expansion and deep subsidence of vast basins (Tyrrhenian, Algeria — Provence, Balearian) began. They were evidently formed at the place of ancient median massifs involved in especially intensive processes of mantle diapirism. They are characterized by extremely high heat flow, rather thinned consolidated crust* and highly elevated anomalously sharply pronounced asthenosphere (BERRY, KNOPF, 1967). In the Tyrrhenian basin, judging from the complicated character of bathymetry and geophysical fields, we deal with strong crust fragmentation and formation of a multitude of narrow horsts, grabens and spreading zones — the so to say dispersed rifting (KHAIN, LEVIN, 1978). In the Algeria-Provence and Balears basins in the Miocene general

* According to seismic data this crust is of "sub-oceanic" character; however, results of dredging in a number of sites of the Tyrrhenian basin demonstrated the outcrops of paleozoic metamorphic rocks on its bottom (MALOVITSKY, 1978).

*Fig. 2.a.*

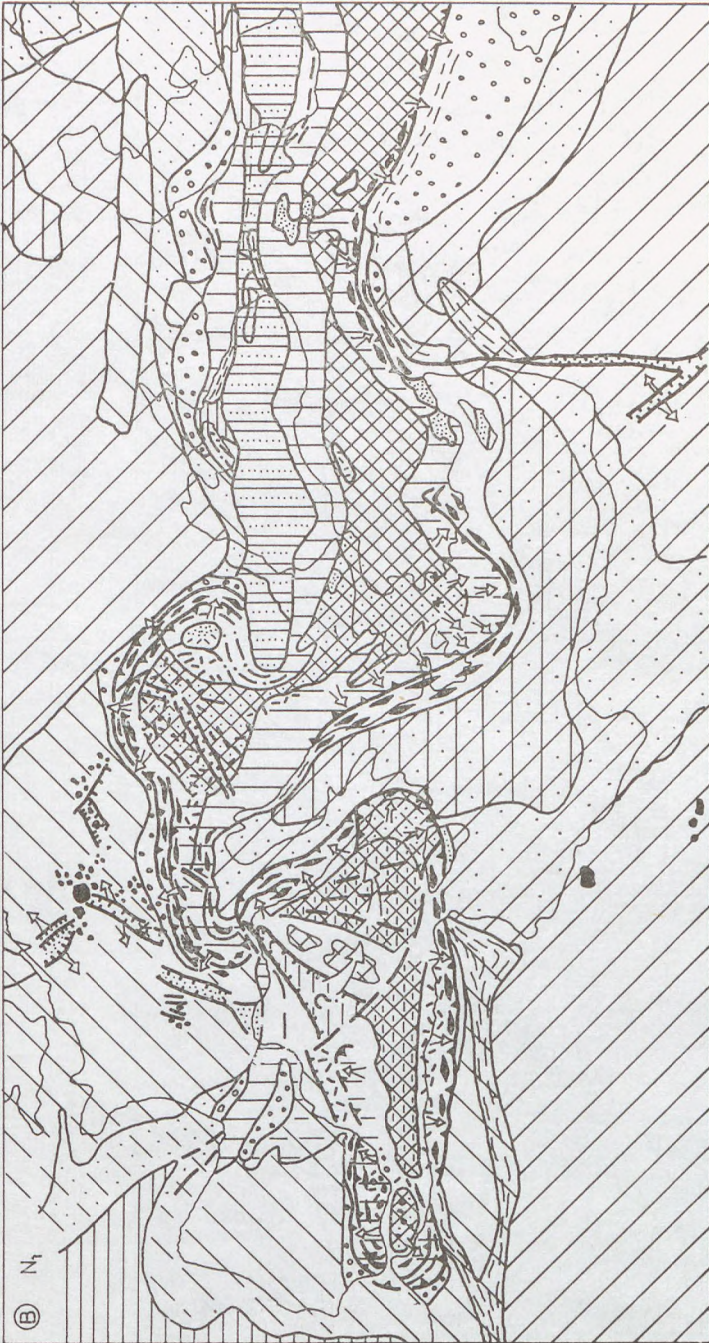


Fig. 2.b.

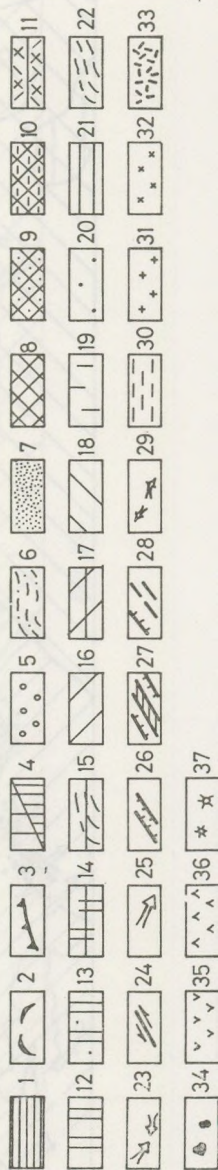
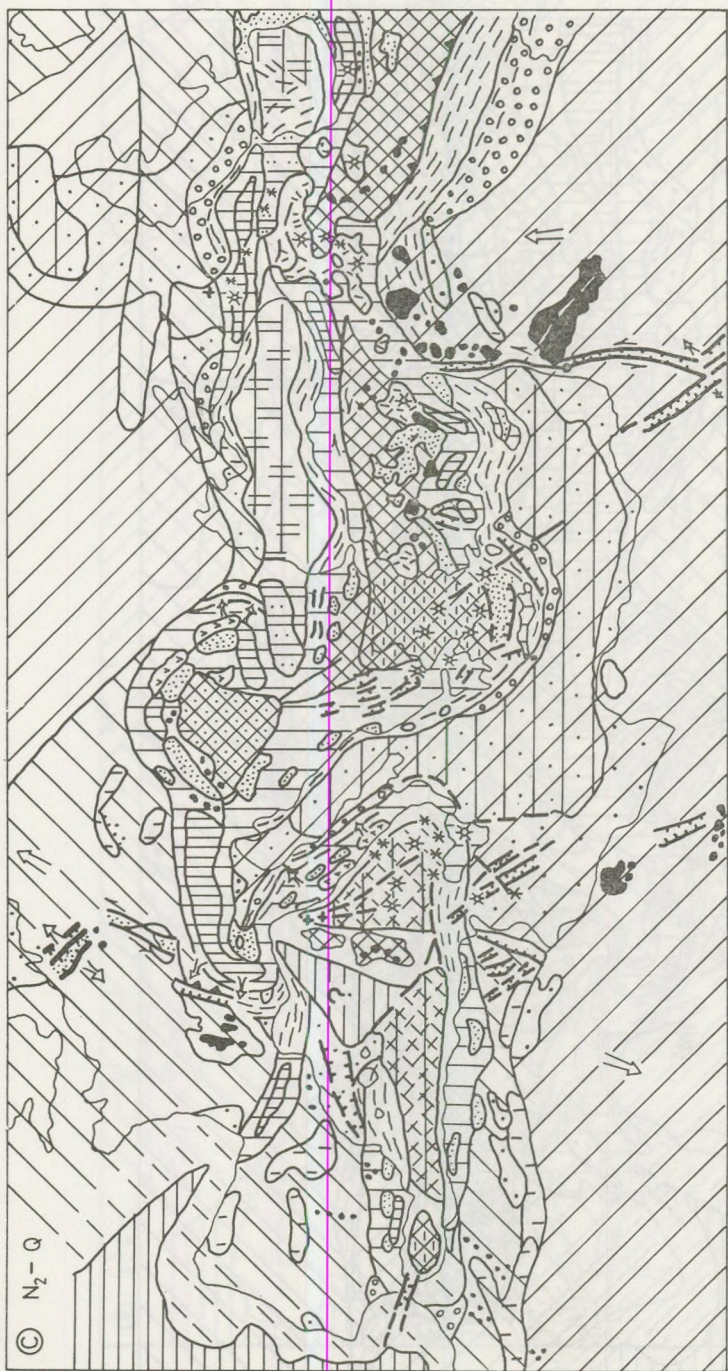


Fig. 2.c.

strong expansion and thinning out of continental crust and perhaps even its total break and wide spreading took place followed by general deep slightly differentiated subsidence since the end of the Miocene.

It is quite likely that the phenomena of horizontal expansion, fragmentation and spreading of large crustal blocks in the Western Mediterranean area were accompanied by their certain general horizontal displacement in relation to the "platform frame" during the Early Orogenic stage. In particular, many authors have recently put forward reasonable assumptions, confirmed by the data of paleomagnetic researchers, on the eastern displacement of Corso-Sardinian and Tyrrhenian blocks with a certain counter clock-wise rotation. This rotating movement was accompanied by strong expansion and spreading in the area situated to the west of the Corso-Sardinian block — in the Algeria-Provence and Valencia basin and strong compression within the Dinarides, Alpine and Apennine geosynclinal systems and East-Corsican zone.

During the Early Orogenic stage the areas of platform framing behaved on the main as relatively rigid monolithic blocks. They were nearly not subjected to horizontal displacements with the exception of some parts adjacent to the Mediterranean belt where their platform cover was folded and partially torn off from its basement, mainly at the end of this stage (Jura mountains, Iberides, Atlasides, Palmirides).

Fig. 2. Structure, kinematics of tectonic movements and volcanic activity in the Mediterranean belt in different stages of the Alpine orogenic period. Compiled by E. E. MILANOVSKY, 1980.

A — early orogenic stage, early substage (P_2^3 — P_3 , 40–55 mln.y.ago); B — early orogenic stage, late substage (N_1 , 25–10 mln.y.ago); C — late (nature) orogenic stage (end of N_1 —Q, 10–0 mln.y.)

1–15 — Mediterranean belt:

1 — residual geosynclinal and periclinal troughs on the stage of subsidence; 2 — zones of intensive folding in the dying of geosynclinal troughs; 3 — gently dipping thrusts and tectonic nappes; 4 — uprising (a — moderately, b — intensively) epigeosynclinal folded structures; 5 — foredeeps on the stage of subsidence; 6 — Mesozoic folded zones (shown on figs 2A and 2B); 7 — intermountain and intramountain depressions in the stage of subsidence; 8 — median massifs (inner Mesozoic folded zones including) with the manifestations of the mantle diapirism on the stage of uplift and initial fragmentation; 9 — the same, in the stage of intensive fragmentation and horizontal extension; 10 — the same, in the stage of general extension, prevailing subsidence, thinning and destruction of continental crust; 11 — the same, in the stage of general extension and formation of "suboceanic" crust; 12 — median and peripheral massifs without manifestations of mantle diapirism, uplifted parts; 13 — the same, subsided and compressed parts; 14 — the same, deeply subsided parts with "suboceanic" crust; 15 — parts of alpine folded structures involved into subsidence of deep sea depression

16–21 — "frame" of Mediterranean belt:

16 — ancient (pre-Cambrian) platforms; 17 — their marginal (pericratonic) depressions with the thinned consolidated crust partly of suboceanic type; 18 — young platforms (areas of paleozoic folding); 19 — areas of intensive uplift on the platforms; 20 — the same, of subsidence; 21 — oceanic basins

22–30 — structural and kinematic symbols:

22 — zones of compression and linear folding on the platforms; median and peripheral massifs and intermountain depressions; 23 — direction of horizontal compression in the upper part of crust; 24 — large-scale wrench faults and the directions of horizontal displacement along them; 25 — supposed directions of horizontal (rotational including) movements of the greatest blocks of the crust; 26 — large grabens, intracontinental rift zones; 27 — intercontinental rift zones; 28 — large fracture zones of fault, gape and fissure types; 29 — directions of horizontal extension in the upper part of crust; 30 — zones of the dispersed horizontal extension

31–37 — magmatism:

31 — granitoid intrusions; 32 — alkaline intrusions; 33 — essentially intermediate-acid (crustal) volcanism; 34 — essentially basic (mantle) volcanism; 35 — mainly intermediate (andesitic) volcanism; 36 — alkaline volcanism; 37 — some large polygenic volcanoes

During the period from the Late Eocene to the Early Miocene the part of the West-European epi-Hercynian platform from the Bohemian to the Central French massif was subjected to horizontal extension in sublatitudinal (more exactly WNW – ESE) direction. This led to the formation of grabens of the Rhone, Rhine and Ohře rift zones and block uplifts adjacent to them and manifestations of alkaline-basic volcanism. Generation of grabens of the Rhine rift system was preceded by the development of the Rhine domal uplift. It started already in Late Cretaceous whereas the Upper Rhine graben was set up only in the Late Eocene, and the other grabens parallel to it – in the Oligocene, i.e. simultaneously with the first powerful compressional deformations in the western part of the Mediterranean belt and were evidently kinematically connected with them. Let us emphasize that in the Late Eocene-Oligocene the main directions of compression in western zones of this belt (Pyrenees, Provence, Alps) were submeridional or NNE – SSW, i.e. strictly transversal in relation to the general direction of the simultaneous horizontal extension in grabens of the northern framing of the belt (ILLIES, 1975). In the Miocene subsidence and extension in the Upper Rhine, Hessen, Rhone grabens stopped. This was evidently connected with the change in the direction of compressing deformations in the Alps from NNE to NNW and NW. Thus, it became almost normal to the striking of these grabens. The Rhine-Rhone graben system is only some part of the extended long developing Rhine-Libyan rift belt. Its southern continuation is traced in the Tunisian strait, Tripolitania and Tibesti massif (ILLIES, 1969; MILANOVSKY, 1971). Thus, this transcontinental rift belt, striking in a parallel to the North-Atlantic one, crosses the Mediterranean geosynclinal-orogenic belt under nearly a right angle and as if “interfering” with it. The Oligocene Campidano graben in Sardinia and the Algerien-Provence basin of the Mediterranean Sea can be considered as elements of the Rhine-Libyan rift belt. The Campidano graben prior to the assumed counter-clockwise turn of the Corso-Sardinian block might strike in the Rhine (NNE) direction.

In the South the middle part of the Mediterranean belt is approached by the longitudinal Afro-Arabian rift belt inheriting a number of ancient extension and tectono-magmatic activation zones. It became a single immense system of rift structures in the Oligocene-Miocene. In contrast to the Rhine-Libyan rift belt it does not cross the Mediterranean belt and only reaches its southern margin (West-Arabian fracture zone). However, in its northern continuation there is the largest Trans-Caucasian zone of transversal uplift, playing a very important role in neotectonics and manifestations of orogenic volcanism of the Caucasus (MILANOVSKY, 1972).

Complicated structural pattern, direction and sequence of compressional and extensional deformations in the Mediterranean belt and its nearest framing that went on during the Early Orogenic stage can hardly be explained by some single simple mechanism, for instance, merely by rapprochement of its northern and southern platform “frame” and subduction of the African and (or) European “lithospheric plates” under this belt. We recognize a definite part played by this factor, e.e. certain rapprochement and

possible relative shift of the African and European blocks, probably connected with general Earth pulsations and periodically intensified at certain moments corresponding to Stille's orogenic phases. Nevertheless we cannot use it to explain either essential difference in time (from the Eocene to the Miocene) of folding of different structural zones, in particular of those located along the northern margin of the Mediterranean belt, or nearly simultaneous folding of arc-like structures along their whole striking, where directions of horizontal movements were different and almost contradictory at different places (Carpathian arc for ex.). We cannot finally give an explanation to the vast zones of horizontal widening and anomalously high heating present within this belt at the Early Orogenic stage. Tectonic deformations in the Mediterranean belt were more likely controlled by the joint effect of a number of factors, in particular the following:

1. Contraction of the width of individual geosynclinal troughs owing to rapprochement of the northern and southern "frame" of the Mediterranean belt and rigid (median and peripheral) massifs located within it during compression phases connected with general Earth pulsations (MILANOVSKY, 1978) might lead to strong compression and folded-nappe deformations of these zones.

2. The rise of heated mantle diapirs located in the inner areas of the Mediterranean belt—mainly under the median massifs—might lead to horizontal diversely directed extension of upper parts of their crust, its fragmentation by a system of grabens, origin of magmatic chambers (including intracrustal) and powerful volcanism (Fig. 4.). Expanding sideways such massifs produced unilateral pressure on arc-like geosynclinal troughs framing them. By this they caused strong compression and "wringing out" of the material that filled them in the form of a system of folds, upthrusts and nappes overturned towards the foreland (e.g. in arc-like systems of the Carpathians, Hellenides, Betides-Rif and oth.)

3. Similar or kindred phenomena could take place in uprising highly heated central zones of some folded structures exerting lateral pressure on its outer zones (Great Caucasus, Pyrenées)

4. Relative horizontal displacements and turnings of individual "rigid" blocks in the inner part of the belt (i.e. certain counter-clockwise rotation of the Corso-Sardinia, and Tyrrhenian blocks) could play an active part in the formation of folded and nappe structures of the Alps and Appennines and in gradual reorientation of the main direction of horizontal compression during the Early Orogenic stage (i.e. in the Alps—from NNE to the meridional and WNW).

Early orogenic volcanism

What part is played in the Mediterranean belt by volcanic formations corresponding to the Early Orogenic stage? How are they distributed in its structure? How are these manifestations of volcanism connected with the kinematics of movements and general geodynamic situation? It has already been noted that the general volume of volcanic products of this

stage is estimated approximately as 40–45,000 km³, which is nearly twice as little as that of the Late Orogenic stage (about 80,000 km³). About 15,000 km³ falls to the Late Eocene and Oligocene, and about 30,000 km³ to the Miocene (see tabl. 1.). Thus, during the Early Orogenic and Orogenic period on the whole the volcanic activity gradually increased. Its mean intensity (with the account of stage and substage continuation) at the Early Orogenic stage yielded not less than 5–6 times that of the Late Orogenic, and its mean intensities in the Late Eocene-Oligocene, Miocene and at the end of Miocene-Anthropogen correlate as 1 : 3 : 8 (see tabl. 1.).

The predominant part of the general volume of volcanics of the Early Orogenic stage (not less than 80–90%) is located in the western (Mediterranean proper) half of the belt, where volcanism was practically absent in the Paleocene-Middle Eocene. The major part of volcanics is represented by rocks of acid and moderately acid composition: rhyolites, rhyo-dacites, dacites; the minor part—by intermediate (andesites, andesite-dacites). Basic rocks (basalts, andesite-basalts) play a negligible part. This allows to believe the magmatic chambers feeding volcanoes to be located mainly in the crust and to have palingenetic character. Rocks of high alkalinity occur rather seldom. Among the volcanic products tephra and nigimbrites sharply dominate over lavas which indicates predominance of explosive, mainly subareal eruptions.

The main part of volcanic rocks is located in inner zones of the Mediterranean belt, mainly in its median massifs. This is first of all the Pannonian massif (about 20,000 km³), Rodopian about 5,000 km³), Corso-Sardinian (more than 7,000 km³) and to much lesser extent, the massifs of Anatolia, Iran and Afghanistan*. These are the areas where geothermic, gravimetric, seismic and tectonic data show significant heating of the interior transformation of the deep crustal structure (rise of seismic boundaries) and versely directed extension (as if "creeping apart") in its upper subsurface part. All these phenomena allow to assume deep mantle diapirs at the Orogenic period within these limits. These processes proceeded more intensively in the western part of the belt, where the Early Orogenic volcanism was manifested most powerfully.

Epochs of volcanic eruptions and formation of extensional structures on median massifs (grabens and graben-like basins, where volcanites are mainly located) are stated to correlate in general in time with epochs of intensive compressional deformations (folds, upthrusts and nappes) in geosynclinal troughs (arc-like on the plan) surrounding these massifs. Vergence of compressional structures and horizontal mass displacement in the latter were always directed away from the median massif, i.e. from the area of volcanism which nowhere at this epoch penetrated to the limits of the zones of folded deformations. Thus, in the Rodopian massif volcanism and extension deformations took place in the Late Eocene-Oligocene. Of the

* One may assume volcanics of Oligocene-Miocene age to exist also within the limits of Alboran, Tyrrhenian, Balearian basins, which were median massifs at that stage. In Alboran basin volcanics of calc-alkaline series were stated with the age of 20 mln years (GIROD, 1977).

same age are on the whole compressional deformations in the Balkanides, Dinarides and the inner zones of the Hellenides, framing this massif in the North and South-West. On the Sardinian massif volcanism and graben formation refers to the Oligocene-beginning of the Miocene. On the whole the epoch of compression and centrifugal displacement (as if "pushing aside") of masses from the median massif in the inner zones of the Apennines and Tell Atlas corresponds to the same time. In the Pannonian massif volcanism and graben formation took part in the Miocene, i.e. on the whole simultaneously with the epoch of folded-nappe deformations in the flysch Carpathian arc surrounding it from three sides. Volcanism in the last region covered not only the median massif proper but the inner zones of Carpathians adjacent to it in the North and East subjected to intensive folding at the Late Cretaceous and as if attached to the rigid Pannonian intermountain area. But in these zones (Slovakian inner Carpathians and Apuseni mountains) volcanic rocks were of less acid, mainly andesite-dacite composition, and, evidently, originated from deeper magmatic chambers. In addition to typical median massifs, horizontal extension deformations and accompanying outbursts of volcanism at the end of Early Orogenic stage touched upon some areas which we propose to call peripheral massifs (MILANOVSKY, 1974; MILANOVSKY, KORONOVSKY, 1973). — In particular, this refers to the eastern part of the Iberian massif where during the last years deep rift-like Valencian basin of the north-eastern striking was revealed, which is a branch of the submeridional Algeria-Provence basin. Intensive extension, subsidence and outbursts of volcanism proceeded here in the Miocene (a series of andesite and dacite tuffs of the age of 20 mln years was stated by drilling).

It should be stressed that in all the marked areas only general correspondence of the epochs of orogenic volcanism and extension in median massifs to compressional deformations in folded areas adjacent to them is observed. But it does not refer to individual folding phases in them and main volcanic paroxysms on the massifs. Thus, for instance, the first (Sahwa) phase of compressional deformations in the western part of flysch Carpathians at the boundary of the Oligocene and the Miocene preceded, and the last one (Post-Sarmatian, Attic) took place after main eruptions on the Pannonian massif occurring since the Helvetian up to the Early Sarmatian. Thus, the main extension deformations in areas of rising mantle diapirs took place, evidently, between the regional compressional paroxysms in alpine folded zones and in the whole Mediterranean belt.

Of lesser significance in the general balance of volcanic material are eruptions that occurred in the innermost zones of some alpine folded structures subjected to intensive compressional deformations in the Late Eocene or Oligocene, in particular, in the inner zones of the Dinarides, Hellenides, Betides, Rif, Tell Atlas and the most eastern part of the axial zone of the Alps. However, in all these areas small subareal eruptions took place at the end of the Oligocene of the Miocene only after folded upthrust deformations in a respective zone had completed. Eruptions in these zones were accompanied or directly preceded by intrusion of granitoid batholiths

and stocks (comagmatic with volcanites), and in the inner zones of the Alps—by manifestations of regional metamorphism. In the Rif and Tell Atlas areas volcanic activity—according to L. GLANGEAU (1954) during the Miocene gradually spread southwards following the wave of folded-nappe compressional deformations. It should be noted that all these volcano-active regions of inner zones of folded structures directly adjoin the median massifs (Pannonian and Rodopian) and also the Alboran and Balearian basins that used to be median massifs up to the Early Orogenic stage. Thus, in the inner zones of the alpine folded structures magmatic melts had access to the surface only when strong horizontal compression in them attenuated and weak expansion spread over to them from the side of the adjacent median massif. The role of main channel along which high heat flow propagated and acid magmatic melts rose to the surface was evidently played by deep tectonic sutures separating median massifs from adjacent folded structures and also the axial suture of the Alps (the suture zone Ivrea-Drava), that is, as if some continuation of the Pannonian massif wedging out westward.

During the Oligocene and the Miocene volcanism was manifested also in certain parts of the "frame" of the Mediterranean belt. The beginning of basalt eruptions in North Arabia and North Africa—i.e. in the northern part of the Afro-Arabian and southern part of the Rhine-Libyan rift belts refers to this time (in both of these zones the volcanism increased sharply during the Late Orogenic stage). Essentially alkaline-basic eruptions within the limits of epihercynian West-European platform—in Central-French massif, Rhine, Bohemian-Sudetic areas were closely connected with processes of horizontal extension accompanying the origin and development of the Rhone, Rhine and Ohře rift systems. In the Rhine area the earliest numerous small manifestations of the alkaline volcanism took place at the end of the Cretaceous-Eocene and, thus, contributed to the development of the Upper Rhine domal uplift and preceded the occurrence of the Upper-Rhine axial graben. Maximum of volcanic activity in the zone of this graben and its flanks and the northern ending refers to the Early-Middle Miocene.

Late Orogenic stage

In Late Orogenic stage that started 5–10 mln years ago i.e. in the Late Miocene or at the boundary of the Miocene and the Pliocene and continuing up to now, the character of tectonic situation in the Mediterranean belt essentially changed as compared with that of the Early Orogenic (Fig. 2c). In particular, this refers to its western, Mediterranean part proper. Here folded-upthrust deformations cease almost everywhere. Only in the beginning of this stage they still went on in some parts of the outermost zones of three folded structures: 1) the zone of Jura mountains with its southern continuation near the outer margin of the Western Alps, which was folded and partially thrust over the Oligocene graben Bress at the boundary of the Miocene and the Pliocene (in the Pontian) in the N–W

direction; 2) the easternmost outer zone of Northern Apennines and 3) southern termination of the eastern (Rumanian) flysch Carpathians with parts of foredeeps adjacent to these structures, where formation of folds and upthrusts ended only in the Pliocene. On the contrary, in the eastern part of the Alpine belt folded upthrust deformations in outer and periclinal zones of a number of folded structures went on in the Pliocene, though not everywhere. They continued also in the inner zones of foredeeps and some inner (intermountain) depressions. Thus, these deformations are known in the eastern half of the Caucasian area in the Terek-Caspian foredeep, Kura intermontane depression, Apsheron periclinal zone, South Caspian basin, outer zone of the Kopet-Dag and Fore-Kopet Dag foredeep, South Tadjik depression and Fore-Pamirs foredeep, and also in the outer zone of the Zagros, Mesopotamian foredeep and outer zones of the Suleiman-Kirtar mountains and their foredeeps.

During the Late Orogenic stage the uplift (evidently of isostatic nature) goes on and is even intensified in a number of large folded structures, mainly of divergent tectonic style (Pyrenées, Alps, Great Caucasus, Elburz) or without clearly expressed vergence (Eastern Pontides, Minor Caucasus, Pamirs, etc.) The amplitude of rise of these alpine structures during the Late Orogenic stage reaches 3–5 km and in some cases more than 7 km (Pamirs). The foredeeps framing them in the western half of the belt die off and become involved in a weak elevation (Fore-Pyrenéan, Fore-Alpine, Fore-Karpathian, Fore-Rif foredeep and oth.). In the eastern half submersion of a number of foredeeps and their outer zones in particular went on in the Late Orogenic stage (Fore-Caucasian, Fore-Kopet Dag, Fore-Pamirs, Fore-Zagros or Mesopotamian, Fore-Suleiman-Kirtar foredeep).

Alongside with this numerous monovergent folded-nappe structures, mostly in the western half of the belt are subjected to some extension during the Late Orogenic stage. Many superimposed intramountain depressions and grabens occur on their bodies — most often longitudinal, less often diagonal or transversal (for instance, Gibraltar, Messina, Corinthian) limited by normal faults. These grabens and basins, as a rule, are filled in with Pliocene and sometimes Miocene (for ex., the Wien and Minor Hungarian basins) and Quaternary sediments and, as a rule, are directly manifested on the relief. These structures are typical for the Carpathians, Balkan (narrow Trans-Balkan grabens), Minor Caucasus (Sevan and other depressions), Apennines, Dinarides (their southern part most of all), Taurus, Tell and Tunisian Atlas and especially for the Bétides and Hellenides, in the eastern parts of which (Balearian islands, Créte arc and South Aegéan basin) the subsiding regions even surpass the elevating zones by their area. These folded structures or at least their inner zones were subjected to more or less considerable horizontal extension during the Late Orogenic stage. In geothermal way they are characterized by the change of high values of the heat flow into the low ones across their striking from inner zones to the outer ones. As a rule more frequent and intensive crustal earthquakes are peculiar rather to these structures than to relatively “monolithic” uplifts like the Pyrenées, the Alps and the Great Caucasus.

During the Late Orogenic stage-late in the Miocene and the Pliocene subsidence of a number of median massifs located mainly in the western half of the belt is intensified. Let us recall their connection with a number of growing deep-mantle diapirs at the Early Orogenic stage. In their place are formed either vast intermountain depressions filled in by thick late Miocene, Pliocene and Quaternary continental molasses (Pannonian for instance) or not quite compensated basins occupied by more or less deep inner seas with rough, highly dissected (Aegean, Alboran, Tyrrhenian) or relatively smooth floor (Balearian, Algerian-Provence basin). These morphological differences evidently reflect a greater extent of the bottom extension and fragmentation, a younger age and relatively lesser thickness of sedimentary cover in the first group of deep sea basins. Their crust is of mosaic or keyboard structure, where relict relatively elevated continental blocks evidently alternate with grabens with thinned crust and small spreading zones filled in with basic and ultrabasic material of mantle origin (zones of dispersed rifting). In contrast to the basins of the second group, they are characterized by high seismicity and intensive manifestation of Late Orogenic and contemporary volcanism. Older (?) basins of the second group are filled in with thick (up to 6–8 km) Cenozoic and Meso-Cenozoic deposits. The crust in them, according to seismic data, is of suboceanic character, probably connected with the extension process that began earlier, went farther here (rifting) and was of more concentrated nature. It is not excluded, however, that the crust of these basins was subjected to transformation process ("oceanization") without strong extension. Both groups of basins are characterized by an extremely high heat flow (ČERMAK, RYBACH, 1979) and significant regional isostatic gravity maxima (ARTEMYEV, 1971). The latter testify evidently to continuing development of mantle diapirs. However, in contrast to the Early Orogenic stage, general regional compression does not hinder it any longer in the western part of the Mediterranean belt. This leads to widening of the whole "column" of the mantle diapir (not only of its uppermost sub-surface part as in the Oligocene and the Miocene) and, respectively, to its general subsidence.

Lastly, at both flanks of the Mediterranean belt, its middle transversal section, there are vast deep basins with ancient probably Pre-Cambrian and perhaps partially Paleozoic basement subjected to subsidence since the Mesozoic or even the Paleozoic. It is an immense East Mediterranean basin with its northern "appendix" – the Adriatic block in the southern part of the belt (d'Argenivea, 1980) and Black Sea and the South Caspian basin in its northern part. During the Late Orogenic stage all these basins were subjected to fast non-compensated subsidence and acquired the character of deep-sea depressions; but its value (several km) is still insignificant in comparison with the total thickness of the cover amounting to 10–15 and even more than 20 km (in the South-Caspian basin).

The East-Mediterranean basin is an area of pericraton subsidence of the ancient African platform. The Black Sea and South-Caspian basins are, evidently, ancient median massifs, separated from the East-European

platform still in the Baikal cycle. Should mantle diapirs ever have existed within their limits it could have been only in the Paleozoic. Consolidated crust in these basins is very thin or might be completely deprived of the so-called "granite" geophysical layer (Black Sea, South Caspian basins). Its disappearance, however, took place much earlier than in the basins of the West Mediterranean. They sharply differ from the latter by normal or even anomalously low heat flow (especially the Black Sea and the East Mediterranean basin), regional isostatic minima, absence of volcanism, aseismicity or poor seismicity of their inner zones. Sediments on their floor occur smoothly or build gentle con-sedimentational developing folds expressed in the floor relief (Southern Caspian). Alpine folded structures framing them do not display centrifugal vergence, but, just the opposite, in a number of places they are more or less upthrust onto such basins (Hellenides, Taurides, Great Caucasus, Elburz and others) and are even separated from them by a peculiar trench or a foredeep (Hellenian trench). Morphological similarity of these peripheral deep basins with those of the West Mediterranean is evidently explained not by similarity of their tectonic position, structure and development, but by the common properties of the geodynamic regime that was established in the Mediterranean belt at the Late Orogenic stage. During the Early Orogenic stage the general horizontal compression which prevailed in it periodically intensified during several orogenic phases. Horizontal extension was manifested only locally in the regions of growth of the mantle diapirs (i.e. in a number of median massifs). Just the opposite, during the Late Orogenic stage in the western half of the belt phenomena of general horizontal extension began to dominate. The latter occurred both in the intermountain area and within the limits of many alpine folded structures. General expansion of the territory of the Mediterranean belt led evidently to "subsidence" of the bottom of the most peripheral basins.

In the eastern half of the belt the role of extension deformations and crustal fragmentation at the Late Orogenic stage also somewhat increases, especially, within its inner parts occupied by median massifs and the oldest, mainly, Mesozoic and partially Late-Eocene (Minor Caucasus) folded zones. However, in outer zones of the eastern half of the belt several phases of rather strong folded deformations are connected with the Late Orogenic stage. These differences in kinematics of movements and general geodynamic conditions in the western and eastern halves of the Mediterranean belt at the Late Orogenic stage should be evidently connected with sinistral horizontal displacements of large amplitude along the West-Arabian (Levantine) shift zone in the northern part of the African-Arabian belt which sets against the southern edge of the Mediterranean belt near the NE corner of the Mediterranean sea. During the Late Orogenic stage along this suture the western-African block was relatively displaced southward whereas the eastern-Arabian — was displaced northward and underthrust ("subducted") under the eastern part of the Mediterranean orogenic belt. This defined a relatively great role of deformations of horizontal compression in its part which is northward and north-eastward of the Arabian platform.

At the end of the Miocene and especially, in the Pliocene and Anthropogen the Afro-Arabian rift belt was activated; the extension in its rift zones (in particular, in the Red Sea rift), the growth of arch-block uplifts connected with them and volcanic activity within its limits (in particular, in the western part of the Arabian platform) increased considerably. It has already been mentioned that in the northern continuation of the Afro-Arabian belt the Mediterranean orogenic belt is crossed by the zone of the Trans-Caucasian transversal uplift where positive undulations of most of the longitudinal tectonic zones of this segment take place. The zone of Trans-Caucasian transversal uplift grows intensively and acquires the role of the principal watershed of the whole Caucasian isthmus during the Orogenic period and especially Late Orogenic stage. Significant part of manifestations of Late Orogenic volcanism in the Mediterranean belt is located here.

During the Pliocene and the Anthropogen the development of another rift belt—the Rhine-Libian one—is also activated. In its southern part adjacent to the margin of the Mediterranean orogenic belt, in the shallow area of the Tunisian-Sicilian strait the whole system of linear grabens and horsts appears NW of the striking, clearly expressed in the bottom relief and studied by seismic methods in details during the last years.

After a long pause (Middle Miocene—Early Pliocene) revived is the Upper Rhine graben. Since the main direction of the extending efforts in the Rhine rift system this time becomes SW—NE, i.e. close to the striking of the Upper Rhine graben, mainly sinistral shifts of blocks occur there. Only its parts of submeridional striking are subjected to considerable extension and subsidence. Simultaneously the development of the Lower Rhine graben extended in NW direction, i.e. approximately normal to the vector of main extending stresses is also activated. It is remarkable that NW, WNW and less often sublatitudinal directions characterize numerous narrow zones of anomalously high heat flow revealed within the limits of the Paleozoic folded area of West Europe. They were evidently “half-open” as a result of the in this area prevailing regional extension in the SW—NE or SSW—NNE direction.

Late orogenic volcanism

During the Late Orogenic stage the intensity of volcanic manifestations in the Mediterranean belt increases 5–6 times in comparison with the Early Orogenic ones. It is remarkable that sharp intensification of volcanism in it coincides with certain attenuation of compression in the eastern half of the belt and their complete cessation and wide development of extensional deformations in its western part. The connection of these phenomena is underlined by the fact that out of the general volume of products of Late Orogenic volcanism (about 80,000 km³) only 10% falls to the eastern part of the belt (Iran, Afghanistan, Pakistan). More than 40% falls to the western, Mediterranean proper, and more than 45% of all volcanic rocks (37,000 km³) falls to the Trans-Caucasian transversal uplifts

dividing these parts. (see tabl. 1.) Comparison of areal of the Late Orogenic volcanism with the distribution of the heat flow in Europe (ČERMAK, RYBACH, 1979) demonstrates their location in the regions with the highest heat flow values. It should be added that some highly thermal regions (e.g. the Pannonian basin) are characterized by considerable manifestations of volcanism that took place mainly not in the late orogenic stage, but at the end of the Early orogenic one — in Middle-Late Miocene (10 — 15 mln years) ago). Evidently, the variations of the thermal field proceed rather slowly, and the crust in such regions nearly did not cool down. At the same time the highest heat flow values show a direct correlation with zones of the recent extension stated by the geological data (rift zones, grabens, areas of dispersed rifting and fragmentation of the crust). The highest sharply expressed heat maxima coincide with the highest regional isostatic gravity maxima (Tyrrhenian, Pannonian, Aegean, Trans Caucasian) evidently, caused by the rise of deep basic and ultrabasic material above these zones (Fig. 3A, B, C).

In the western (Mediterranean proper) part of the belt the prevailing part of volcanic manifestations at the Late Orogenic stage, the way it was at the Early Orogenic one, is located at the inter-mountain areas — the Central Anatolian, Aegean-Rodopian, Pannonian, Tyrrhenian. However, powerful subareal eruptions of products of intermediate-acid composition, including large masses of ignimbrites, occurred (mainly early at the Late Orogenic stage) only in those inter-mountain areas where development of mantle diapirs proceeded at a slower rate and which at this stage were rather strongly, dissected by fractures but on the whole relatively uplifted median massifs (Kirshekhir and Menderes massifs in Anatolia). Ignimbrite eruption of acid palingenetic magma at the Anatolian massifs alternated (at the beginning of the stage) and then (at its end) were totally replaced by extrusions of basic lavas (basalts and andesite-basalts) originating from deeper magmatic chambers. In more "mature" inter-mountain areas, where development of mantle diapirs progressed further and which after fragmentation and extension of their surface were subjected to general significant subsidence at the end of the Miocene and in the Pliocene (Pannonian, Tyrrhenian, Central part of the Aegean) the zones of the highest volcanic activity were removed to their periphery and appeared to be located mainly in the half-open at the Late Orogenic stage longitudinal rear sutures separating these intermountain areas from the adjacent folded-nappe structures (Eastern Carpathians, Apennines and others) and partially even to deep diagonal and transversal faults crossing them (volcanic range Kaliman-Hargita, Etna and others) and even to deep fractures and linear grabens, spreading beyond the limits of the Mediterranean belt to its platform (volcanoes of the Pantellerian graben, basalts of Trans-Balkan transversal fault and oth.)

Volcanic activity went on somewhere in the central parts of the inter-mountain areas transformed into vast intermountain depressions (Pannonian) and deep-sea basins (Tyrrhenian) with some inner horst-like basement blocks but was much less intensive on the whole here than in the peripheric

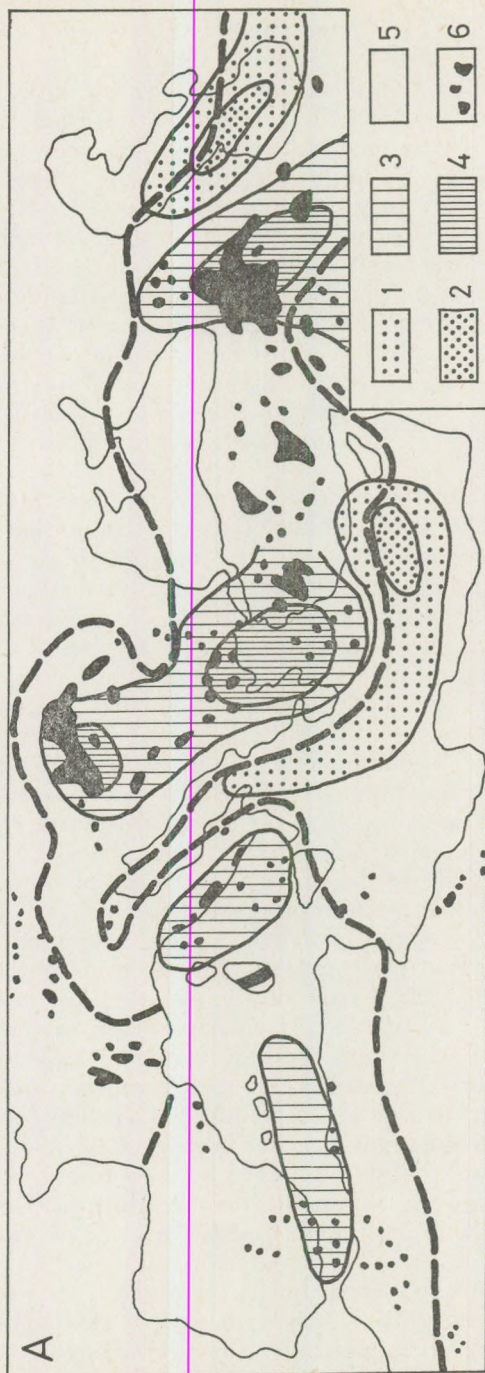
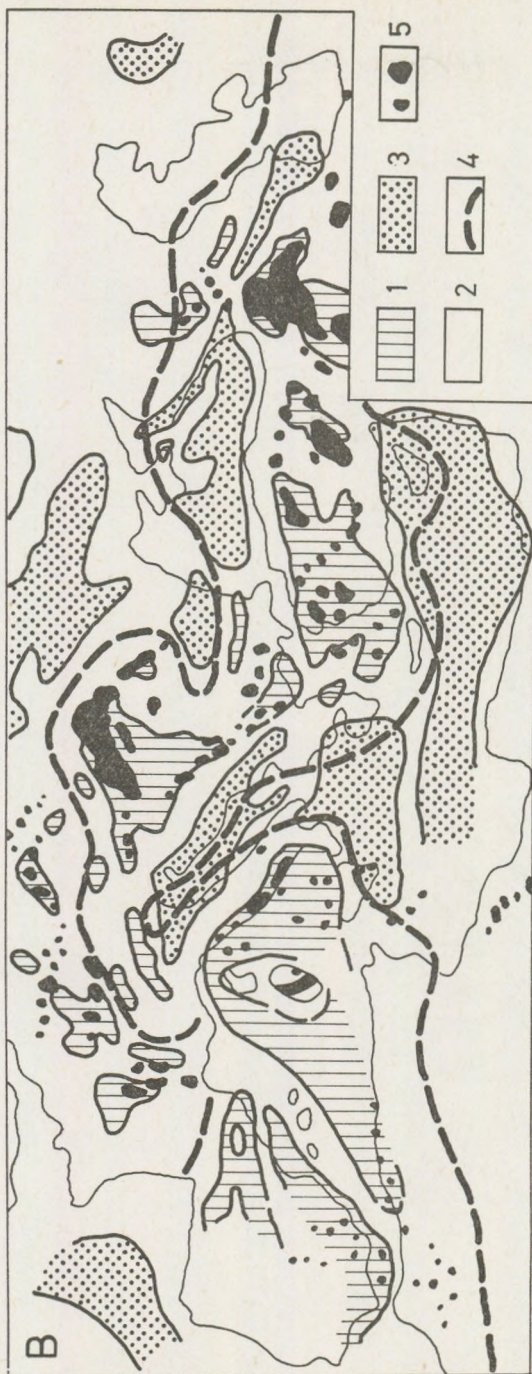


Fig. 3. Correlation between regional isostatic gravianomalies, heat flow distribution, areas of Late Cenozoic mantle diapirism and extension in the Mediterranean belt and its "frame" and localisation of Late Cenozoic volcanic manifestations.

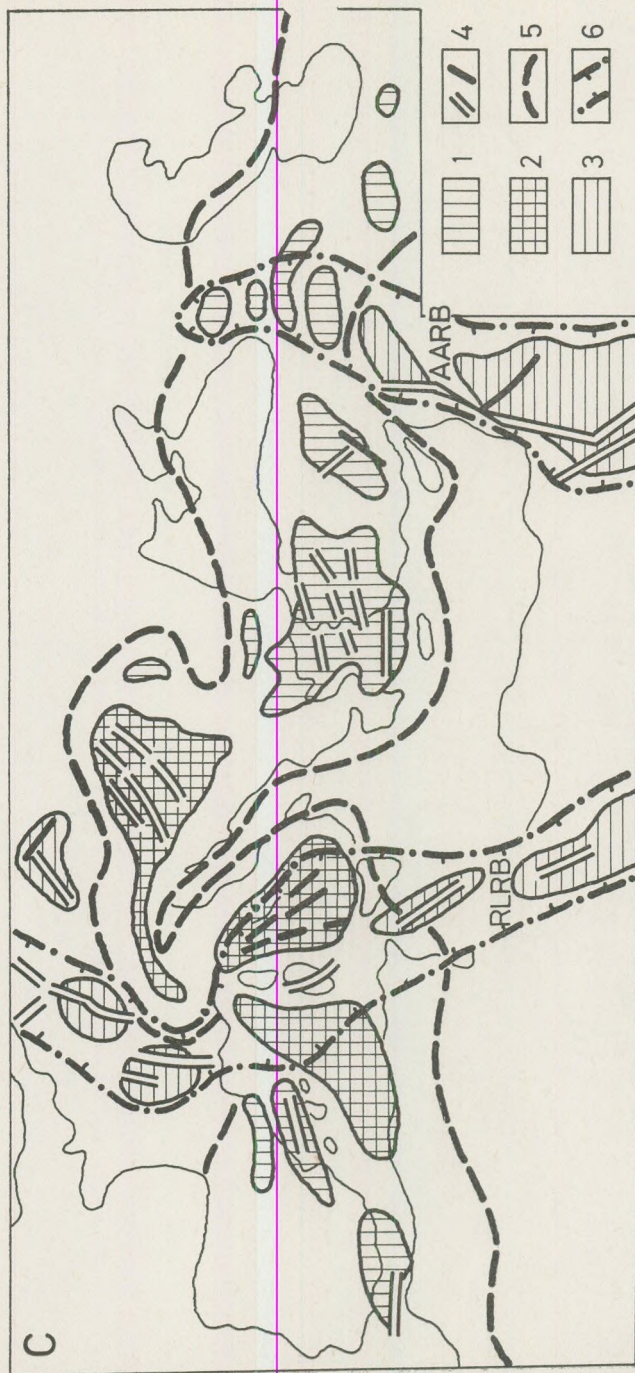
A — main regional isostatic anomalies (according to M. E. ARTEMYEV, 1971)

1 — regional minimum of moderate intensity; 2 — the same, of great intensity; 3 — regional maximum of moderate intensity; 4 — the same, of great intensity; 5 — boundaries of the Mediterranean belt (peripheral massifs and adjacent part of young platforms with alpine folded deformations including); 6 — areas of Late Cenozoic volcanism manifestations



B — scheme of heat flow distribution in the Mediterranean belt and its northern "frame" (compiled by E. E. MILANOVSKY according to the heat flow map of Europe, ČERMAK, RYBACH, 1979)

1 — regions with high heat flow values ($\geq 80 \text{ mw} \cdot \text{m}^{-2}$); 2 — the same, intermediate values ($40 - 80 \text{ mw} \cdot \text{m}^{-2}$); 3 — the same, low values ($< 40 \text{ mw} \cdot \text{m}^{-2}$); 4 — boundaries of the Mediterranean belt; 5 — areas of Late Cenozoic volcanism manifestations



C — distribution of areas of Late Cenozoic mantle diapirism and horizontal extension in the Mediterranean belt and its "frame"

1 — mantle diapirs in the Mediterranean belt; 2 — the same, most developed and deeply subsided since the end of the Miocene, with strongly thinned, extended and reworked continental crust; 3 — mantle diapirs in the limits of adjacent platforms; 4 — grabens and great fracture zones; 5 — boundaries of the Mediterranean belt; 6 — boundaries of the transcontinental rift belts (RLRB—Rhine-Lybian rift belt, AARB—Afro-Arabian rift belt).

zones of intermountain areas. Character and composition of volcanic rocks in "mature" inter-mountain areas at the Late Orogenic stage changes essentially: the part of ignimbrites sharply decreases, explosive activity on the whole yields to predominance of lava extrusions, outbursts of acid and intermediate-acid material are replaced by eruptions of andesites, andesite-basalts and basalts. In a number of regions appear subalkaline and alkaline products, essentially potassic volcanites in the Naples region including.

In the eastern part of the belt, after nearly total absence of volcanic activity in the Oligocene-Miocene, the latter flashes again at the end of the Miocene and in the Pliocene. Quantitatively it yields significantly to the western part of the belt. Its manifestations at the Late Orogenic stage are connected with median massifs (e.g. the Lut volcanic area on the Lut massif) and their parts subjected to reworking and folding at the end of the Mesozoic (Gazni, Kokh-i-Sultan, Taftan, Bazman, Yezd, Sahend and other areas on the Afghanistan and Iran massifs). On the whole all these volcanic areas trend to the periphery of massifs and tectonic sutures bordering and complicating them. Of peculiar position is a large poligenous Demavend volcano located at the transversal tectonic zone in the Elburz anticlinorium formed at the Early orogenic stage. Prevailing part of the volcanites is represented by andesites, the lesser one — by dacites and trachi-andesites (Demavend), i.e. by rocks more typical in the western part of the belt for the Early Orogenic stage. There are also rather many monogenous basaltic cones.

The strongest manifestations of the Late Orogenic volcanism are associated with the zone of Trans-Caucasian transversal uplift where at the Early Orogenic stage volcanic activity was nearly absent. Volcanic regions at this zone are located in the rigid "inner massifs" of the Great and, mainly, Minor Caucasus and Eastern Taurus, North-Caucasian "marginal massif", some parts of the Georgian and Iranian median massifs and also to much lesser extent — in certain longitudinal and transversal tectonic sutures crossing the zones of Mesozoic and Oligocene folding adjacent to these rigid blocks. On the whole, however, all the volcanic areas of the Caucasus and Armenian highland trend to a wide submeridional zone, crossing practically the whole Mediterranean belt. Many volcanic regions and chains of volcanoes are located in a number of transversal faults and deep fractures of submeridional and north-eastern striking. During the Late Orogenic stage the Trans-Caucasian transversal zone was subjected to a gentle arch-like bulging up accompanied by weak extension in sublatitudinal (i.e. longitudinal in relation to main tectonic zones of the Caucasian segment of the Mediterranean belt) direction. The uplift of Transcaucasian zone was evidently associated with the rise of a vast deep asthenolith which is in essence the northern termination of the grandiose submeridional zone of mantle diapirism controlling the development of Afro-Arabian rift belt (Fig. 3C). High heat flow values, extensive positive regional isostatic gravity anomalies and an area of relatively lower density upper mantle material recently revealed under them (VINNIK, 1976) testify in favour of the existence of active mantle diapir under the Trans-Caucasian transver-

sal tectonovolcanic zone. It is interesting to mention that the Trans-Caucasian tectono-volcanic transversal zone jointly with West-Arabian (Levantine) wrench fault zone of Afro-Arabian rift belt separates the western part of the Mediterranean orogenic belt with sharp prevalence of horizontal extension at the Late Orogenic stage from its eastern part with simultaneous manifestations of compression.

During the first, most powerful phase of the Late Orogenic volcanism (at the end of the Miocene-beginning of the Pliocene) explosive eruptions of essentially andesite and also more acid products (up to rhyolites) prevailed in the Trans-Caucasian zone. During the successive phases (in the Late Pliocene and Anthropogen) intensity of eruptions decreases on the whole, the part of extrusions of basic andesite-basalt and basalt lavas among their products increases. However, some local intracrustal magmatic chambers are preserved producing volcanic material of andesite-dacite, dacite and even rhyolite composition (Elbrus, Aragaz and other polygenic volcanoes).

In the platform framing of the Mediterranean belt significant intensification of volcanic activity also corresponds on the whole to the Late-Orogenic stage of its development. It is especially sharply displayed in the West-Arabian basalt province, i.e. in the northern part of the Afro-Arabian rift belt, directly eastward of the Red Sea rift and Levantine sinistral wrench fault zone.

The West-Arabian province with its immense Pliocene and Quaternary basalt extrusions almost directly joins the volcanic fields of the Trans-Caucasian transversal zone in the North. This testifies in favour of the direct connection between their deep magmatic sources.

In the Pliocene-Anthropogen volcanism is activated in both parts of Rhine-Lybian rift belt—its southern, North-African part (vast basalt fields of Tripolitania, contrast basaltrhyolite series of the Tibesti highland) and its northern, West-European part (volcanoes of the Central French massif). Reorientation of the direction of main extending stresses at the Late Orogenic stage in comparison with the Early Orogenic stage from WNW—ESE to SSW—NNE did not favour to wide manifestation of volcanism within the Rhine rift system.

In the Pliocene-Anthropogen basalt volcanism is activated on the westernmost parts of the platform frame of the Mediterranean belt—in Morocco and on the Iberian peripheral massif.

Conclusion

The brief review of Cenozoic volcanism in the Mediterranean belt and its relations with tectonic movements and structures given above show three main stages to be observed in the history of tectonic development and volcanism in this belt in the Cenozoic. These stages are: Late-geosynclinal or Pre-Orogenic (P_1 — P_2^{1-2}), Early Orogenic (P_2^3 — N_1) and Late Orogenic (the end of N_1 — Q).

During a peculiar tectonic pause separating Late Mesozoic and Cenozoic epochs of the strongest compressional deformations in the Mediterranean belt the most immense at the whole alpine cycle eruptions of calc-alkaline essentially andesitic series took place in the Early-Middle Eocene. Being so, volcanism occurred only in the eastern half of this belt, where nearly total absence of compressional deformations corresponds to the Early-Middle Eocene.

The Early Orogenic stage—the time of the most intensive compressional deformations, folding and nappe formation in most of the mountain structures of the Mediterranean belt and, evidently, of its general narrowing, — yields strongly, not less than 5 times, to the late geosynclinal stage by total volume of volcanic products, by the energy of volcanic processes and even more sharply— by volcanism intensity. It was especially low early in this stage (in the Late Eocene) and then in the Oligocene and the Miocene began to grow gradually. Volcanic areas at this stage were almost totally located on these median massifs under which development of mantle diapirs started at this epoch. Volcanic activity was directly connected with the intensity of deep material rise and interiors heating within their limits. In the uppermost part of the Earth's crust of such massifs differentiated block movements occurred and numerous extensional structures (horsts, deep grabens, faults, fractures) appeared. Thus, in spite of the regional compressional conditions in the Mediterranean belt the horizontal expansion of the intermountain arcas took place as if they were "crawling away" (Fig. 4.). Phases of volcanism intensification in median massifs do not generally coincide with phases of folding, i.e. intensification of the Mediterranean belt general compression but alternate with them.

During the Late Orogenic stage general compression in the western half of the belt sharply decreases and even ceases and processes of extension and graben formation are widely displayed. The latter involve even many alpine folded structures. Median massifs (intermountain areas) are subjected to deep subsidence ("collapse"). Deformations of compression go on only in the eastern part of the belt, mainly in its outer-most zones. Volcanism at this stage is considerably intensified, its mean intensity increases 5–6 times as compared with that of the Early Orogenic stage. Volcanic activity of the western part developing under conditions of certain general extension on the whole exceeds several times the one of the eastern part of the belt where compressional deformations go on. The main zones of volcanism remain (intermountain areas i.e. median massifs) and inner basins formed at some of their places. Volcanic areas, however, are displaced to their periphery spreading to those zones of adjacent folded structures, where compression conditions were replaced by those of certain extension at the Late Orogenic stage. Essentially intracrustal anatectic foci of acid volcanism in the western part of the belt predominant at the Early Orogenic stage are gradually replaced by the eruptions basic and alkaline-basaltic magmas of deeper (mantle) origin.

At the Late Orogenic stage the zone of Trans-Caucasian transversal uplift separating the western and eastern parts of the Mediterranean belt

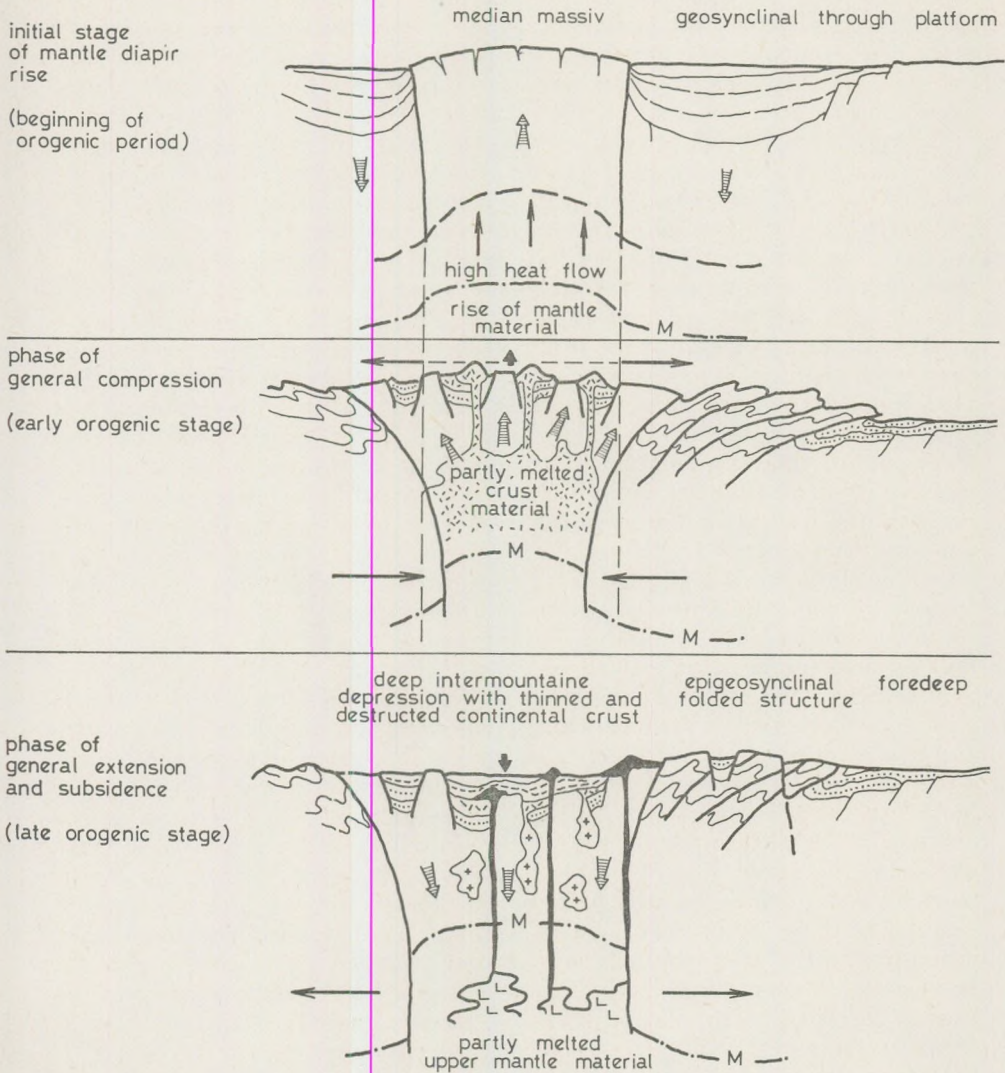


Fig. 4. Idealised scheme of mantle diapir evolution during the orogenic period of the development of the Mediterranean belt.

acquires the role of the most important volcanic province of this orogenic belt. This zone lies on a direct continuation of the submeridional Afro-Arabian rift belt, activated late in the Miocene-Pliocene and is its northern ending crossing the Alpine orogenic belt. Thus volcanic processes and tectonic deformations in the Trans-Caucasian transversal zone were evidently controlled by the development of a great submeridional system of mantle asthenoliths interacting in a complicated way with that of sublatitudinal deep structures of the Mediterranean belt.

As seen from all the above-said, manifestation and intensity of Cenozoic volcanism in the Mediterranean belt in time directly depended on the phenomena of extension and inversely — on those of compression. Volcanic zones were located in the areas of anomalously high heat flow subjected to horizontal extension (in a number of cases — local extension which took place under conditions of general compression). These empirical regularities concerning the conditions of orogenic volcanism manifestations appear to be common in principle with those of volcanism of rift zones, platforms and other tectonic structures. They can hardly be combined with the interpretation of the Cenozoic volcanism of the Mediterranean belt put forward by some researchers who try to explain it in the light of "classical" global tectonics conception — i.e. as island-arc type volcanism proceeding under conditions of collision and subduction of lithospheric plates.

REFERENCES

- ARTEMYEV, M. E. (1971): Some peculiarities of the deep structure of Mediterranean type depressions according data of isostatic gravity anomalies. — Bull. Moscow Soc. Natur., geol. section, N 4, pp. 39–52 (in Russian).
- BELLON, H., BROUSE, R. (1971): Le magmatisme perimediterranéen occidental. Essai de synthèse. — Bull. Soc. geol. France, t. XIX, D3, pp. 469–480.
- BELLON, H., COULON, CH., EDEL, I. B. (1977): Le déplacement de la Sardaigne. Synthèse des données géochronologiques, magnétiques et paléomagnétiques. — Bull. Soc. geol. France, t. XIX, N 4, pp. 825–831.
- BERRY, M. J., KNOPOFF, L. (1967): Structure of the upper mantle under the Western Mediterranean basin. — Journ. Geophys. Res. 72, 14.
- ČERMAK, V., RYBÁČEK, L. (ed.) (1979): Terrestrial heat flow in Europe. — Berlin, Heidelberg, Springer-Verlag, 328 pp.
- D'ARGENIO, B., HORVATH, F., CHANNEL, I. (1980): Paleotectonic evolution of adriatic African promontory. — In: Colloque C. 5. Géologie des chaînes alpines issues de la Tethys, du 26. OGI. Paris, pp. 331–351.
- GROD, M., GROD, N. (1977): Contribution de la pétrologie à la connaissance de l'évolution de la Méditerranée occidentale depuis l'oligocène. — Bull. Soc. geol., France, t. XIX, N 3, pp. 481–488.
- GLANGEAUD, L. (1954): Les éruptions tertiaires Nord-Africaines, leurs relations avec la tectonique Méditerranéenne. — Compt. rendu XIX Section Congr. geol. Intern. Alger, 1952. Section XI Fasc. XVII. Alger.
- ILLIES, J. H. (1969): An intercontinental belt of the world rift system. — Tectonophysics, 8(1), pp. 5–29.
- ILLIES, J. H. (1975): Recent and paleo-intraplate tectonics in stable Europe and Rhinegraben rift system. — Tectonophysics, 29, pp. 251, 264.
- KHAIN, V. E. and LEVIN, L. E. (1978): Tectonic types of the marginal and interior seas with oceanic and suboceanic crust. — Vestnik Moscovskogo Universiteta, series geol., N 6, p. 3–18. (in Russian).
- KORONOVSKY, N. V. (1979): Paleogene volcanism at the geological history of the east part of the Alpine folded belt. — Vestnik Moscovskogo Universiteta, series geol., N 2, p. 3–16, N 3, pp. 30–42. (in Russian).
- MALOVITSKY, J. A. P. (1978): Tectonics of the Mediterranean Sea bottom. — Moscow, "Nauka", 96 pp. (in Russian).
- MILANOVSKY, E. E. (1969): Regularities in distribution and development of orogenic cenozoic volcanism in Alpine belt of South-Western part of Eurasia. — In: "Problems of connection between tectonics and magmatism" Moscow, "Nauka", pp. 153–184 (in Russian).
- MILANOVSKY, E. E. (1972): To the problem of spatial interrelations between geosynclinal-orogenic and rift belts. — Vestnik Moscovskogo Universiteta, series geol., N 4, pp. 3–18, (in Russian).
- MILANOVSKY, E. E. (1974): Geodynamics and volcanism of orogenic belts. — In: "Geodynamics, generation of magma and volcanism". Petropavlovsk-Kamchatskiy, pp. 32–50 (in Russian).
- MILANOVSKY, E. E. (1974): Consolidated massifs and deep-sea depressions. — In: "Tectonics of median massifs", Moscow, p. 4–8.
- MILANOVSKY, E. E. (1978): Some regularities of tectonic development and volcanism of the Earth during phanerozoic (problems of the Earth pulsations and expansion). — "Geotectonics", N 6, pp. 3–16 (in Russian).

- MILANOVSKY, E. E., KORONOVSKY, N. V. (1973): Der orogene spätkänozoische Vulkanismus Eurasiens und seine Beziehungen zur Tektonik. — "Stockwerkbau und Felderteilung"; Veröff. Zentralinst. Physik der Erde, N 14, Potsdam, pp. 257—267.
- MILANOVSKY, E. E., KORONOVSKY, N. V. (1973): Orogenic volcanism and tectonics of Alpine belt of Eurasia. — Moscow, "Nedra", (in Russian), 280 pp.
- MILANOVSKY, E. E., KORONOVSKY, N. V. (1976): Quantitative estimation of products of orogenic volcanism in Alpine belt of Eurasia. — Transactions of X. Congr. Karpato-Balkan. geol., Ass. Bratislava.
- LE PICHON, X. and ANGELIER, Y. (1979): The hellenic arc and trench system: a key to the neotectonic evolution of the Eastern Mediterranean. — Tectonophysics, 60, pp. 1—52.
- STEGENA, L., GÉCZY, B., HORVÁTH, F. (1975): Late cenozoic evolution of the Pannonian basin. — Tectonophysics, 26, pp. 71—90.
- TRÜMPI, R. (1973): The timing of orogenic events in the Central Alps. — In: Gravity and tectonics. K. A. De Yong and R. Scholten (eds.). John Wiley and Sons. New York, pp. 229—251.
- VYNNIK, L. P. (1976): Earth mantle investigations by means of seismic methods. — Moscow, "Nauka", 200 pp. (in Russian).

LATE OLIGOCENE MOLLUSCS FROM A SAND-PIT NEAR MÁRIAHALOM (HUNGARY): A PRELIMINARY STUDY

by

A. W. JANSSEN

Rijksmuseum van Geologie en Mineralogie, Hooglandse Kerkgracht 17,

Leiden - The Netherlands

(Received: 15th March, 1981)

Introduction

In Hungary Late Oligocene deposits are known to occur in an area with a length of about 300 km and a width of 50 to 100 km, situated in the central-northern part of the country. This area forms part of the Paratethyan Carpathian Basin. The deposits, occurring in a large variety of sediments and containing many different types of faunas, are mostly known from borings, and from relatively few outcrops. The sediments and their faunas have been the subject of a large number of publications. The general geology and the mollusc faunas of the Hungarian Late Oligocene were investigated extensively by BÁLDI (1973). The stratigraphy of the Late Oligocene sediments in the central Paratethys has been revised substantially in the first volumen of "Chronostratigraphie und Neostratotypen", edited by Báldi and Senes, with the cooperation of many well-known specialists (BÁLDI and SENES, 1975). For further details on the deposits concerned, the reader is referred to these two publications.

The outcrop of Máriahalom was mentioned for the first time by BÁLDI and CSÁGOLY (in BÁLDI and SENES, 1975), who designated the exposed sediments as a facies stratotype of the Egerian stage and gave a list of the mollusc species found by them. BÁLDI (1976) also gives a list of the mollusc fauna.

In October 1979, accompanied by Dr. T. Báldi, I had the occasion to visit the sand-pit near Máriahalom and to collect mollusc material for the collections of the Rijksmuseum van Geologie en Mineralogie at Leiden (RGM). This visit was realized within the framework of a field-trip to Poland and Hungary during which many Oligocene and Miocene localities in both countries were visited (JANSSEN, 1980).

In this paper, which is a slightly modified version of an internal report (RGM, dept. of European Caenozoic Mollusca, report nr. bg. 25 June 1980) the material collected at Máriahalom is evaluated provisionally. I wish to express my sincere gratitude to Dr. Báldi for his guidance to this and several other localities in Hungary, thus enabling me to collect very valuable additions to our museum's collections.

Location of the sand-pit and collecting methods

The village of Máriahalom lies about 30 km NW of Budapest. The sand-pit is exploited on the southern side of the road between Uny and Máriahalom (see map in BÁLDI & CSÁGOLY, 1975, p. 134, fig. 20).

The height of the outcrop at the time of the visit was approximately 10 meters (see text-fig. 1.). Greyish, rather coarse quartz sands were exposed, containing abundant shells, sometimes in sharply delimited pockets and lenses (text-fig. 2 and 3.). The sediment shows many cross-beddings and other sedimentary structures. The faunal composition seems to differ slightly in the various lenses and pockets. On the bottom of the pit large concretionary blocks and slabs are present, containing imprints of tree leaves and stems and pieces of driftwood, frequently attacked by Terebinthids. In text-fig. 1. such slabs are visible in situ. Small fragments of these concretions were found in the residues.

Mollusc material was collected by picking isolated specimens from the sediment (mainly the larger species) and by sieving the sediment on meshes of 0.5 and 2.5 mm. Therefore the residues can be used only for a qualitative investigation of the fauna.

The preservation of the molluscs is moderate. Some specimens show signs of transportation. The sediment is in an early stage of decalcification, so the shells are very brittle and especially the larger specimens have to be packed carefully before transportation. All shells are covered with quartz grains sticking to their surface and difficult to remove, especially from the smaller specimens. Afterwards it was necessary to impregnate many shells with a plastic/acetone solution to achieve a lasting preservation in the collection.

Altogether some 38 kg of samples were collected. In the laboratory these samples were dried and fractionated. Each fraction was picked out and many specimens were subsequently treated with the plastic solution. The laboratory treatment of the samples was mainly done by Mr C. P. BARNARD, whose dedication is gratefully acknowledged.

Stratigraphy

According to BÁLDI & CSÁGOLY (1975, p. 134), the Late Oligocene Mány Formation in the Máriahalom area unconformably overlies Triassic or Eocene deposits. The entire formation has a thickness of 300 to 500 m. It shows a transgressive sequence with freshwater and brackish deposits at its base, changing into shallow marine and medium-depth sublittoral deposits higher in the section. On top of the Mány Formation Miocene sediments are present, separated by a sedimentary hiatus. The entire section of the Mány Formation is assumed to be of Late Oligocene (Egerian) age (BÁLDI, 1976).

In the sand-pit only a small part of the Mány Formation is visible. Comparison with some nearby boring-sections made it clear that the sediments in the outcrop represent a small section from the lower part of the formation (BÁLDI & CSÁGOLY, 1975), which is in accordance with the mollusc-fauna composition.

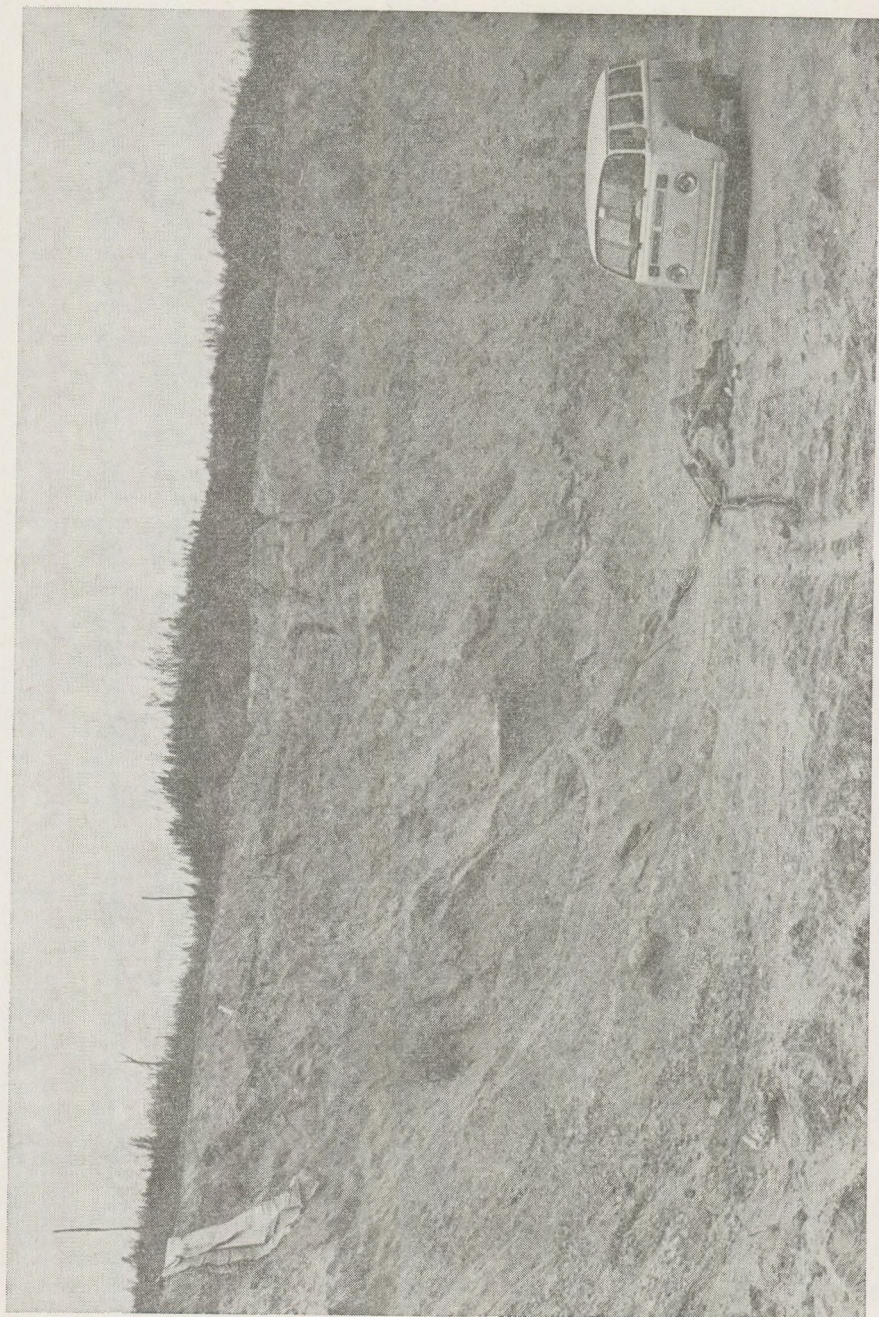


Fig. 1. General view of the Máriahalom sand-pit. Fossiliferous sands of the Late Oligocene (Egerian) Many Formation, about 10 m in height, are cropping out. October 1979



Fig. 2. Detail of the excavation-front of the Máriahalom sand-pit, upper part of the section
October 1979



Fig. 3. Detail of a pocket-like shell concentration in the upper part of the excavation-front of the Máriahalom sand-pit. Many specimens of *Potamides margaritaceus*, *P. lamarcki* and *Pirenella plicata* s. lat. October 1979.

Annotated list of mollusc species

Below all mollusc species found by me are listed. In each case the number of specimens is indicated approximately. Wherever relevant the name presumably assigned to a species by BÁLDI & CSÁGOLY (1975) is added. Several species, apparently new to this fauna or otherwise of interest, are represented on the accompanying plates.

It is emphatically stated that many names have a provisional character. It was especially difficult to establish sound identifications, for those species not treated in Báldi's 1973 monograph as a large part of the Paratethys mollusc literature is not at my disposal. Therefore this study should be regarded merely as a tentative indication of which forms are present. For a final elaboration of this fauna extensive comparisons will be necessary, with other Paratethys faunas as well as with Atlantic-Boreal ones.

1. *Nucula (Nucula) aff. nucleus* (LINNÉ, 1758)

Plate 1, fig. 1/a – b

Not mentioned by BÁLDI and CSÁGOLY (1975). Material: 3/1, 26/2 and 25/2 defective specimens. The maximal shell-length is about 6 mm. The umbonal angle is relatively small. The shell-surface sometimes shows an interruption of regular growth. Very fine radial sculpture is always present. This form belongs to a group of species that urgently needs revision.

2. *Nuculana (Saccella) anticeplicata* (ROTH von TELEGD, 1914)

Not mentioned by BÁLDI & CSÁGOLY. Material: 4/2 specimens and 14 fragments. All specimens have distinctly coarser concentric sculpture than those figured by BÁLDI (1973, p. 161, pl. 2, fig. 1 – 2). Some shells show a reduction of this sculpture to an almost completely smooth surface. Maximal shell-length about 6 mm.

3. *Glycymeris (Glycymeris) latiradiata latiradiata* (GÜMBEL, 1861)

Glycymeris latiradiata Sandb., 1861 juv. in BÁLDI & CSÁGOLY (1975). *Glycymeris obovata* Lamarck, in BÁLDI (1976). Material: 2/1, 25/2 and 25/2 juvenile specimens. Dimensions and ratios of the present specimens correspond completely with the nominal subspecies, judging from the statistical data given by BÁLDI (1973, p. 171). The largest specimen has a length of about 60 mm. This is the typical species of the so-called "Pectunculus sands", a shallow-marine deposit of the Hungarian Egerian. Its common occurrence, even in double-valved specimens, in the Máriahalom fauna with a mainly euryhaline character is remarkable!

4. *Mytilus (Mytilus) sp.*

Mytilus aquitanicus May., 1858 in BÁLDI & CSÁGOLY (?). Material: 1/2 mould with remnants of the actual shell and about 35 shell-fragments. The ventral margin of the shell is almost straight and not concave, as in *M. aquitanicus*. Also the Máriahalom specimen is distinctly less convex and wider in relation to its length. In *M. chatticus* GÖRGES, 1952 the shell is

more slender. As only one specimen is available it is impossible to obtain an impression of the variability of this species, therefore it is mentioned here in open nomenclature.

5. *Musculus (Musculus) sp.*

Plate 1, fig. 3

Not mentioned by BÁLDI & CSÁGOLY. Material: 2/2 juvenile specimens. Length approximately 1.5 mm. These specimens are too small for specific identification. *Musculus philippi* (MAYER in WOLFF, 1897) mentioned by BÁLDI (1973, p. 174. pl. 4, fig. 3) from the Hungarian Oligocene belongs, according to R. JANSSEN (1979, p. 42), to the genus *Modiolus*.

6. *Pinctada phalaenacea (Lamarck, 1819)*

Not mentioned by BÁLDI & CSÁGOLY (1975), but BÁLDI (1973) recognized this species in Late-Oligocene medium-depth sublittoral facies, especially in the Pitar beyrichi community. Material: 200/2 defective specimens. All shells are juvenile, so in fact it is impossible to distinguish between this species and *P. Stampinensis (Deshayes)*. The latter species is mainly known, however, from Middle-Oligocene deposits.

7. *Isognomon (Isognomon) heberti (COSSMANN and LAMBER, 1884)*

Plate 1, fig. 2

Isognomon of. *heberti* COSSM. et LAMB., 1884 in BÁLDI & CSÁGOLY (1975). Material: 1/2 juvenile specimen. The form of the ligamental furrows corresponds completely with the description in ZILCH (1938. pl. 1, fig. 3).

8. *Anomia (Anomia) ephippium LINNÉ, 1758*

Anomia ephippium Linné, 1758 in BÁLDI & CSÁGOLY (1975). Material: 1/1 juvenile and 21/2 adult specimens. In all specimens the adductor scars are very well visible. The position corresponds perfectly with equal-sized recent specimens of this species: one large circular scar with two smaller ones horizontally below it. In larger Recent specimens the two smaller scars are situated on an oblique line. In each case the scars are completely separated.

9. *Ostrea cyathula LAMARCK, 1806*

Ostrea cyathula LAM., 1806 in BÁLDI & CSÁGOLY (1975). Material: many isolated valves, some of them attached to gastropods. From 1965 onwards this species was included in the genus *Crassostrea* (fide R. JANSSEN, 1979 and Neuffer, 1973). I. agree with DR. BÁLDI (in litt.) however that it should be incorporated into *Ostrea*: The roundish outline, the form and the position of the adductor scar and the presence of chomata settle the matter convincingly.

10. *Linga (Linga) oligocaenica (COSSMANN, 1921)*

Linga columbella LAM., 1818 in BÁLDI & CSÁGOLY (1975). Material: 21/2 specimens and 66 fragments. This form is smaller, and much less con-

vex than *L. columbella* (Lamarck, 1819). Furthermore the concentric sculpture is considerably coarser. No doubt this is the Oligocene precursor of *L. columbella*. I cannot decide whether or not it might be preferable to consider *oligocaenica* as a subspecies of *columbella*.

11. *Parvilucina* (*Microloripes*) sp.

Plate 1, fig. 4

Material: 351/2 and 5/1 specimens. This species is not mentioned by BÁLDI & CSÁGOLY, which is surprising because it is quite abundant. Maximal shell-length to somewhat over 4 mm. The shell is slightly higher than long and has a very weak concentric sculpture.

12. *Saxolucina* (*Saxolucina*) *heberti* (DESHAYES, 1857)

Plate 1, fig. 5

Saxolucina bellardiana May., 1864 in BÁLDI & CSÁGOLY (1975). Material: 4/2 specimens and 11 fragments. This species may be identical with *S. bellardiana*, judging from photographs given by SACCO (1901, pl. 17, fig. 29–37), but the present material is too poor for a final decision. Some specimens have radial folds, concentric sculpture may be present or absent. Directly compared specimens of *S. heberti* from the Oligocene of the Etampes Basin (France) correspond perfectly, also in their variations.

13. *Divalinga* (*Divalinga*) *ornata* (AGASSIZ, 1845)

Divalinga ornata AGASSIZ, 1845 in BÁLDI & CSÁGOLY (1975). Material: 4/1 and numerous loose valves.

14. *Felaniella* (*Felaniella*) aff. *nysti* (BOSQUET, 1868)

Plate 1, fig. 6

Diplodonta fragilis Braun, 1851 in BÁLDI & CSÁGOLY (1975)? Material: 41/2 more or less defective specimens. The species *D. rotundata* could not be recognized among the available material. It is mentioned by BÁLDI & CSÁGOLY, so it might be present between the hinge fragments. In my opinion the Máriahalom shells correspond much better, although not completely, with *F. nysti* (compare GLIBERT & de HEINZELIN, 1954, pl. 2, fig. 13) than with *F. fragilis* (SANDBERGER, 1863). The latter species has a rounded outline, whereas *F. nysti* has a more or less straightened posterior margin. *F. nysti*, however, seems to be somewhat longer in relation to its height than the Máriahalom specimens.

15. *Mysella* (*Mysella*) sp.

Plate 1, fig. 7

Not mentioned by BÁLDI & CSÁGOLY (1975). Material: 2/2 juvenile specimens. Shell length about 1 mm. Both specimens, a left and a right valve, are obliquely oval, with their umbones behind the midline. The right valve has two long lateral teeth (pl. 1, fig. 7), left valve without any teeth. In both valves a ligamental resilium is visible in an oblique view from the ventral margin. The material is insufficient for specific identification.

16. *Venericardia (Venericardia) sp.*

Cardita monilifera Duj., 1837 in BÁLDI & CSÁGOLY (1975). Material: 2/1, 21/2, 50/2 juveniles and 20 fragments. *V. monilifera* (compare COSSMANN & PEYROT, 1912, pl. 3, fig. 9–12) has an entirely different outline. The present material resembles much more closely *V. bazini* (Deshayes), from the Oligocene of the Etampes area in France. In this latter species, however, the radial ribs are narrower and more pronounced, with obvious spines. The shell of *V. bazini* is somewhat more convex, and in the left valve the lateral tooth is more developed. Still, in general form and further hinge details there are many similarities with the Máriahalom specimens. The specimens from Dömös, shown by BÁLDI (1973, pl. 12, fig. 2–3) seem to agree better with *V. monilifera*. The shell of fig. 1 is again very different in outline. *V. monilifera* is only known from the Miocene (Helvetian and? Tortonian, see GLIBERT and van de POEL, 1970, p. 124) sediments, which restrains me from considering both forms to be identical without a direct comparison. For the time being the best indication for the Dömös specimens seems to be *V. (V.) aff. monilifera*, which is also Dr Báldi's view now (in litt.).

17. *Erycinella clara (von KOENEN, 1893)*

Plate 1, fig. 8a–b

Not mentioned by BÁLDI & CSÁGOLY (1975). Material: 7/2 specimens. These specimens fit very well within the description by von Koenen, as well as within that of COSSMANN (1922, p. 127, pl. 7, fig. 45–49). All specimens remain below a shell length of 2 mm.

18. *Goodallia (? Goodallia) sp.*

Plate 1, fig. 9a–b

Not mentioned by BÁLDI & CSÁGOLY (1975). Material: 1/1 and 1/2 specimen. This form differs from *Goodallia* s. str. in the presence of a well-developed anterior lateral tooth in both valves. The ventral margin is not crenulated. The outer surface is devoid of any concentric sculpture.

19. *Laevicardium (? Dinocardium) kovacovense (SENES, 1958)*

Not mentioned by BÁLDI and CSÁGOLY. Material: 16 fragments. Unfortunately only very defective material was collected, which however corresponds much better with *L. kovacovense* than with *Cardium neglectum*. This latter species was found at Máriahalom by BÁLDI & CSÁGOLY. It is not impossible that the two species occur in the present material, but the state of preservation of many fragments is poor. The radial sculpture of *C. neglectum* is so different that it is not very probable, however, that this species is represented in my material.

20. *Parvicardium sp.*

Plate 1, fig. 10

Not mentioned by BÁLDI & CSÁGOLY. Material: 1/2 very defective juvenile specimen. The shell has about 25 radial ribs with obvious knobs.

The outline of the shell must have been somewhat squarish, an obtuse carina is present near the seventeenth radial rib.

21. *Spisula (Spisula) subtruncata* (da COSTA, 1778)

Not mentioned by BÁLDI & CSÁGOLY (1975). Material: 30 fragments. One or two complete valves were observed during collecting, but they did not stand the transportation, because of their extreme fragility. Both lunula and area carry obvious fan sculpture, characteristic for *S. subtruncata*. For further details of the occurrence of this species in Late Oligocene deposits see R. JANSSEN (1979, p. 105).

22. *Angulus (Peronaea) ancestralis* BÁLDI, 1973.

Tellina (Serratina) serrata RENIER, 1804 in BÁLDI & CSÁGOLY? Material: 13 fragments. This material too is very fragmentary, so it might be heterogeneous. *A. lamellosus* (DOLLFUS, BERKELEY COTTER & GOMEZ), which could be directly compared (specimens from the locus typicus Caccella), has a much coarser concentric sculpture. *A. serrata* could be compared from several localities. Rostral fragments of the present species look very much like *serrata* at first sight, but closer examination reveals important differences. BÁLDI (1976) mentions also *T. perrandoi* Mayer; this species seems to be absent in my material.

23. *Arcopagia (Arcopagia) cf. subelegans* (d'ORBIGNY, 1852)

Not mentioned by BÁLDI & CSÁGOLY (1975). Material: 1 fragment. The concentric sculpture is finer than in the specimens represented by BÁLDI (1973, pl. 20, fig. 7).

24. *Macoma (Psammacoma) elliptica* (BROCCHI, 1814)

Not mentioned by BÁLDI & CSÁGOLY (1975). Material: 4 fragments.

25. *Gari (Psammotaena) sp.*

Gari protracta May., 1893 in BÁLDI & CSÁGOLY (1975). Material: 21 fragments. The material is too fragmentary for a judgement of the general outline, so it is very difficult to decide which species it belongs to. Apparently the present species is very close to *G. protracta*, as described and illustrated by BÁLDI (1973, p. 221, pl. 20, figs. 1 and 4). On the other hand, a direct comparison with *G. angusta* (PHILIPPI, 1943) from the Late Oligocene of the Lower Rhine area (compare R. JANSSEN, 1979, p. 114, pl. 3, fig. 60) revealed only minor differences. Therefore I consider the available material insufficient for a sound identification. A final decision will have to wait until specimens with a complete outline are available.

26. *Congeria basteroti* (DESHAYES, 1836)

Congeria basteroti Desh., 1836 in BÁLDI & CSÁGOLY. Material: 5/2 specimens and 28 fragments. The name *basteroti* is applied to this material on the authority of BÁLDI (1973, p. 197). My material is insufficient to decide whether or not this form could be identical with *C. nystiana* (d'ORBIGNY,

1852) or *C. brardi* (BRONGNIART, 1823). Both of the latter two species are known from Oligocene deposits, whereas *C. basteroti* occurs in Miocene faunas.

27. *Coralliophaga* sp.

Plate 1, fig. 11

Not mentioned by BÁLDI & CSÁGOLY. Material: 4 fragments. One of the defective shells shows remnants of a fine radial sculpture. At least one of the other specimens seems to be devoid of this sculpture, but its surface is strongly affected as a result of sand grains sticking to the shell.

28. *Dentonia gestlini* (DESHAYES, 1830)

Plate 1, fig. 13

Not mentioned in BÁLDI & CSÁGOLY (1975). Material: 2/2 and 2/2 defective specimens. This species is easily distinguished from *Polymesoda convexa brongniarti* by its flatter and more roundish shell, the absence of the pallial sinus and differences in the hinge elements. This is the first record of this species from Hungary.

29. *Polymesoda (Pseudocyrena) convexa brongniarti* (BASTEROT, 1825)

Polymesoda convexa s. str. Brong., 1822 and *Polymesoda convexa brongniarti* Bast., 1825 in BÁLDI & CSÁGOLY (1975). Material: 16/2 specimens and 30 fragments. As two subspecific forms of one and the same species should not occur together I reckon also the smaller specimens to the subsp. *brongniarti*. The largest shell has a length of almost 70 mm and therefore the identification seems to be correct indeed, in spite of the fact that this subspecies is only known from Miocene faunas. Also other characteristics (form, sculpture) correspond to *brongniarti*.

30. *Callista (Costacallista)* sp.

Not mentioned by BÁLDI & CSÁGOLY (1975). Material: 34/2, mainly juvenile specimens and 25 fragments. The sculpture of the outer surface varies from regular and dense concentric riblets to almost completely smooth. In this respect there is analogy with the sculptured *C. beyrichi* (SEMPER, 1861) and the almost smooth *C. reussi* (SPEYER, 1866), both occurring in the North Sea Basin Late Oligocene, and very often hard to distinguish by means of the sculpture. Both latter forms can, however, always be separated by hinge characteristics (e.g. the angle between the cardinal teeth in both valves). But even the specimens with the strongest concentric sculpture from Máriahalom have the hinge features of the smooth *C. reussi*. Final identification therefore requires a more profound study and more material.

31. *Callista* (s. lat.) sp.

Plate 1, fig. 12

Callista undata Basterot, 1825 in BÁLDI & CSÁGOLY? Material: 5/1 juvenile and 120/2 adult specimens. This species may be distinguished from

Callista (Costacallista) sp. by its more triangular shell form, resembling the genus *Tivelina*. In this latter genus, however, the cardinal teeth diverge considerably more than in the Máriahalom specimens. *C. undata* Basterot has a length of about 35 mm and is only known from Miocene deposits. The material from Máriahalom has a maximal length of approximately 9 mm. It might represent an ancestral form of *undata*.

32. *Venus (Ventricoloidea) multilamella interstriata* (ROTH von TELEGD, 1914)

Not mentioned by BÁLDI & CSÁGOLY (1975). Material: 4/2 juvenile specimens and 7 fragments.

33. *Pelecypora (Cordiopsis) polytropa suborbicularis* (COLDFUSS, 1841)

Pelecypora (Cordiopsis) polytropa And., 1858 (sic!) in BÁLDI & CSÁGOLY. Material: 8/2, 4 fragments, 2/1 and 21/2 juvenile specimens. The Hungarian form corresponds with the subspecies *suborbicularis*, which is also a regular component of the Late Oligocene faunas in the North Sea Basin. Juvenile specimens from Máriahalom show a wide range of variability, so it is not excluded that among them another species (? *Dosinia* sp.) is present.

34. *Chamelea* sp.

Plate 2, fig. 1–2

Not mentioned by BÁLDI & CSÁGOLY. Material: 2/2 defective specimens. Both shells are too poorly preserved for a sound identification. The shell form is rounded triangular, the outer surface bears a vague concentric ribbing.

– Veneridae sp. indet.

Material: many fragments. These fragments belong to some venerid species, judging from their hinge structure, but they are too badly preserved to enable identifications. Presumably most of them will belong to one of the two *Callista* species or to *Pelecypora*, mentioned above.

35. *Corbula (Varicorbula) gibba gibba* (OLIVI, 1792)

Not mentioned by BÁLDI & CSÁGOLY (1975). Material: 1/2 specimen. Only one, very typical right valve was found. Its length (6.7 mm) indicates that it belongs to *C. gibba* s. str.

36. *Caryocorbula (Caryocorbula) basteroti* (HOERNES, 1870)

Corbula basteroti HÖRNES, 1870 in BÁLDI & CSÁGOLY. Material: 2/2 specimens and 16 fragments. The specimens fit perfectly within the descriptions in the literature (e.g. HOERNES, 1870; ANDERSON, 1959; BÁLDI, 1973). Apparently this is not an extreme form of the next species, although juvenile specimens are very similar.

37. *Caryocorbula (Caryocorbula) revoluta hoernesii* (COSSMANN & PEYROT, 1909)

Corbula carinata Duj., 1837 in BÁLDI & CSÁGOLY. Material: abundant isolated valves and several double-valved specimens. The shells seem to be somewhat longer (on the average), than those illustrated by COSSMANN & PEYROT (1909, pl. 2, fig. 61–65). BÁLDI (1973, p. 234, sub nomen *Corbula carinata*) also agreed with the identity of this form with *hoernesii*. For the denomination of the various forms of *C. revoluta* the reader is referred to GLIBERT & van de POEL (1966, p. 51). In contrast to their opinion, however, I do not regard *C. basteroti* (*Hoernes*) as a nomen nudum!

38. *Lentidium (Lentidium) modelli* (HÖLZL, 1958)

Lentidium modelli HÖLZL, 1958 in BÁLDI & CSÁGOLY (1975). Material: 140/2, mainly defective specimens. This species belongs to a group of related forms (*sphenoides* Sandberger, *elongatum* Sandberger, *donaciforme* Nyst, *morleti* Meunier, *burdigalense* Benoist, may be also *subcomplanatum* d'Orbigny and others) for which it would be convenient to establish a separate subgenus.

39. *Lentidium (Lentidium)* sp.

Plate 2, fig. 6–8

Lentidium tournoueri May., 1864 in BÁLDI & CSÁGOLY. Material: 70/1 and 350/2 specimens, mainly juveniles. The present material is very heterogeneous in its length/height-ratio and may therefore belong to more than one species. All specimens, however, belong in the group of species in which the shell is inaequivalve, with the left valve resting in the right valve and leaving there an obvious scar (see plate 2, fig. 6–7). In another group of species the shell is aequivalve with the ventral margins touching each other. To this latter group belongs e.g. *L. triangula* (Nyst).

40. *Martesia (Martesia)* sp.

Plate 2, fig. 3–4

Not mentioned by BÁLDI & CSÁGOLY (1975). Material: 2/2 juvenile valves, 17 fragments, 1 defective mesoplax. The material is in general too much worn for a detailed description. The sculpture of the outer surface is usually only very locally preserved. The anterior side of the shell is beaked, the callum reaches almost to the umbo. The posterior side is irregularly produced. The mesoplax has a pentagonal form, its dorsal side is gibbose, ventrally the septum shows concentric growth lines and a longitudinal seam.

41. ? *Teredina* sp.

Plate 2, fig. 5

Not mentioned by BÁLDI & CSÁGOLY. Material: 1 fragment of calcareous tube. The posterior end of the tube shows an opening in the form of an 8, with a crown of denticles on the inside (compare MOORE, 1969, p. N726, fig. E189–6a–b).

42. *Teredinidae* sp. indet.

Teredo sp. in BÁLDI & CSÁGOLY. Material: 2 shell fragments, 22 fragments of calcareous tubes. Many specimens with only the calcareous tubes visible, are present in a concretion collected from the bottom of the sand-pit. The available material is insufficient even to identify the genus.

43. *Dentalium (Antalis) seminudum* Deshayes, 1861

Plate 2, fig. 9

Not found by BÁLDI & CSÁGOLY (1975). Material: 18 more or less defective specimens, most of them rather strogly worn. There are about 12 primary ribs and no secondary ones. The sculpture fades away in the direction of the aperture. The radial sculpture corresponds very well with specimens of this species from Ormoy (Étampes area, France), it is much coarser and stronger than in *D. (A.) pseudofissura* R. JANSSEN, 1978, from Late Oligocene deposits in the North Sea Basin.

44. *Cadulus (Dischides)* sp.

Plate 2, fig. 10–11

Not mentioned in BÁLDI & CSÁGOLY. Material: 28 fragments. The smooth surface, the rate of curvature and the fact that the aperture is narrowed again (plate 2, fig. 11) are characteristic for this group. Unfortunately the apical lobes of the shell are not preserved. This species is at least related to *C. (D.) subpolitum* (COSSMAN & PEYROT, 1916). *C. (D.) rhenanus* R. JANSSEN, 1978, found in Late Oligocene sediments of the North Sea Basin, is markedly more slender.

45. *Patella (Patella)* aff. *neglecta* Michelotti, 1847

Not mentioned by BÁLDI & CSÁGOLY. Material: 1 defective shell and 2 fragments. The form and the sculpture of the only specimen from Máriahalom correspond fairly well with the literature data of *P. neglecta*, but its size is remarkable (length about 45 mm!). As I have no material at my disposal for a direct comparison I prefer to mention this species in open nomenclature.

46. *Jujubinus (Scrobiculinus)* sp.

Plate 2, fig. 12

Calliostoma tournoueri C. et P., 1917 in BÁLDI & CSÁGOLY. Material: 225 specimens, among which many juveniles. The various species in this group described from Oligocene and Miocene deposits are so variable and resemble each other so strongly that I find it impossible to apply any of the available names to the Hungarian specimens with some degree of certainty.

47. *Skenea* sp.

Plate 2, fig. 18

Not mentioned by BÁLDI & CSÁGOLY (1975). Material: 1 specimen. Very small shell (diameter just over 1 mm), wider than high, with three convex whorls. The nucleus of the protoconch is obliquely embedded. There is a wide umbilicus, very vague spiral lines are visible around it.

48. *Circulus* sp.

Plate 2, fig. 13

Not found by BÁLDI & CSÁGOLY (1975). Material: 4 specimens. The shells resemble very much the strongly sculptured form of *C. dubius* (PHILIPPI, 1843) (see R. JANSSEN, 1978, p. 159, pl. 11, fig. 35–36), but their diameter is about twice that of *dubius* and they are relatively somewhat higher. I could compare the material with specimens from the Late Oligocene of the Lower Rhine area, having the same number of whorls as the Máriahalom specimens, which may represent a local subspecies of *dubius*.

49. *Clithon* (*Vittoclython*) aff. *pictus* (FÉRUSAC, 1825)

Plate 2, fig. 15–17

Theodoxus pictus FÉR., 1825 in BÁLDI & CSÁGOLY. Material: many hundreds of specimens. The larger specimens are relatively more conical and higher than the smaller shells (compare drawings). For this reason this material differs strongly from the typical Miocene form of *C. pictus*, which is globular or even carinated (compare e.g. HOERNES, 1856, p. 535, pl. 47, fig. 14); such forms are absent in the Máriahalom fauna. The Máriahalom specimens correspond better with *C. buekkensis* (*Roth von Teledt*) as represented in BÁLDI (1973, pl. 24, fig. 8–9), but Báldi's description indicates that the shell form of this species is identical with *C. pictus* and that the main differences between these two species lie in the patterns. So I find it difficult to decide what name to use for this material.

50. *Theodoxus* (*Calvertia*) aff. *grateloupianus* (FÉRUSAC, 1821)

Plate 2, fig. 14

Theodoxus grateloupianus FÉR., 1821 in BÁLDI & CSÁGOLY. Material: 1 slightly defective specimen. Differs in form and colour pattern strongly from the foregoing species, but the shell is not as much broadened as indicated by BÁLDI (1973, p. 245, pl. 25, fig. 1–2). The only available specimen is insufficient for further considerations. Apart from that *T. grateloupianus* is also one of the species with an exclusive Miocene distribution pattern.

51. *Nerita* (*Theliostyla*) *plutonis* BASTEROT, 1825

Nerita plutonis BASTEROT, 1825 in BÁLDI & CSÁGOLY (1975). Material: 30 specimens. Although also *N. plutonis* is a "Miocene species" the Máriahalom material agrees so well with the various literature data that the identification seems to be certain. Oligocene ancestral forms are known from Northern Italy (SACCO, 1896).

52. *Littorina* (*Melaraphe*) sp.

Plate 3, fig. 9

Littorina sp. in BÁLDI & CSÁGOLY? Material: 3 specimens. This form differs from *L. obtusangula* Sandberger by its relatively wide body-whorl, which is not angular.

53. Hydrobiidae sp.

Plate 3, fig. 5a–b

Not mentioned by BÁLDI & CSÁGOLY (1975). Material: 4 specimens. Small, conical shell with rather convex and smooth whorls. The umbilicus is closed in juvenile specimens and only a narrow fissure in adult ones. The apertural lip is slightly thickened externally.

54. *Stenothyrella* sp. (div. ?)

Plate 3, fig. 7–8

Not mentioned by BÁLDI & CSÁGOLY (1975). Material: 6 specimens. The variability in size and convexity of the whorls and also the fact that there are specimens with two small teeth in the aperture while others have none, leads to the assumption that the sample is heterogeneous. The number of specimens is, however, too small for specific identifications, especially because *Stenothyrella* species as a rule resemble each other closely.

55. *Rissoidea* sp. 1

Plate 3, fig. 6

Not found by BÁLDI & CSÁGOLY. Material: 19 specimens in rather bad state of preservation. Height of the shell about 8 mm. The shell is thick-walled, conical, with rather flat whorls; there is only a very slight indication of radial sculpture. The apertural lip is slightly thickened externally, internally are several solid teeth, lying on a weak ridge.

56. *Rissoidea* sp. 2

Plate 3, fig. 3a–b

Not mentioned by BÁLDI & CSÁGOLY (1975). Material: 1 defective shell. The height of the shell must have been almost 3 mm. The whorls are slightly convex, smooth, but with spiral sculpture on the basal part of the body-whorl. The umbilicus is open. The apertural lip is strongly thickened externally. The inner lip is thickened in the right upper corner of the aperture.

57. *Rissoidea* sp. 3

Plate 3, fig. 4

Not mentioned by BÁLDI & CSÁGOLY. Material: 1 defective shell. Still smaller than the foregoing species (height about 2 mm). The umbilicus is only a narrow fissure. Apertural margin slightly thickened internally and externally.

58. *Teinostoma* (*Teinostoma*) sp.

Plate 3, fig. 1

Not mentioned by BÁLDI & CSÁGOLY (1975). Material: 57 specimens. Diameter slightly more than 3 mm. Shell surface with spiral sculpture. The first whorls have also a fine radial sculpture, causing reticulation. The umbilicus is completely covered by a callosity. This is not *T. egerensis* BÁLDI (1973, p. 242, pl. 24, fig. 5–6), which is a *Solariorbis*.

59. *Teinostoma (Megatyloma)* sp.

Plate 3, fig. 2

Not found by BÁLDI & CSÁGOLY. Material: 1 specimen. Its diameter is about 1.4 mm, the shell is higher than wide. The umbilicus is completely covered. Shell surface without sculpture.

60. *Pseudomalaxis (Pseudomalaxis) semiclastrata* (SPEYER, 1869)

Not mentioned in BÁLDI & CSÁGOLY. Material: 2 fragments. Although only two small fragments were found the resemblance with North Sea Basin material is striking, because of the Square section of the whorls, which obviously were touching each other. They carry strong, threadlike spirals on the upper and lower carinae.

61. *Haustator (Haustator)* sp. aff. *venus* (D'ORBIGNY, 1852) sensu HÖLZL, 1962.

Turritella genitzi SPEYER, 1866 in BÁLDI CSÁGOLY. Material: several hundreds of specimens. The shells correspond very well with the photographs and the description of HÖLZL (1962, p. 139, pl. 8, fig. 11–12), but remain distinctly smaller. Transitions to the form *confusa* HÖLZL, 1962 are also present at Máriahalom. This species is very different from *H. goettenstrupensis* (COSSMANN, 1899) (= *T. geinitzi* SPEYER, non d'ORBIGNY), especially in size and development of the spiral sculpture. A photograph of the Máriahalom species is given by BÁLDI & STEININGER (1975, pl. 8, fig. 9). The very confused taxonomy of the family Turritellidae induces me to apply a rather careful denomination for the specimens from Máriahalom.

62. *Melanopsis (Lyrcaea) impressa hantkeni* HOFMANN, 1870

Melanopsis impressa hantkeni Hofmann, 1870 in BÁLDI & CSÁGOLY (1975). Material: 19 specimens. The shells correspond perfectly with those figured in BÁLDI (1973, p. 258, pl. 27, fig. 1–3).

63. *Potamides (Potamides) lamarcki* BRONGNIART, 1810

Potamides lamarcki margaritaceus n. subsp. in BÁLDI & CSÁGOLY. Material: numerous specimens. The largest shells reach a height of more than 5 cm and a basal diameter of more than 15 mm! They reach considerably larger dimensions than the largest specimens from the North Sea Basin (viz. the Boutersem Sands in Belgium), and they are also somewhat more coarsely sculptured. Considering the extreme variability of this species in its many Oligocene and Miocene occurrences I am not sure whether these differences justify a separate subspecies for the Máriahalom form. The name *margaritaceus* was merely mentioned by BÁLDI & CSÁGOLY. BÁLDI & STEININGER (1975) represent this form on their plate 10, fig. 4 with the denomination *Potamides lamarcki* n. ssp. On page 344, however, they mention *P. lamarcki margaritaceus* CSÁGOLY, 1974 and refer to plate 10, fig. 4. So, to avoid all possible misunderstandings about the authorship of this subspecies and considering the fact that "CSÁGOLY, 1974" apparently

refers to an unpublished paper I think it wise to consider *margaritaceus* as a nomen nudum. As a formal ground for this it may be stated that nowhere has a diagnosis been published.

64. *Potamides (Ptychopotamides) margaritaceus* (BROCCHI, 1814)

Tympanotonus margaritaceus BROCC., 1814 in BÁLDI & CSÁGOLY (1975). Material: abundant specimens. The shells from Máriahalom reach a height to over 6 cm. A specimen from this locality was represented by BÁLDI & STEININGER (1975, pl. 10, fig. 1).

65. *Pirenella plicata* (BRUGUIÈRE, 1792) s. lat.

Pirenella plicata BRUGUIÈRE, 1792 in BÁLDI & CSÁGOLY. Material: abundant specimens. Like the two foregoing species this form too has very large dimensions. Form and sculpture situate the Máriahalom material somewhere between the typical form and the subspecies *papillata* SANDBERGER, 1859. Adult specimens have relatively fine-granulated basal spiral threads on the body-whorl.

66. *Pirenella plicata bavarica* (GÜMBEL, 1861)

Not mentioned by BÁLDI & CSÁGOLY (1975). Material: 125 specimens. Much smaller than the foregoing form (height to about 10 mm), characterized by a very weak radial sculpture, which may only be present on the two uppermost spirals, but is more often completely absent. This form looks somewhat like the subsp. *monilifera* (DESHAYES, 1833), which is larger, however, and has a more developed sculpture.

The presence of two sharply delimited forms of *Pirenella plicata* at Máriahalom offers some problems. If one refuses to accept the occurrence of two subspecies of one and the same species together in a fauna (which I am inclined to do!), then there are two possible solutions: firstly there is the possibility of the original presence of the two subspecies in different bio-coenoses that were later washed together to one thanatocoenosis. The other solution is to regard one of the two forms as an independant species or a forma. For the time being I am not able to decide which of the two interpretations would apply in this case.

67. *Pirenella laevisissima* (GOLDFUSS, 1844)

Not mentioned in BÁLDI & CSÁGOLY. Material: 15 more or less defective shells. *P. laevisissima* is sometimes considered to be merely a subspecies or even a forma of *P. plicata*. In the Máriahalom specimens there is not the slightest indication of transitional forms. Also the higher number of spiral lines (see also SANDBERGER, 1859, p. 100, pl. 9, fig. 8b) seems to be an indication that *laevisissima* is a separate species. See also GLIBERT (1962, p. 165).

68. *Pirenella* sp. n. ?

Plate 3, fig. 17

Not found by BÁLDI & CSÁGOLY (1975). Material: 160 specimens. The height of the shell may reach some 12 mm. The shell is conical with rather

convex, relatively low whorls. The sculpture is composed of four spiral threads, of which the third (counting abapically) is the strongest, and 15–20 radial ribs are slightly arched. On the intersections lie distinct knobs. The basis of the body-whorl is bordered by two narrow but relatively high spiral lines. Sometimes varix may be developed. The variability of this species concerns mainly the apical angle and the number of radial ribs.

I did not succeed in finding this species in the literature, so it might be an undescribed form. It resembles more or less the typical form of *P. hartbergensis* (HILBER, 1891), but there are significant differences on ornamentation and range of variability.

69. *Terebralia* aff. *lignitarum* (EICHWALD, 1853)

Terebralia bidentata FR., 1832 in BÁLDI & CSÁGOLY. Material: 80 more or less defective specimens and 27 juvenile shells. *T. bidentata* (DEFRANCE, 1832) differs from the Máriahalom material in its more inflated base. The present species is more closely related to *T. lignitarum* and *T. rahtii* (SANDBERGER, 1859). Unfortunately I have no material at my disposal of this latter species.

70. *Diastoma grateloupi* (d' ORBIGNY, 1852)

Not mentioned in BÁLDI & CSÁGOLY. Material: 20 juvenile specimens. The largest shell has a height of about 9 mm, so the material is insufficient to decide whether or not it should be attributed to the form *turritoapenninica* SACCO, 1895 (compare BÁLDI, 1973, p. 263: pl. 29, fig. 7–8).

71. *Sandbergeria secalina* (PHILIPPI, 1843)

Not mentioned by BÁLDI & CSÁGOLY. Material: 302 shells. The specimens are on the average somewhat more slender than shells from the Late Oligocene of Glimmerode (see R. JANSSEN, 1978, pl. 11, fig. 38), but equally slender shells are also present, so I do not think that the Hungarian specimens should be separated specifically.

72. *Bittium (Bittium) spina* (HOERNES, 1855)

Not found by BÁLDI & CSÁGOLY. Material: 9 specimens. The size of the shells (height to about 5 mm) and the convex whorls indicate that this form does not belong to the subspecies *agriense* BÁLDI, 1966.

73. *Cerithiopsis* (s. lat.) sp.

Not mentioned by BÁLDI & CSÁGOLY (1975). Material: 1 specimen. The height of this shell is about 2.4 mm. Two smooth (or worn?) embryonic whorls are still present. The upper part of the shell is distinctly cyrtocoid, the younger part becomes more cylindrical. The teleoconch comprises 5 1/2, moderately convex whorls. The sculpture consists of three spirals and axially directed radial ribs. On the intersections lie distinct knobs. The base of the body-whorl is damaged.

74. *Acirsa (Acirsa) sp.*

Plate 3, fig. 16

Not mentioned in BÁLDI & CSÁGOLY (1975). Material: 6 defective specimens. The sculpture comprises 4 to 5 wide spiral threads, separated by narrow grooves. Locally this sculpture may be somewhat obscure. The radial sculpture exists of prosoclyne furrows in the same direction as the growth-lines. There are 15–18 such furrows on the body-whorl. Judging from the regular distances between them these furrows will not have been caused by external influences.

75. *Cirsotrema (s. lat.) sp.*

Amaea cf. amoena PHILL., 1843 in BÁLDI & CSÁGOLY? Material: 1 fragment. The body-whorl has 18 strong radial ribs, of which four are developed like varices. In between these ribs a much finer spiral sculpture is present, five of such spirals are visible above the basal disc, which is also sculptured with many very fine spiral threads. The material is insufficient for a closer identification.

76. *Eulima (Eulima) glabra hebe* (SEMPER, 1861)

Plate 3, fig. 12

Not found by BÁLDI & CSÁGOLY (1975). Material: 1 defective specimen. The only available shell was compared with Late Oligocene specimens from the North Sea Basin, no important differences were found (compare R. JANSSEN, 1978, p. 187, pl. 13, fig. 75).

77. *Balcis (Balcis) alba naumanni* (VON KOENEN, 1867)

Plate 3, fig. 10–11

Not mentioned by BÁLDI & CSÁGOLY. Material: 4 defective shells. Although only few badly preserved specimens were found I do not think that they are different from the North Sea Basin form, occurring in Late Oligocene deposits.

78. *Calyptrea (Calyptrea) chinensis* (LINNÉ, 1758)

Not found by BÁLDI & CSÁGOLY. Material: 63 more or less damaged shells.

79. *Eratopsis (Eratopsis) prolaevis prolaevis* SACCO, 1894

Plate 3, fig. 13

Not mentioned in BÁLDI & CSÁGOLY. Material: 1 shell. The inner side of the outer apertural lip bears weak denticles in this specimen. In this respect it differs from the material described by BÁLDI (1973, p. 279, pl. 34, fig. 5)

80. *Globularia gibberosa sanctistephani* (COSSMANN & PEYROT, 1919)

Not mentioned by BÁLDI & CSÁGOLY. Material: 2 adult and 2 juvenile shells. In both of the larger specimens the umbilicus is completely covered, in one of the juveniles it is still open. The largest shell has a height of 22 mm.

This form was described from the Hungarian Late Oligocene by BÁLDI (1973, p. 276, pl. 32, fig. 4–5). There are some slight differences between the Máriahalom material and the specimens described by COSSMANN & PEYROT (1919, p. 449, pl. 12, fig. 30–33): the Hungarian shells have a more depressed spira, a less obvious subsutural depression and a distinctly more concave columella. As far as is visible from his photographs the same seems to be the case in the specimens represented by BÁLDI. So, a study of more material may prove that the Hungarian Late Oligocene shells represent a separate subspecies.

81. *Cernina (Cernina) rothi* (COSSMAN, 1925)

Globularia rothi COSSM., 1825 (sic!) in BÁLDI & CSÁGOLY (1975). Material: 1 very fine specimen, with a height of 32 mm.

82. *Neverita josephinia olla* (de SERRES, 1829)

Polinices jos. olla DE SERRES, 1829 in BÁLDI & CSÁGOLY. Material: 15 specimens.

83. *Euspira helicina* (BROCCHI, 1814) s. lat.

Polinices catena DA COSTA, 1778 s. l. in BÁLDI & CSÁGOLY, 1975. Material: 56 specimens. The umbilical callosity below the base of the body-whorl is only very slightly constricted, but in spite of this the Máriahalom material may be attributed to this species. Further investigation will be necessary for determination of the subspecies. Also the nomenclature of the representatives of this group in the Oligocene of Western Europe needs reconsideration.

84. *Euspira* sp.

Plate 3, fig. 15

Not found by BÁLDI & CSÁGOLY. Material: 1 specimen. Its height is only 4 mm. The shell is strikingly high in habitus. The umbilical callus is constricted below the base of the body-whorl. In spite of its size this shell looks rather adult. Its surface is badly corroded.

85. *Ampullinopsis crassatina* (LAMARCK, 1804)

Ampullina crassatina LAMARCK, 1904 (sic!) in BÁLDI & CSÁGOLY (1975). Material: 23 specimens and 5 juvenile shells. This form belongs to the smaller type, as described by BÁLDI (1973, p. 278).

86. *Natica neglecta* MAYER, 1858

Plate 3, fig. 14

Natica sp. in BÁLDI & CSÁGOLY? Material: 1 shell. This specimen most certainly does not belong to *N. tigrina* DeFrance, which has a much more shouldered appearance. *N. neglecta*, widely distributed in Miocene deposits of Western Europe, seems to be present also in Late Oligocene deposits of the North Sea Basin (compare R. JANSSEN, 1978, p. 195, pl. 14, fig. 84).

87. *Ocinebrina* aff. *conspicua* (SANDBERGER, 1861)

Plate 3, fig. 18

Ocinebrina schönni HÖRNES, 1856 in BÁLDI & CSÁGOLY? Material: 2, specimens, 9 juveniles and 1 fragment. *O. schoenni* differs from the present species by the occurrence of varices on the body-whorl, causing an obvious triangular horizontal section of the stell. *O. conspicua* is certainly more closely related, but reaches a larger size (height 22 mm instead of 14 mm for the Máriahalom shells). From *O. crassilabiata trivariocosa* BÁLDI, 1964, mentioned from Máriahalom by BÁLDI & CSÁGOLY (1975) and BÁLDI (1976), the present material differs in the absence of varices on the body-whorl, the presence of a pronounced spiral thread causing subcarinated whorls, and in the completely different spiral sculpture.

88. *Mitrella* (*Macrurella*) sp.

Plate 4, fig. 4

Not mentioned in BÁLDI & CSÁGOLY. Material: 1 defective juvenile shell, which is insufficient for specific identification.

89. *Babylonia* (*Peridipsaccus*) *matheroni* MAGNE, 1942 subsp. n.

Babylonia eburnoides umbilicosiformis T. ROTH, 1914 in BÁLDI & CSÁGOLY (1975). *Babylonia caronis* BRONGNIART *B. eburnoides* átm. in BÁLDI (1976). Material: 13 specimens. Some specimens have the pseudumbilicus closed, while it is open in others. The shells from Máriahalom are markedly more slender than the specimens that I collected at Eger (Wind brickyard, bed K). A specimen of this form from Máriahalom was represented by BÁLDI & STEININGER (1975, p. 345, pl. 9, fig. 1–2).

It agrees with a specimen from Sárísáp illustrated by BÁLDI (1973, pl. 51, fig. 7). From *B. matheroni* MAGNE, 1942 (= *eburnoides* MATHERON, 1842, non GRATELOUP, 1834) and its related forms this material differs by the more or less open pseudumbilicus (which, by the way, places this form somewhere between *Babylonia* s. str. and *Peridipsaccus*!) and the different proportions of the spira. *B. Caronis* (BRONGNIART, 1823) approaches the present form in outline, but has also a closed pseudumbilicus. Most probably, however, it is more closely related to *B. matheroni*; it should be introduced as a new subspecies.

90. Melongenidae sp. (div. ?)

Plate 4, fig. 1–3

Galeodes ex. gr. *semseyana* ERDÖS, 1900, and *Galeodes* sp. in BÁLDI & CSÁGOLY (1975). Material: 8 more or less defective specimens and 2 fragments. The shells that I collected at Máriahalom are very variable in habitus. The three main forms are illustrated on pl. 3, fig. 1–3. All the specimens have in common that the growth-lines are strikingly foliaceous on the sutures. All have an obvious thickening around the pseudumbilicus (as far as visible). The form represented here in fig. 1 looks very much like *Galeodes basilica* (BELLARDI) as described by BÁLDI (1973, p. 295, pl. 40, fig.

3–4), whereas the shell of fig. 2 has some resemblance with *G. semseyana* ERDÖS (see BÁLDI, 1973, p. 295, pl. 40, fig. 1–2), although my specimen has a higher spira and lacks the basal row of spines, whereas the foliaceous growth-lines on the suture seem to be absent in Báldi's specimen. Most probably BÁLDI (1976) meant this form with the indication *Volema* ex aff. *subcarinata* LAMARCK. In the third form the carina is absent, as a result of which the shell looks like a muricid species. Judging from my very limited and badly preserved material this could very well be one extremely variable species, but just as well it might belong to three different taxa.

91. *Dorsanum* (*Dorsanum*) *gradatum* (WOLFF, 1897)

Bullia gradata WOLFF, 1897 in BÁLDI & CSÁGOLY. Material: 19 specimens. This species belongs to the group of *D. baccatum* (Basterot) and *D. subpolitum* (d'ORBIGNY) and should not be attributed to *Bullia*.

92. *Dorsanum* (? *Dorsanum*) *hungaricum* (GÁBOR, 1936)

Bullia hungarica GÁBOR, 1936 in BÁLDI & CSÁGOLY (1975). Material: 112 more or less defective specimens. This species differs from *Dorsanum* s. str. in its strongly developed spiral sculpture. It seems to be linked up with *D. rudium* PEYROT, 1927. It should be preferable to introduce a new subgenus for these two species.

93. *Hinia* (*Tritonella*) sp.

Not found by BÁLDI & CSÁGOLY. Material: 51 more or less defective shells. This species differs from *Dorsanum hungaricum* in its much coarser spiral sculpture and the presence of distinct teeth on the inner side of the apertural lip. There is also one parietal tooth. The available material is extremely variable in general form, from slender to thick-set, and also in the number of radial ribs. Therefore it might be expected that it belongs to more than one species, which cannot however, be ascertained because of insufficient adult specimens.

94. *Olivella* (*Lamprodoma*) *clavula vindobonensis* CSEPREGHY – MEZNERICS, 1954

Olivella clavula vindobonensis Cs. MENZ., 1954 in BÁLDI & CSÁGOLY, 1975. Material: 110 specimens, more or less damaged. My material fits completely within the description and illustrations of BÁLDI (1973, p. 301, pl. 44, fig. 7–8). It differs, however, from the description of CSEPREGHY – MEZNERICS (1954, p. 139, pl. 6, fig. 3, 9) in its higher spira. Thus this form seems to be intermediate between the nominal subspecies and *vindobonensis*.

95. *Athleta* (*Athleta*) *rarispinga* (LAMARCK, 1811)

Athleta rarispinga LAMARCK, 1811 in BÁLDI & CSÁGOLY. Material: 22 specimens. All shells have an obvious depression adapically of the row of spines on the body-whorl. In Miocene specimens this seems to be absent or much less important (PEYROT 1928, p. 155, pl. 11, fig. 18–22). Also the

Máriaalom specimens have more spines (even up to six!) and close to the apertural lip obvious radial folds are present. A direct comparison would possibly point out that both forms are not identical. I do not have such material at my disposal and therefore I maintain, for the time being, the name usually attributed to the Hungarian material. The specimen shown in BÁLDI (1973, p. 306, pl. 42, fig. 6–7) and also the one illustrated by BÁLDI & STEININGER (1975, p. 346, pl. 6, fig. 3–4) are identical with my specimens. DR. BÁLDI (in litt.) informed me that GAÁL (1937–1938, p. 9) described a similar form as *Voluthilites telegdyi*. Unfortunately Gaál's paper is not available to me, but if he really had the same form it should be named *Athleta (Athleta) rarispina telegdyi* (GAÁL).

96. *Turrinae* sp.

Not mentioned by BÁLDI & CSÁGOLY. Material: 1 defective shell. The whorls have about five spiral lines, of which the fourth is the strongest. Above this spiral the whorls are slightly concave. Secondary spiral lines occur on the youngest whorls. Radial sculpture is absent. As the specimen lacks the protoconch and early whorls, and because the form of the growth-lines is difficult to observe, it is impossible to give further identification.

97. *Clavinae* sp. 1

Plate 4, fig. 5

Not found by BÁLDI & CSÁGOLY. Material: 2 specimens. The material is insufficient for identification.

98. *Clavinae* sp. 2

Not mentioned by BÁLDI & CSÁGOLY. Only one defective specimen, apparently different from the other two *Clavinae*.

99. *Clavinae* sp. 3

Not mentioned by BÁLDI & CSÁGOLY (1975). Material: 2 juvenile shells. None of the three *Clavinae* mentioned here could be identified with the species described by BÁLDI (1973). Additional material will be necessary for further investigation.

100. *Bela* sp.

Plate 4, fig. 6

Not mentioned by BÁLDI & CSÁGOLY. Material: 14 specimens of which several are badly damaged. The shell is spindle-shaped, slender, with rather strong radial ribs. Fine spiral threads are visible between the ribs.

101. *Hastula (Hastula)* sp.

Plate 4, fig. 7

Not mentioned in BÁLDI & CSÁGOLY (1975). Material: 22 defective specimens. This species has no spiral groove below the suture. A vague axial sculpture is only visible on the oldest whorls, but most shells are strongly corroded.

102. *Phasianema* sp.

Plate 4, fig. 13

Not mentioned by BÁLDI & CSÁGOLY. Material: 1 specimen. This shell has approximately the form of *P. costatum* (BROCCHI), but it has only a very weak spiral sculpture, very badly visible because of surface corrosion. The specimen has no columellar tooth.

103. *Odostomia* (*Megastomia*) sp.

Plate 4, fig. 8

Not mentioned by BÁLDI & CSÁGOLY (1975). Material: 3 specimens. Insufficient for a closer identification.

104. *Syrnola* (*Syrnola*) sp.

Plate 4, fig. 9

Not found by BÁLDI & CSÁGOLY. Material: 18 more or less damaged shells. The height is up to more than 7 mm. The shell is long and slender, with almost completely flat whorls. In juvenile specimens the base is angular, in larger shells it is rounded. The columella has a strong fold. The material shows some resemblance to *S. laterariae* BÁLDI, 1966 (see BÁLDI, 1973, p. 331, pl. 49, fig. 7), which is, however, much smaller. As there are several other species with which the present material should be compared I prefer to mention the species in open nomenclature.

105. *Syrnola* (*Puposyrnola*) sp.

Not mentioned by BÁLDI & CSÁGOLY (1975). Material: 6 specimens. The height of the specimens is maximally 3 mm. Their surface is smooth, the shell-form is cyrtoconoid. The columella bears a solid spiral fold.

106. *Tiberia* (*Loxoptyxis*) sp.

Plate 4, fig. 11

Not mentioned in BÁLDI & CSÁGOLY (1975). Material: 1 specimen. Its height is about 3 mm. The last whorl has an angular base. The columella has two strong folds. The apical angle is much smaller than in *Pyramidella* (*Milda*) sp.

107. *Pyramidella* (*Milda*) sp.

Plate 4, fig. 10

Not mentioned in BÁLDI & CSÁGOLY. Material: 2 complete and 19 defective specimens. Height up to 10 mm. Columella with a very strong upper spiral fold and two much weaker ones below it. A weak ridge is present around the very small umbilicus. The shell surface is smooth. The outline of the shell is clearly cyrtoconoid.

108. *Ringicula* (*Ringiculina*) sp.

Plate 4, fig. 15

Ringicula auriculata paulucciae MORLET, 1878 in BÁLDI & CSÁGOLY. Material: 37 specimens. The shells are much smaller than *R. paulucciae*

MORLET (as described in BÁLDI, 1973, p. 333, pl. 50, fig. 3). *Ringicula* species are difficult to distinguish and therefore further identification will be postponed until more material is available for comparison.

109. *Actaeon (Actaeon) punctatosulcatus* (PHILIPPI, 1843)

Not mentioned by BÁLDI & CSÁGOLY. Material: 1 specimen. The shell corresponds perfectly with specimens from the Late Oligocene deposits of the Lower Rhine area.

110. *Acteocina exerta* (DESHAYES, 1862)

Plate 4, fig. 14

Not mentioned by BÁLDI & CSÁGOLY (1975). Material: 121 specimens. The shells correspond very well with specimens from Ormoy (Etampes Basin, France), except for their slightly higher spira.

111. *Ellobium (Ellobium) cf. subjudae* (d'ORBIGNY, 1852)

Plate 4, fig. 16–17

Ellobium sp. in BÁLDI & CSÁGOLY (1975); *Ellobium* n. sp. ex aff. *vicentina* FUCHS in BÁLDI (1976). Material: 11 specimens. This species is one of the very rare representatives in Europe of a group of terrestrial species which has its main area of distribution in southern Asia. The shell reaches a height of 42 mm, the shell surface is rather coarsely sculptured with granules arranged in radial lines. The relative height of the spira is variable (compare drawings). The columella has two obvious spiral folds, the parietal labrum is slightly thickened in its middle part. Also the higher part of the callus lying against the base of the body-whorl is somewhat thickened.

The material bears some resemblance with *E. vicentinum* (FUCHS, 1870) from the (? Early Oligocene, Tongrien, see WENZ, 1923, p. 1121) locality Soggio di Brin in northern Italy. This latter species, however, is considerably smaller (somewhat less than 30 mm) and it has only one columellar fold. *E. subjudae* (d'ORBIGNY, 1852) (= *Auricula Judae* GRATELOUP, 1827, non LAMARCK = *A. aquitanica* SANDBERGER, 1873) from the Rupelian of Gaas etc. in south-western France, is more closely related. It has 2–3 folds on the columella and reaches a height of 45 mm, which compares very well with the Máriahalom material. The drawing in GRATELOUP (1840, pl. 11, fig. 1), however, represents (if correctly drawn!) a shell with a relatively higher spira and more convex whorls. The illustration in SANDBERGER (1873, pl. 19, fig. 24) is a copy of Grateloup's drawing. On the other hand VERGNEAU (1959, p. 173) described this species as "... , de forme ovoïde-oblongue. Spire courte à sommet arrondi.", which matches the Hungarian form very well. She compares the French Oligocene species with a Miocene form from the Loire and Aquitaine Basins in France, *Auricula oblonga* DESHAYES, 1830 (compare TOURNOUËR, 1872, p. 96, pl. 4, fig. 2a–b). This species, however, has nothing to do with the Hungarian material: it is considerably smaller, has a smooth shell surface and an obvious subsutural depression. In spite of these differences *A. oblonga* was included in *Ellobium* s. str. by WENZ (1923, p. 1117) and by GLIBERT (1952, p. 405).

Summarizing I think that the Máriahalom material is closely related and perhaps even identical with *E. subjudae*. A direct comparison will be necessary for a final decision.

NON-MOLLUSCA

In the samples from Máriahalom that were investigated for their mollusc content also some fossils of other animal groups were found. Of these the bony fish otoliths were shown to DR. P. A. M. CAEMERS (Leiden), who is a specialist in this group of fossils. Although he had only a glance at the material he could ascertain that the fauna contains some unexpected elements.

The following non-molluscs were encountered:

Crustacea – *Cirripedia*

many fragments and operculae (tergum and scutum) of *Balanidae* sp.

Crustacea – *Decapoda*

29 fragments of crab pincers

Pisces – *Elasmobranchii*

4 shark teeth, 1 tooth of a ray, 1 dental segment of *Myliobatis* sp.

Pisces – *Teleostei*

46 otoliths and 82 teeth and other skeleton fragments.

Furthermore six fragments were found of concretions containing imprints of tree leaves and stems, and attacked by *Teredinids*.

From the bottom of the sand-pit a larger fragment of such concretions was collected. The original level of these concretions is not known, but presumably they occur scattered in the sediment (compare text-fig. 1).

Discussion and conclusions

BÁLDI & CSÁGOLY (1975) mentioned in their list a mollusc fauna comprising 64 species. Of these 14 species are not present in my material. These are:

Anadara diluvii LAM., 1805

Diplodonta rotundata MONT., 1803

Cardium neglectum HÖLZL, 1962

Semicorbula cf. *nadali* C. et. P., 1909

Diloma amedei BROGNIART, 1823

Protoma cathedralis BROGNIART, 1823

Protoma diversicostata SANDB., 1861

Thais sumeghyi n. sp.

Hadriania cf. *egerensis* GÁBOR, 1936

Ocenebrina crassilabiata trivaricosa BÁLDI, 1964

Euthriofusus cf. *burdigalensis* DEFR., 1820

Athleta ficulina LAMARCK, 1811

Egereia cf. *collectiva* GÁBOR, 1936

Turricula cf. *regularis* KONINCK, 1837.

BÁLDI (1976) listed 59 species, including one further species not found by me (*Tellina perrandoi* Mayer).

Together with the 111 species present in my samples the total number of species of the Máriahalom mollusc fauna is brought to 126, which is almost twice the number of species mentioned by BÁLDI & CSÁGOLY.

When taking a closer look at those species not mentioned by BÁLDI & CSÁGOLY, it is very striking that among them there is quite a number of species present in my material in rather high numbers and consequently should be considered as important elements of the fauna, especially:

Nucula aff. *nucleus*
Pinctada phalaenacea
Parvilucina (Microloripes) sp.
Lentidium (Lentidium) sp.
Teinostoma (Teinostoma) sp.
Pirenella plicata bavarica
Pirenella sp. ? n.
Sandbergeria secalina
Calyptraea chinensis
Acteocina exerta.

It is hardly a coincidence, in my opinion, that all these species have relatively small shells (say less than 10 mm). The same is the case for almost all other species not found by BÁLDI & CSÁGOLY. Therefore I presume that only few or no sieving residues were inspected by them. It is obvious that in this way many species remain unnoticed.

At least for some of the species newly found it must be stated, however, that they may not have been present in the outcrop earlier. Ever since the time of collecting by BÁLDI & CSÁGOLY (\pm 1974) the exploitation in the sand-pit have been making some progress and it is very well possible that sediments with a slightly different faunal composition are being excavated today. This is in agreement with my own observation that the various pockets and lenses in the sediment seem to differ slightly in species composition. DR. BÁLDI (in litt.) confirms this. He wrote to me, that some taxa of which I found some fragments only, were found earlier in large quantities.

Although the mollusc fauna record of this sand-pit is almost doubled now I think it quite likely that more new species will be found rather easily; considering the short time that I spent at the locality extensions of the fauna may be expected.

PALAEOENVIRONMENT

According to an analysis made by MRS. CSÁGOLY the mollusc fauna found at Máriahalom is attributed to the so-called *Tympanotonus-Pirenella* community (as described by BÁLDI, 1973, p. 107) by BÁLDI & CSÁGOLY (1975). Judging from the most common species at Máriahalom I can agree with this statement, but it is most certainly not a typical representative of this association, as there are many species present at Máriahalom that have a more open marine character than indicated by the *Tympanotonus*-

Pirenella community. There are also typical elements of the *Mytilus aquitanicus* community and especially also of the *Glycymeris latiradiata* community. Summarizing we may conclude that the Máriahalom fauna indicates an euryhaline environment as part of a lagoon or coastal lake, situated rather closely to a connection with open sea. The heterogeneous composition of the fauna and the observed differences in the various pockets and lenses in the sediment point to a biotop with quickly changing environmental conditions, which is, by the way, a general characteristic of euryhaline communities.

AGE OF THE SEDIMENT

Among the mollusc taxa known from the Máriahalom fauna there are several that are known only from Middle Oligocene faunas, but just as well there are species that are not known to occur in faunas older than Miocene. It is obvious that the vertical distribution of many species is still imperfectly known, or will prove to be different in Hungary from the distribution in other basins. So, there are no obvious reasons to assume this fauna not to be of Late Oligocene (Egerian) age.

LIST OF SPECIES AND REGISTRATION NUMBERS FOR RGM COMPUTER REGISTRATION

RGM	Name	Number of specimens
223.881	<i>Nucula</i> (<i>Nucula</i>) aff. <i>nucleus</i> (LINNÉ, 1758)	3/1, 25/2 and 25/2 def.
223.882	ditto, represented specimen	1/2
223.883	<i>Nuculana</i> (<i>Sacella</i>) <i>anticepicata</i> (ROTH VON TELEGD, 1914)	4/2, 14 fragm.
223.884	<i>Glycymeris</i> (<i>Glycymeris</i>) <i>latiradia latiradiata</i> (GÜMBEL, 1861)	2/1, 25/2
223.885	ditto	25/2 juv.
223.886	<i>Mytilus</i> (<i>Mytilus</i>) sp.	1/2 mould
223.887	ditto	35 fragm.
223.888	<i>Musculus</i> (<i>Musculus</i>) sp.	2/2 juv.
223.889	<i>Pinctada phalaenacea</i> (LAMARCK, 1819)	200/2 def.
223.890	<i>Isognomon</i> (<i>Isognomon</i>) <i>heberti</i> (COSSMANN & LAMBERT, 1884) represented specimen	1/2 juv.
223.891	<i>Anomia</i> (<i>Anomia</i>) <i>ephippium</i> LINNÉ, 1758	1/1 juv., 21/2
223.892	<i>Ostrea cyathula</i> (LAMARCK, 1806)	many
223.893	ditto	many, on gastropods
223.894	<i>Linga</i> (<i>Linga</i>) <i>oligocaenica</i> (COSSMANN, 1921)	21/2, 66 fragm.
223.895	<i>Parvilucina</i> (<i>Microloripes</i>) sp.	many/2
223.896	ditto, represented specimen	1/2
223.897	<i>Saxolucina</i> (<i>Saxolucina</i>) <i>heberti</i> (DESHAYES, 1857)	3/2, 11 fragm.
223.898	ditto, represented specimen	1/2
223.899	<i>Divalinga</i> (<i>Divalinga</i>) <i>ornata</i> (AGASSIZ, 1845)	4/1, many/2
223.900	<i>Felaniella</i> (<i>Felaniella</i>) aff. <i>nysti</i> (BOSQUET, 1868)	40/2 (\pm def.)
223.901	ditto, represented specimen	1/2
223.902	<i>Mysella</i> (<i>Mysella</i>) sp.	1/2
223.903	ditto, represented specimen	1/2
223.904	<i>Venericardia</i> (<i>Venericardia</i>) sp.	2/1, 21/2, 50/2 juv., 20 fragm.
223.905	<i>Erycinella clara</i> (VON KOENEN, 1893)	6/2

RGM	Name	Number of specimens
223.906	ditto, represented specimen	1/2
223.907	<i>Goodallia</i> (? <i>Goodallia</i>) sp.	1/2
223.908	ditto, represented specimen	1/1
223.909	<i>Laevicardium</i> (? <i>Dinocardium</i>) <i>kovacovense</i> (SENEŠ, 1958)	16 fragm.
223.910	<i>Parvicardium</i> sp., represented specimen	1/2 def.
223.911	<i>Spisula</i> (<i>Spisula</i>) <i>subtruncata</i> (DA COSTA, 1778)	30 fragm.
223.912	<i>Angulus</i> (<i>Peronaea</i>) <i>ancestralis</i> BALDI, 1973	13 fragm.
223.913	<i>Arcopagia</i> (<i>Arcopagia</i>) cf. <i>subelegans</i> (D'ORBIGNY, 1852)	1 fragm.
223.914	<i>Macoma</i> (<i>Psammacoma</i>) <i>elliptica</i> (BROCCHI, 1814)	4 fragm.
223.915	<i>Gari</i> (<i>Psammotaena</i>) sp.	21 fragm.
223.916	<i>Congerina</i> <i>basteroti</i> (DESHAYES, 1836)	5/2. 28 fragm.
223.917	<i>Coralliophaga</i> sp.	3 fragm.
223.918	ditto, represented specimen	1 fragm.
223.919	<i>Dentonia</i> <i>geslini</i> (DESHAYES, 1830)	1/2, 2/2 def.
223.920	ditto, represented specimen	1/2
223.921	<i>Polymesoda</i> (<i>Pseudocyrena</i>) <i>convexa</i> brongniarti (BASTEROT, 1825)	16/2, 30 fragm.
223.922	<i>Callista</i> (<i>Costacallista</i>) sp.	34/2, 25 fragm.
223.923	<i>Callista</i> (s.lat.) sp.	5/1 juv., 119/2
223.924	ditto, represented specimen	1/2
223.925	<i>Venus</i> (<i>Ventricoloidea</i>) <i>multilamella</i> <i>interstriata</i> (ROTH VON TELEGD, 1914)	4/2 juv., 7 fragm.
223.926	<i>Pelecypora</i> (<i>Cordiopsis</i>) <i>polytropa</i> <i>suborbicularis</i> (GOLDFUSS, 1841)	8/2, 4 fragm.
223.927	ditto	2/1 juv., 21/2 juv.
223.928	<i>Chamelea</i> sp., represented specimen	1/2 def.
223.929	ditto, represented specimen	1/2 def.
223.930	Veneridae sp. indet.	many fragm.
223.931	<i>Corbula</i> (<i>Varicorbula</i>) <i>gibba</i> <i>gibba</i> (OLIVI, 1792)	1/2
223.932	<i>Caryocorbula</i> (<i>Caryocorbula</i>) <i>basteroti</i> (HOERNES, 1870)	2/2, 16 fragm.
223.933	<i>Caryocorbula</i> (<i>Caryocorbula</i>) <i>revoluta</i> <i>hoernesii</i> (COSSMANN & PEYROT, 1909)	many
223.934	<i>Lentidium</i> (<i>Lentidium</i>) <i>modelli</i> (HÖLZL, 1958)	140/2, mainly def.
223.935	<i>Lentidium</i> (<i>Lentidium</i>) sp.	70/1, 348/2
223.936	ditto, represented specimen	1/2
223.937	ditto, represented specimen	1/2
223.938	ditto, represented specimen	1/2
223.939	<i>Martesia</i> (<i>Martesia</i>) sp.	1/2 juv., 17 fragm.
223.940	ditto, represented specimen	1/2 juv.
223.941	ditto, represented specimen	1 mesoplax
223.942	? <i>Teredina</i> sp., represented specimen	1 fragm. calc. tube
223.943	Teredinidae sp.	2/2 def., 22 fragm. of calc. tubes
223.944	<i>Dentalium</i> (<i>Antalis</i>) <i>seminudum</i> DESHAYES, 1861	17 (\pm def.)
223.945	ditto, represented specimen	1
223.946	<i>Cadulus</i> (<i>Dischides</i>) sp.	26 fragm.
223.947	ditto, represented specimen	1 fragm.
223.948	ditto, represented specimen	1 fragm.
223.949	<i>Patella</i> (<i>Patella</i>) aff. <i>neglecta</i> MICHELOTTI, 1847	1 def., 2 fragm.
223.950	<i>Jujubinus</i> (<i>Scrobiculinus</i>) sp.	224
223.951	ditto, represented specimen	1
223.952	<i>Skenea</i> sp., represented specimen	1
223.953	<i>Circulus</i> sp.	3
223.954	ditto, represented specimen	1

RGM	Name	Number of specimens
223.955	<i>Clithon (Vitocliton) aff. pictus</i> (FÉRUSSAC, 1825)	many
223.956	ditto, represented specimen	1
223.957	ditto, represented specimen	1
223.958	ditto, represented specimen	1
223.959	<i>Theodoxus (Calvertia) aff. grateloupianus</i> (FÉRUSSAC, 1821), represented specimen	1
223.960	<i>Nerita (Theiostyla) plutonis</i> BASTEROT, 1825	30
223.961	<i>Littorina (Melaraphe) sp.</i>	2
223.962	ditto, represented specimen	1
223.963	Hydrobiidae sp.	3
223.964	ditto, represented specimen	1
223.965	<i>Stenothyrella sp.</i>	5
223.966	ditto, represented specimen	1
223.967	ditto, represented specimen	1
223.968	Rissoidae sp. 1	18 (± def.)
223.969	ditto, represented specimen	1
223.970	Rissoidae sp. 2, represented specimen	1 def.
223.971	Rissoidae sp. 3, represented specimen	1 def.
223.972	<i>Teinostoma (Teinostoma) sp.</i>	56
223.973	ditto, represented specimen	1
223.974	<i>Teinostoma (Megatyloma) sp.</i> , represented specimen	1
223.975	<i>Pseudomalaxis (Pseudomalaxis) semiclastrata</i> (SPEYER, 1869)	2 fragm.
223.976	<i>Haustator (Haustator) sp. aff. venus</i> (d'ORBIGNY, 1852), sensu HÖLZL, 1962	many
223.977	<i>Melanopsis (Lyrcaea) impressa hantkeni</i> HOFMANN, 1870	19
223.978	<i>Potamides (Potamides) lamarcki</i> BRONGNIART, 1810	many
223.979	ditto	many juv.
223.980	<i>Potamides (Ptychopotamides) margaritaceus</i> (BROCCH, 1814)	many
223.981	ditto	many
223.982	ditto	many
223.983	ditto	many
223.984	ditto	many
223.985	<i>Pirenella plicata</i> (BRUGUIÈRE, 1792) s.lat.	many
223.986	ditto	many
223.987	<i>Pirenella plicata bavarica</i> (GÜMBEL, 1861)	125
223.988	<i>Pirenella laevisissima</i> (GOLDFUSS, 1844)	15 (± def.)
223.989	<i>Pirenella sp. ? n.</i>	159
223.990	ditto, represented specimen	1
223.991	<i>Terebralia aff. lignitarum</i> (EICHWALD, 1853)	80 (± def.)
223.992	ditto	27 juv.
223.993	<i>Diastoma grateloupi</i> (d'ORBIGNY, 1852)	20 juv.
223.994	<i>Sandbergeria secalina</i> (PHILIPPI, 1843)	302
223.995	<i>Bitium (Bitium) spina</i> (HOERNES, 1855)	9 (± def.)
223.996	<i>Cerithiopsis</i> (s.lat.) sp.	1
223.997	<i>Acirsa (Acirsa) sp.</i>	5 def.
223.998	ditto, represented specimen	1 def.
223.999	<i>Cirsotrema</i> (s.lat.) sp.	1 fragm.
224.000	<i>Eulima (Eulima) glabra hebe</i> (SEMPER, 1861), represented specimen	1 def.
224.001	<i>Balcis (Balcis) alba naumannii</i> (VON KOENEN, 1867)	2 def.
224.002	ditto, represented specimen	1 def.
224.003	ditto, represented specimen	1 def.
224.004	<i>Calyptraea (Calyptraea) chinensis</i> (LINNÉ, 1758)	63 (± def.)

RGM	Name	Number of specimens
224.005	<i>Erato (Eratopsis) prolaevis prolaevis</i> SACCO, 1894, represented specimen	1
224.006	<i>Globularia gibberosa sanctistephani</i> (COSSMANN & PEYROT, 1919)	2, 2 juv.
224.007	<i>Cernina (Cernina) rothi</i> (COSSMANN, 1925)	1
224.008	<i>Neverita josephina olla</i> (DE SERRES, 1829)	15
224.009	<i>Euspira helicina</i> (BROCCHI, 1814) s. lat.	56
224.010	<i>Euspira</i> sp., represented specimen	1
224.011	<i>Ampullinopsis crassatina</i> (LAMARCK, 1804)	23
224.012	ditto	5 juv.
224.013	<i>Natica neglecta</i> MAYER, 1858, represented specimen	1
224.014	<i>Ocenebrina</i> aff. <i>conspicua</i> (SANDBERGER, 1861)	1, 9 juv., 1 fragm.
224.015	ditto, represented specimen	1
224.016	<i>Mitrella (Macrurella)</i> sp., represented specimen	1 juv. def.
224.017	<i>Babylonia (Peridipsaccus) matheroni</i> MAGNE, 1942, subsp. n.	13
224.018	Melongenidae sp.	5 (\pm def.)
224.019	ditto, represented specimen	1 def.
224.020	ditto, represented specimen	1 def.
224.021	ditto, represented specimen	1 def.
224.022	<i>Dorsanum (Dorsanum) gradatum</i> (WOLFF, 1897)	19
224.023	<i>Dorsanum</i> (? <i>Dorsanum</i>) <i>hungaricum</i> (GÁBOR, 1936)	112 (\pm def.)
224.024	<i>Hinia (Tritonella)</i> sp.	51 (\pm def.)
224.025	<i>Olivella (Lamprodoma) clavula vindobonensis</i> CSEPREGHY - MEZNERICS, 1954	110 (\pm def.)
224.026	<i>Athleta (Athleta) rarispina</i> (LAMARCK, 1811)	22
224.027	Turrinae sp.	1 def.
224.028	Clavinae sp. 1	1
224.029	ditto, represented specimen	1
224.030	Clavinae sp. 2	1 def.
224.031	Clavinae sp. 3	2 juv.
224.032	<i>Bela</i> sp.	13 (\pm def.)
224.033	ditto, represented specimen	1
224.034	<i>Hastula (Hastula)</i> sp.	21 def.
224.035	ditto, represented specimen	1 def.
224.036	<i>Phasianema</i> sp., represented specimen	1
224.037	<i>Odostomia (Megastomia)</i> sp.	2
224.038	ditto, represented specimen	1
224.039	<i>Syrnola (Syrnola)</i> sp.	17 (\pm def.)
224.040	ditto, represented specimen	1 def.
224.041	<i>Syrnola (Puposyrnola)</i> sp.	6
224.042	<i>Tiberia (Loxoptysis)</i> sp., represented specimen	1
224.043	<i>Pyramidella (Milda)</i> sp.	1, 19 def.
224.044	ditto, represented specimen	1
224.045	<i>Ringicula (Ringiculina)</i> sp.	36
224.046	ditto, represented specimen	1
224.047	<i>Actaeon (Actaeon) punctatosulcatus</i> (PHILIPPI, 1843)	1
224.048	<i>Acteocina exerta</i> (DESHAYES, 1862)	120
224.049	ditto, represented specimen	1
224.050	<i>Ellobium (Ellobium) cf. subjudae</i> (D'ORBIGNY, 1852)	9
224.051	ditto, represented specimen	1
224.052	ditto, represented specimen	1
224.053	Crustacea, Cirripedia, Balanidae sp.	many specimens and fragments
224.054	Crustacea, Decapoda	29 fragm. of crab pincers

RGM	Name	Number of specimens
—	Pisces, Elasmobranchii	4 shark teeth
—	Pisces, Elasmobranchii	1 tooth of ray
—	Pisces, Elasmobranchii, <i>Myliobatis</i> sp.	1 dental segment
—	Pisces, Teleostei	46 otoliths
—	Pisces, Teleostei	82 teeth and other skeleton fragm.
224.055	concretions with tree leaves and stems, and attacked by Teredinids	6 fragm.
224.056	ditto	1 large fragm.
—	uninspected residue	about 1.5 kg
—	uninspected residue	about 1.5 kg
—	uninspected residue	about 1.5 kg

PLATE 1

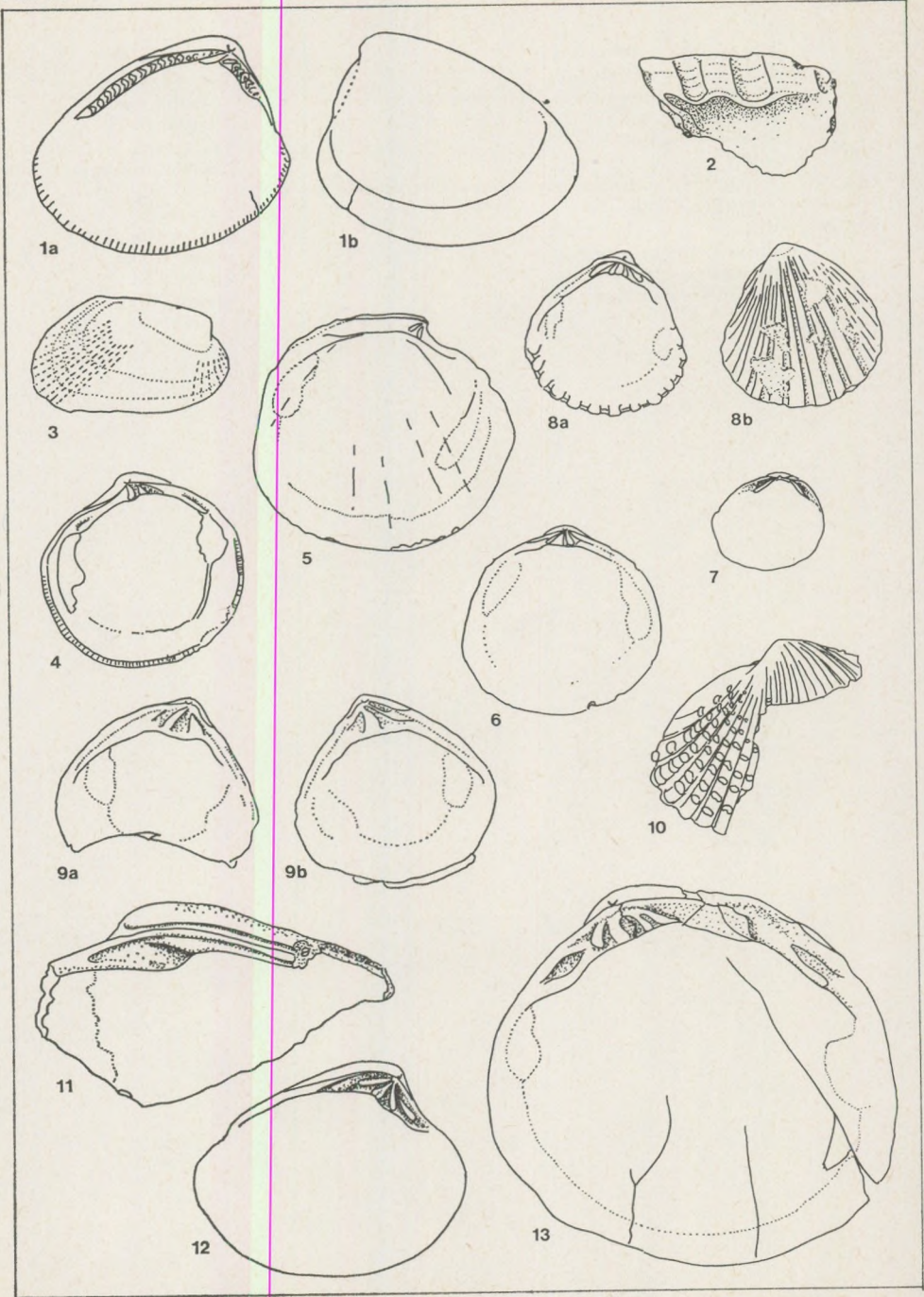


PLATE 1

- Fig. 1a-b *Nucula* (*Nucula*) aff. *nucleus* (LINNÉ, 1758), X 8.
2 *Isognomon* (*Isognomon*) *heberti* (COSSMANN & LAMBERT, 1884), X 4.
3 *Musculus* (*Musculus*) sp., X 17.
4 *Parvilucina* (*Microloripes*) sp., X 4.
5 *Saxolucina* (*Saxolucina*) *heberti* (DESHAYES, 1857), X 4.
6 *Felaniella* (*Felaniella*) sp., X 4.
7 *Mysella* (*Mysella*) sp., X 17.
8a-b *Erycinella clara* (VON KOENEN, 1891), X 17.
9a-b *Goodallia* (? *Goodallia*) sp., X 8. Left and right valve of same individual.
10 *Parvicardium* sp., X 17.
11 *Coralliophaga* sp., X 8.
12 *Callista* (s.lat.) sp., X 4.
13 *Dentonia gestini* (DESHAYES, 1830), slightly enlarged (H = 46 mm).

All specimens from Máriahalom, Hungary. Late Oligocene, Egerian, lower part of Mány Formation.
Material kept in RGM collections (Leiden, The Netherlands).

PLATE 2

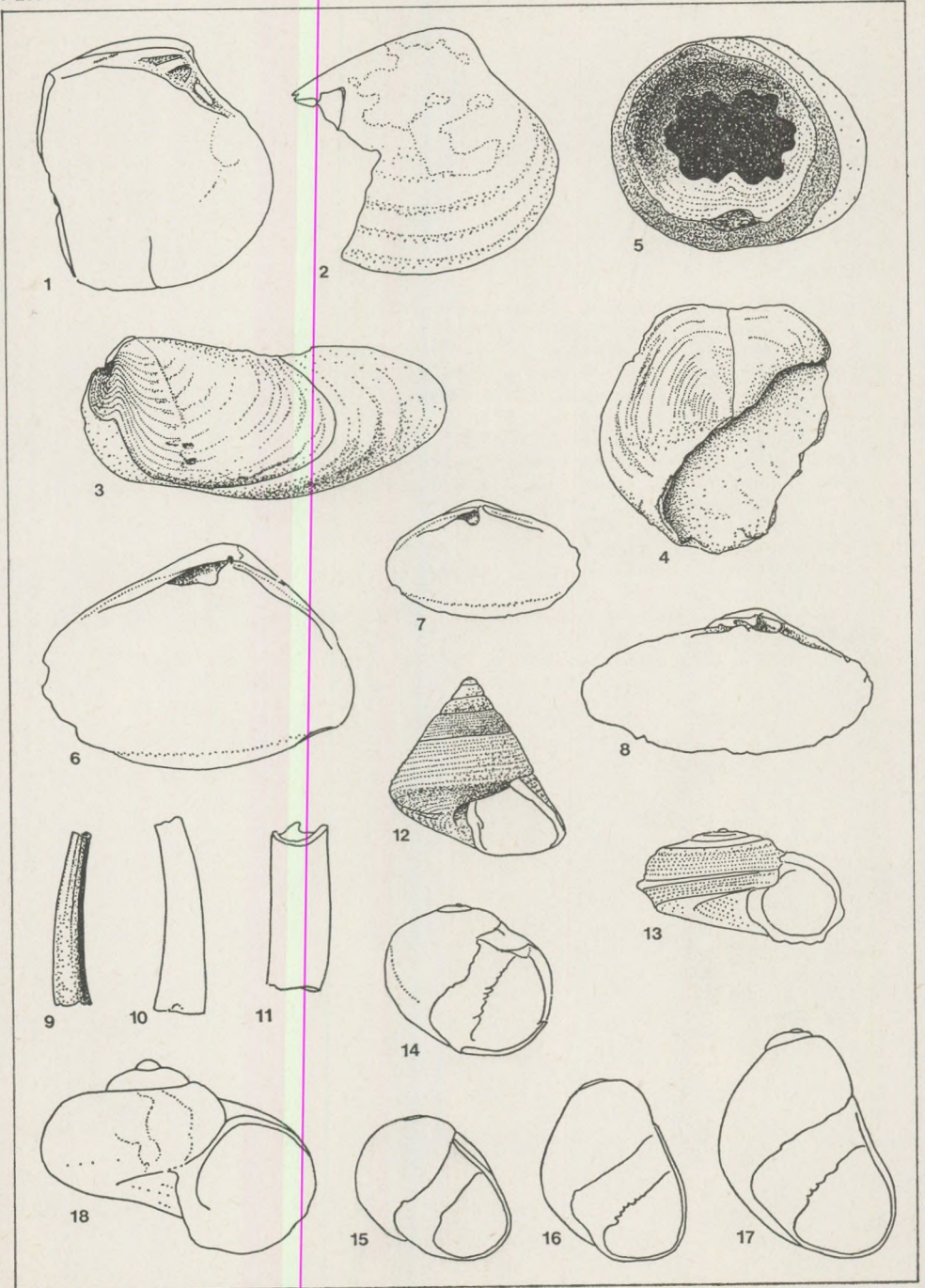


PLATE 2

- Fig. 1–2 *Chamelea* sp., X 4.
3 *Martesia* (*Martesia*) sp., X 8.
4 *Martesia* (*Martesia*) sp., mesoplax, X 8.
5 *Teredina* sp. ?, X 4. Distal view of calcareous tube.
6–8 *Lentidium* (*Lentidium*) sp., X 8.
9 *Dentalium* (*Antalis*) *seminudum* DESHAYES, 1861, X 4.
10–11 *Cadulus* (*Dischides*) sp., X 8.
12 *Jujubinus* (*Scrobiculinus*) sp., X 4.
13 *Circulus* sp., X 8.
14 *Theodoxus* (*Calvertia*) aff. *grateloupianus* (FÉRUSAC, 1821), X 4.
15–17 *Clithon* (*Vitoclithon*) aff. *pictus* (FÉRUSAC, 1825), X 4.
18 *Skenea* sp., X 34.

All specimens from Máriahalom, Hungary. Late Oligocene, Egerian, lower part of Mány Formation.

Material kept in RGM collections (Leiden, The Netherlands).

PLATE 3

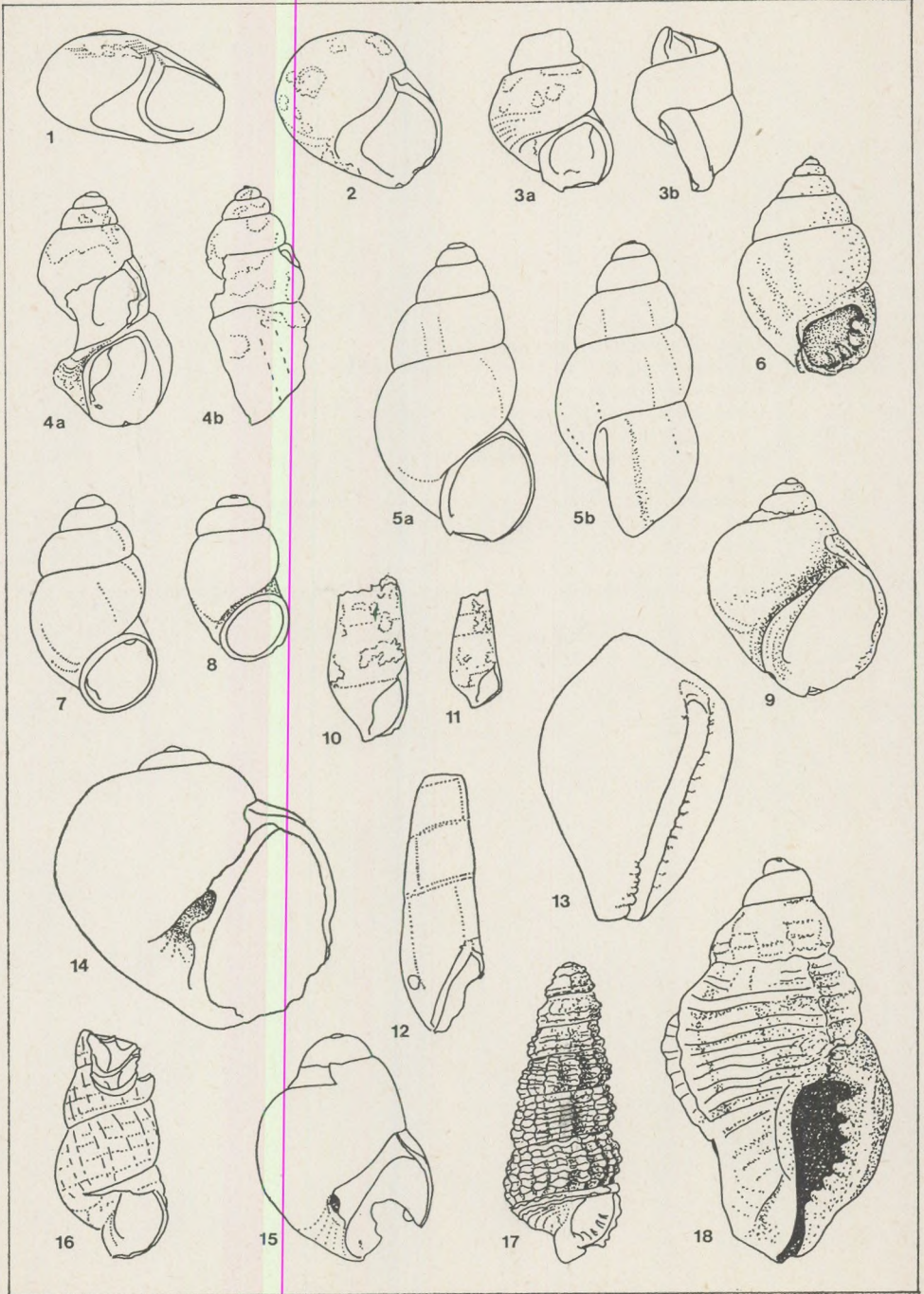


PLATE 3

- Fig. 1 *Teinostoma (Teinostoma)* sp., X 8.
 2 *Teinostoma (Megatyloma)* sp., X 17.
 3a-b Rissoidae sp. 2, X 8.
 4a-b Rissoidae sp. 3, X 17.
 5a-b Hydrobiidae sp., X 17.
 6 Rissoidae sp. 1, X 4.
 7-8 *Stenothyrella* sp. (? div.), X 17.
 9 *Littorina (Melaraphe)* sp., X 17.
 10-11 *Balcis (Balcis) alba naumanni* (VON KOENEN, 1867), X 8.
 12 *Eulima (Eulima) glabra hebe* SEMPER 1861, X 8.
 13 *Erato (Eratopsis) prolaevis prolaevis* SACCO, 1894, X 8.
 14 *Natica neglecta* MAYER, 1858, X 4.
 15 *Euspira* sp., X 8.
 16 *Acirsa (Acirsa)* sp., X 4.
 17 *Pirenella* sp. n. ?, X 4.
 18 *Ocenebrina* aff. *conspicua* (SANDBERGER, 1861)

All specimens from Máriahalom, Hungary. Late Oligocene, Egerian, lower part of Mány Formation.

Material kept in RGM collections (Leiden, The Netherlands).

PLATE 4

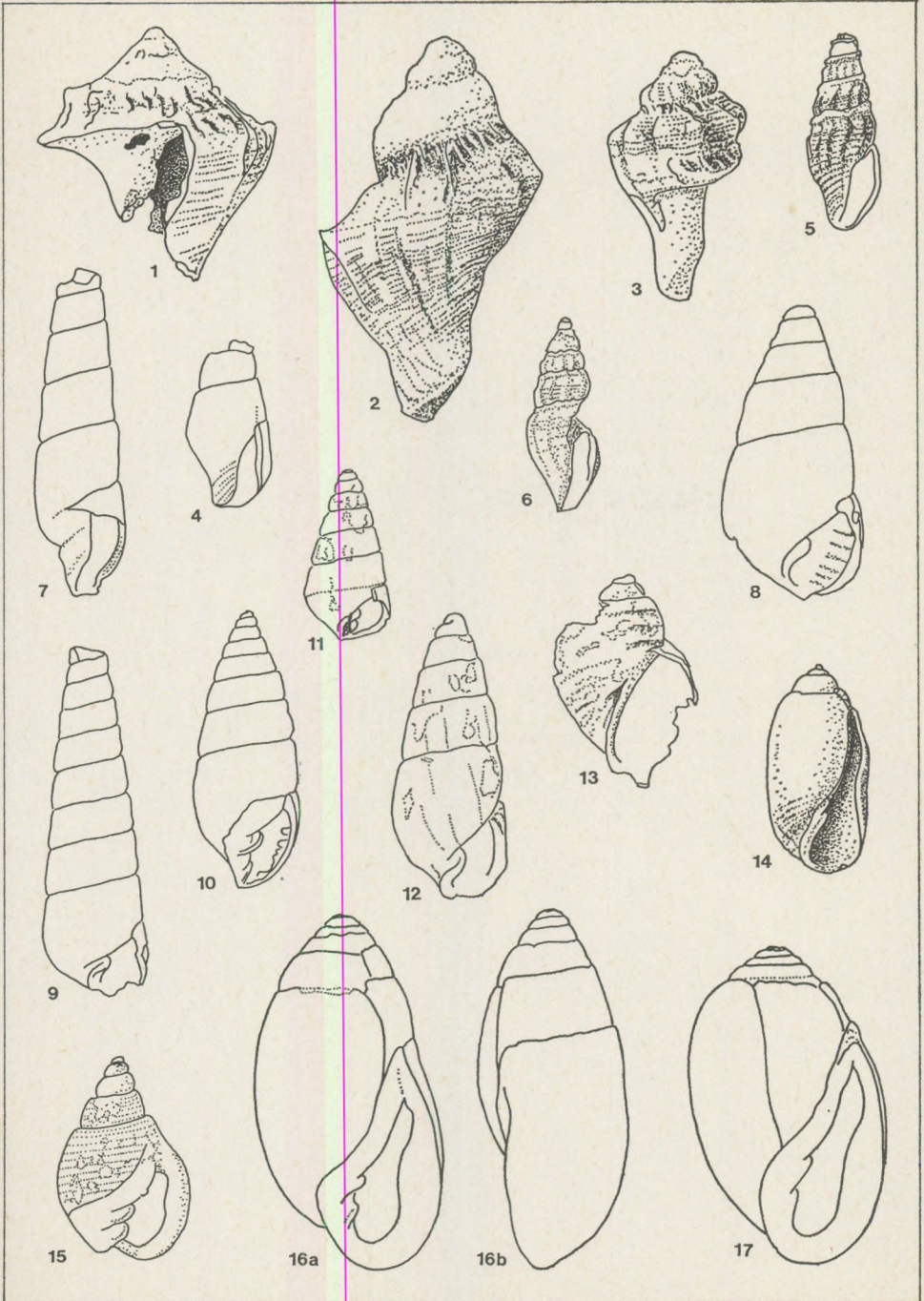


PLATE 4

- Fig. 1-3 Melongenidae sp., slightly enlarged (H = 30 mm, 45 mm, and 30 mm resp.).
4 *Mitrella (Macrurella)* sp., X 8.
5 *Clavinae* sp. 1, X 4.
6 *Bela* sp., X 4.
7 *Hastula (Hastula)* sp., X 4.
8 *Odostomia (Megastomia)* sp., X 17.
9 *Syrnola (Syrnola)* sp., X 8.
10 *Pyramidella (Milda)* sp., X 4.
11 *Tiberia (Loxoptyxis)* sp., X 8.
12 *Syrnola (Puposyrnola)* sp., X 17.
13 *Phasianema* sp., X 8.
14 *Acteocina exerta* (DESHAYES, 1962), X 8.
15 *Ringicula (Ringiculina)* sp., X 8.
16-17 *Ellobium (Ellobium)* of *subjudae* (D'ORBIGNY, 1952), slightly enlarged (H=42 mm and 38 mm resp.).

All specimens from Máriahalom, Hungary. Late Oligocene, Egerian, lower part of Máty Formation.

Material kept in RGM collections (Leiden, The Netherlands).

REFERENCES

- ANDERSON, H.-J. (1959): Die Muschelfauna des nordwestdeutschen Untermiozän. — *Palaeontographica*, (A) 113 (4-6): 61-179, 2 tab., 9 fig., pl. 13-18.
- BÁLDI, T. (1973): Mollusc fauna of the Hungarian Upper Oligocene (Egerian). Studies in stratigraphy, palaeoecology, palaeogeography and systematics. — Budapest (Akad. Kiadó), 511 pp., 55 fig., 4 tab., 51 pl.
- BÁLDI, T. (1976): A Dunántúli Középhegység és Észak-Magyarország oligocénjének korrelációja. — *Földt. Közl.*, 106 (4): 407-424, 19 figs., 9 tabs.
- BÁLDI, T., & E. CSÁGÓLY (1975): Faziostratotypus: Máriahalom. Sand pit. In: Báldi & Senes (ed.), 1975. OM Egerien. Die Egerer, Pouzdfaner, Puchkirchener Schichtengruppe etc. etc., pp. 134-137.
- BÁLDI, T. & F. STEININGER (1975): Die Molluskenfauna des Egerien. In: Báldi & Senes (ed.), 1975. OM Egerien. Die Egerer, Pouzdfaner, Puchkirchener Schichtengruppe etc. etc., pp. 341-375, 14 pl.
- BÁLDI, T. & J. SENEŠ (ed.) (1975): OM Egerien. Die Egerer, Pouzdfaner, Puchkirchener Schichtengruppe und die Bretkaer Formation. — *Chronostratigraphie und Neostratotypen. Miozän der Zentralen Paratethys*, 5, 577 pp., many tab., figs. and plates.
- COSSMANN, M. (1921-1922): Synopsis illustré des mollusques de l'Éocène et de l'Oligocène en Aquitaine. — *Mém. Soc. géol. France, (Paléont.)* 55 (1): 1-112, pl. 1-8 (1921); (2): 113-220, pl. 9-15 (1922).
- COSSMANN, M. & J. LAMBERT (1884): Etude paléontologique et stratigraphique sur le terrain oligocène marin aux environs d'Etampes. — *Mém. Soc. géol. France*, (3) 3: 1-187, pl. 1-6.
- COSSMANN, M. & A. PEYROT (1909-1935): Conchologie néogénique de l'Aquitaine. — *Act. Soc. linn. Bordeaux*, 63-86 (1909-1935, and Ouvr. cour. Acad. Sci. Arts Bell.-Lett. Bordeaux, 1-6 (1909-1932). Two parallel series were published, started by Cossmann & Peyrot, after 1925 continued by Peyrot. For a detail specification see H.-J. Anderson, 1954. Die miozäne Reinkb-Stufe in Nord- und Westdeutschland und ihre Mollusken-Fauna. — *Fortschr. Geol. Rheinl. Westf.*, 14, pp. 122.
- FUCHS, T. (1870): Beitrag zur Kenntnis der Conchylienfauna des videntinischen Tertiärgebirges. — *Denkschr. k. Akad. Wissensch., mathem.-naturwissensch. Classe*, 30: 137-216, pl. 1-11.
- GLIBERT, M. (1952): Gastropodes du Miocène moyen du Bassin de la Loire; 2. — *Mém. Inst. r. Sc. natur. Belgique*, (2) 46: 243-450, 2 tab., pl. 1-15.
- GAÁL, I. (1937-1938): Az egriekkel azonos harmadkori puhatestűk Balassagyarmaton és az oligocén kérdése. — *Ann. Mus. Nat. Hung.*, 32 pars *Min. Geol. Pal.*: 1-87 (cited after Báldi, 1973).
- GLIBERT, M. (1962): Les Mesogastropoda du Cénozoïque étranger des collections de l'Institut royal des Sciences naturelles de Belgique. 1- partie. Cyclophoridae à Stifiliferidae (inclus). — *Mém. Inst. r. Sc. nat. Belgique*, (2) 69: 1-305.
- GLIBERT, M. & J. DE HEINZELIN DE BRAUCOURT (1954): L'Oligocène inférieur belge. — *Mém. Inst. r. Sc. nat. Belgique*, vol. Jub. Victor van Straelen, 1: 281-438, pl. 1-7.
- GLIBERT, M. & L. VAN DE POEL (1966): Les Bivalvia fossiles du Cénozoïque étranger des collections de l'Institut royal des Sciences naturelles de Belgique. 3 Heteroconchia, 1^e partie. Laternulidae à Chamidae. — *Mém. Inst. r. Sc. nat. Belgique*, (2) 81: 1-82, 6 (fin). Oligodontina (2). Astartodontina et Septibranchida. — *Mém. Inst. r. Sc. nat. Belgique*, (2) 84: 1-185.
- GRATELOUP, (J.P.S. DE) (1836-1846): Conchyliologie des terrains tertiaires du Bassin de l'Adour. — *Actes Soc. Linn. Bordeaux*, 8: 247-302, 2 pl., 1836; 9: 365-432, 1 pl., 1837; 10: 92-152, 180-214, 1 pl., 251-290, 1 pl., 1838; 11: 109-146, 1839. Atlas 1. Univalves, 45 pl. with explanations, Bordeaux (Lafargue), 1840; suppl., pl. 46-48 with explanations, Bordeaux (Lafargue), 1846.
- HÖLZL, O. (1962): Die Molluskenfauna der oberbayerischen marinen Oligozänmolasse zwischen Iear und Inn und ihre stratigraphische Auswertung. — *Geol. Bavarica*, 50: 5-271, 13 fig., 12 pl.
- HOERNES, M. (1851-1870): Die fossilen Mollusken des Tertiärbeckens von Wien. — *Abh. k. k. geol. Reichsanst.* 3-4.
- JANSSEN, A. W. (1980): Report on a field-trip to the German Democratic Republic, Poland and Hungary. September/October 1979, made by A. W. Janssen. Leiden (Rijksmus. Geol. Mineral., report Nr. 61, dept. Eur. Caen. Moll.), 33 pp., 12 fig. (not published, photostatic copies available on request).
- JANSSEN, R. (1978-1979): Die Mollusken des Oberoligozäns (Chattium) im Nordsee-Becken. 1. Archopoda, Archaeogastropoda, Mesogastropoda, 2. Neogastropoda, Euthyneura, Cephalopoda. — *Arch. Moll.*, 109 (1-3): 137-227, pl. 9-14, 1978 (1), 109 (4-6): 277-376, pl. 15-18, 18a, 1979 (2).
- JANSSEN, R. (1979): Revision der Bivalvia des Oberoligozäns (Chattium, Kasseler Meeressand). — *Geol. Abhand. Hessen*, 78: 1-181, 1 fig., 4 pl.
- MAYER, C. (1861-1903): Description de coquilles fossiles des terrains tertiaires inférieurs. — *Journ. Conchyl.*, 9-51.
- MOORE, R. C. (ed.) (1969-1971): Treatise on invertebrate paleontology, 1. Mollusca 6, Bivalvia 1-3. Boulder (Geol. Soc. Am., Univ. Kansas), 1224 pp., many fig.
- NEUFFER, F. O. (1973): Die Bivalven des Unteren Meeressandes (Rupelium) im Mainzer Becken. — *Abh. hess. L.-Amt. Bodenforsch.*, 684 1-113, 13 pl.
- ROTH VON TELEGD, K. (1914): Eine ober-oligozäne Fauna aus Ungarn. — *Geol. Hung.*, 1 (1): 5-77, 6 pl.
- SACCO, F. (1890-1904): I molluschi dei terreni terziarii del Piemonte e della Liguria, 7-30, many pl. (vol. 1-6 appeared under the authorship of L. Bellardi).
- SANDBERGER, F. (1858-1863): Die Conchylien des Mainzer Tertiärbeckens. Wiesbaden (Kreidel), 468 pp., 35 pl.
- SANDBERGER, F. (1870-1875): Die Land- und Süßwasser Conchylien der Vorwelt. Wiesbaden (Kreidel), VIII + 1000 pp., atlas with 36 plates (4 vols.).
- TOURNOUER, R. (1872): Auriculidées fossiles des faluns. — *J. Conchylol.*, 20: 77-116, pl. 3-4.
- VERGNEAU, A. M. (1959): Observations paléontologiques et paléocécologiques sur les gastropodes du Stampien de Gaas, Landes. Thèse (3e cycle, Univ. Bordeaux), 210 pp., 4 tab., 12 pl.
- WENZ, W. (1923): Gastropoda extramarina tertiaria, 4. — *Fossilium Catalogus, 1. Animalia*, 21: 1069-1420.
- ZILCH, A. (1938): Die Pedalion-Arten des mitteleuropäischen Tertiärs. — *Senckenbergiana*, 20 (5): 363-380.

CONTRIBUTION TO THE LITHOLOGY OF THE REWORKED CLASTIC DOLOMITE COMPLEX OF THE SOUTHERN GERECESE FORELANDS (TRANSDANUBIA, HUNGARY)

by

FÁY-TÁTRAY, M.

Eötvös L. University, Budapest; Department for Applied- and Engineering Geology
Budapest VIII., Múzeum krt 4/A

SUMMARY

It was during the seventies that intense exploration in the Gerecse Forelands disclosed the presence of a fanglomerate-like, reworked, clastic dolomite complex almost all over the area concerned. Genetics and the possibilities of lithological classification of the said complex are presented in the paper.

* * *

The reworked clastic dolomite complex of the Nagyegyháza-basin (discovered during the exploration of the bauxite and coal reserves of the area) has been recognized in the form of more or less continuous patches also in almost all of the small basins adjoining the Gerecse Forelands and is the subject of exploration even now.

In the Nagyegyháza basin it occurs as an essentially continuous sheet, the thickness of which is 25 to 30 meters, while at Mány it is only about 20 meters thick and is confined to two basin-like troughs divided by an unproductive "barren" zone. At Mány-East — instead of being continuous — it occurs locally in the form of patches of various size the thickness of which does not exceed 10 meters.

In the Tarján — Héreg — Bajna area its occurrence is restricted to small sinkhole-like depressions of the bedrock.

At Nagyegyháza the reworked dolomite complex is immediately underlain by a workable, strata-like bauxite-sheet, while at Mány only scattered patches of bauxite are found beneath the dolomite-scrée, the latter indicating that it was only the depressions of the carbonate terrain which were filled with bauxite in that case. It will be discussed later on that the accumulation of bauxites has been repeatedly recurrent in this area. Based on its shape and extension the reworked dolomite complex can be confined to tectonically controlled depressions of the carbonatic basement.

As to its lithological composition, the scree consists mainly of fragments of Middle to Upper Triassic rocks (predominantly dolomites and somewhat less commonly also "dachstein" limestones). It is assumed that these rocks were subject to intense physical and chemical weathering as a result of which they disintegrated and were transported and redeposited either by means of simple gravitation-controlled mass-movements (= phanglomerate-like depositions) or by ephemeral water courses (see also Тóти,

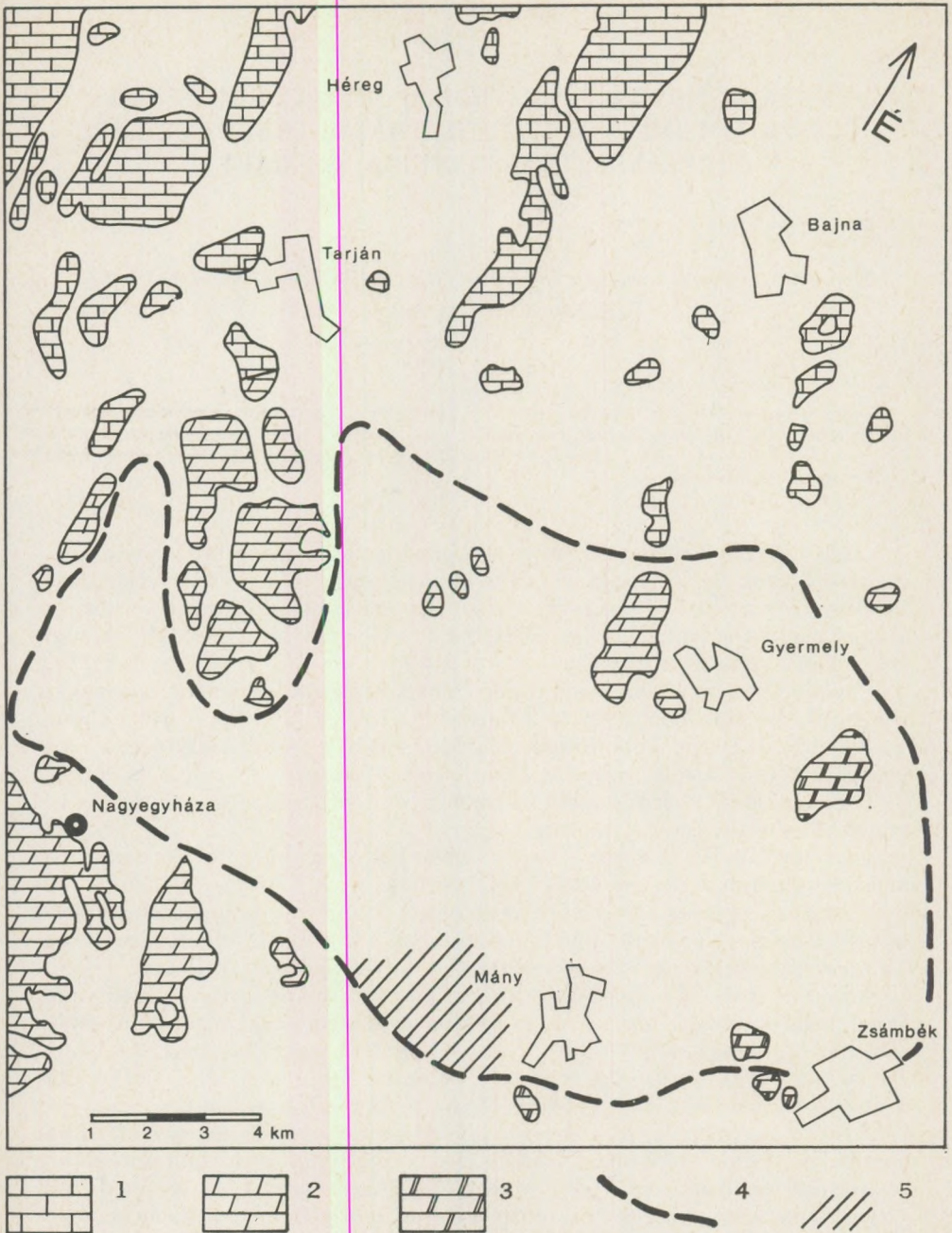


Fig. 1. Areal extension of the reworked elastic dolomite complex

Legends: (1) "Dachstein" limestone, Norian to Raethian "Hauptdolomit" Carnian-Norian (3) Diplopóra-Dolomites Ladinian (4) Boundaries of the reworked dolomite complex (5) Occurrences of the "upper" reworked dolomite complex

Á. 1974). As to grain-size, the material is rather varied: it contains boulders of several tens of centimeters or even meters diameter and fine, silt-size dolomite-powder as well, the latter being considered as the matrix of the reworked clastic dolomite complex.

As to its origin, part of the silt-size dolomite-powder is of clastic nature, i.e. it was formed by disintegration, as a result of the intense physical and chemical weathering and was transported to its present position together with the coarse fraction of the complex. Part of it, however, in undoubtedly of in situ origin, having been formed by postdepositional, mainly chemical processes such as diagenic dissolution and disintegration.

The amount of the powder matrix varies between 0 to 100 percent in most samples. Whether the percentage of the fine-grained dolomite powder conforms to the powder content of the original sediment can be established in the case of the cemented clastics only. Cementation may have been brought about by dissolution and reprecipitation of the carbonatic material either in contact with downward percolating, SO_4 -rich waters of the overlying swamp, or at the time of postdepositional inundation. When drilling at places of no cementation it is impossible to get any representative sample from the uncemented clastic complex. Fine grains are washed off namely by the flushing medium and consequently cores are relatively "enriched" in coarse ones, thus the original grain-size distribution is distorted.

Nevertheless, a definite upward decrease of the average grain size of the dolomite debris within the vertical profile seems to be a general rule all over the area. It can be related to the geomorphological evolution of both the source area and the sedimentary basin. Due to intense denudation the relative height of the source area must have been gradually decreased while the rate of sedimentation being rather high the sedimentary basin became gradually filled up. Thus, with the relief getting increasingly gentle, the grain-size of the transported material became finer and finer. Another consequence of the intense denudation is the fact that the deeper the erosion penetrated, the wider the scope of the eroded material. After stripping the more-or-less homogeneous uppermost Triassic strata, the erosion reached namely an originally deeper seated level consisting of various types of dolomites which gave rise to the deposition of the heterogeneous "polymict" dolomite-breccias in the uppermost parts of the clastic dolomite complex. This heterogeneous breccia consists of dolomite fragments of different colour and texture.

Together with the dolomite scree bauxites were also transported onto the area of deposition. Part of the bauxite was literally mixed with the scree and when laid down it was washed into the open pore-spaces of the previously deposited loose clastics. Part of it, however, was laid down in the form of smaller or larger lenticular bodies of reworked bauxite interbedded within the dolomite-scree (= this is the so called "interlayered" horizon of the Nagygyháza bauxite deposit).

After the relief had been essentially levelled but swamps had not yet formed, there was another period of reworking and redeposition of bauxite

at Nagyegyháza, which resulted in the formation of the so-called "upper bauxite horizon", the final member of the reworked complex. As to lithology, this upper bauxite horizon exhibits rather unique characteristics: it is generally gray and rich in pyrite — clear signs of a most probably epigenetic reduction which was brought about by descendant low-Ph solutions originating in the overlying coal-swamp. Although of limited extent, the same horizon occurs in the Mány-basin, too.

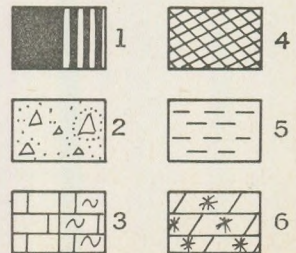
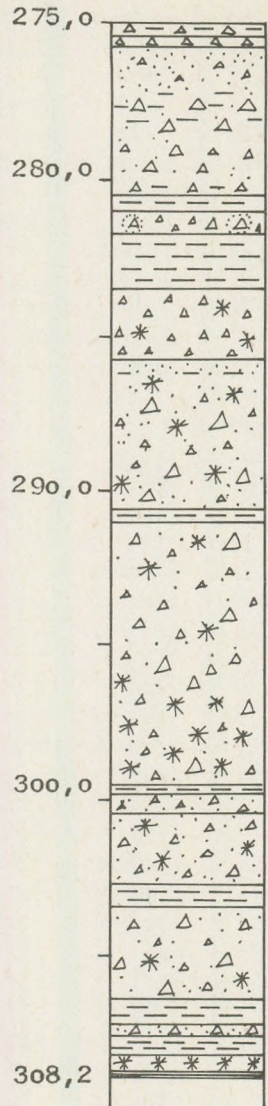
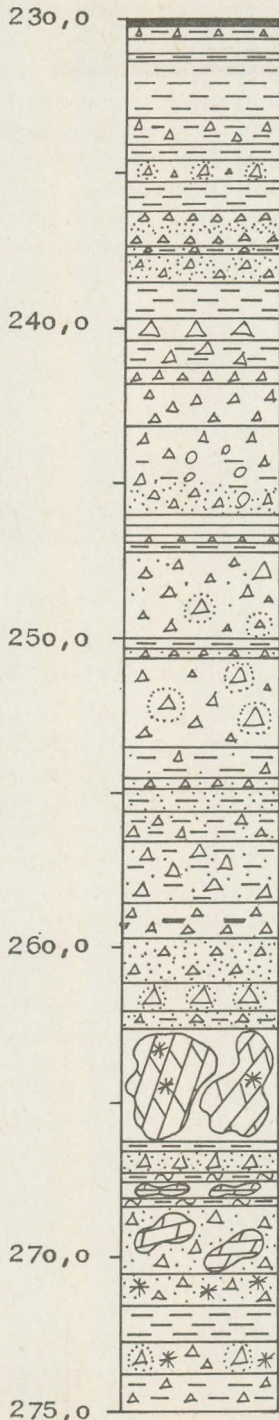
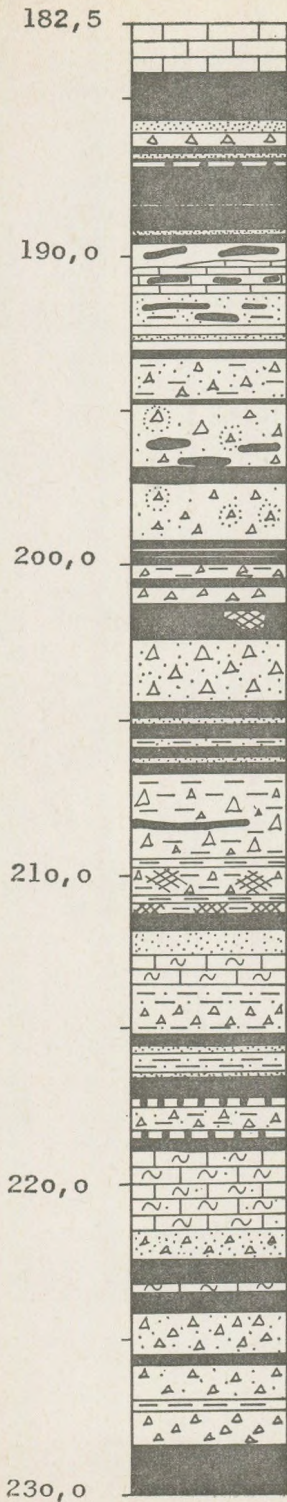
With the beginnings of the formation of the coal-measures, the accumulation of the reworked dolomite scree gradually ceased. It is the carbonaceous clays containing yet smaller or larger amounts of dolomite debris and belonging essentially to the coal-measures, that can be taken for the transition between the two. One of the most prominent representatives of the transition-member was found in borehole No Zs-29 (See Fig. 2.) which penetrated the pinched-out end of the coal-seam consisting of 45 meters of alternating minor coal-seams, carbonaceous clays, dolomite debris argillaceous dolomite-powder, angular dolomite fragments embedded into bauxite and with only 3 meters of the otherwise rather common calcareous marls. Beneath this transitional series the hole penetrated 123 meters of dolomite-scrée, the silt-size (=powdery) dolomite content of which markedly decreased downwards. At the basis of the here extraordinarily thick clastic complex there were also large blocks and boulders of dolomite.

In the Southern part of the Mány area (See Fig. 1.) there is an additional horizon of reworked dolomite, overlying the coal-measures, and belonging to the lowermost section of the Eocene Alveolina-Limestone series. It consists either of well-rounded dolomite pebbles cemented into a conglomerate or it may be represented merely by huge dolomite blocks of several meters diameter. Based on its geometry and the facies of the surrounding formations this uppermost "reworked" dolomite horizon should be taken for an abrasion conglomerate rather than the equivalent of the lower, terrestrial dolomite debris depositions. As to the age of the reworked dolomite complex, it is the carbonaceous intercalations, the palynological study of which serves as a basis for a reliable estimation. According to the palynological investigations of L. RÁKOSI, they can be taken for Eocene (Lutetian). The Foraminifera fauna found in the "upper" dolomite-clastite horizon of Mány definitely proves the Middle Eocene age of the complex (KÉCSKEMÉTI, T)

As to lithology, there are basically two possible ways of classifying the Nagyegyháza — Csordakút — Mány-type clastic complexes. One possibility is the creation of independent taxa for every one of the charac-

Fig. 2. Stratigraphic column of borehole Zs-29 showing the transitional (lignitiferous) part of the reworked dolomite complex

Legends: (1) Coal-carbonaceous clay (2) Dolomite-debris with dolomite-powder (3) Limestone, calcareous marl (4) Bauxite (5) Clay (6) Cherty dolomite. Further: combination of all the above symbols



teristic specimens comprising the series. The other — and much more convenient — one is to establish a restricted number of so-called “ideal” types, by the combination of which all members of the series can be easily deduced.

During the early stages of the exploration of the Nagyegyháza — Csordakút — Máty area the first method was used when trying to standardize the description of the core-samples recovered from the reworked dolomite complex. With the number of the investigated core-samples increasing, the grouping of the specimens into “ideal” types became facilitated. The establishment of the “ideal” types was based the investigation of 180 boreholes sunk at Nagyegyháza, 200 at Máty and about 100 on other sections of the area in question.

When defining the said ideal types the following lithological characteristics were taken into consideration:

- material
- shape of the clastic elements
- the nature of the cement

(As to the fine-clastic matrix, it could not be used for a criterion of classification because it invariably consisted of fine — less than 1 mm diameter — dolomite-grains, i.e. of dolomite-powder.)

Based on the above principles classification was carried out along the following main lines:

- (1) According to the material of its clastic constituents the reworked dolomite complex may be
 - homogenous, consisting of one particular kind of dolomite
 - heterogeneous, consisting of several kinds of dolomite
 - heterogeneous, consisting of fragments of dolomite and limestone
 - heterogeneous, consisting of dolomite, and/or limestone, and clay, or grains of red- or gray bauxite
 - heterogeneous, consisting of dolomite, and/or limestone, and carbonaceous clay and/or coaly detritus
- (2) According to the shape of the clastic constituents, they may be reworked clastics consisting of
 - angular fragments, exhibiting no rounding at all
 - fragments with signs of some slight wear at the most protruding points
 - well rounded fragments
 - angular *and* rounded fragments (that is, they may be heterogeneous, i.e. conglobreccias)
- (3) As to the nature of the cement they may be
 - carbonatic
 - pyritic
 - argillaceous (red or gray)
 - carbonaceous-argillaceous

The minimum number of variations of the above listed types is 64. It is only about 15 to 20 of them which proved to be common up to now. The most characteristic of them are shown by Photos Nos.

This seemingly mechanical classification has its geological implications, too. As to the material of the clastic constituents, it may be indicative of the age of the blocks which, at the time of the accumulation of the clastic dolomite complex had been elevated, and thus the sites of denudation. Although most of the clastic grains are rather undistinctive, i.e. they were hard to identify even in their original (Upper Triassic) position, some of them are characteristic even in fragments. Examples are the stromatolites of Norian age, the brown and purple-coloured Upper Carnian dolomites, then the Lower Carnian dark-gray, sometimes even black dolomites and – perhaps the most distinct of all – the Lower Carnian “Hornstein”.

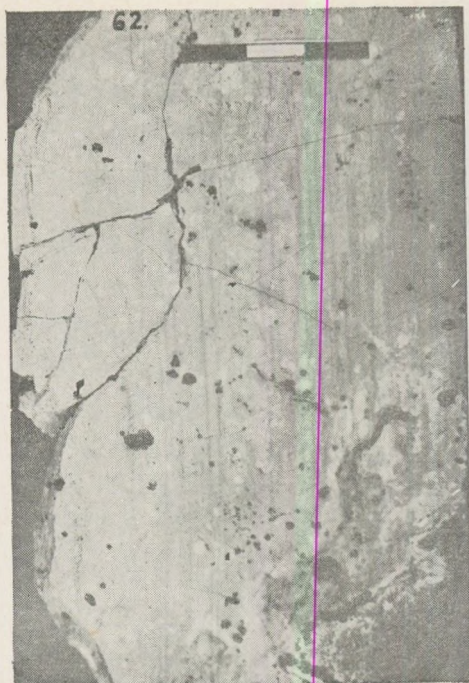
Since the shape of any transported clastic grain is principally determined by the distance of the transportation on the one hand and by the transporting medium (i.e. permanent- or ephemeral watercourses, etc.) on the other hand; the shape, as such, may be indicative of either of the two. Being influenced, however, by some other factors (such as physical properties like brittleness, friability or pulverulency of the rock) too, the shape of the clastic grains alone is not to be taken for a decisive argument when trying to re-construct palaeogeomorphological environments.

Shape and size together, or more exactly their variations may facilitate, however, the establishment of the direction of transport, which in the case of both the Nagygyháza and the Mány area must have been from South to North.

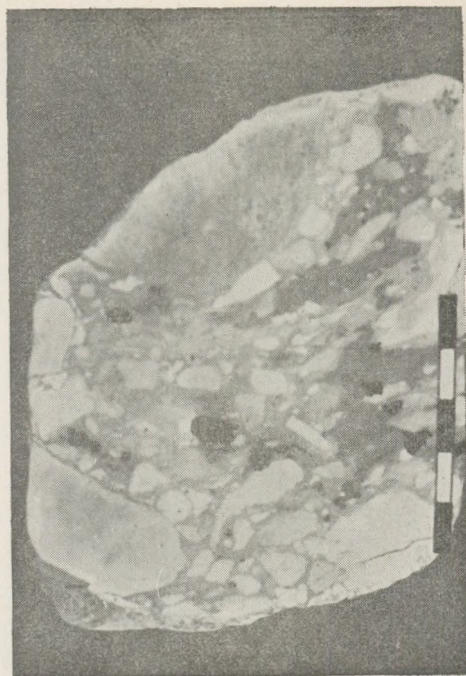
It is the nature of the cement and also the fine matrix which are most important from the practical point of view. They are namely responsible for both the permeability and the stability of the clastic dolomite complex.

The presence of any bauxitic or argillaceous bauxitic members may considerably decrease the permeability of the sequence and thus is of remarkable importance from point of view of protection against karstic water-inrushes.

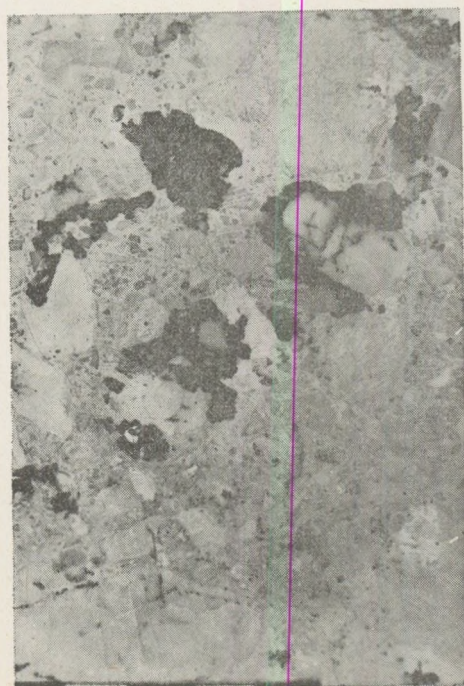
The extremely fine-grained “powder” dolomite matrix also deserves attention when present, because either the intergranular spaces may be filled by it, or it may occur in the form of smaller or larger (several tens of centimetres or even metres/thick) “layers” interbedded in the coarse clastic sequence. It may be taken for a permeability-decreasing factor only when sufficiently cemented, and thus providing no load into the waters passing through.



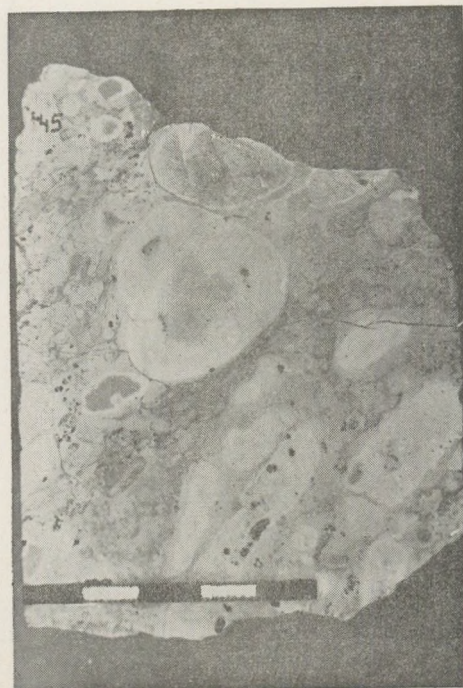
1



2



3



4

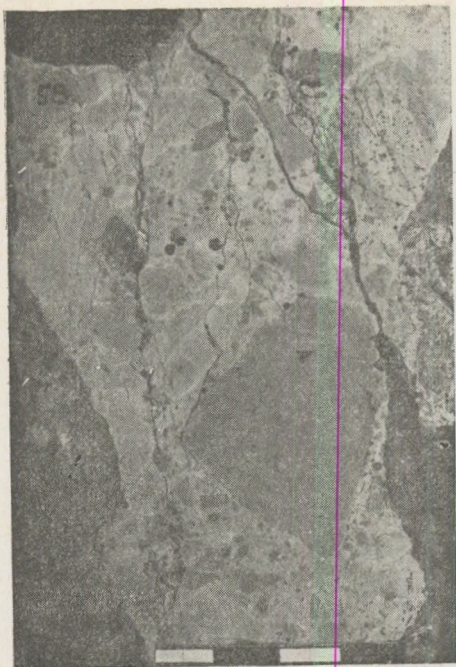
PLATE 1.

Fig. 1. Heterogeneous, unsorted dolomite scree with angular grains embedded into a powdery dolomitic matrix cemented by carbonatic material. The black spots are small aggregates of pyrite

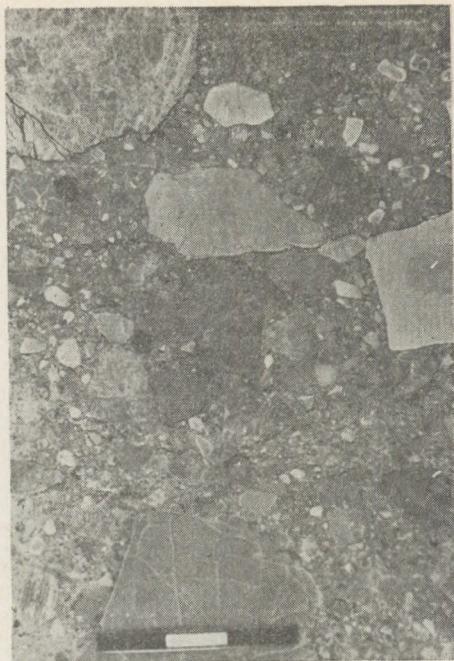
Fig. 2. Heterogeneous, unsorted dolomite scree with angular to subangular grains embedded in a loose powdery-dolomitic matrix, slightly cemented by some carbonatic material

Fig. 3. Heterogeneous, unsorted dolomite-scree, with angular to rounded grains. The matrix is scarce and only slightly cemented by carbonatic material

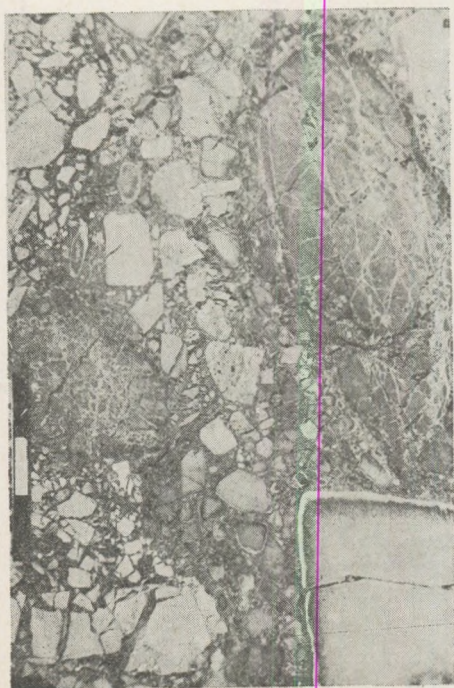
Fig. 4. Heterogeneous, medium-sorted dolomite-scree with angular to rounded grains embedded in a limonite-coloured matrix. Rounding is mainly due to pulverization along a surficial "crust" of the grains



5



6



7



8

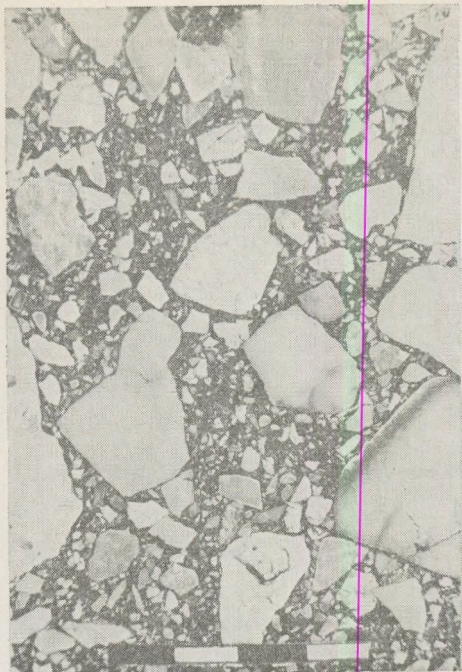
PLATE 2.

Fig. 5. Rounded, well-sorted, fine-grained dolomite-scrée with the dolomite grains embedded in a powdery dolomitic matrix rich in disseminated pyrite

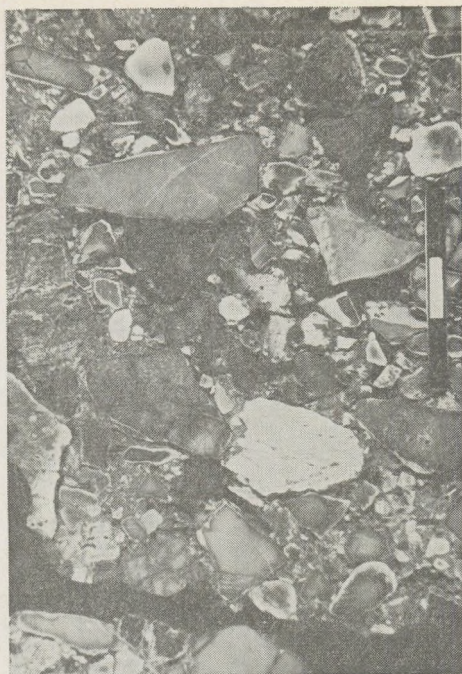
Fig. 6. Heterogeneous, unsorted dolomite scree, with the edges of the dolomite grains rounded. Matrix: powdered dolomite. Cement: gray, argillaceous with large patches of pyrite

Fig. 7. Heterogeneous, unsorted, angular to subangular dolomite scree, with the dolomite-grains embedded in a powdery dolomitic matrix with disseminated pyrite and — at places — also with pyritic impregnations

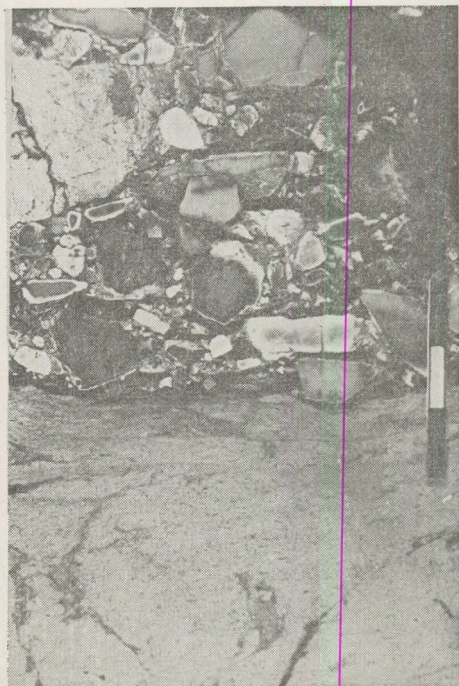
Fig. 8. Heterogeneous, slightly sorted but well-rounded dolomite scree embedded into a powdery dolomitic matrix cemented by a gray, argillaceous-pyritic material



9



10



11



12

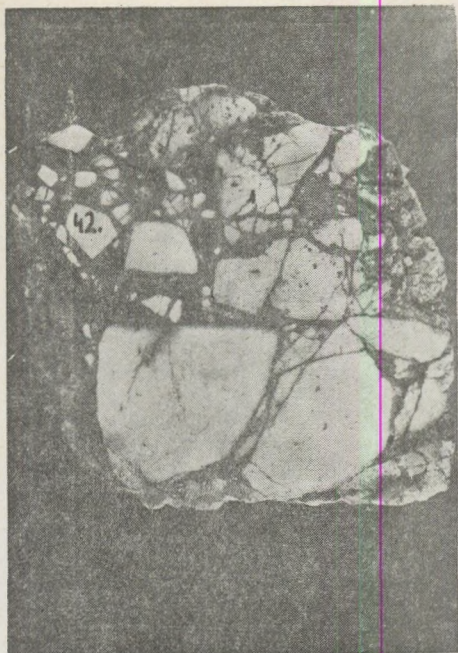
PLATE 3.

Fig. 9. Heterogeneous, medium-sorted dolomite scree, with the angular to subangular dolomite grains embedded into a powdery dolomitic matrix and cemented by a carbonaceous argillaceous material

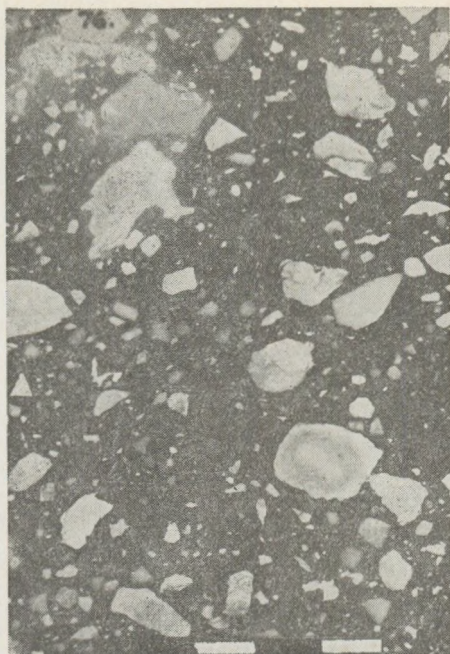
Fig. 10. Heterogeneous, medium-sorted dolomite scree with angular dolomite grains and coal-detritus embedded in subordinated amounts of powdered dolomite, cemented by a gray, clayey, lignitiferous material

Fig. 11. Heterogeneous, medium-sorted, loose dolomite-scrree with subordinated amounts of dolomite-powder, immediately overlying the lignitiferous clays or the calcareous marls of the coal-measures

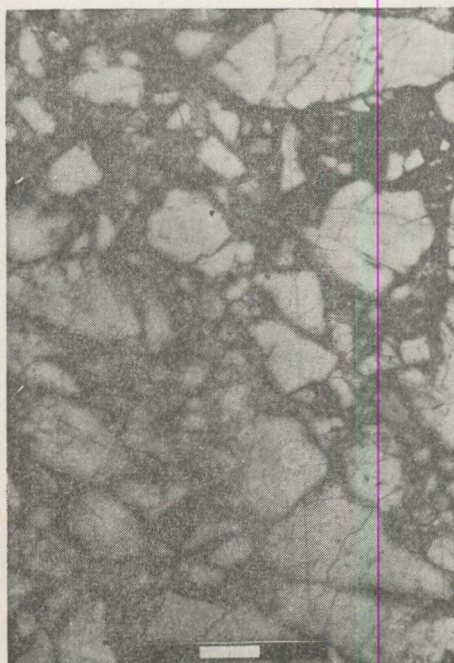
Fig. 12. Stromatolitic dolomite boulder (bottom) with heterogeneous angular dolomite fragments embedded into brown-coal



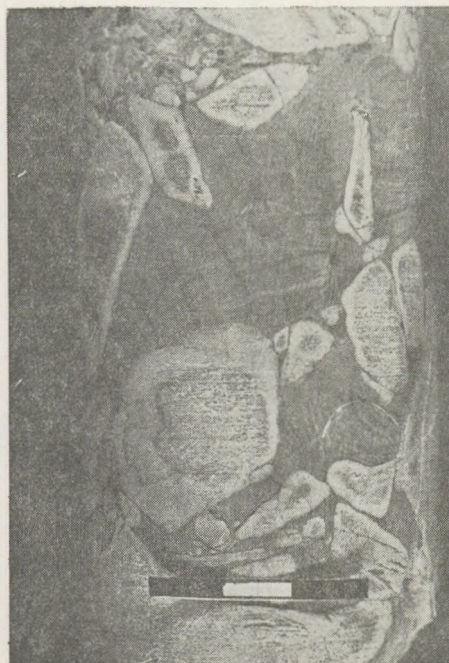
13



14



15



16

PLATE 4.

Fig. 13. Unsorted, subangular dolomite fragments embedded into a powdered dolomite matrix cemented by red limonitic clay

Fig. 14. Poorly sorted, heterogeneous dolomite scree with subordinated amounts of dolomite powder, cemented by large amounts of red argillaceous-bauxitic(?) material

Fig. 15. Poorly sorted, subangular debris of "Dachstein" limestone cemented by a red clayey and partly also carbonatic material

Fig. 16. Unsorted, homogeneous dolomite scree, with the edge of the dolomite grains pulverized. The matrix consists of dolomite powder and is coloured by rhythmical precipitations of iron-oxide

REFERENCES

- TÓTH, Á. (1974): A short review of the dolomite conglomeration-breccia complex overlying the main bauite horizon of the Nagygyháza basin. Balatonalmádi, manuscript. (in Hungarian)
- VÉGH, E. (1972): Expert Report on the Dolomitic Core-samples Recovered from Exploratory holes of the Nagygyháza - Mány area. Bp. manuscript. (in Hungarian)
- WILLEMS, T., SCHMIEDER, A., BAGDY, I., SZILÁGYI, G., KESSERÜ, Zs. (1973): On the possibilities of protection against karstic water inrushes in the Nagygyháza - Csordakút - Mány mining district, with special regard to certain environmental conditions disclosed by the latest drilling campaigns. Bp. manuscript. (in Hungarian)
- (1976): Final Report on Exploration for Coal-, Bauxite- and Water resources in the Nagygyháza basin. Tatabánya, Manuscript. (in Hungarian)
- Working Committee of the Geol. Soc. of Hungary (1970): Report on the complex geological investigation of the reworked dolomites of the Nagygyháza - Csordakút - Mány area. Bp. Manuscript. (in Hungarian)

AMMONITES AND STRATIGRAPHY OF THE BATHONIAN AT ÓFALU, EASTERN MECSEK MOUNTAINS (S. HUNGARY)

A. GALÁ CZ

Department of Paleontology, Eötvös L. University, Budapest

(Received: 15th March, 1982)

РЕЗЮМЕ

Новые раскопки в средне-юрских слоях местности Кохтал (Сенвэлдь), находящейся около деревни Офалу в восточной части гор Мечек и известной как классическое палеонтологическое месторождение, дали новую очень богатую аммонитовую фауну. На основании собранных послойно аммонитов появилась возможность для ревизии прежней литостратиграфической классификации. В красной желваковой известняково-мергелевой формации были обнаружены нижнебатский Zigzag, среднебатский *Progracilis* и *Subcontractus*, а также верхнебатские зоны Ходсона. Среднебатскую зону Морриса, по-видимому, нельзя было выявить только из-за отсутствия ее форм-указателей.

Из-за преобладания видов *Phylloceras* и *Lytoceras* аммонитовая фауна указывает на средиземноморские черты, однако найдено и большое количество таксонов северо-западной Европы. Примечательно относительно большое число микроконховых аммонитов. Самые важные с биостратиграфической точки зрения виды аммонитов были обсуждены и представлены подробнее. Данная работа представляет собой первый шаг в переоценке батских аммонитов гор Мечек.

Introduction

In 1880—81 J. Böckh published the stratigraphical and paleontological results of his studies on the Middle Jurassic of the Mecsek Mountains. The paleontological work, abreast of the time, is the first Hungarian Jurassic ammonite monograph. Regrettably the work was published only in Hungarian, thus it remained neglected in the international literature.

In 1981 geology students taking summer field exercises, revisited the Kohltal at Ófalu, one of the classical Middle Jurassic localities of the Mecsek Mountains, which was also studied by Böckh. They carried out petrographical, sedimentological investigations and collected a rich ammonite fauna, which was handed over to the present author for determination. The material, which was collected layer-by-layer, made possible to give an accurate stratigraphic arrangement of the red, nodular calcareous marl. The here exposed formation is of a wide-spread occurrence in the Mecsek Mountains, and is regarded as an important marker horizon.

The Kohltal of Ófalu is an important locality, because this is the type area (Eszterpuszta in earlier times) from where Böckh described *Bullatimorphites eszterense*, an ammonite indexing his stratigraphical unit the "Eszterense beds".

The Middle Jurassic rocks of Ófalu have been repeatedly studied during the last 120 years. The good outcrops with rich fauna were the bases for significant stratigraphical conclusions. The present work reviews critically the results of these previous studies, and presents a detailed stratigraphic arrangement and the stratigraphically most important ammonite finds.

History of previous studies and former stratigraphic arrangements

The Ófalu sequence is the easternmost surface outcrop of Jurassic rocks in the Mecsek Mountains. Its most interesting feature is its relatively small thickness, which can be due mainly to the reduced Lower Jurassic series (HETÉNYI et al. 1976). The reduced thickness of the sequence was explained by tectonic causes (VADÁSZ 1935, p. 97), but primary, paleogeographic causes can also be taken into consideration (WEIN 1967, p. 380).

The Middle Jurassic beds of Ófalu were first mentioned by PETERS (1862, p. 39), but he disregarded the detailed study, because his work was focused on the Lower Jurassic formations. HOFMANN and BÖCKH (in HAUER 1876, pp. 22, 25) were the first to call attention to the rich ammonite fauna of the Middle Jurassic in the Mecsek Mountains, at Ófalu among others. Later BÖCKH in his 1880–81 work gave a detailed description of the sequence and the fauna of these localities.

BÖCKH (1880–81, p. 36) described the Middle Jurassic of Ófalu under the locality name "Eszter" in the Stratigraphical part of his monograph. He studied two outcrops of the red, nodular, ammonitic sequence. The lower part of the sequence was exposed in the road-cutting along the Kohltal. He gave the following list of ammonites from this outcrop:

- Lytoceras tripartitum* RASP. sp.
- L.* cfr. *Adeloides* KUD. sp.
- Phylloceras euphyllum* NEUM.
- Ph. disputabile* ZITT.
- Ph. mediterraneum* NEUM.
- Ph. Zignoanum* D'ORB. sp.
- Oppelia (Oekotraustes)* sp. indet.
- Stephanoceras linguiferum* D'ORB. sp.
- S.* n. sp. indet. (cfr. *rectelobatum* HAUER sp.)
- S. Eszterense* n. sp.
- S.* n. sp. indet. (cfr. *Eszterense*)
- S.* sp. indet. (cf. *Ymir* OPPEL sp.)
- S.* cfr. *bombur* OPP. sp.
- Perisphinctes curvicosta* OPP. sp.
- P. funatus* OPP. sp.
- P.* cfr. *wagneri* OPP. sp.

He named the succession yielding this fauna as "Stephanoceras Eszterense beds", and placed it into the Upper Bathonian. However, he regarded the

fauna as a mixed assemblage, with forms (*Lytoceras tripartitum*, *Stephanoceras linguiferum*) indicating the Lower Bathonian and with elements (*Perisphinctes curvicostis*, *P. funatus*) suggesting the Lower Callovian. He pointed out that the Eszterense beds are not contemporaneous with other Mecsek Mts. occurrences of the red, nodular ammonitic beds, because these represent in other outcrops the Lower Bathonian (= "Stephanoceras recelobatum beds" of БÖCKH), or belong to the Lower Callovian.

БÖCKH gave an other Middle Jurassic faunal list from Ófalu, of which elements were collected from the yellowish-reddish limestone overlying the Eszterense beds that had been exposed in a small quarry near the entrance of the Kohltal.

These ammonites are as follows:

- Phylloceras euphyllum* NEUM.
- Ph. disputabile* ZITT;
- Ph. mediterraneum* NEUM.
- Haploceras vallis-calcis* n. sp.
- Stephonoceras bullatum* D'ORB. sp.
- Perisphinctes Recuperoi* GEMM.
- P. patina* NEUM.
- P. cfr. leptus* GEMM.

He regarded this fauna as of Lower Callovian, and ranged it into the "Stephanoceras macrocephalum horizon".

LÓCZY (1915, pp. 213–214), working on the Callovian ammonites of Villány, revised the faunal lists of БÖCKH (e.g. he determined *S. linguiferum* of БÖCKH as *S. extinctus* QUENST.), but regarded the original stratigraphic arrangement as correct, interpreting the Eszterense beds as uppermost Bradfordian, i.e. Upper Bathonian.

VADÁSZ (1935, pp. 57–60), in his monograph of the Mecsek Mountains gave a summarised description on the several outcrops of the red nodular beds in the mountains. He added new elements to the faunal lists of БÖCKH, and he subdivided the succession into three units: *Parkinsonia ferruginea*, *Oppelia aspidoides* and *Macrocephalites macrocephalus* horizons. It is not clear which elements of his synthetic faunal lists came from Ófalu, but he mentioned that he found all the three horizons in the Kohltal. He ranged the Eszterense beds into the *Oppelia aspidoides* horizon of the Bradfordian (= Upper Bathonian sensu VADÁSZ).

KOVÁCS (1953) made new collections at the previously described localities of the red, ammonitic Middle Jurassic beds. He mentioned the following, preliminary determined ammonites from the Kohltal of Ófalu:

- Calliphylloceras* sp. ex aff. *frechi* PRINZ
- Lytoceras tripartitum* D'ORB. (sic!)
- Perisphinctes banaticus* ZITT.
- P. orion* OPP.
- P. sp.* ex aff. *moorei* OPP.
- P. lytoceratoides* LÓCZY

- Stephanoceras linguiferum* D'ORB.
Macrocephalites macrocephalum (SCHLOTH.)
Cosmoceras sp. ex. aff. *globosum* (TILL)

On the basis of these forms, he ranged the whole fauna into the Lower Callovian.

HETÉNYI et al. (1976, pp. 25–27) gave a detailed description of the Middle Jurassic sequence of Ófalu.

The extended faunal list from the red, greyish-red marl contains the following ammonites:

- Zetoceras* cf. *plicatum* (NEUM.)
Phylloceras cf. *kudernatschi* HAUER
Ph. euphyllum NEUM.
Ph. cf. *euphyllum* NEUM.
Ph. hatzegi LÓCZY jun.
Ph. cf. *hatzegi* LÓCZY jun.
Phylloceras sp.
Calliphylloceras demidoffi (ROUSS.)
C. cf. *demidoffi* (ROUSS.)
C. disputabile (ZITTEL)
C. aff. *frechi* (PRINZ)
Ptychophylloceras euphyllloides (TILL)
Pt. cf. *euphyllloides* (TILL)
Holcophylloceras mediterraneum NEUM.
Sowerbyceras cf. *tietzei* (TILL)
Lytoceras adeloides KUD.
Nannolytoceras tripartitum (RASP.)
Oxycerites tilli LÓCZY
Oxycerites sp.
Hecticoceras sp.
Cadomites rectelobatum (HAU.)
C. cf. *rectelobatum* (HAU.)
Polyplectites linguiferum (D'ORB.)
P. cf. *linguiferum* (D'ORB.)
Bullatimorphites bullatum (D'ORB.)
B. aff. *bullatum* (D'ORB.)
B. eszterense BÖCKH
B. sp.
Macrocephalites macrocephalus (SCHLOTH.)
M. sp.
Parkinsonia cf. *parkinsoni* (SOW.)
P. sp.
Leptosphinctes cf. *leptus* (GEM.)
Wagnericeras cf. *wagneri* (OPP.)
Choffatia remperoi (GEM.) (sic!)
Siemiradzka aurigera (OPP.)
Indosphinctes patina (NEUM.)

This is a composite list, uniting all the previous determinations of BÖCKH, VADÁSZ and KOVÁCS. The work does not mention the possibility of further subdivisioning, and ranges the succession into the Bathonian and Callovian.

HETÉNYI (in FÜLÖP, 1978, pp. 199–200), describing the Eszterense beds with type locality in Ófalu, mentions the following characteristic ammonites:

- Oxycerites aspidoides* (OPP.)
- Proecticoceras haugi* POP. et HATZ. (sic!)
- Polyplectites linguiferum* (D'ORB.)
- Bullatimorphites eszterense* (BÖCKH)
- B. ymir* (OPP.)
- Wagnericeras wagneri* (OPP.)

On the basis of these forms, he dated the Eszterense beds as of Bathonian.

This literature review shows clearly the necessity of stratigraphical revision of the Middle Jurassic red, nodular, calcareous marl of the Mecsek Mountains. Despite the fact that even BÖCKH pointed out the heterochronism of these beds, later authors regarded the sequence as general marker beds of the Bathonian, Callovian, or the Bathonian-Callovian age.

On the basis of the literature, the age of the Ófalu occurrence cannot be ascertained. The present work is not aimed at revising the ammonites collected previously from this locality. However, even a check of the formerly published faunal lists reveals that inferences to wide stratigraphic intervals were probably based on the rather arbitrary interpretation of certain ammonite species. For example *Stephanoceras*/*Polyplectites linguiferum* could be any of the Bathonian *Polyplectites* species, especially when the macroconch pair (*Cadomites*) is also recorded. "*Stephanoceras* cfr. *Bombur* OPP." (BÖCKH 1881, p. 52) is probably a microconch pair of the here abundant *Bullatimorphites* (see below). The two perisphinctids which were mentioned first by BÖCKH ("*Perisphinctes*" *funatus* and "*P.*" *curvicosta*) are species interpreted 100 years ago so widely that their diagnostic value in inherited faunal lists is rather little.

The usefulness of the faunal lists of KOVÁCS (1953, p. 92) is greatly reduced by the fact that he did not give the horizons of his specimens, thus it is problematic whether his Lower Callovian ammonites (e.g. *Macrocephalites macrocephalus*) belong to the Callovian beds of BÖCKH, to the Eszterense beds, or to both.

The faunal list presented by HETÉNYI et al. (1976, pp. 26–27) gives neither the revision of the previous determinations, nor the exact horizons of the specimens from the new collections. This faunal list contains (probably after VADÁSZ, 1935) even Bajocian forms (e.g. *Parkinsonia* cf. *parkinsoni*), and some newer Callovian elements which can be interpreted widely (*Hecticoceras*, *Indosphinctes patina*). It is very likely that all these forms are in fact Bathonian ammonites.

The recent faunal list of HETÉNYI (1978, p. 200) makes a more precise arrangement possible, suggesting only the Middle and the lower part of the Upper Bathonian.

Summing up, it can be stated that БÖCKН gave a rather narrow interval for the age of the Ófalu red marly beds, but later the workers widened this stratigraphic interval, first because they took all occurrences of these beds into consideration. The new collections, which were made recently in the Kohltal of Ófalu, may serve as a proper starting point for a revision of the Middle Jurassic ammonites and stratigraphy of the Mecsek Mountains.

The Middle Jurassic succession of the Kohltal at Ófalu

The Jurassic sequence of the Kohltal was recently discussed by a detailed petrologic-sedimentologic study (PATAKY et al. 1982). This work treated also the Middle Jurassic beds cropping out in the lower part of the valley. They divided the series into three units. The uppermost unit, which is the closing member of the Jurassic sequence in the Kohltal, is a greyish-brown, massive, siliceous limestone (*unit G*) overlying the red marls. During recent studies this limestone has not yielded any diagnostic fossils, but previous records mentioned the occurrence of Lower Callovian ammonites (HETÉNYI et al. 1976, p. 28). Its microfacies is dominated by recrystallized radiolarians, a feature very similar to that of the Callovian-Oxfordian limestone described from other parts of the Mecsek Mountains (NAGY 1967, pl. I, fig. 1).

The underlying *unit F* is a succession of yellowish, greyish, then reddish marls and nodular limestone. Its total thickness is about 18 metres. The contact of *units F* and *G* could not be studied, thus the origin of Lower Callovian ammonites recorded previously from the red marls, remained uncertain. The Bathonian sequence of *unit F*, with the collected ammonites, is as follows [ammonites with asterisk are discussed and figured below; zonal scheme after TORRENS (in COPE et al. 1980)].

a) Yellowish clayey marl with limestone layers	thickness 0.8 m
b) Greyish-yellow, pink, hard limestone with clayey patches	1.0 m
c) Red, thinly-bedded clayey nodular limestone. Abundance of nodules increases downward	
* <i>Choffatia (Subgrossowria)</i> sp. aff. <i>acuticosta</i> (ROEM.)	
<i>Choffatia (Subgrossowria)</i> sp.	
<i>Choffatia</i> sp.	0.3 m

UPPER BATHONIAN; HODSONI ZONE 2.1 m

Same lithology

Phylloceras sp.

Holcophylloceras zignodianum (D'ORB.)

Phychophylloceras flabellatum (NEUM.)

Ptychophylloceras sp.

0.9 m

-
- d) Nodular limestone and marl, with flattened, mainly ca. 1 cm nodules. Nodules are pale, matrix is red marl. In the lower part the lower 0.3 m thick interval is repeated by a small local fault

- Phylloceras* sp.
Phylloceras sp. indet.
Calliphylloceras disputabile (ZITT.)
Calliphylloceras sp.
Holcophylloceras zignodianum (D'ORB.)
Holcophylloceras sp. indet.
Ptychophylloceras flabellatum (NEUM.)
Ptychophylloceras euphyllum (NEUM.)
Ptychophylloceras sp. indet.
Lytoceras adeloides (KUD.)
 **Strigoceras dorsocavatum* (QUENST.)
Lissoceras sp.
 **Paralcidia subdiscus* (D'ORB.)
 **Bullatimorphites* (*B.*) *eszterense* (BÖCKH)
Bullatimorphites (*B.*) sp.
Tulites (*Rugiferistes*) sp.
 **Wagnericeras* cf. *fortecostatum* (DE GROSS.) 0.7 m
 SUBCONTRACTUS ZONE 1.6 m

Same lithology

- Phylloceras* sp.
Phylloceras sp. indet.
Calliphylloceras disputabile (ZITT.)
Calliphylloceras sp.
Holcophylloceras zignodianum (D'ORB.)
Holcophylloceras sp. indet.
Ptychophylloceras flabellatum (NEUM.)
Ptychophylloceras euphyllum (NEUM.)
Ptychophylloceras sp.
Ptychophylloceras sp. indet.
Prohecticoceras sp. indet.
Cadomites sp.
Bullatimorphites (*B.*) cf. *ymir* (OPPEL)
Bullatimorphites (*B.*) sp.

MIDDLE BATHONIAN; PROGRACILIS ZONE 0.5 m

e) Red, thinly-bedded claymarl, with red limestone nodules. Abundance of nodules increases downward, with a change of colour into yellowish

- Phylloceras* sp. indet.
Calliphylloceras disputabile (ZITT.)
Holcophylloceras sp.
Holcophylloceras sp. indet.
Ptychophylloceras flabellatum (NEUM.)
 **Siemiradzka* sp. 2.2 m

f) Greyish, light-brown limestone weathering nodularly <i>Phylloceras</i> sp. <i>Adabofoloceras</i> sp.	0.7 m
g) Red, thinly-bedded claymarl, with few calcareous nodules	0.4 m
h) Red, thinly-bedded claymarl, with flattened, light-grey and pink calcareous nodules * <i>Lissoceras psilodiscus</i> (SCHLOENB.)	0.3 m
i) Red, thinly-bedded claymarl, with small (0.5–1 cm) nodules in the lower part	0.2 m
j) Light-green, clayey nodular limestone	0.5 m
k) Red marl with yellowish bands	0.7 m
l) Red clay, claymarl with light-grey or red nodules	0.2 m
m) Red clay	0.15 m
n) Red, thinly-bedded calcareous clay alternating with yellowish nodular limestone layers <i>Phylloceras</i> sp. indet. <i>Calliphylloceras</i> sp. indet. <i>Lytoceras</i> sp. <i>Nannolytoceras tripartitum</i> (RASP.) <i>Nannolytoceras</i> cf. <i>polyhelictum</i> (BÖCKH) <i>Nannolytoceras</i> sp. indet. <i>Lissoceras psilodiscus</i> (SCHLOENB.) ? <i>Cadomites</i> sp. ? <i>Polysphinctites</i> sp.	1.0 m
LOWER BATHONIAN; ZIGZAG ZONE 6.95 m	
Total thickness: 11.15 m	

Unit F, below its Bathonian part, continues downward, with a ca. 10 m thick, predominantly reddish marl series, with interbedded yellowish, grey and green marls and limestones. The new collections did not yield any fossils, but this is probably the source of the previously recorded Upper Bajocian fossils.

The lowermost Middle Jurassic beds exposed in the Kohlthal are the yellowish-grey marls and alternating siliceous limestone and clay beds of *unit E*. Fossils are rare. This is the succession which yielded the ammonites *Stephanoceras humphriesianum* (Sow.), *Teloceras blagdeni* (Sow.) and *Strenoceras subfurcatum* (ZLET.) of previous authors (BÖCKH 1881, p. 40; VADÁSZ 1935, pp. 53–57; HETÉNYI et al. 1976, pp. 24–25). These forms indicate the Humphriesianum and Subfurcatum Zones.

The most important new data concerning the stratigraphic arrangement of *unit F* are as follows:

- The red colour of the rocks is dominant down to about 13 m from the top, and the first ammonites indicating the Lower Bathonian came from about 11 m. Thus the preliminarily drawn Bajocian/Bathonian boundary is near to, but does not coincide with the local lithostratigraphic boundary;
- The succession belonging to the Lower Bathonian is relatively thick (i.e. 6.95 m), but yielded few fossils, without the forms needed for subzonal identification;
- At 4.2 m from the top the first Middle Bathonian ammonites appear, indicating the Progracilis Zone, thus the Lower/Middle Bathonian boundary can be drawn as between the *e* and *d* beds;
- At 3.7 m from the top, ammonites suggesting the Subcontractus Zone of the Middle Bathonian occur. Thus the thickness of the Progracilis Zone is 0.5 m altogether, and its upper boundary does not coincide with lithological change: it should be drawn within the *d* beds. Subcontractus Zone yielded the richest ammonite fauna. BÖCKH (1881, p. 54), from an other Mecsek Mountains locality of these beds, recorded *Morrisiceras morrissi*, indexing the highest Middle Bathonian zone. However, the Ófalu sequence did not yield any ammonites indicating this zone so far, but traces of lack of this zone are also missing.
- The fauna diminishes toward the top of the sequence, and at 2.1 m from the top occur some forms suggesting the basal Upper Bathonian Hodsoni Zone (=Retrocostatum Zone auctt.). The Middle/Upper Bathonian boundary does not coincide again with lithological change; it can be drawn within the *c* beds.
- The ammonites of highest position within the now exposed red sequence came from 1.6 m from the top. New collections from the highest one and a half metre thick interval in this, or nearby localities may clear the exact chronostratigraphic position of the boundary as between the red marl (*unit F*) and the overlying limestone (*unit G*). It seems possible that the highest part of the red marls belong into the higher Upper Bathonian, however the Lower Callovian arrangement is rather unlikely.

General comments on the fauna and the most important ammonite finds

The Bathonian beds of Ófalu yielded a rather rich ammonite fauna. Even the recent, small-scale collection totalled about 200 specimens, mainly phylloceratids. It is remarkable that the ammonite fauna is dimorphic: associated macroconch and microconch oppeliids, perisphinctids and stephanoceratids occur together. This is unusual in an otherwise Mediterranean fauna.

Other invertebrate fossils are also abundant. The rich sponge-fauna is well-known—this was one of the localities of POČTA (1886). Several bivalves (epi- and inbenthonic), some brachiopods and nautiloids and a number of belemnites also occurred.

The sequence consists of red, nodular, ammonite-rich rocks, but its varied lithology and mainly its varied fauna with rich benthonic elements differs substantially from that of the Jurassic ammonitico rosso known from the Transdanubian Central Mountains of Hungary. Future studies on the faunas may reveal interesting data on the relation of these two petrographically similar, but sedimentologically and faunistically different formations.

The following discussion gives some comments on the stratigraphically most important, recently collected ammonites.

Strigoceras dorsocavatum (QUENSTEDT, 1857); Pl. II, figs. 1a—b.

It is worth to mention this imperfectly-preserved ammonite, because the representatives of the genus *Strigoceras* are rather rare in the Bathonian. The stratigraphical position of the majority of the *S. dorsocavatum* specimens mentioned in the literature are somewhat uncertain. In North Germany it comes from the Lower Bathonian (WESTERMANN 1958, p. 54), in western France it is characteristic for the "Orbigny subzone" (= basal Subcontractus Zone) (GABILLY in MANGOLD et al. 1971, p. 107). The Ófalu specimen came from the Subcontractus Zone.

Lissoceras (Lissoceras) psilodiscus (SCHLOENBACH, 1846); Pl. II, fig. 2.

One of the several *Lissoceras* species common in Ófalu. The figured specimen is a well-preserved example, but partially crushed by sediment compaction. A whole phragmocone, with a short body-chamber portion. This species is generally characteristic for the Lower Bathonian (see GALÁČZ 1980, p. 59). The Ófalu profile yielded several specimens; the figured one came from the middle part of the Lower Bathonian.

Paralcidia subdiscus (D'ORBIGNY, 1846); Pl. I, 1a—b.

A complete specimen of the type species of this rarely recorded genus. The well-preserved ammonite shows the characteristic features clearly; the excentric coiling of the body-chamber, the rounded umbilical margin, and the flattened venter, especially near the end of the body-chamber. WAAGEN (1869, pp. 212—214) gave a new description of this species, and he mentioned its occurrence, among others, from Crussol, south-eastern

France. Subsequently the species was described and figured from this locality (RICHE and ROMAN 1921, p. 155, pl. VIII, fig. 3). ELMI (1967, pp. 262–263, fig. 85) dated the species as of the Subcontractus Zone. The Ófalu specimen came also from this middle part of the Middle Bathonian.

It is possible that on the basis of their first-glance similarity and their large size, the specimens of this form had previously been misidentified as *Oxycerites tilli* (see VADÁSZ 1935, p. 59; HETÉNYI et al. 1976, p. 27).

Bullatimorphites (Bullatimorphites) eszterense (BÖCKH, 1881); Pl. II, fig. 3.

The figured specimen is one of the several collected topotypes. This collection work resulted in only poorly-preserved specimens, and this is the most entire specimen. While fragmentary and subsoluted, this internal cast shows the same dimensions and ribbing as the holotype. The specimens came from the beds corresponding to the Subcontractus Zone. Other occurrence of this form in Hungary shows that this species characterizes the upper part of the Subcontractus Zone (GALÁ CZ 1980, p. 81).

Bullatimorphites (Sphaeroptychius) marginatus (ARKELL, 1951); Pl. II, fig. 4.

A somewhat fragmentary, but well-preserved, nearly complete specimen. The broad inner whorls, the dense ribbing, the lateral lappets and the ventral flare, all characteristic to this species, are well visible. Both ARKELL (1951, p. 14) and ENAY (1959, p. 257) placed this species into the Subcontractus Zone, while the Ófalu specimen, together with macroconch *Bullatimorphites*, came from the Progracilis Zone.

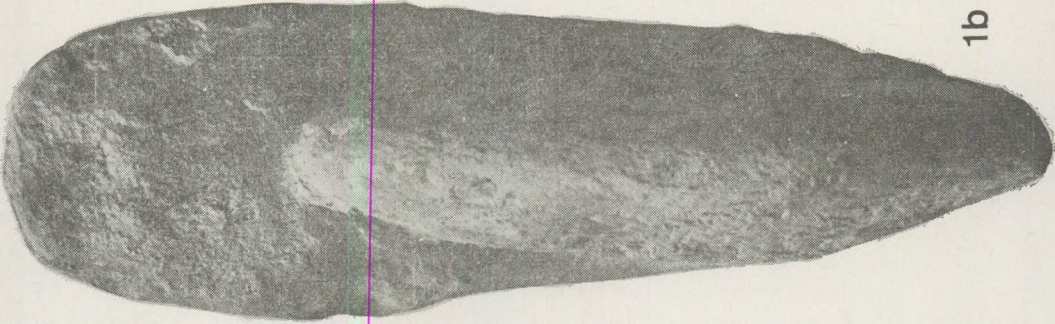
It is possible that similar *Sphaeroptychius* specimens were the bases of the previously recorded "*Sphaeroceras* cf. *Bombur* OPP. sp." (see BÖCKH 1881, p. 52; VADÁ SZ 1935, p. 59).

Procerites (Gracilisphinctes) progracilis COX et ARKELL, 1950; Pl. III, fig. 1.

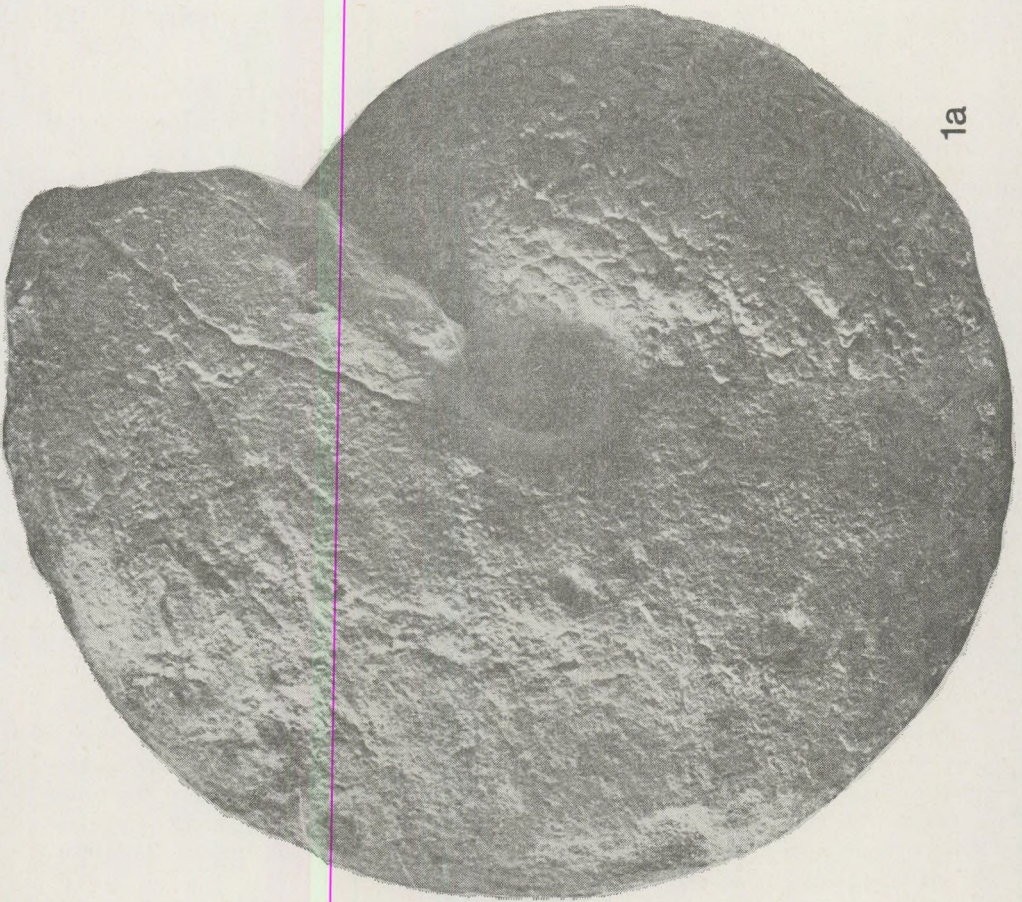
This wholly-chambered internal cast, with its evolute inner whorls bearing constrictions and with its whorl-section, agrees well with *P. (G.) progracilis* figured in the literature. The agreement is especially good with the "finely ribbed specimen" of ARKELL (1951–58, p. 198, pl. XXVIII, fig. 1). The figured Ófalu specimen came from a loose block, however an other poorly-preserved specimen was found *in situ* in the lower part of *d* beds. Being a zonal index in the basal Middle Bathonian, this is a stratigraphically important find.

Procerites (Procerites) imitator (BUCKMAN, 1922); Pl. III, fig. 2.

A phragmocone of a large-sized *Procerites*. Its dimensions, the rare strong ribs of the middle whorls match well with the features of the specimens figured by ARKELL (1951–58, pl. XXVI, figs. 2–4). This species seems to be a very abundant form in the Progracilis Zone where the holotype came from, but TORRENS (in COPE et al. 1980, p. 38) mentions some occurrences from higher horizons (see e.g. GABILLY 1964, p. 69). The figured form came from the Progracilis Zone.



1b



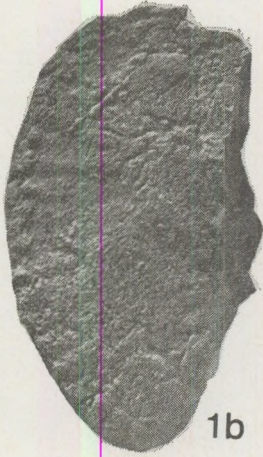
1a

PLATE I.

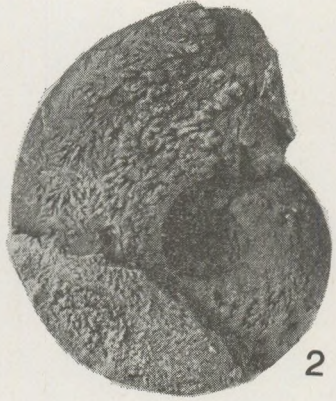
Fig. 1a–b *Paralcidia subdiscus* (D'ORB.), *d* beds, upper part; Middle Bathonian, Tulites subcontractus Zone.
1a: lateral view; 1b: apertural view.
Natural size



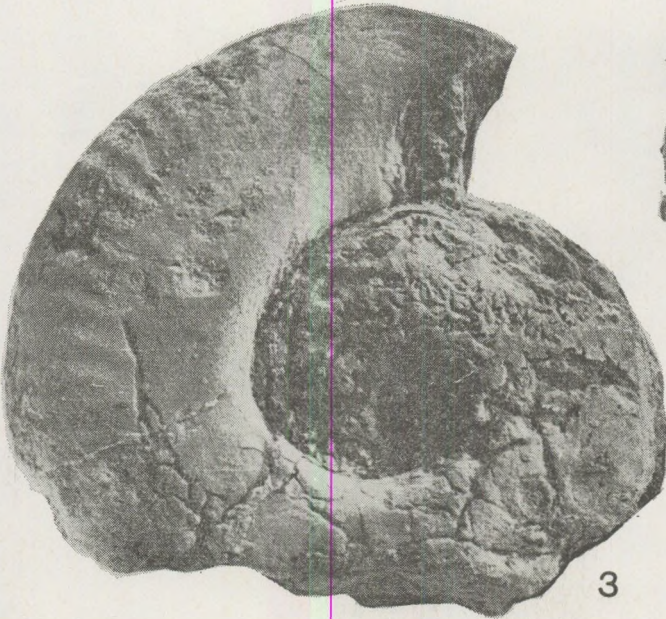
1a



1b



2



3



4

PLATE II.

- Fig. 1a – b *Strigoceras dorsocavatum* (QUENST.), *d* beds, upper part; Middle Bathonian, Tulites subcontractus Zone.
1a: ventral view; 1b: lateral view
- Fig. 2. *Lissoceras* (*L.*) *psilodiscus* (SCHLOENB.), *h* beds; Lower Bathonian, Zigzagiceras zigzag Zone
- Fig. 3. *Bullatimorphites* (*B.*) *eszterense* (BÖCKH), topotype, *d* beds, upper part; Middle Bathonian, Tulites subcontractus Zone
- Fig. 4. *Bullatimorphites* (*Sphaeroptychius*) *marginatus* (ARKELL), *d* beds, lower part; Middle Bathonian, Procerites (*G.*) *progracilis* Zone
All natural size

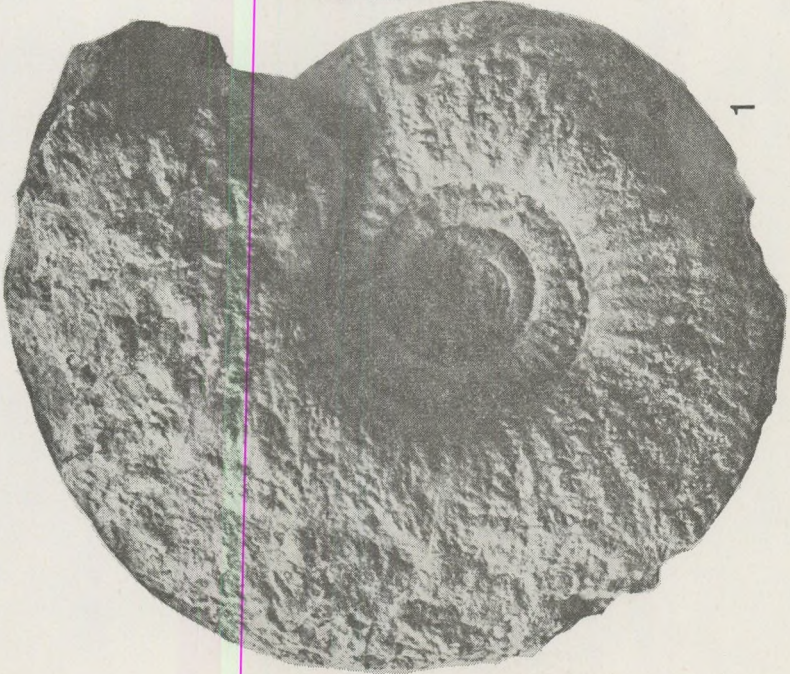
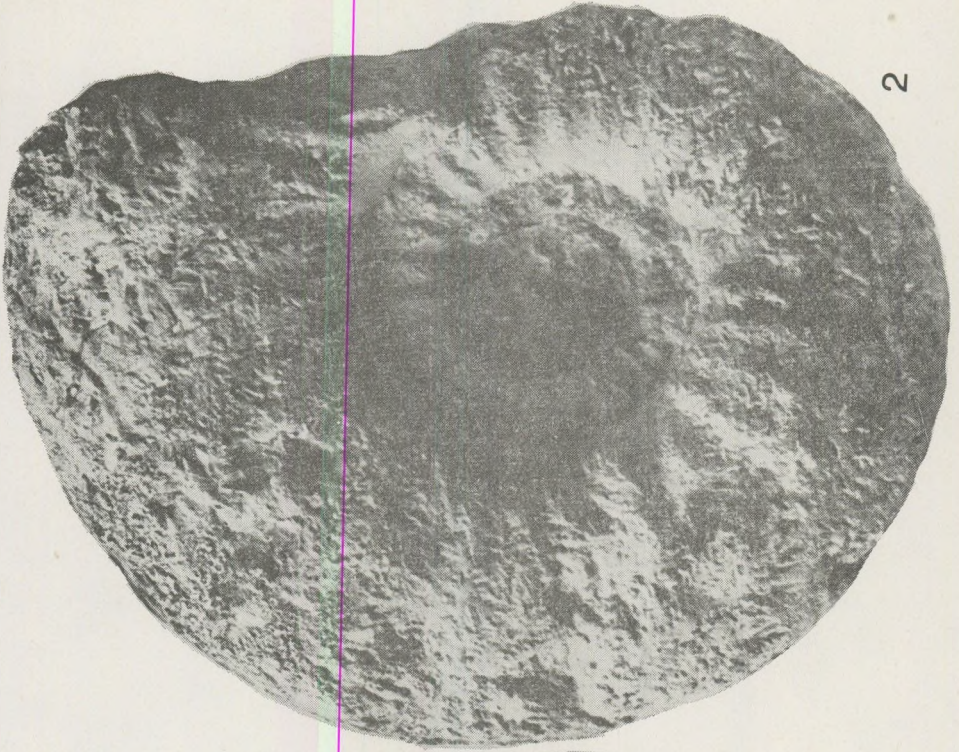


PLATE III.

- Fig. 1. *Procerites (Gracilisphinctes) progracilis* COX et ARKELL, from a loose block
Fig. 2. *Procerites (P.) imitator* (BUCKM.), *d* beds, lower part; Middle Bathonian, *Procerites*
(G.) *progracilis* Zone
Both natural size

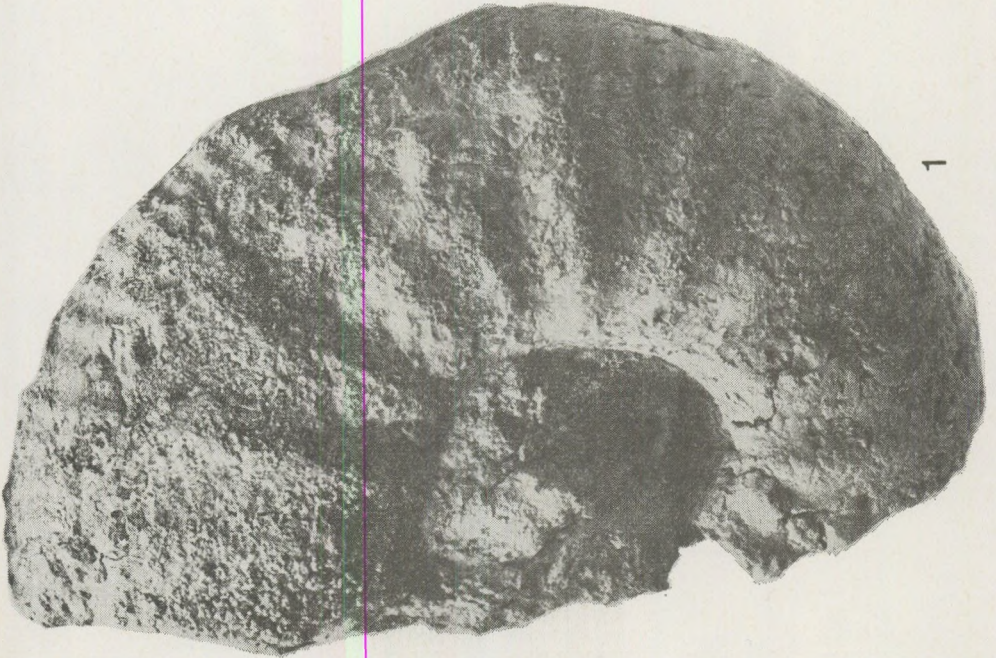
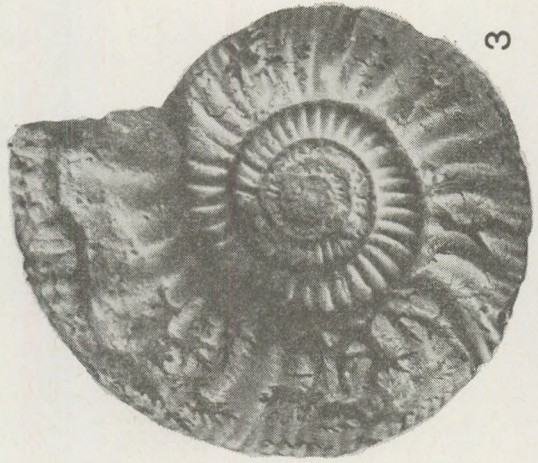


PLATE IV.

- Fig. 1. *Wagnericeras* (*W.*) sp. aff. *fortecostatum* (DE GROSS.), *d* beds, upper part; Middle Bathonian, *Tulites subcontractus* Zone
- Fig. 2. *Siemiradzka* sp., *e* beds; Lower Bathonian, *Zigzagiceras zigzag* Zone
- Fig. 3. *Choffatia* (*Subgrossouvria*) sp. aff. *acuticosta* (ROEM.), *c* beds, upper part; Upper Bathonian, *Procerites hodsoni* Zone
- All natural size

Siemiradzka sp.; Pl. IV, fig. 2.

A small-sized body-chamber fragment. A parabolic node and the base of the lateral lappet are visible. These features and the style of ribbing makes the generic arrangement certain, but the state of preservation enables no specific determination. The first Bathonian flourishing of the genus *Siemiradzka* dates in the middle and upper Zigzag Zone. The Ófalu specimen came from the uppermost assemblage of the Lower Bathonian.

Choffatia (*Subgrossouvria*) sp. aff. *acuticosta* (ROEMER, 1911); Pl. IV, fig. 3.

A well-preserved phragmocone with a fragment of the body-chamber. It differs from the holotype in its denser secondary ribs, showing resemblance to the specimens figured by HAHN (1968, pp. 72–74, pl. 7, fig. 3; pl. 8, fig. 6). On the basis of the literature, the age of *C. acuticosta* is basal Upper Bathonian (see e.g. HAHN loc. cit.; MANGOLD 1970, pp. 63–64). The figured specimen was the ammonite found in the highest stratigraphic position during the new collection, and suggests the Hodsoni Zone.

Perhaps similar *Subgrossouvria* specimens served as bases for citing *P. moorei*, *P. recuperoi* and other perisphinctids in the earlier faunal lists.

Wagnericeras (*W.*) sp. aff. *fortecostatium* (DE GROSSOUVRE, 1930), Pl. IV, fig. 1.

A comparatively large, fragmentary phragmocone. The generic arrangement is suggested by the type of ribbing and the relatively simple suture line, but the specific arrangement is uncertain. As compared to the type of *W. fortecostatium*, the primary ribs are stronger and more distant. Typical *W. fortecostatium* is characteristic in England in the Progracilis Zone (TORRENS in COPE et al. 1980, p. 31) and this closely-allied form came from the Subcontractus Zone of Ófalu.

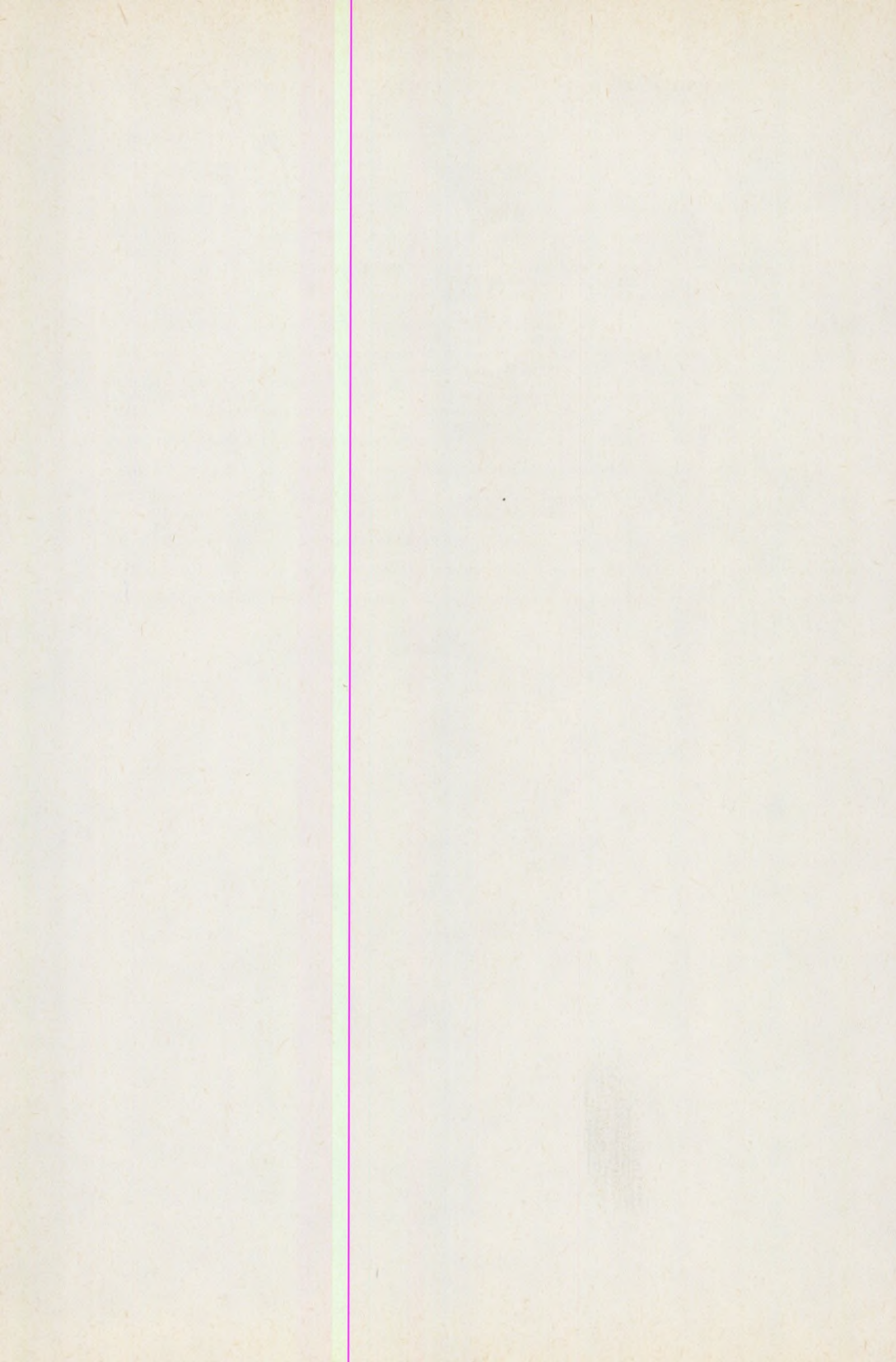
Acknowledgements

The author wishes to thank geology students L. CSONTOS, I. DUNKL, S. JÓZSA and N. PATAKY for allowing to use their unpublished data, for presenting their collected material and for their help in the field.

REFERENCES

- ARKELL, W. J. (1951): A Middle Bathonian ammonite fauna from Schwandorf, northern Bavaria. — Schweiz. paläont. Abh., 69, pp. 1–18.
- ARKELL, W. J. (1951–58): A monograph of English Bathonian ammonites. — Monogr. Palaeontogr. Soc. London, pp. 1–264.
- BÖCKH, J. (1880–81): (Data to the knowledge on the Jurassic deposits of the Mecsek Mountains and adjacent area. Part. I. Stratigraphy, Part II. Paleontology) — Ért. Term. Tud. Közlem., Vol. XI., No. IX., pp. 1–50; 1–107 (In Hungarian)
- COPE, J. C. W., DUFF, K. L., PARSONS, C. F., TORRENS, H. S., WIMBLETON, W. A. and WRIGHT, J. K. (1980): A correlation of Jurassic rocks in the British Isles, Part 2: Middle and Upper Jurassic. — Geol. Soc. London, Spec. Rep. No. 15., pp. 1–109.
- ELMI, S. (1967): Les Lias supérieur et le Jurassique moyen de l'Ardeche. — Doc. Labo. Géol. Fac. Sci. Lyon, No. 19, fasc. 1–2., pp. 1–507.
- ENAY, R. (1959): Note sur quelques Tullitides (Ammonitina) du Bathonien. — Bull. Soc. géol. France, 7 Sér. I., pp. 252–259.
- FÜLÖP, J. (ed.) (1978): Lex. Stratigr. Int., Vol. I., Europe, fasc. 9: Hongrie (2^e ed.). CNRS Paris, pp. 1–666.
- GABILLY, J. (1964): Le Jurassique inférieur et moyen sur le littoral Vendéen. — Trav. Inst. Géol., Anthropol., Préhist., Fasc. Sci. Poitiers, t. V., pp. 65–107.

- GALÁ CZ, A. (1980): Bajocian and Bathonian ammonites of Gyenespuszta, Bakony Mts., Hungary — *Geol. Hung.*, Ser. Palaeont., fasc. 39, pp. 1—227
- HAHN, W. (1969): Die Perisphinctidae STEINMANN (Ammonoidea) des Bathoniums (Brauner Jura epsilon) im südwestdeutschen Jura. — *Jh. geol. Landesamt Baden-Württemberg*, 11, pp. 29—86.
- HAUER, F. (1876): Jahresbericht des Direktors, Beil. II: Mitteilungen der Geologen der K. ung. geologischen Anstalt über ihre Aufnahmearbeiten in den Jahren 1874 und 1875. — *Verh. k.-k. geol. Reichsanst.*, Jg. 1876, Nr. 1., pp. 19—27
- HETÉNYI, R., FÖLDI, M., HÁMOR, G., NAGY, I., BILIK, I. and JANTSKY, B. (1976): (Explication to the 10 000 geological map of the Mecsek Mts., Ófalu) — *Hung. Geol. Survey, Budapest*, pp. 1—74. (In Hungarian)
- KOVÁCS, L. (1953): Les couches du Dogger supérieur de la montagne Mecsek. — *MÁFI Évi Jel.* (1950), pp. 89—95. (In Hungarian, with French and Russian abstracts)
- LÓCZY, L. jun. (1915): Monographie der Villányer Callovien-Ammoniten. — *Geol. Hung.*, 1., fasc. 3—4, pp. 1—248,
- MANGOLD, C. (1970): Les Perisphinctidae (Ammonitina) du Jura meridional au Bathonien et au Callovien. — *Doc. Lab. Géol. Fac. Sci. Lyon*, No. 41, fasc. 2, pp. 1—246,
- MANGOLD, C., ELMI, S. and GABILLY, S. (1971): Les faunes du Bathonien dans le moitié sud de la France. Essai de zonation et correlations. — *Coll. Jurassique Luxembourg*, 1976, *Mém. BRGM*, No. 75, pp. 103—132.
- NAGY, I. (1967): Sur le rapport entre le Jurassique supérieur et les roches volcaniques Crétacées dans la Montagne Mecsek. — *MÁFI Évi Jel.*, (1961), pp. 149—168. (In Hungarian, with French and Russian abstracts)
- PATAKY, N., JÓZSA, S., DUNKL, I. (1982): The Jurassic sequence of the Kohltal, Ófalu, Mecsek Mts. — *Földt. Közl.*, 112, 4., pp. 333—394. (In Hungarian, with English abstract)
- PETERS, K. F. (1862): Über den Lias von Fünfkirchen. — *Sitzungsb. math.-naturwiss. Cl. k. Akad. Wiss. Wien*, 46, 1. pp. 1—53.
- POČTA, P. (1886): Über einige Spongien aus dem Dogger des Fünfkirchener Gebirges. — *M. Kir. Földt. Int. Évk.*, VIII, pp. 103—116.
- RICHE, A. and ROMAN, F. (1921): La montagne de Crussol. — *Trav. Lab. Géol. Univ. Lyon*, fasc. 1., pp. 1—196.
- VADÁSZ, E. (1935): Das Mecsek-Gebirge. — *Magyar Tájak Földt. Leírása*, I., pp. 1—180. (In Hungarian, with German abstract)
- WAAGEN, W. (1869): Die Formenreiche des Ammonites subradiatus. In: *Benecke's Geogn.-Palaeont.*, Beitr. II, 2. pp. 181—256.
- WEIN, GY. (1976): Über die Tektonik Südost-Transdanubiens. — *Földt. Közl.*, 97, 4, pp. 371—395. (In Hungarian, with German abstract)
- WESTERMANN, G. (1958): Ammoniten-fauna und Stratigraphie des Bathonien NW-Deutschlands. — *Beih. Geol. Jb.*, 32, pp. 1—103.



THE JURASSIC AMMONITES OF VILLÁNY

B. GÉCZY

Department of Paleontology, Eötvös L. University, Budapest

Received: 15th March, 1982)

РЕЗЮМЕ

С вилланьской горы Темплом и с находящейся вблизи нее горы Сомшич было собрано 180 видов аммонитов, относящихся к 17 семействам. На основании фауны было с несомненностью доказано наличие ярусов нижнеплинсбахского (самого верхне-несинемюрского?) и верхнебатского, а также почти полного келловейского яруса. Исключительное богатство форм фауны можно объяснить тремя факторами. Прежде всего несмотря на малую толщину слоя фауны, она охватывает большой интервал времени. С другой стороны, фауна перемешана и переработана, то есть наслоение и перемыв привели к последующей ее концентрации. И наконец, но не в последнюю очередь, этот район, по-видимому, находился на стыке двух фауна-провинций, где одинаково встречались группы, характерные как для островных морей стабильной Европы, так и для открытого моря Тетис.

Introduction

The Templom-hill of Villány is one of the world's richest Jurassic ammonite localities. The classic monographs of TILL (1910) and LÓCZY (1915) gave 131 species descriptions, and this number exceeds by 27 the other world-famous fauna of Chanaz (Savoie).

In 1915 LÓCZY stated that the ammonite-rich bank of the Templom-hill had been completely outmined. RAKUSZ and STRAUSZ (1953) also regarded the bank as extracted. As a matter of fact, only the quarrying was stopped probably a century ago. After World War II., G. KOPEK collected a valuable fauna from the ammonite-rich bank. This was completed with a small collection by P. SZABÓ in 1959, then G. VIGN carried out a systematic, layer-by-layer collection, on the initiative and under the guidance of J. FÜLÖP in 1962. A. VÖRÖS called attention to another outcrop of the bank at the Somsich-hill nearby. From 1967, with the help of A. VÖRÖS and A. GALÁ CZ, repeated collections were made at both the Templom-hill and the Somsich-hill localities. This work has been supported by R. HETÉNYI from the Geological Institute of Hungary. Before the Mediterranean Jurassic Colloquium (1969) the author was commissioned by J. FÜLÖP to work out a revision of the ammonite fauna of Villány. At the same time, all the collections and the original — but unfortunately incomplete — material of LÓCZY, kept in the Geological Institute of Hungary, were made available. This honourable confidence of J. FÜLÖP is greatly appreciated. A part

of the ammonites described by TILL (Deverman-collection, now in the Senckenberg Museum, Frankfurt an Main) was available for determination on loan. The material was completed by further collections of A. KASZAP and A. VÖRÖS. The specimen-number of the new collections surpasses the amount of TILL's and LÓCZY's material.

The most important stratigraphical recognition of the recent decades is that the "Cornbrash-Bradfordian" beds of LÓCZY belong into the Pliensbachian, instead of the original Bathonian assignment. This correction has been made by British researchers (D. AGER, J CALLOMON and D. DONOVAN), during the excursion of the Mediterranean Jurassic Colloquium in 1969. Thus Villány is a good example of international co-operation in the earth-sciences. The first one to discover the Templom-hill locality was O. LENZ from Prague (1872), TILL prepared his monograph in Vienna, and LÓCZY in Zurich, under the guidance of ROLLIER. The stromatolitic fabric of the ammonite-rich bank was first recognized by Polish researchers (RADWANSKI and SZULCZEWSKI, 1965) and the first publication of the Pliensbachian brachiopods and ammonites was given by AGER and CALLOMON (1971). Detailed description of the sequence is due to A. VÖRÖS (1972).

Lower Jurassic

On the Templom-hill and Somsich-hill the Lower Jurassic beds overly conformably the Upper Triassic variegated marls. On the basis of the thrust structure of the Villány Mountains, it is possible that the contact is tectonic. The Lower Jurassic calcareous series contains terrigenous material in large quantity and silicified woods as well. The total thickness is about 12 metres.

CALLOMON (in AGER and CALLOMON, 1971) reported the following ammonite species. *Apoderoceras* cf. *lobulatum* BUCKMAN, 1921, *A.* cf. *aculeatum* (SIMPSON, 1843), *A.* cf. *ferox* BUCKMAN, 1925; ?*Epideroceras* sp. juv.; *E. rollieri* (LÓCZY, 1915); *Villania densilobata* TILL, 1909. The infilling material of *Liparoceras* cf. *cheltiense* (MURCHISON) (= "*Cosmoceras globosum*" TILL) differs from that of the other specimens from Villány so much that its Villány origin should be questioned.

The recent revision of the whole fauna extended the faunal list of CALLOMON and resulted in the following:

Phylloceratidae ZITTEL, 1884

Phylloceras cf. *hebertinum* (REYNÈS, 1868)

Partschiceras cf. *striatocostatum* (MENEHINI, 1853)

Juraphyllitidae ARKELL, 1950

Tragophylloceras numismale (QUENSTEDT, 1846)

Lytoceratidae NEUAMYR, 1875

Lytoceras cf. *fimbriatum* (SOWERBY, 1817)

Lytoceras sp.

Oxynoticeratidae HYATT, 1875

- Radstockiceras* cf. *evolutum* (FUCINI, 1901)
Radstockiceras cf. *buvignieri* (D'ORBIGNY, 1844)
Radstockiceras cf. *involutum* (POMPECKJ, 1907)

Eoderoceratidae SPATH, 1929

- Apoderoceras?* *antiquum* (LÓCZY, 1915)
Apoderoceras cf. *sociale* (SIMPSON, 1855)
Epideroceras cf. *exhaeredatum* BUCKMAN, 1923
Epideroceras cf. *grande* DONOVAN, 1958
Epideroceras n. sp.
Epideroceras? sp.
Villania densilobata TILL, 1909
Villania cf. *densilobata* TILL, 1909
Villania n. sp.
Villania rollieri (LÓCZY, 1915)
Villania sp. aff. *rollieri* (LÓCZY, 1915)
Tetraspidoceras quadrarmatum (DUMORTIER, 1869) n. subsp.
Coeloderoceras? *vermiforme* (TILL, 1911)

Polymorphitidae HAUG, 1887

- Uptonia* cf. *jamesoni* (SOWERBY, 1827)
Tropidoceras sp. aff. *frischmanni* (OPPEL, 1862)

This Lower Jurassic fauna of Villány is characterized by poor preservation, scattered occurrence, large size of the forms, relative abundance of NW European forms and subordinate appearance of Mediterranean elements, as well as the abundance of endemic species. The collection of TILL, LÓCZY and FÜLÖP resulted in 4312 ammonites from Villány, and this total comprised 8 Lower Jurassic specimens altogether. This low value can be probably due to the fact that the underlying beds of the ammonite-rich bank were recorded previously as faunal-free, and the lower, sandy, pebbly beds were worthless for quarrying. When the collection work at the Somsich-hill was focused on the Lower Jurassic beds, relatively numerous (i.e. 25) specimens were yielded. Probably the bad preservation caused the determination of these Lower Jurassic ammonites as of Bathonian ones. It is also probable that the fauna, beside subsequent solution and wearing and deformation by tectonic movements, has been sorted out, and this resulted in the disappearance or redeposition of the majority of the smaller forms. The greater part of the specimens are of large-sized, the diameter of one wholly-septate *Radstockiceras* exceeds 370 mm and *Apoderoceras*, *Epideroceras* and *Villania* specimens with diameter over 200 mm are also common.

Remarkable is the small proportion (5%) of Phylloceratidae in the fauna; that of the Lytoceratidae is 10%, but the common *Lytoceras fimbriatum* occurs both in the Mediterranean and NW European areas. The paleobiogeographic interpretation of the Eoderoceratidae is difficult, because the revision of this group is still lacking. Beside the forms known in

England, southern France, southern Germany and Switzerland, there are probably some definitely Tethyan forms (e.g. *Villania*), too.

Reineckeia vermiformis TILL is probably a form from the *Coeloderoceras*-group. The type seems to have been lost, and no similar specimens were obtained during the new collections, thus this problem cannot be solved.

The Lower Jurassic fauna of Villány is dated by the occurrence of the Lower Pliensbachian zonal index *Uptonia jamesoni*. The genus *Uptonia* is restricted to the Jamesoni Zone. On the basis of the occurrence of numerous *Epideroceras* species, the possibility arises that the uppermost Sinemurian Raricostatum Zone is also represented in Villány. On the other hand, *Echio-ceras*, characteristic for this latter zone, has not come from the fauna so far. It is possible that in the Villány fauna the last, large-sized *Epideroceras* species coexisted with the *Radstockiceras* and *Apoderoceras*, characteristic for the Jamesoni Zone.

Middle Jurassic

VÖRÖS (1972) distinguished, on lithological grounds, the Bathonian sandy limestone from the Lower Callovian limestone with iron-oxide, and from the Callovian ammonite-rich bank. The Bathonian beds vary 0 to 8 cm in thickness, filling usually the surface depressions of the underlying rocks. The lower part of the Lower Callovian is represented also in certain profiles. Its thickness varies between 0 and 10 centimetres. The horizontal occurrence of the Callovian bank of 15 to 40 cm thickness is far greater.

The Bathonian-Callovian beds yielded the following ammonite fauna:

Phylloceratidae ZITTEL, 1884

- Phylloceras kundernatschi* (HAUER, 1854)
- Phylloceras plicatum* NEUMAYR, 1871
- Phylloceras* sp.
- Adabofolloceras villanyense* (TRAUTH, 1923)
- Calliphylloceras demidoffi* (ROUSSEAU, 1842)
- Calliphylloceras* sp.
- Holcophylloceras mediterraneum* (NEUMAYR, 1871)
- Holcophylloceras* sp.
- Ptychophylloceras euphyllum* (NEUMAYR, 1870)
- Ptychophylloceras euphylloides* (TILL, 1910)
- Ptychophylloceras flabellatum* (NEUMAYR, 1871)
- Ptychophylloceras* sp.
- Sowerbyceras tietzei* (TILL, 1910)
- Sowerbyceras transiens* (POMECKJ, 1893)
- Sowerbyceras* sp.

Lytoceratidae NEUMAYR, 1875

- Lytoceras adeloides* (KUDERNATSCH, 1852)
- Lytoceras depressum* (TILL, 1910)
- Lytoceras* n. sp.

Haploceratidae ZITTEL, 1884

Lissoceras vouttense (OPPEL, 1865)*Lissoceras jullieni* DOUVILLÉ, 1914

Oppeliidae BONARELLI, 1894

Oxycerites tilli LÓCZY, 1915*Oxycerites* sp.*Paralcidia virgata* (LÓCZY, 1915)*Paralcidia?* cf. *mariorae* (POPOVICI-HATZEG, 1905)*Paralcidia* sp.*Thraxites thrax* STEPHANOV, 1966*Oecotraustes?* sp.*Prohcticoceras angulicostatum* (LÓCZY, 1915)*Prohcticoceras subpunctatum* (SCHLIPPE, 1888)*Prohcticoceras haugi* (POPOVICI-HATZEG, 1905)*Chanasia turgida* (LÓCZY, 1915)*Chanasia* sp.*Hectioceras* sp.*Lunuloceras pseudopunctatum* (LAHUSEN, 1883)*Lunuloceras paulowi* (TSYTOVITCH, 1911)*Lunuloceras taeniolum* (BONARELLI, 1894)*Lunuloceras lahusei* (TSYTOVITCH, 1911)*Lunuloceras* sp.*Sublunuloceras?* sp.*Putealicerias paucifalcatum* (TILL, 1910)*Putealicerias punctatum arcuatum* ZEISS, 1956*Putealicerias lugeoni* (TSYTOVICH, 1911)*Putealicerias* sp.*Rossienceras regulare* (TILL, 1910)*Rossienceras rossiense* (TEISSEYRE, 1883)*Rossienceras uhligi* (TILL, 1910)*Rossienceras laubei* (NEUMAYR, 1871)*Rossienceras bukowskii* (BONARELLI, 1894)*Rossienceras* sp.*Jeanneticeras?* sp.*Kheraites* sp.*Horioceras semseyi* (LÓCZY, 1915)*Horioceras* sp.*Petitclercia hungarica* LÓCZY, 1915*Lorioloceras kormosi* (LÓCZY, 1915)*Lorioloceras?* n. sp.*Phlycticeras* cf. *schaumburgi* (WAAGEN, 1875)*Phlycticeras* cf. *waageni* BUCKMAN, 1914*Phlycticeras* n. sp. aff. *polygonium* (ZIETEN, 1831)

Tulitidae BUCKMAN, 1921

Bullatimorphites cf. *hannoveranus* (ROEMER, 1911)*Bullatimorphites* cf. *davaiacensis* (LISSAJOUS, 1923)

Bullatimorphites? sp.

Bullatimorphites? n. sp.

Bomburites cf. *bombur* (OPPEL, 1862)

Bomburites globuliforme (GEMMELLARO, 1872)

Bomburites cf. *devauxi* (GROSSOUVRE, 1891)

Bomburites sp.

Treptoceras microstoma (D'ORBIGNY, 1846)

Macrocephalitidae BUCKMAN, 1922

Macrocephalites s.l. sp.

Oecoptychiidae ARKELL, 1957

Oecoptychius refractus (ZIETEN, 1818)

Pachyceratidae BUCKMAN, 1918

Erymnoceras coronatum (BRUGUIÉRE in D'ORBIGNY, 1845)

Erymnoceras triplicatum (TILL, 1911)

Kosmoceratidae HAUG, 1887

Kosmoceras (*Zugocosmoceras*) *zugium* BUCKMAN, 1923

Kosmoceras (*Kosmoceras*) cf. *castorianum* TINTANT, 1963

Epicosmoceras cf. *fuchsi* (NEUMAYR, 1871)

Epicosmoceras? sp.

Reineckeidae HYATT, 1900

Rehmannia revili (PARONA et BONARELLI, 1897)

Rehmannia hungarica (TILL, 1911)

Loczyceras robustum (TILL, 1911)

Loczyceras vesuntianum BOURQUIN, 1968

Loczyceras inacuticostatum (LÓCZY, 1915)

Loczyceras crassicostatum (LÓCZY, 1915)

Loczyceras reissi (STEINMANN, 1881)

Loczyceras balusseauii CARIOU, 1980

Loczyceras densicostatum (TILL, 1911)

Loczyceras segestanum (GEMMELLARO, 1871)

Loczyceras loczyi BOURQUIN, 1968

Loczyceras euumbilicatum (LÓCZY, 1915)

Tyrannites savarensis (BOURQUIN, 1968)

Tyrannites eusculptus (TILL, 1911)

Reineckeia lata LÓCZY, 1915

Reineckeia fehlmanni JEANNET, 1951?

Reineckeia douvillei STEINMANN, 1881

Reineckeia anceps (REINECKE, 1818)

Reineckeia kiliani PARONA et BONARELLI, 1897

Reineckeia stuebeli (STEINMANN, 1881)

Reineckeia nodonsa TILL, 1911

Reineckeia tilli FISHER, 1915

Collotia falcata (TILL, 1911)

Collotia thiebauti (GERARD et CONTAUT, 1936)

- Collotia multicostata* (PETITCLERC, 1915)
Collotia paronai (PETITCLERC, 1915)
Collotia oxypticha (NEUMAYR, 1870)
Collotia heretica (MAYER, 1865)
Collotia sp.
Collotia? sp. aff. *decora* (WAAGEN, 1875)?

Perisphinctidae STEINMANN, 1890

- Procerites?* *proceroides* (TILL, 1911)
Wagnericeras? *banaticum* (ZITTEL, 1868)
Siemiradzkia cf. *demariae* (PARONA et BONARELLI, 1897)
Siemiradzkia cf. *procera* (SEEBACH, 1864)
Siemiradzkia sp.
Homoeoplanulites furculus (NEUMAYR, 1871)
Homoeoplanulites lenzi (TILL, 1911)
Homoeoplanulites leptus (GEMMELLARO, 1872)
Homoeoplanulites sp.
Homoeoplanulites? *plicatissimus* (LÓCZY, 1915)
Choffatia waageni (TEISSEYRE, 1889)
Choffatia subbalinense (SIEMIRADZKI, 1894)
Choffatia villanoides (TILL, 1911)
Choffatia pannonica (LÓCZY, 1915)
Choffatia tilli MANGOLD, 1970?
Choffatia prorsocostata (SIEMIRADZKI, 1894)
Choffatia dumortieri MANGOLD et ELMI, 1966
Choffatia hofmanni (TILL, 1911)
Choffatia sp. aff. *caucasica* (NEUMAYR et UHLIG, 1892)
Choffatia sp.
Subgrossouvria eurypticha (NEUMAYR, 1871)
Subgrossouvria coroneiformis (LÓCZY, 1915)
Subgrossouvria lycoceratoides (LÓCZY, 1915)
Subgrossouvria sp. aff. *aberrans* (WAAGEN, 1875)
Subgrossouvria sp.
Grossouvria konkievitzi (SIEMIRADZKI, 1894)
Grossouvria evoluta MANGOLD, 1970
Grossouvria variabilifera (LÓCZY, 1915)
Grossouvria sp.
Indosphinctes drevermanni (TILL, 1911)
Indosphinctes patina (NEUMAYR, 1871)
Indosphinctes pseudopatina (PARONA et BONARELLI, 1897)
Indosphinctes errans SPATH, 1931?
Indosphinctes n. sp.
Indosphinctes sp.
Elatmites leptoides (TILL, 1911)
Elatmites graciosus (SIEMIRADZKI, 1894)
Flabellisphinctes villanyensis (TILL, 1911)
Flabellisphinctes pseudolothari (LÓCZY, 1915)

Flabellisphinctes baranyaensis (LÓCZY, 1915)

Flabellisphinctes sp.

Okaites calloviensis (LÓCZY, 1915)

Okaites mosquensis (FISCHER in SIEMIRADZKI, 1894)

Okaites sp.

Poculisphinctes fascisculptus (LÓCZY, 1915)

Aspidoceratidae ZITTEL, 1895

Metapeltoceras? sp.

Bullatimorphites cf. *hannoveranus* and *B.* cf. *davaiacensis* characterize the Upper Bathonian, and *Prohecticoceras angulicostatum* is the index of the Angulicostatum Horizon within the Retrocostatum Zone. However, this latter specimen greatly differs, with its matrix, from the fossils of the ammonite-rich bank. The Bathonian is suggested also by *Procerites?* *proceroides*, *Wagnericeras?* *banaticum* and the *Siemiradzkia* specimens. The extraordinarily rich fauna contains relatively few Bathonian forms.

The Callovian elements are by far the most frequent. The original horizon of the characteristic fossils cannot be reconstructed, however, these suggest distinct parts of the Callovian. In the evaluation of the Callovian fauna, the synthesis made by CARIOU (1980) was especially valuable, because this work emphasizes the chronostratigraphic value of Reineckeidae, instead of the Kosmocerotidae. CARIOU distinguished 6 zones, 12 subzones and 20 horizons within the Callovian. In Villány, all but the uppermost 3 horizons are represented.

Callovian

Lower Callovian

The Praequense Horizon of the Macrocephalus Zone is suggested by *Choffatia hofmanni* (TILL). The upper part of this zone and the lower part of the Gracilis Zone (Rehmanni Horizon—Pictava Horizon) is suggested by *Rehmannia revili* (= *Reineckeia espinazitensis* in LÓCZY, pl. VII, fig. 10; *R. eusculpta* TILL in LÓCZY, pl. VIII, fig. 6, *partim*). *Bomburites globuliforme* characterizes the Laugieri Horizon. *Indosphinctes pseudopatina* and *Collotia oxypticha* (= *Reineckeia* cf. *greppini* in TILL, pl. II, fig. 7), as well as *Collotia paronai* (= *Reineckeia* cf. *greppini* in TILL, pl. II, figs. 4–6) characterize the Proximum Horizon.

Middle Callovian

The Bannense Horizon of the Jason Zone is indicated by *Chanasia turgida* (LÓCZY, 1915) and *Loczyceras densicostatum* (= *Reineckeia densicostata* TILL, pl. I, fig. 5). The Bannense and Medea Horizons are suggested by *Loczyceras segestana* (= *Reineckeia bukowskii* TILL, pl. I, figs. 7–8; *R. prorsocostata* in TILL, pl. I, fig. 6), and *Reineckeia stuebeli* (= *Reineckeia waageni* TILL, pl. II, fig. 11). *Loczyceras reissi* (= *R. transiens* TILL, pl. II, fig. 8) is characteristic to the Medea Horizon, and *Loczyceras balussei*

(=*R. anceps* in TILL, pl. IV, fig. 3) to the Medea and Jason Horizons. The Jason Subzone is suggested by the presence of *Rehmannia hungarica* TILL, pl. I, fig. 1 and *Collotia multicosata* (= *Reineckeia palfyi* TILL, pl. II, figs. 9–10). The Jason Zone is suggested also by *Oecoptychius refractus*.

The following Reineckeids occur both in the Jason and Coronatum Zones: *R. anceps* (Bannense to Villanyensis Horizons), *R. fehlmanni* (= *R. anceps* in LÓCZY, pl. VIII, fig. 1) (Jason Subzone to Waageni Horizon).

The base of the Coronatum Zone is definitely indicated by *Flabelliphinctes villanyensis* (Villanyensis Horizon). *Loczyceras vesuntianum* (= *Reineckeia* cf. *hungarica* TILL, pl. I, fig. 4) and *Loczyceras crassicosatum* (LÓCZY, pl. VII, figs. 3–4) are characteristic to the Baylei Horizon. *Rossiniceras regulare* indicates the Leuthardti Subzone. *Choffatia waageni*, the index form of the Waageni Horizon, appears also in Villány. *Okaites calloviensis* ranges also into this horizon. *Erymnoceras coronatum* is an unequivocal proof for the Coronatum Zone. *Reineckeia lata* suggests the uppermost Coronatum Zone.

Loczyceras inacuticosatum (LÓCZY, pl. VIII, fig. 3), *Collotia falcata* (TILL, pl. I, fig. 12) and *Reineckeia nodosa* TILL, pl. IV, figs. 4–6 range from the Coronatum Zone to the basal Athleta Zone (Rota to Trezeense Horizons).

Upper Callovian

The presence of the Athleta Zone is indicated by *Collotia nivernensis* (= *Reineckeia* cf. *fraasi* in LÓCZY, pl. VIII, fig. 7), which is characteristic for the Trezeense Horizon, and *Collotia thibauti* (= *Reineckeia hungarica* LÓCZY in LÓCZY, pl. IX, fig. 1), which ranges in the Trezeense and Piveteau Horizons. *Collotia* sp. aff. *decora* (= *Parkinsonia calloviensis* LÓCZY, pl. IV, fig. 11; pl. VI, fig. 11) ranges from the Trezeense to the Collotiformis Horizon.

Conclusions

In spite of the reduced thickness, the fauna of the Villány ammonite-rich bank ranges over a wide temporal interval. AGER and CALLOMON (1971) rightly regarded the Callovian bank as a good example of heterogeneous condensation, where the faunal enrichment was the combined result of subsequent disappearance of the original matrix, reworking, and faunal mixing. On the other hand, Villány was originally situated near the boundary of two different faunal provinces. The fauna contains North-West European forms (Kosmoceratidae) indicating the archipelago of stable Europe, together with the abundant elements (firstly the Phylloceratidae and Lytoceratidae) of the Tethyan ocean surrounding in south the stable Europe. LÓCZY (1915)—somewhat inappropriately—regarded the ammonite-rich bank as a shore deposit, having been formed on the “beach of an open sea”. Villány was more probably a fragment of the southern margin of stable Europe, which subsequently was broken off and came to the present site through lateral movements (GÉCZY 1972).

REFERENCES

- AGER, D. V. and CALLOMON, J. H. (1971): On the Liassic age of the "Bathonian" of Villány (Baranya). — *Ann. Univ. Sci. Budapest., Sect. Geol.*, 14., pp. 5–16.
- CARIOU, E. (1980): L'étage Callovien dans le Centre-Ouest de la France. — *Thèse Univ. Poitiers Doct. Sci. Nat.*, No. 325.
- GÉCZY, B. (1972): (The formation of the Jurassic faunal provinces and the Mediterranean plate tectonics). *MTA X. Oszt. Közl.*, 5., 3–4, pp. 297–311. (In Hungarian)
- KASZAP, A. (1959): Doggerschichten im Villányer Gebirge (Südungarn). — *Földt. Közl.*, 89., 3., pp. 262–269. (In Hungarian, with German abstract)
- LENZ, O. (1872): Aus dem Baranyaer Comitat. — *Verh. k. k. geol. Reichsanst.*, Jg. 1872, No. 14., pp. 290–294.
- LÓCZY, L. (1915): Monographie der Villányer Callovien-Ammoniten. — *Geol. Hung.*, 1., 3–4, pp. 1–253.
- RADWANSEKI, A. and SZULCZEWSKI, M. (1966): Jurassic stromatolites of the Villány Mountains (Southern Hungary). — *Ann. Univ. Sci. Budapest., Sect. Geol.* 9., pp. 87–107.
- RAKUSZ, GY., STRAUZ, L. (1953): La géologie de la Montagne de Villány. — *MÁFI Évk.*, 41., 2., pp. 1–43. (In Hungarian, with French and Russian abstracts)
- TILL, A. (1910–11): Die Ammonitenfauna des Kelloway von Villány (Ungarn). — *Beitr. Paläont. Geol. Öster., Ungarns u. Orient*, 23–24.
- VÖRÖS, A. (1972): Lower and Middle Jurassic formations of the Villány Mountains. — *Földt. Közl.*, 102. 1. pp. 12–28. (In Hungarian, with English abstract)

THE PROBLEM OF EXTINCTION

M. MONOSTORI

Department of Paleontology, Eötvös University, Budapest

(Received: 15th March, 1982)

РЕЗЮМЕ

1. Вымирание является естественной составляющей процесса развития живого мира, оно неотделимо от этого процесса и происходило в течение всей истории Земли.

2. Вымирание нельзя отделить от генетических особенностей и их изменения.

3. Изменения условий среды, особенно неожиданные, играют существенную роль при вымирании.

4. Существенную роль в вымирании играют также размеры популяции, степень их изоляции и изменения этих факторов. Эта связь в зависимости от конкретных условий может быть многосторонней.

5. В связи с этими последними имеют большое значение возникающие под влиянием тектонических и других причин изменения уровня моря и перемещения континентов.

6. Важную роль мог играть также климат, установление условий питания, появление конкурентов и врагов и много остальных факторов живого и неживого мира, в особенности их радикальные изменения.

7. Вымирание на более высоком таксономическом уровне обычно является ключительным аккордом процесса, который измеряется геологической шкалой времени и которому предшествуют ареальные и таксономические сужения (уменьшение численности форм и района их распространения).

8. Причины вымирания должны исследоваться в каждой группе и на каждом таксономическом уровне. Искать общие причины не имеет смысла (это, конечно, не исключает частичного или полного совпадения причин вымирания у некоторых таксонов).

9. Вымирание является таким же сложным, материально детерминированным и проявляющимся диалектически процессом, как любой из процессов развития органической жизни.

1. Evolution and extinction

The evolution of the organic world shows that certain groups, within a more or less limited time interval, disappear from the Earth without leaving any representatives in rocks formed afterwards. The extinction of certain animal groups is not unusual, because the organic world, just as the whole material world, exists and evolves through the dynamics and dialectics of origin and death. Extinction is restricted here to the meaning of the phenomenon when a certain organic group disappears without descendants, phyletic extinction, i.e. the transition into new forms is disregarded.

The so-called "mass extinctions" are discussed widely in the literature. In some relatively short interval of geological time the number of taxa

becoming extinct is relatively high, i.e. the organic world shows abrupt changes.

The phenomenon of extinction has been known from the beginning of paleontological investigations. The fixist (creationist) views hardly integrated this fact, and this resulted in the nearly ridiculous recreationist theories which take repeated creations into consideration. On the other hand, some followers of the evolutionary theories, who believed in the gradual development of the organic world, denied the fact of extinction, arguing that these are apparent phenomena arising from our incomplete knowledge (in fact, there are some—rather exceptional—animal groups which had been regarded as extinct, and were discovered later).

Nowadays it is hardly doubted that extinction is an important and inseparable part of the evolution of the organic world.

2. Theories explaining extinction

2.1. *Theories favouring internal factors*

A part of the theories of extinction can be characterized by a measure of mysticism. These theories regard the living world as an object which follows only its internal principles, developing independently of external circumstances. These theories interpret the organic world as a superorganism. Formerly they used to blame the running out of some mysterious "vital force" to account for the extinction. The hypothesis of VERNADSKY on the mass of biosphere as constant during Earth's history led some researchers to the supposition that from the origin of new species one may infer the extinction of former ones. The cause of extinction is an "internal command" manifested in the total living world. Thus the extinction takes place for the goal of evolution.

2.2. *Theories favouring external factors*

A rather great part of the theories explains extinctions by external causes independent of the organic world. These are materialistic views, but comprise true, as well as false explanations.

2.2.1. *Theories based on cosmic factors*

The authors of these theories study the problem of the so-called mass extinctions, separating it from the temporally random extinctions which appear permanently through Earth's history. The catastrophic nature of the events is strongly emphasized.

There are many extraterrestrial causes which have been called to account for the mass extinctions. Impact of cosmic bodies, extreme changes in tidal movements and changes in light can be mentioned, as well as the recently arisen theories which are based on abnormal increase of external radiation destructive for living forms.

Geological and geophysical studies have made it clear that the magnetic field of the Earth changed rapidly during Earth's history, and these were accompanied with polarity reversals, causing temporal ceasing of the

magnetic field. This might have resulted in the loss of the Van Allen belt, and the concomitant high ultraviolet and cosmic radiation on Earth's surface. However, accurate calculations revealed (WADDINGTON, 1967) that the excess radiation originating in this way is insignificant as compared to the value of the existing radiation. The polarity reversals and the faunal changes are not coincidental, furthermore the terrestrial and marine extinctions show temporal differences, too (SIMPSON, 1968; MAYR, 1970; RAUP and STANLEY, 1971). The followers of this theory suggested recently the direct physiological effects of the magnetic field (FOSTER, 1976).

Another theory regards the excess radiation of supernova eruptions as the cause of the extinctions. Calculations of probabilities show that the temporal distances between mass extinctions correspond to the probabilities of cosmic catastrophes in sufficient vicinity. Beside radiation, equilibrium disturbance of the atmosphere also might cause climatic catastrophe (TERRY, 1968; RUSSEL and TUCKER, 1971). They interpreted the temporal differences of the floral and faunal mass extinctions, as well as the selective extinctions of the faunas as a result of different resistances. On the other hand, they have no explanations to the problem that how these very short supernova effects could cause long, geologically measured extinction processes. The interpretations disregard also the fact that extinctions appear continuously in the whole of Earth's history, without the need of any, so drastic external factors (SIMPSON, 1968). Recent studies have suggested that the degree of decrease in the atmospheric protection can be questioned also, on the basis of hitherto disregarded physical and chemical processes (REID, 1976). Especially the Late Cretaceous (65 m.y.B.P.) mass extinction was connected to a supernova eruption, however, no remains of a contemporary eruption have been discovered so far (TUCKER and FELDMAN, 1976).

Hsü (1980) inferred the Late Cretaceous extinction from an impact of a cosmic body (asteroid). He argued that the cyanide compounds carried by this cosmic body caused the mass devastation of the marine plankton, the warming up related to the impact resulted in the terrestrial extinctions, while the originated dust caused the significant climatic cooling later. However, the problem why these drastic changes did not have any effects on the numerous organisms living together with the extinct ones in the same habitats remained unsolved.

To sum up, it can be stated that there is no sufficient basis to assign main role to the various cosmic effects in the mass extinctions. On the other hand, it cannot be declared that cosmic effects have had no influence on the course of evolution, including extinctions.

2.2.2. Theories based on terrestrial causes

Extremely high is the number of theories explaining mass extinctions by terrestrial causes. These include large-size crustal movements, sea level changes, climatic changes, changes in the salinity of oceans or in the gaseous composition of the atmosphere, or changes in the quantity of the terrestrial radioactive or other elements.

Some examples

FRÖHLICH (1977) argued that the terrestrial radioactive element release during geologically active periods may cause subsequent extinctions.

FISCHER (1964) explained the Late Permian extinction by the evaporation of epicontinental seas, which caused the hypersalinity of the oceanic deep waters and slight dilution of the waters above, and this might have led to the extinction of many stenohaline forms. He based his theory on the presence of extensive salt-deposits.

MCALISTER (1970) recognized correlation between the oxygen consumption and the rate of extinction of some animal groups. He concluded that the changes in atmospheric oxygen content had a decisive (and selective) role, and this is why the extinctions of terrestrial and marine animals appear coincidentally in many cases.

DAVITASHVILI (1969) based his hypothesis on the theory of Darwinian struggle for life, claiming that the main cause of extinction is the "biological stress" i.e. the perfection of concurrents and enemies.

All these theories, alike the cosmic hypotheses, are characteristically one-factor models. The authors usually search for a single cause for the extinction. However, the mass extinctions affected several animal groups, and this cannot be put under the cover of single environmental factors. There is no question of the abandonment of the effect of these factors, but it is probably insufficient to argue for one-factor theories for the complicated phenomena of mass extinctions.

2.3. *Theories supposing interaction of several factors*

The development in the knowledge of theoretical paleontology and evolutionary biology made it clear that the phenomenon of extinction, as a part of evolution, cannot be studied as taken from its context of the development of the organic world.

There are several known mass-extinction periods within Earth's history. Those in the Late Ordovician and Late Devonian are relatively less-known. According to some authors (JOHNSON, 1974; BOUCOT, 1975), these periods were characterized by maximal marine expansions with sudden and short-duration lowering of the sea level, during which the break in the sedimentation left no, or hardly discernible traces. This was completed by the effect of glaciation in the Late Ordovician. The radical sea level change resulted in circumstances which made impossible the gradual adaptation and the migration of the previously adapted associations, decreased the sizes of the populations and increased the concurrence between the groups.

Similar was the case of the Late Permian, greater, so better-known extinction. In this extinction great importance is attached to the coincidental total disappearance of the reef environment (BOUCOT, 1975). The areal decrease accompanying the lowering of the sea level is a cause of the extinction at the Permian/Triassic boundary by the equilibrium theory too, because there is close correlation between the size of the area and the number of the inhabiting taxa (SIMBERLOFF, 1974). The maximal extinction of

the terrestrial vertebrate fauna is not coincidental with the Permian/Triassic boundary, but precedes and is substantially slighter than that of the marine invertebrates. The extinction of the marine vertebrates can be correlated with that of the marine invertebrates (PITRAT, 1973).

According to these theories, part of the mass extinctions were caused by sudden short environmental destruction during stable domination of circumstances favourable for special adaptations. Thus the mass extinction can be explained as a function of complex biological-anorganic natural relationships.

The best-known extinction took place in the Late Cretaceous. This affected many animal groups, including terrestrial and marine vertebrates, as well as marine invertebrates. The effect was substantial on the shallow-water benthos and on the pelagic plankton of the marine invertebrates. It was a rather selective extinction, because certain forms or groups became extinct, while others showed continuous development within the same environment.

Some authors regard here the sea level changes and the climatic decline as of especially importance (WORSLEY, 1971; BOUCOT, 1975; COOPER, 1977).

During the Late Cretaceous tectonic respite the terrestrial material supply of the seas diminished substantially, and this might have caused the nutrient-insufficiency of the oceanic plankton. The sudden decrease of the plankton had been completed by the undifferentiated oceanic distribution and the lack of oceanic circulation, thus the nutrient-loss of the higher water-levels could not be replaced from the depth (BRAMLETTE, 1965a, b; NEWELL, 1965). The loss of the planktonic flora caused food-web disruption, and contributed to the extinction of a number of consumers (planktonic foraminifers, ammonites, belemnites).

The Late Cretaceous regression was similar in extreme speed and significance to those mentioned above; some calculations have indicated that its speed might have been ten-times higher than the average. All the effects mentioned above at the Paleozoic extinctions might have also contributed in this case (COOPER, 1977).

The cooling and becoming continental of the terrestrial climate might be related to the decrease of the phytoplankton, thus influencing the atmospheric composition. The terrestrial ecological niches became narrower and the competition between certain forms became increased. The floral turnover changed the food resources. Regression ceased many terrestrial isolations and resulted in new competitions (COOPER, 1977).

SLOAN (1976), on the basis of studies in North America, disputed the catastrophic extinction of dinosaurs in the Late Cretaceous. He argued that the extinction took place here in humid subtropical—warm temperate forests dominated by angiosperms which were gradually replaced by colder temperate forests rich in pinaceans, while the *Triceratops*-fauna was replaced with gradual dominance changes by *Protungulatum-Stygimys* (mammal) fauna.

These above examples are some of the theories which try to show the phenomenon in its interrelations. Some authors have pointed out that the mass extinctions are not the consequences of special causes, but the results of those same internal and external factors which cause the continuously appearing ordinary extinctions. The differences lie in the extreme measure, coincidence and rapidness of these factors (COOPER, 1977).

3. Problems

The above-mentioned complex theories, good approximations as they may seem, usually arise several unanswered questions in the case of studies on actual living groups.

One of the problems is that the judgement of the extent of extinction depends on the studied taxonomic level. Different pictures can be drawn of the extinction periods if one regards them from phyla to genera. According to VALENTINE (1974), the species-level studies could be most important, because species are the primary elements of evolution.

Another important question is how the genetic characteristics of organisms regulate the extinctions. Some authors argue that stable environment results in loss of genetic variability for adaptation. The stability and instability of the environment may be in different correlation with the genetic variability of the population. BRETSKY and LORENZ (1970) show theoretically that the probability of extinction is maximal when stable environmental circumstances change into instable ones, especially in the case of rapid phenomena. SCHOFF and GOOCH (1972), on the basis of studies on some forms living in 1000 to 2000 m water depth, denied the role of loss of genetic variability. However, to decide this important question, single studies seem to be insufficient because knowledge about the development of deep-sea faunas is limited, and we do not know whether the studied stable environment was really stable for extended times, and the forms in question were really living there, or not.

MAYR (1970), RAUP and STANLEY (1971), JABLOKOV and JUSUF OV (1976), IVANOVSKI (1976) accept that extinction is realized through genetic factors. Referring to the fact that extinctions affect taxonomical and not ecological groups, RAUP and STANLEY attach less importance to ecological adaptations. GABUNIA (1969; 1971), on the other hand, assigns the extinction of certain forms to inadaptable evolution (rapid, but imperfect adaptation), which results subsequently from the forms being unable to concur with the forms which have undergone slow, but perfect environmental adaptation.

A third and important question is the influence of sea level changes on the faunas. It is well-documented that the Mediterranean Sea in Late Miocene times—because of probable world-wide eustatic lowering of the sea level—became disconnected from the Atlantic Ocean, and was separated into brackish-water or evaporating lagoons, with the formation of vast evaporite masses. Sea level changes appeared rapidly and repeatedly with temporary re-established connections, and these resulted in the inflow of

water and salts. Recent studies suggest that almost the whole Mediterranean fauna was obliterated, and the area was repopulated only in the Pliocene, after the final establishment of a connection to the Atlantic. These truly great changes did not cause any apparent extinctions in the fauna (the migrating Pliocene forms reappeared as elements identical with those of the Miocene fauna). This is why this important event was recognized so late (BENSON, 1976; ČITA, 1976; ADAMS, 1976). These facts call attention to the fact that even the sudden sea level changes and regressions may not cause mass extinctions in themselves.

On the basis of studies on the extinction of an animal group, the dinosaurs, VOSS—FOUCART (1971) concluded that all the previously suggested external environmental or internal evolutionary factors could have influenced only a respective part of the so differentiated fauna. Thus, he suggested that the extinction of this group was a complicated process, the result of interactions of several factors.

According to RAUP (1978), the extinction of families and orders is the inevitable and natural result of evolution. The basic phenomenon is the species extinction, which is usually related to certain common organizational features, but there are extinctions arising from specific features, producing cummulation of unrelated species extinctions. Extreme is the sustained life-span, not the extinction!

4. Conclusions

a) Extinction is a natural and inseparable phenomenon of the development of the organic world, appearing throughout geological history;

b) Extinction cannot be rendered independent of the genetic features and their changes,

c) In extinction considerable is the role of the shaping of environmental conditions, especially the sudden changes;

d) Considerable is the role of population size, and the extent and changes of isolation. The relationship may be manifold, depending on the circumstances (BOUCOT, 1975);

e) Concerning these previous facts, the sea level changes and conti-nent movements caused by tectonic and other effects are of great importance;

f) Important factors might have been the climate, the development of food-supply, the appearance of concurents and enemies, as well as many other elements of the organic and inorganic environment, and especially their radical changes;

g) Extinction on higher taxonomic level is generally the final event of a geo-historically measurable process, which is anticipated by areal and taxonomic restriction (i.e. decrease in areal distribution and in the number of forms);

h) Mass extinctions are not different basically, being caused by special-ly coincident effects, which are especially unfavourable for organic life;

i) The causes of extinctions should be studied separately for all groups and in every taxonomic level; search for general causes seems meaningless (this is not a necessary exclusion of total or partial coincidence of causes for certain taxa);

j) Extinction is a complex, materially determined and dialectically manifested phenomenon, just like the other phenomena of the development of organic life.

REFERENCES

- ADAMS, C. G. (1976): Larger Foraminifera and the Late Cenozoic history of the Mediterranean region. — *Palaeogeogr., Palaeoclimatol., Palaeoecol.*, 20, pp. 147—176.
- BENSON, R. H. (1976): Testing the Messinian salinity crisis biodynamically: an introduction. — *Palaeogeogr., Palaeoclimatol., Palaeoecol.*, 20, pp. 3—11.
- BENSON, R. H. (1976): Changes in the ostracodes of the Mediterranean with the Messinian salinity crisis. — *Palaeogeogr., Palaeoclimatol., Palaeoecol.*, 20, pp. 147—170.
- BOUCOT, A. (1975): *Evolution and Extinction Rate Controls*. Elsevier, Amsterdam, pp. 1—427.
- BRAMLETTE, M. N. (1965a): Massive extinctions in biota at the end of Mesozoic time. — *Science*, 148, pp. 1696—1699.
- BRAMLETTE, M. N. (1965b): Mass extinctions of Mesozoic biota. — *Science*, 150, p. 1240.
- BRETSKY, P. W., LORENZ, D. M. (1970): An essay on genetic-adaptive strategies and mass extinctions. — *Bull. Geol. Soc. Amer.*, 81, pp. 2449—2456.
- СИТА, М. В. (1976): Биодинамические эффекты кризиса Мессинской солености на эволюцию planktonic foraminifera в Средиземном море. — *Palaeogeogr., Palaeoclimatol., Palaeoecol.*, 20, pp. 23—42.
- COOPER, M. R. (1977): Eustasy during the Cretaceous: its implications and importance. — *Palaeogeogr., Palaeoclimatol., Palaeoecol.*, 22, pp. 1—60.
- Cretaceous/Tertiary extinctions and possible terrestrial and extraterrestrial causes. — *Syllogeus*, No. 12, Ottawa, 1976, pp. 1—162.
- ДАВИТАИВИЛИ, Л. Ш. (1969): Причины вымирания организмов. — *Наука*, Москва, pp. 1—144.
- FISCHER, A. G. (1964): Brackish oceans as the cause of the Permo-Triassic marine faunal crisis. In: Nairn, A. E. M. (Ed.): *Problems in Paleoclimatology*. Wiley and Sons, New York, pp. 566—579.
- FOSTER, J. (1976): in *Cretaceous/Tertiary ...*
- FRÖHLICH, K. (1977): Bemerkungen zur Faunenincisionen und ihren möglichen physikalischen Ursachen. — *Freiberger Forschungshefte*, C, 326, pp. 71—72.
- ГАБУНИЯ, Л. К. (1969): Вымирание древних рептилий и млекопитающих. — *Медниереба, Тбилиси*, pp. 1—233.
- ГАБУНИЯ, Л. К. (1971): Инадаптивная эволюция как одно из важнейших общих условий вымирания млекопитающих. — *Труды Пал. Инст. АН СССР*, 130, 32—38.
- Hsü, K. (1980): Terrestrial catastrophe caused by cometary impact at the end of the Cretaceous. — *Nature*, 285, No. 5762, pp. 201—203.
- ИВАНОВСКИЙ, И. А. (1976): Палеонтология и теория эволюции. — *Наука*, Новосибирск, pp. 1—78.
- ЯБЛОКОВ, А. В., ЮСУФОВ, А. Г. (1976): Эволюционное учение. — *Высшая школа*, Москва, pp. 1—335.
- JOHNSON, J. G. (1974): Extinction of perched faunas. — *Geology*, 2, pp. 479—482.
- MAYR, E. (1970): *Populations, Species and Evolution*. Cambridge, Mass., Harvard Univ. Press, pp. 1—453.
- MCALISTER, A. L. (1970): Animal extinctions, oxygen consumption, and atmospheric history. *Journ. Paleont.* 44, pp. 405—409.
- NEWELL, N. D. (1965): Mass extinctions at the end of the Cretaceous period. — *Science*, 149, pp. 922—924.
- PITRAT, C. W. (1973): Vertebrates and the Permo-Triassic extinction. — *Palaeogeogr., Palaeoclimatol., Palaeoecol.*, 14, pp. 249—264.
- RAUP, D. M., STANLEY, S. M. (1971): *Principles of Paleontology*. Freeman and Co., San Francisco, pp. 1—388.
- RAUP, D. M. (1978): Approaches to the extinction problem. — *Journ. Paleont.*, 52, pp. 517—523.
- REID, J. (1976): in *Cretaceous/Tertiary ...*
- RUSSEL, D., TUCKER, W. (1971): Supernovae and the extinction of the dinosaurs. — *Nature*, 229, No. 5286, pp. 553—554.
- SCHOPF, T. J., GOOCH, J. L. (1972): A natural experiment to test the hypothesis that loss of genetic variability was responsible for mass extinctions of the fossil record. — *Journ. Geol.*, 80, pp. 481—483.
- SIMBERLOFF, D. S. (1974): Permo-Triassic extinctions: effects of area on biotic equilibrium. — *Journ. Geol.*, 82, pp. 267—274.
- SIMPSON, G. G. (1968): Evolutionary effects of cosmic radiation. — *Science*, 162, pp. 140—141.
- SLOAN, R. E. (1976): The ecology of dinosaur extinction. In: *Athlon Essays in Paleontology in Honour of Loris Shano Russel*, Royal Ontario Museum, pp. 134—154.
- TERRY, E. D. (1968): Biologic effects of supernovae. — *Science*, 159, pp. 421—423.
- TUCKER, W., FELDMAN, P. (1976): in *Cretaceous/Tertiary ...*
- VALENTINE, J. W. (1974): Temporal bias in extinctions among taxonomic categories. *Journ. Paleont.*, 48, pp. 549—552.
- VOSS-FOUCART, M. F. (1971): Est-il possible d'expliquer l'extinction des dinosaures a la fin du Crétacé. — *Natur. Belg.*, 52, pp. 101—108.
- WADDINGTON, C. J. (1967): Paleomagnetic field reversals and cosmic radiation. — *Science*, 158, pp. 913—915.
- WORSLEY, T. R. (1971): Terminal Cretaceous events. — *Nature*, 230, No. 5292, pp. 318—320.

LOWER AND MIDDLE JURASSIC BRACHIOPOD PROVINCES IN THE WESTERN TETHYS

by

A. VÖRÖS

Palaeontological Department, Hungarian Natural History Museum, Budapest

(Received: 15th March, 1982)

РЕЗЮМЕ

На основании проведенного численными методами сравнения 19 синемюрских, 30 плинсбахских, 14 ааленских, 18 верхне-байосских и 17 келловейских составляющих видов фауны брахиоподов на территории западного Тетиса юрского периода можно с уверенностью выявить одну «европейскую», одну «средиземноморскую» и одну «эфиопскую» провинцию брахиоподов, последняя из которых в течение доггера становится все более ярко очерченной. Максимальная разница между европейской и средиземноморской провинциями достигается в течение аалена-байоса. Средиземноморская и эфиопская провинции не показывают связи друг с другом. На основании анализа палеогеографических условий и факторов, определяющих разделение на провинции, можно прийти к выводу, что европейская и эфиопская провинции распространялись на евразийский и гондванский шельфы, а также и на эпиконтинентальные морские участки Тетиса, в то время как средиземноморские брахиоподы жили на подводных хребтах Тетиса, расположенных далеко от больших континентов. Континентальные фрагменты, содержащие средиземноморских брахиоподов, после закрытия Тетиса были разбросаны по участку альпийского орогенного пояса от Марокко до Кавказа, причем большая их часть группируется в периадриатическом регионе.

Introduction

In the past two decades there has been an increase in the number of works published on the geographical distribution of former marine faunas. Palaeobiogeography became a fashionable topic, giving useful data for related fields in the earth sciences. The geographical distribution of the Jurassic Tethyan brachiopods served as basis for several treatments (e.g. DELANCE, 1972; ROUSSELLE, 1975), outstandingly the one by AGER (1967; 1971; 1973), who distinguished, among others, the NW European, the Mediterranean and the Abessinian, i.e. Ethiopian provinces, on the basis of the occurrences of certain characteristic genera and morphological groups.

The definition of faunal province may be interpreted in a rather wide sense, and a strict interpretation is generally impossible. According to CAMPBELL and VALENTINE (1977, p. 55.), faunal provinces are "regions within which fossil communities maintain a characteristic species composition and between which they tend to differ significantly". Specialists working on a special fossil group of a special age in detail may feel, or even understand these identities and differences. On the other hand, the unbiased expression and representation of these conditions need the application

of numerical methods. The present paper gives a comparison of the West Tethyan Sinemurian, Pliensbachian, Aalenian, Upper Bajocian and Callovian brachiopod faunas by numerical methods, but does not discuss the faunas of the Toarcian and Bathonian stages which are very poorly represented in the Mediterranean brachiopod faunas in Hungary.

Methods

For pairwise comparison of faunal lists there are several similarity coefficients available (see CHEETHAM and HAZEL, 1969), from which the present work used those two suggested by GÉCZY (1974): the Jaccard- and the Simpson-coefficients (equations: $J.C. = \frac{C}{N_1 + N_2 - C}$; $S.C. = \frac{C}{N_1}$, where N_1 is the taxon number of the smaller, N_2 is of that of larger, and C is the number of the common taxa in the two faunas). The separation of faunal provinces was done by the method elaborated previously (VÖRÖS, 1977). Within the studied Jurassic stages there were designated faunistic units represented by data of individual sites or by summarized data of some nearby localities. Well-documented monographs are available about most localities, in other cases only species descriptions accompanied with figures were taken into consideration. As a next step, respective "type faunas" were selected within the previously quantitatively outlined faunal provinces, which type faunas characteristically represent each province in species number and composition alike. Then the faunas of all other localities were compared to the type faunas. (N.B. This comparison would be real only if the same specialist was to revise all the faunas by studies on the original material. However, this claim meets objective difficulties, which have been partially overcome now: I could study only some of the here compared faunas in museum collections. Thus my judgement is based on more or less reliable knowledge through direct studies on Lower Jurassic brachiopod faunas of the NW Carpathians, the Northern Calcareous Alps, the Southern Alps and the Central Apennines.) The results of the pairwise comparisons (i.e. the Simpson- and Jaccard-coefficient values) are figured in systems of co-ordinates plotted against the character related to the type fauna (see e.g. Fig. 1.). The faunas are represented by points the positions of which within the system show the measure of similarity to the type faunas. The quarter-field of the system of co-ordinates can be divided into six equal parts with lines starting from the origin where the two outermost parts comprise the faunas most similar to the type fauna, while the intermediate segments contain those of transitional character. In the maps these features are represented by sector tradings (see e.g. Fig 2.).

Brachiopod provinces separated by numerical methods

Sinemurian

The comparison is made for 19 faunas, totalling in 243 species, of which majority is Upper Sinemurian (Lotharingian) in age.

1. South Germany + Alsace-Lorraine (QUENSTEDT, 1858, 1868 – 71; OPPEL, 1861; HAAS and PETRI, 1882)	25 species
2. England (DAVIDSON, 1878; AGER, 1956 – 67)	15 species
3. Rhone basin (DUMORTIER, 1867)	13 species
4. Portugal (CHOFFAT, 1947)	8 species
5. Hauts Plateux (Morocco and Algeria) (FLAMAND, 1911; DARESTE de la CHAVANNE, 1930; GOURION, 1960)	8 species
6. Taormina (Sicily) (DI STEFANO, 1887)	34 species
7. Calabria (FUCINI, 1892; GRECO, 1894)	29 species
8. Alpes Vaudoises (Préalpes Médiannes) (HAAS, 1885; PETERHANS, 1926)	16 species
9. Mecsek Mts. (South Hungary) (VADÁSZ, 1935)	17 species
10. Southern Carpathians (JEKELIUS, 1915; RAILEANU and JORDAN, 1964)	15 species
11. The Rif (DUBAR, 1938)	8 species
12. Saharan Atlas (DUBAR, 1942; GOURION, 1960)	12 species
13. Western Sicily (GEMMELLARO, 1878)	15 species
14. Central Appennines (CANAVARI, 1879, 1882; DE STEFANI, 1887; FUCINI, 1893, 1895; RUGGIERO, 1964)	60 species
15. Southern Alps (PARONA, 1884; DEL CAMPANA, 1907; DAL PIAZ, 1909; CONTI, 1954; POZZI, 1960; SACCHI VIALLI, 1964)	24 species
16. Northern Calcareous Alps (OPPEL, 1861; FRAUSCHER, 1883; GEYER, 1889)	56 species
17. Gerecse Mts. (NW Hungary) (VIGH, 1943)	30 species
18. Bakony Mts. (Hungary) (BÖCKH, 1874; ORMÓS, 1937; VÖRÖS, unpubl.)	38 species
19. External Dinarides (Risan) (EICHENBAUM, 1883; BITTNER, 1895; MIHAJLOVIĆ, 1955)	10 species

The type fauna of the European province comprises the summarized data of South Germany and Alsace-Lorraine, while the type fauna of the Mediterranean is that of the Northern Calcareous Alps. The faunal characters of the localities are plotted in a system of co-ordinates in Fig. 1. Rather numerous are the faunas within the transitional fields; especially interesting are No. 6 (Taormina) and No. 7 (Calabria) with significant Mediterranean, and No. 12 (Saharan Atlas) and No. 15 (Southern Alps) with strong European affinity. On the basis of distributional abundance, some characteristic European and Mediterranean species can be designated. The characteristic European species are those appearing in at least four of the definitely European faunas (Nos: 1 to 5, 8 to 10) and not found in the definitely Mediterranean faunas (Nos. 11, 13, 14, 16 to 19), namely: *Zeilleria numismalis*, *Z. perforata*, *Spiriferina walcotti*. Characteristic Mediterranean species are those represented in at least four distinctly Mediterranean faunas, and lacking in the distinctly European faunas: *Linguithyris aspasia*, *Zeilleria? venusta*, *Spiriferina angulata*, *S. obtusa*. These species can be used in maps to express the faunistic features of the localities which can-

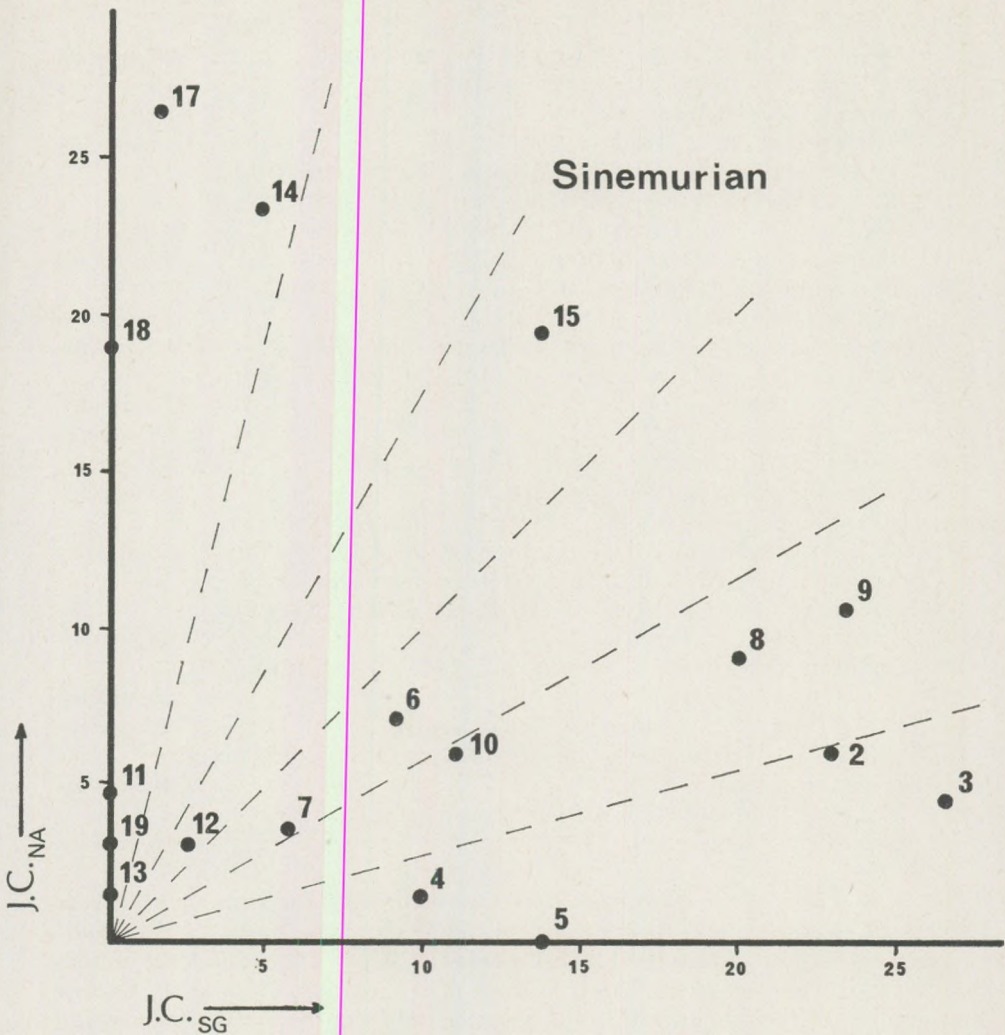


Fig. 1. Jaccard-coefficient values of Sinemurian faunas compared with the South German (horizontal axis) and the North Alpine (vertical axis) faunas, respectively

not be evaluated quantitatively because of the low (<5) species number. For example (see Fig. 2), in Sweden (TROEDSSON, 1951) all the characteristic European species occur, while in Provence (LANQUINE, 1929), *Zeilleria perforata* and *Spiriferina walcotti* are known. The Mediterranean character of the NW Carpathians (Stratenska Hornatina; MAHEL, 1958) is indicated by the occurrence of *Spiriferina obtusa*. The geographical distribution of the qualitatively compared faunas (Fig. 2.) shows a contradictory pattern for Hungary, Southern Italy and in the Atlas Range, calling attention to paleogeographic and large-scale tectonic problems.

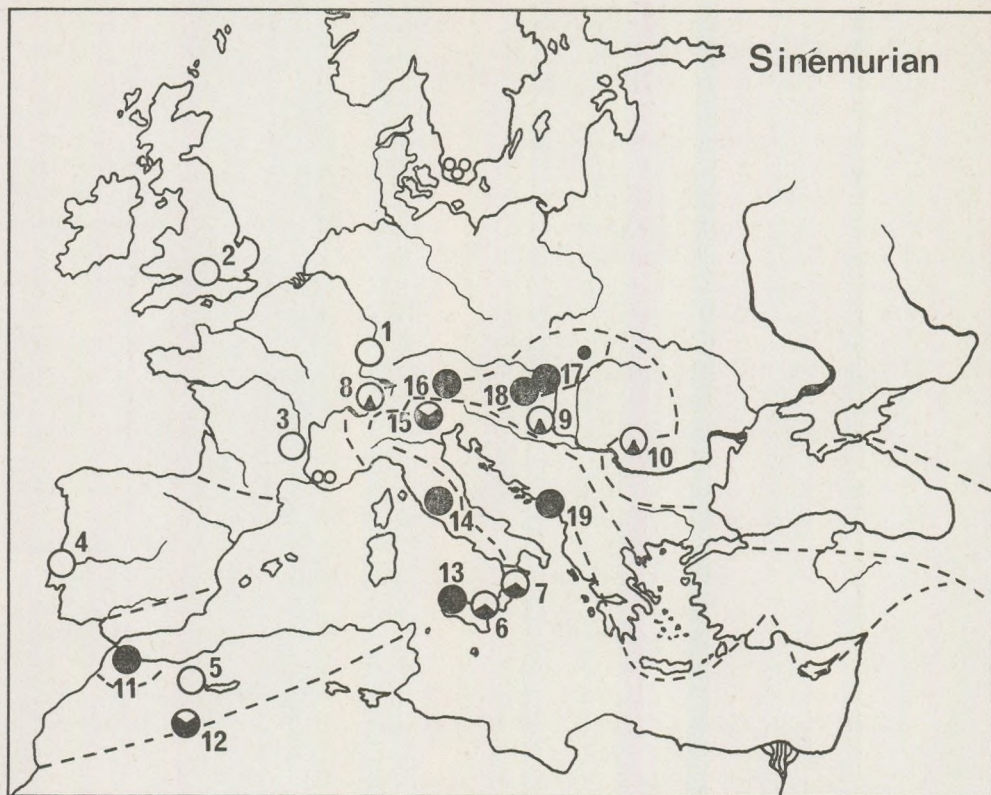


Fig. 2. Geographical distribution of Sinemurian faunas. Open circles: faunas of European character; full circles: faunas of Mediterranean character (the division of other circles into sectors is proportional to their faunal character); \circ : characteristic European species; \triangle : characteristic Mediterranean species; broken lines: major Alpine tectonic lines

Pliensbachian

The present comparison is an extended version of a previously published paper (VÖRÖS, 1977) on the Pliensbachian (Carixian and Domerian) brachiopod distribution, being based upon more data, totalling in 30 faunas with 306 species altogether.

- | | |
|------------------------------------------------------------------------------------------------|------------|
| 1. Southern Alps (UHLIG, 1880; PARONA, 1880; BÖSE and SCHLOSSER, 1900; HAAS, 1912; RENZ, 1932) | 73 species |
| 2. Central Apennines (CANAVARI, 1880, 1881, 1883; ZITTEL, 1869; RAMACCIONI, 1936) | 56 species |
| 3. Western Sicily (GEMMELLARO, 1874; DI STEFANO, 1892) | 45 species |
| 4. External Hellenides (RENZ, 1932) | 28 species |
| 5. External Dinarides (ČIRIĆ, 1949) | 9 species |
| 6. Bakony Mts. (VÖRÖS, 1970) | 40 species |
| 7. Great Fatras (Belanska Dolina) (SIBLÍK, 1964) | 8 species |

8. Northern Calcareous Alps (BÖSE, 1898)	42 species
9. Betic Cordilleras (Murcia) (CISNEROS, 1923)	14 species
10. South Germany (QUENSTEDT 1858, 1868—71; RAU, 1905)	67 species
11. Alsace-Lorraine (HAAS and PETRI, 1882)	21 species
12. Pirenees (DUBAR, 1925)	8 species
13. Catalonia (Lérida) (DELANCE, 1969)	15 species
14. Morocco (Oudjda) (DARESTE de la CHAVANNE, 1930)	10 species
15. Anatolia (Yakacik) (AGER, 1959)	10 species
16. Crimea (MOISEIEV, 1934)	24 species
17. Yugoslavian Southern Carpathians (RADOVANOVIĆ, 1888; SUČIĆ—PROTIĆ, 1969, 1971)	50 species
18. Rumanian Southern Carpathians (Svinița) (RAILEANU and IORDAN, 1964)	21 species
19. Padurea Craiului (PREDĂ, 1967)	24 species
20. Mecsek and Villány Mts. (South Hungary) (VADÁSZ, 1935; AGER and CALLOMON, 1971)	15 species
21. Little Carpathians (Pristodolok) PEVNY, 1964; SIBLÍK, 1967)	7 species
22. Kostelec (W. Slovakia) (SIBLÍK, 1965, 1966, 1967, 1968)	16 species
23. Gresten (TRAUTH, 1909)	19 species
24. Great Britain (AGER, 1956)	32 species
25. Rhone basin (DUMORTIER, 1869)	11 species
26. Iberian Cordilleras (HINKELBEIN, 1969; HEVIA and DEL POZO, 1972; COMAS RENGIFO and GOY, 1975)	15 species
27. Portugal (CHOFFAT, 1947)	10 species
28. Oranian High Plateau (Saida) (FLAMAND, 1911; GOURION, 1960)	21 species
29. Eastern Atlas (Guelma) (DARESTE de la CHAVANNE, 1920)	22 species
30. Western Balkan Mts. (Teteven) (COHEN, 1931; TZANKOV and BONČEV, 1932)	17 species

As type faunas, the European and Mediterranean provinces are represented by the faunas of South Germany and the Southern Alps, respectively. The features of the Pliensbachian faunal localities are plotted in the system of co-ordinates in Fig. 3. The majority of the faunas show South German affinities, making a distinction of a European province clear, however, striking is the fact that the faunas of localities No.5 (External Dinarides) and No.16 (Crimea) appear as transitional, with European characters.

Characteristic European species, with occurrence in at least five distinctly European faunas (Nos. 10 to 12, 14, 17 to 20, 22, 24 to 28) and lack in distinctly Mediterranean faunas (Nos. 1, 2, 6, 8, 9) are: *Gibbirhynchia curviceps*, *Tetrarhynchia tetrahedra*, *Prionorhynchia quinqueplicata*, *Lobothyris edwardsi*, *L. punctata*, *L. subpunctata*, *Zeilleria subnumismalis*, *Z. mariae*, *Z. indentata*, *Z. quadrifida*, *Aulacothyris resupinata*. Characteristic Mediterranean species with occurrences in at least three distinctly Medi-

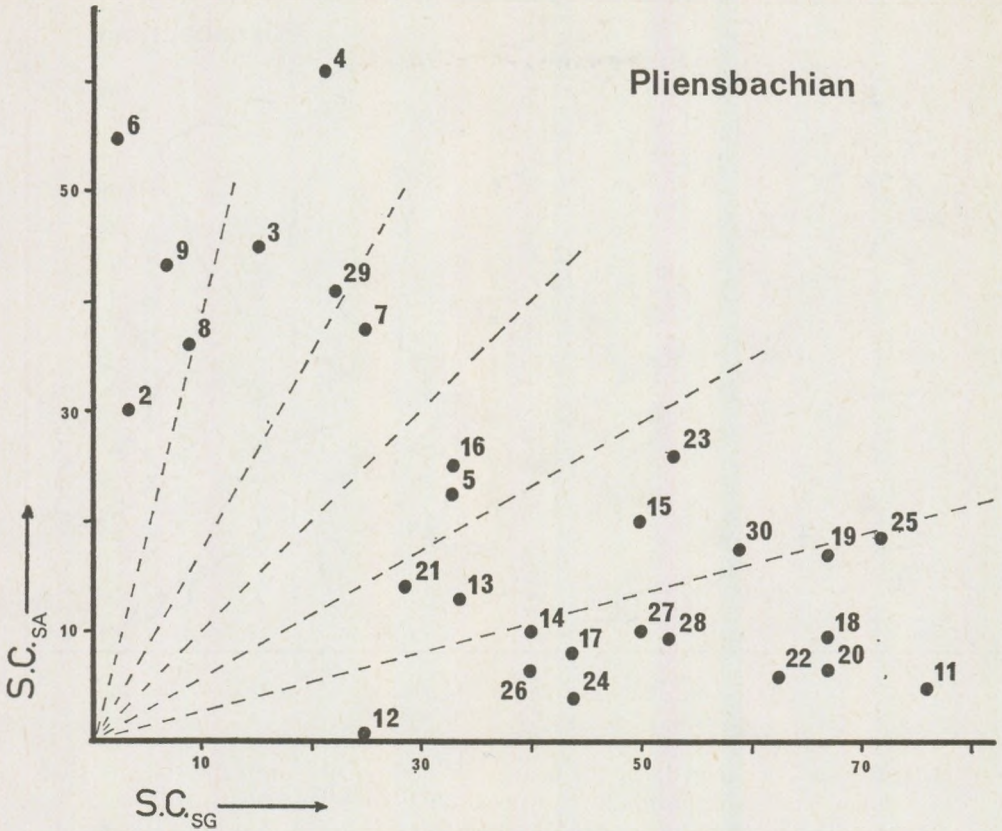


Fig. 3. Simpson-coefficient values of Pliensbachian faunas compared with the South German (horizontal axis) and the South Alpine (vertical axis) faunas, respectively

terranean faunas and lack in all the distinctly European faunas are: *Pisirhynchia retroplicata*, *P. inversa*, *Prionorhynchia? flabellum*, *P.? scherina*, *Apringia piccininii*, *A. mariottii*, *A.? stoppanii*, *Gibbirhynchia? sordellii*, *Linguithyris aspasia*, *Phymatothyris rheumatica*, *Viallithyris gozzanensis*, *V.? delorenzoi*, *Securithyris adnethensis*, *Aulacothyris? furlana*, *A.? apenninica*, *A.? pedemontana*. Fig. 4 shows the occurrences of some characteristic species. *Lobothyris punctata* is known from the Bukovina nappe of the Eastern Carpathians (TURCULET, 1971), while *Tetrarhynchia tetrahedra* and *Zeilleria quadrifida* occurs also near Brasov (in the Keresztélyfalva Lias ranged into the Geta nappe) (JEKELIUS, 1915). Interesting is the appearance of *Linguithyris aspasia*, a characteristic Mediterranean species in the Saharan Atlas (FLAMAND, 1911) and in the western part of the Betic Cordilleras (KILIAN, 1889), here associated with *Securithyris adnethensis*. The geographical distribution of the quantitatively compared faunas shows contradictory pattern in many places. The transitional (mixed?) character of the Anatolian

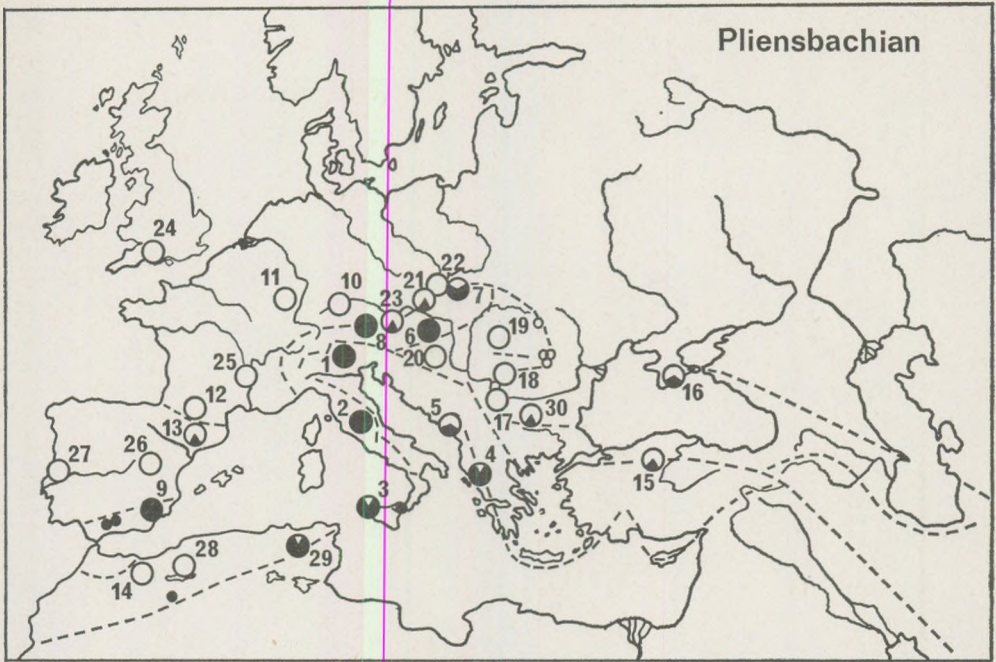


Fig. 4. Geographical distribution of Pliensbachian faunas. Legend: same as in Fig. 2

(No. 15) and Crimean (No. 16) faunas is hardly interpretable. In the case of faunas Nos. 5, 21 and 22 the possibility of misidentifications can be inferred. The position of faunas Nos. 6 and 20 emphasizes the paleogeographical importance of the Central Hungarian lineament. The particular pattern of the European and Mediterranean faunas (similar to that in the Sinemurian) in Iberia and in the Atlas calls probably for large-scale tectonic explanation, too.

Aalenian

The comparison is based on 14 faunas of a total of 141 species.

- | | |
|-------------------------------------------------------------------------------------------------------------|------------|
| 1. South Germany and Alsace-Lorraine (QUENSTEDT, 1868 – 71; HAAS and PETRI, 1881; BRANCO, 1879; DROT, 1952) | 12 species |
| 2. England (DAVIDSON, 1878) | 28 species |
| 3. NW France (Sarthe) (FRENEIX et al., 1956) | 6 species |
| 4. Rhone basin (ROCHÉ, 1939) | 16 species |
| 5. Morocco (Moyen Atlas) (ROUSSELLE, 1965) | 4 species |
| 6. Sardinia (TADDEI RUGGIERO, 1966) | 7 species |
| 7. Mecsek Mts. (VADÁSZ, 1935) | 5 species |
| 8. Western Sicily (DI STEFANO, 1884) | 10 species |
| 9. Calabria (GRECO, 1899) | 13 species |

- | | |
|-------------------------------------------------------------------------------------------------------------------------------------|------------|
| 10. Southern Apennines, (Lagonegro) (GRECO, 1900) | 6 species |
| 11. Southern Alps (PARONA and CANAVARI, 1880; VAČEK, 1886; FINKELSTEIN, 1889; BÖSE and FINKELSTEIN, 1892; FERRARI and MANARA, 1972) | 40 species |
| 12. Northern Calcareous Alps (ROTHPLETZ, 1886; FINKELSTEIN, 1889) | 48 species |
| 13. External Dinarides (Crna Gora) (MARTELLI, 1906) | 16 species |
| 14. NW Caucasus (KAMYSHAN and BABANOVA, 1973) | 25 species |

The faunal characters of the Aalenian localities are shown in the system of co-ordinates in Fig. 5. The separation seems to be significantly sharp, the majority of the points representing the faunas are assembled along the axes, the faunas of transitional character are those of No. 6 (Sardinia) and No. 12 (Northern Calcareous Alps) only. Characteristic European species occurring in at least three distinctly European faunas (Nos. 1 to 5) and la-

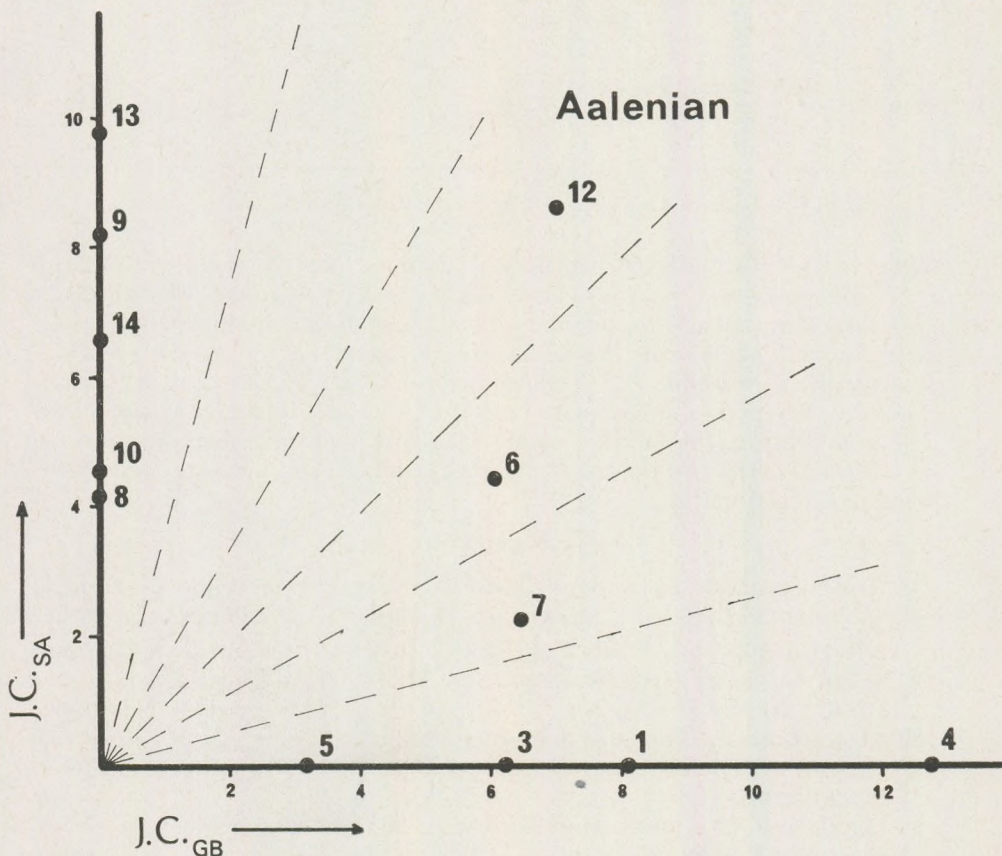


Fig. 5. Jaccard-coefficient values of Aalenian faunas compared with the British (horizontal axis) and the South Alpine (vertical axis) faunas, respectively

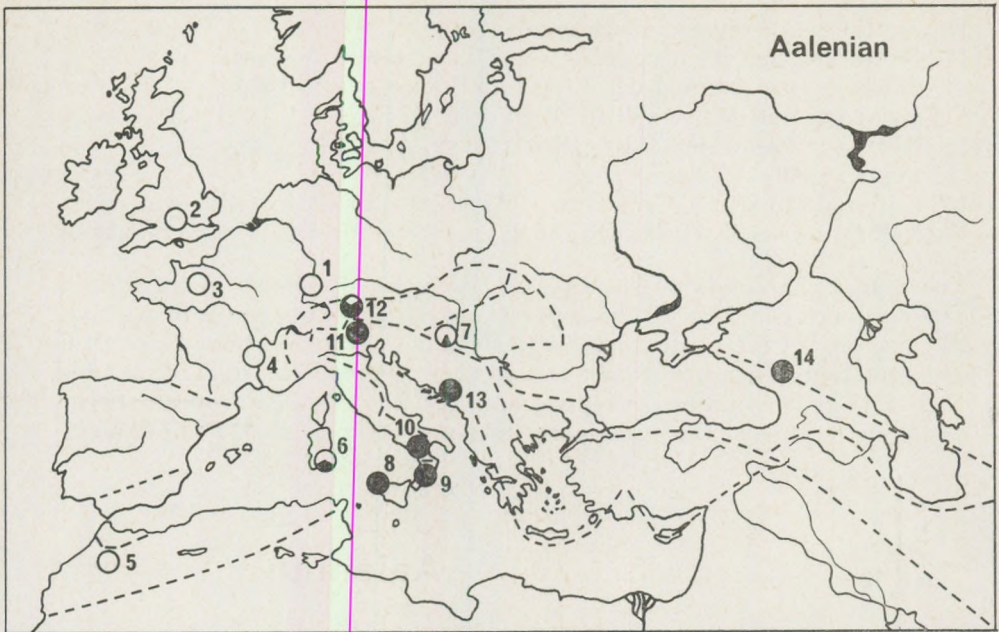


Fig. 6. Geographical distribution of Aalenian faunas. Legend: same as in Fig. 2

cking in the distinctly Mediterranean faunas (Nos. 8 to 11, 13, 14) are *Pseudoglossothyris curvifrons* and *Epithyris submaxillata*. Characteristic Mediterranean species (appearance in at least three distinctly Mediterranean faunas and lack in the distinctly European ones): *Pseudogibbirhynchia vigili*, *P. erycina*, *Parvirhynchia ximenesi*, *P. waehneri*, and *Zeilleria ippolitae*. The geographical distribution of the Aalenian faunas are shown in Fig. 6. Despite the relatively few data, the Mediterranean province can be outlined distinctly, only the interpretation of the Caucasian occurrence meets some difficulties.

Bajocian

The comparison below refers to the upper part of the Bajocian (Humphriesianum to Parkinsoni Zones), with 18 faunas of 241 species altogether.

- | | |
|-----------------------------------------------------------------------------|------------|
| 1. NW Caucasus (KAMYSHAN and BABANOVA, 1973) | 17 species |
| 2. South Germany (QUENSTEDT, 1858, 1868 – 71; KUHN, 1938; SEIFERT, 1963) | 41 species |
| 3. Alsace-Lorraine (HAAS and PETRI, 1882) | 16 species |
| 4. Jura Mts. (HAAS, 1889; GREPPIN, 1900; CONTINI and ROLLET, 1970) | 20 species |
| 5. Rhône-area (ARCELIN and ROCHÉ, 1936; MARZLOFF et al., 1936; ROCHÉ, 1939) | 63 species |
| 6. England (DAVIDSON, 1878) | 63 species |
| 7. Portugal (CHOFFAT, 1947) | 15 species |

8. Morocco (Moyen Atlas) (ROUSSELLE, 1965)	19 species
9. Váh-valley (PEVNY, 1969)	9 species
10. Eastern Carpathians (JEKELIUS, 1916; TURCOULET, 1971; PREDÁ, 1976)	11 species
11. Southern Carpathians (JORDAN, 1966)	18 species
12. Balkan Mts. (TCHOUMATCHENKO, 1978)	8 species
13. Somalia (Jubaland) (WEIR, 1929)	11 species
14. Western Sicily (GEMMELLARO, 1877)	5 species
15. Southern Alps (OPPEL, 1863; PARONA, 1880, 1896; BÖSE and FINKELSTEIN, 1892; POINTINGHER, 1959; FERRARI and MANARA, 1972)	23 species
16. Northern Calcareous Alps (OPPEL, 1863; ROTHPLETZ, 1886)	17 species
17. NW Carpathians (PEVNY, 1964; SIBLÍK, 1966)	11 species
18. Bakony Mts. (Vörös, unpubl.)	15 species

Representative type faunas for the European and Mediterranean provinces are those of South Germany and the Southern Alps, respectively. The characteristics of the Bajocian faunas are plotted in the system of co-ordinates in Fig. 7. The separation is extremely significant: all the points

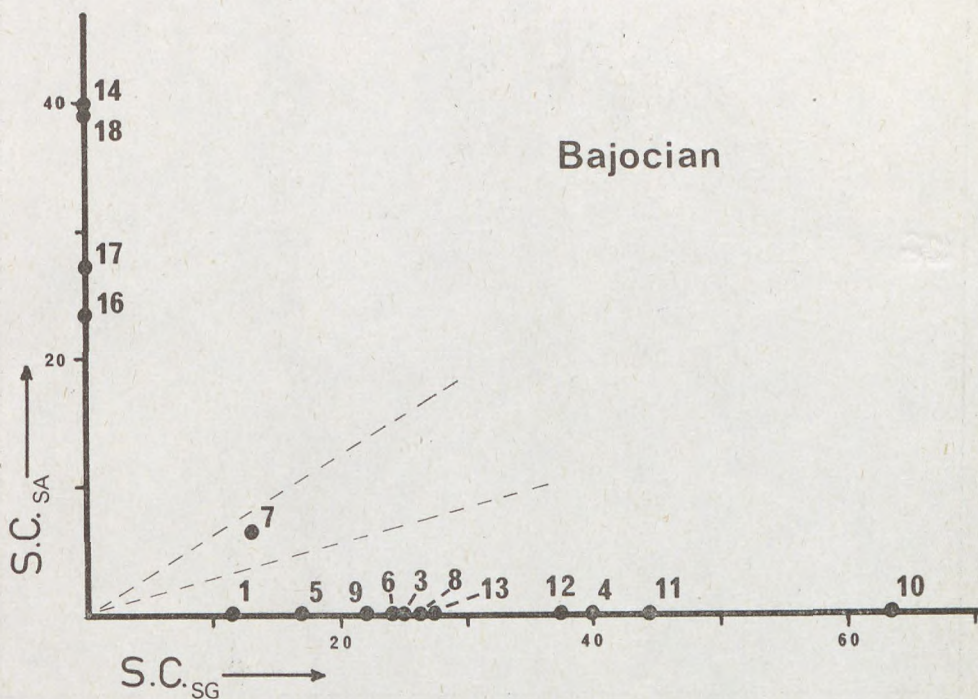


Fig. 7. Simpson-coefficient values of Bajocian faunas compared with the South German (horizontal axis) and the South Alpine (vertical axis) faunas, respectively

representing the faunas except No. 7 (Portugal), are assembled along the axes. It is remarkable that the Somalian fauna (No. 13) has no Mediterranean features, but shows European affinities. Characteristic European species, with occurrences in at least five distinctly European faunas, are as follows: *Cymatorhynchia quadriplicata*, *Acanthothyris spinosa*, *Lobothyris perovalis*, *Tubithyris globata*, *Epithyris maxillata*, *Monsardithyris ventricosa* and *Aulacothyris carinata*. Characteristic Mediterranean species, which occur in at least three Mediterranean faunas: *Apringia? atla*, *Striirhynchia? subechinata*, "*Rhynchcnella*" *berchta*, "*Terebratula*" *fylogia* and *Placothyris gerda*. The geographical distribution of the Bajocian faunas is shown in Fig. 8. Noteworthy are the occurrence of some characteristic European species at the Jordan River (MUIR—WOOD, 1925) and in Eritrea (DIAZ—ROMERO, 1931), associated with some species, which appear

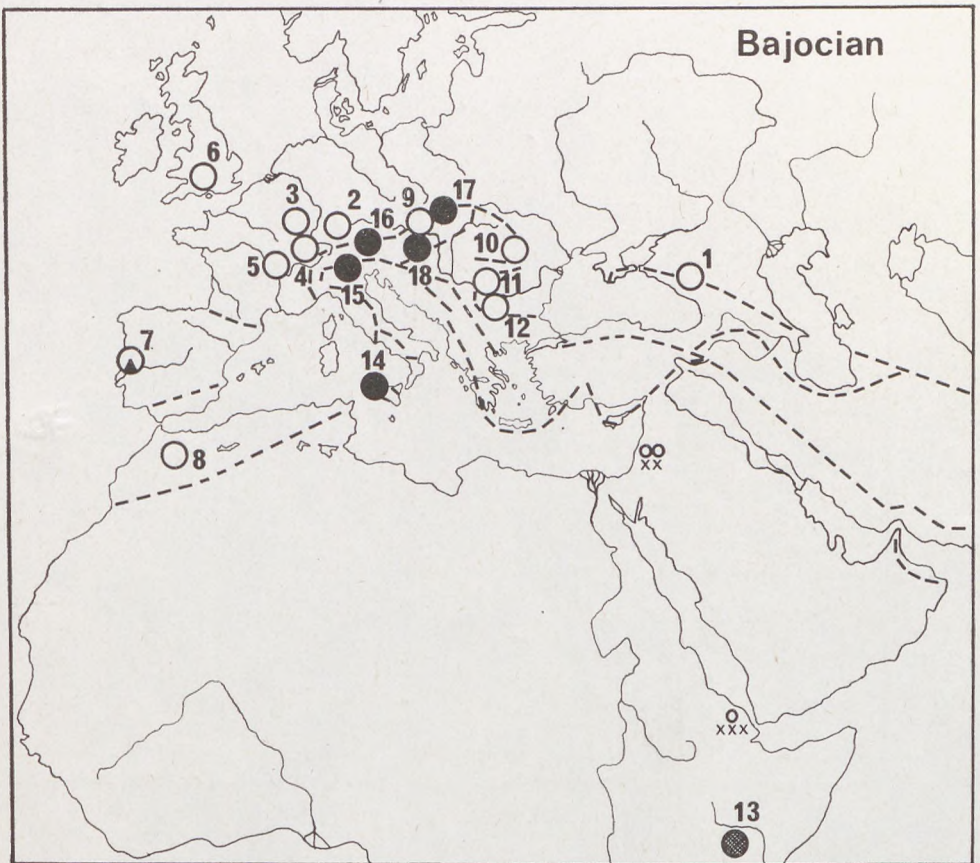


Fig. 8. Geographical distribution of Bajocian faunas. Legend: same as in Fig. 2. and: cross-hatched circles: faunas of Ethiopian character; x: characteristic Ethiopian species

also in Somalia. Taking these facts into consideration, an Ethiopian province of strong European influence can be outlined. The Mediterranean province is markedly delimited from the European one the only disturbing element is the Váh-valley occurrence (No. 9).

Callovian

This comparison is based on 17 faunas with 222 species, mainly Lower Callovian in age.

- | | |
|-----------------------------------------------------------------------------------------------------|------------|
| 1. Turkmenia (MOISEIEV, 1944; PROZOROVSKAYA, 1968) | 24 species |
| 2. Northern Caucasus (NEUMAYR and UHLIG, 1892; MOISEIEV, 1934) | 23 species |
| 3. Crimea (MOISEIEV, 1934; BABANOVA, 1964; KAMYSHAN and BABANOVA, 1973) | 38 species |
| 4. Russian platform (LAHUSEN, 1883; MAKRIDIN, 1964) | 20 species |
| 5. Silesia (Balin) (SZAJNOCHA, 1879) | 24 species |
| 6. South Germany and Alsace-Lorraine (QUENSTEDT, 1858, 1868-71; HAAS and PETRI, 1882; CORROY, 1932) | 55 species |
| 7. NW France (DESLONGCHAMPS, 1859a; 1860; GROSSOUVRE, 1891; BIZET, 1894; COUFFON, 1919) | 48 species |
| 8. England (DAVIDSON, 1978) | 19 species |
| 9. Portugal (CHOFFAT, 1947) | 10 species |
| 10. Southern France (DESLONGCHAMPS, 1859b; PARONA and BONARELLI, 1897) | 8 species |
| 11. Mecsek and Villány Mts. (VADÁSZ, 1935; VÖRÖS, unpubl.) | 13 species |
| 12. Tunisia and Lybia (DESIO et al., 1960; DUBAR, 1967) | 16 species |
| 13. Ethiopia and Somalia (DOUVILLÉ, 1886; DIAZ-ROMERO, 1931; MUIR-WOOD, 1935) | 25 species |
| 14. Northern India (NOETLING, 1985; MUIR-WOOD, 1937) | 5 species |
| 15. Northern Calcareous Alps (OPPEL, 1861; ROTHPLETZ, 1886; KUNZ, 1967) | 12 species |
| 16. NW Carpathians (UHLIG, 1881; KSIĄZKIEWICZ, 1956) | 9 species |
| 17. Southern Carpathians (Rucar) (SIMIONESCU, 1899) | 7 species |

The type fauna of the European province is the combined data of South Germany and Alsace-Lorraine, while the type fauna of the Mediterranean province is that of the Northern Calcareous Alps. As a type fauna of the Ethiopian province, individualized for this age, the combined Ethiopian and Somalian fauna appeared sufficient. The features of the Callovian faunas are shown in Fig. 9. The European and Mediterranean provinces show an almost continuous transition. It is striking that significant Mediterranean affinities are shown by the faunas of No. 10 (Southern France) and No. 11 (Mecsek and Villány Mts.), which can be related to the European shelf by other paleogeographic criteria. It is interesting that the three faunas representing the Ethiopian province do not show Mediterranean influence, but two of them (i.e. Nos. 12 and 14) have some European

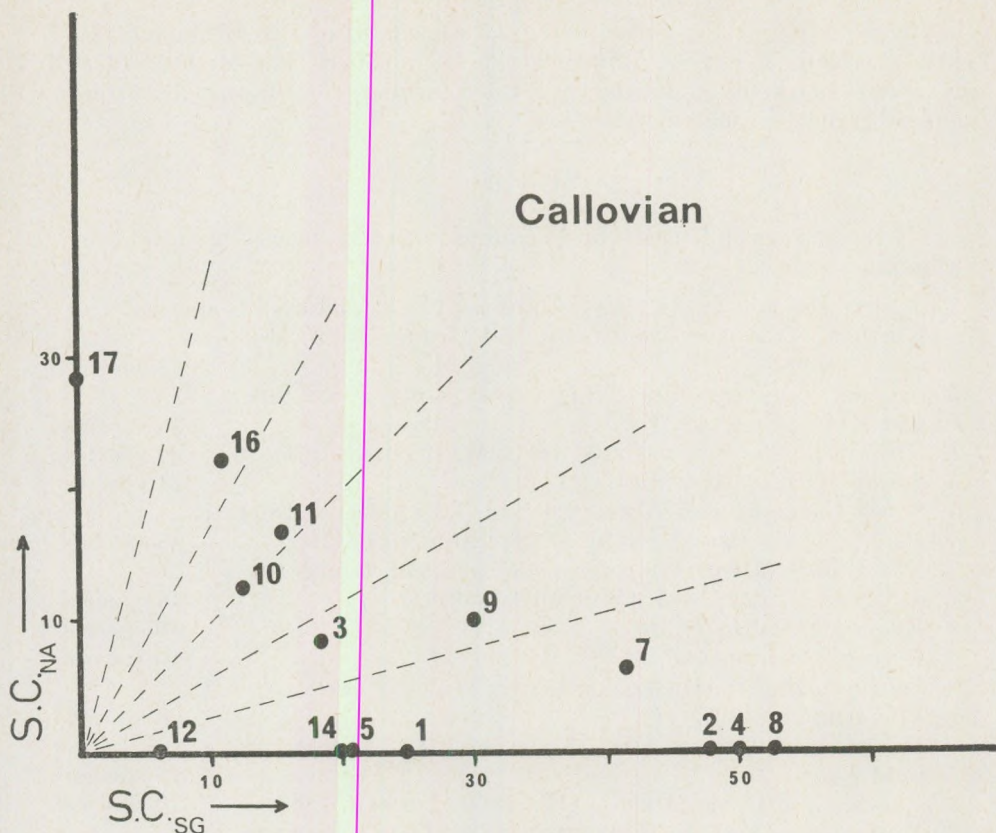


Fig. 9. Simpson-coefficient values of Callovian faunas compared with the South German (horizontal axis) and the North Alpine (vertical axis) faunas, respectively

character. Characteristic European species, which occur in at least five distinctly European faunas (Nos. 1, 2, 4 to 8) and lack in the Mediterranean (Nos. 15 to 17) or the Ethiopian (Nos. 12 to 14) faunas, are: *Ivanoviella alemanica*, *Rhynchonelloidella varians*, *Goniothyris? eggensis*, *Ptyctothyris dorsoplicata*, *P. subcanaliculata*, *Aulacothyris pala* and *Ornithella lagenalis*. Characteristic Ethiopian species, occurring in at least two Ethiopian faunas and lacking in the other two provinces: *Burmihynchia parva*, *B. weiri*, *Daghanirhynchia subversabilis*, *Pseudoglossothyris sulcata*, "*Terebratula*" *subsella*. Characteristic Mediterranean species (with occurrences in at least two Mediterranean faunas and lacking in the two other provinces): *Calvirhynchia contraversa*, *Septocrurella? defluxoides*. The geographical distribution of the Callovian faunas is shown in Fig. 10. Not surprising are the occurrences of the characteristic *Rhynchonelloidella varians* and *Ptyctothyris dorsoplicata* in the Baltic area (KRENKEL, 1915; STOLL, 1934), and *Daghanirhynchia daghaniensis* in the Sinai (DOUVILLÉ, 1916). In some faunas of

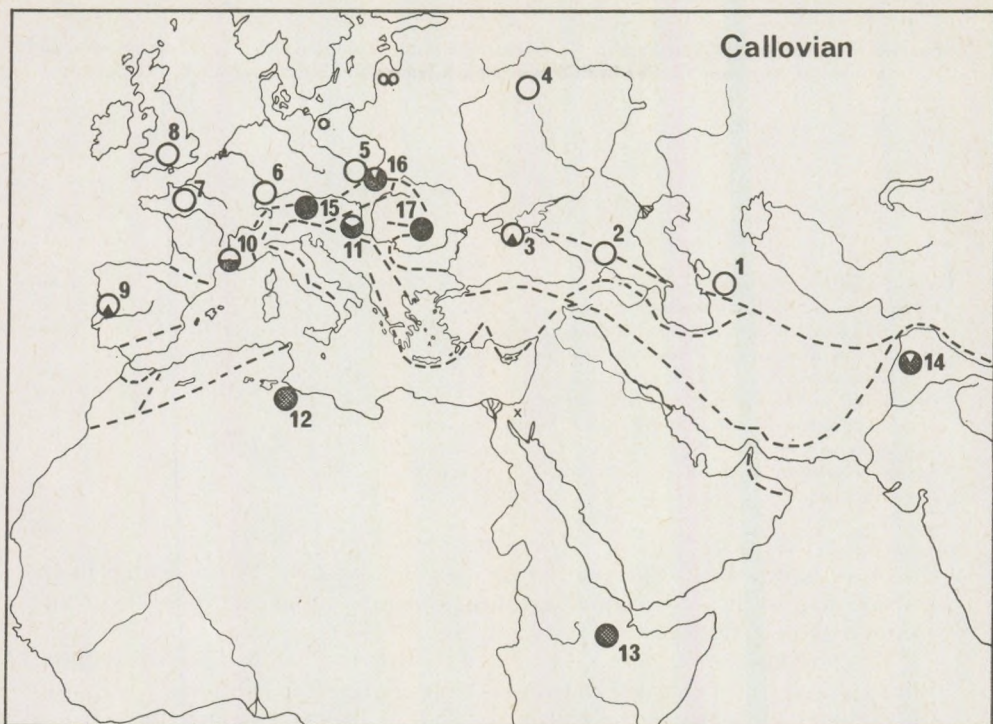


Fig. 10. Geographical distribution of Callovian faunas. Legend: same as in Figs 2. and 8

the European province (Nos. 3, 9, 10, 11) strong Mediterranean influence appears. Extremely peculiar is the occurrence of a clearly Mediterranean fauna in the Southern Carpathians (No. 17), a range all tectonic units of which showed European characters during the previous Jurassic intervals.

Temporal changes in provinciality

The European, Mediterranean and (in the Callovian) the Ethiopian brachiopod provinces distinguished above by numerical methods as individual faunistic units, can be compared to each other, too. The quantitative data of the provinces are tabulated in Table I.

In the Sinemurian and the Pliensbachian species number increases in both the European and the Mediterranean provinces. Following the Aalenian minimum, species number in the European province regains high values, while in the Mediterranean areas the drastic decrease in species number continues through the Bajocian and Callovian. Undoubtedly, the actual turnover took place in the Toarcian, when the whole western Tethys underwent significant paleogeographic changes. These were probably connected to the start of the opening of the Atlantic ocean. It is striking, on

Table I.

Species numbers of the European, Mediterranean and Ethiopian brachiopod provinces and numbers of common species in different stages from the Sinemurian to the Callovian

	Sinemurian	Pliensbachian	Aalenian	Bajocian	Callovian
Total number of counted species	243	306	171	241	222
Occurring in the European province	114	167	66	191	170
Occurring in the Mediterranean province	156	184	113	59	24
Species common to the European and Mediterranean provinces	27	45	8	6	8
Occurring in the Ethiopian province	—	—	—	—	39
Species common to the Ethiopian and Mediterranean provinces	—	—	—	—	—
Species common to the Ethiopian and European provinces	—	—	—	—	2

the other hand, that while this "crisis" was gotten over by the faunas of the European province by Bajocian times, the fall of the Mediterranean brachiopod fauna went on.

Fig. 11 shows the Simpson- and Jaccard-coefficient values calculated from the data in Table I. Continuous lines figure the temporal changes in the similarities between the European and Mediterranean provinces, based on the values of the two coefficients. It is clear that the similarity is closest in the Pliensbachian and Callovian, while the minimum (i.e. the maximum of the provinciality) is shown in the Aalenian and Bajocian. Remarkable is that provinciality was higher in the Sinemurian than in the Pliensbachian. If the difference between the European and Mediterranean provinces had been formed only at the beginning of the Jurassic, the Sinemurian would have shown still high similarity values. However, as the differences appear great even in this time, one has to suppose the timing of the individualization of the Mediterranean province as considerably earlier (probably the Middle Triassic, VÖRÖS, 1977). The similarity between the European and the Ethiopian provinces (in the Callovian) is low, considerably lower than that between the European and the Mediterranean one. The high degree of endemism and the strong isolation of the Ethiopian province is emphasized by the fact that it shows no connections and similarities to the Mediterranean province.

Factors resulting in provinciality

As a starting point to this discussion, one can take the paleogeographic pattern which shows the Jurassic Tethys as a large "V"-shaped ocean open to the East and closed in the West. This ocean was bordered on both the Eurasian and the African (Gondwanian) continental sides by extended

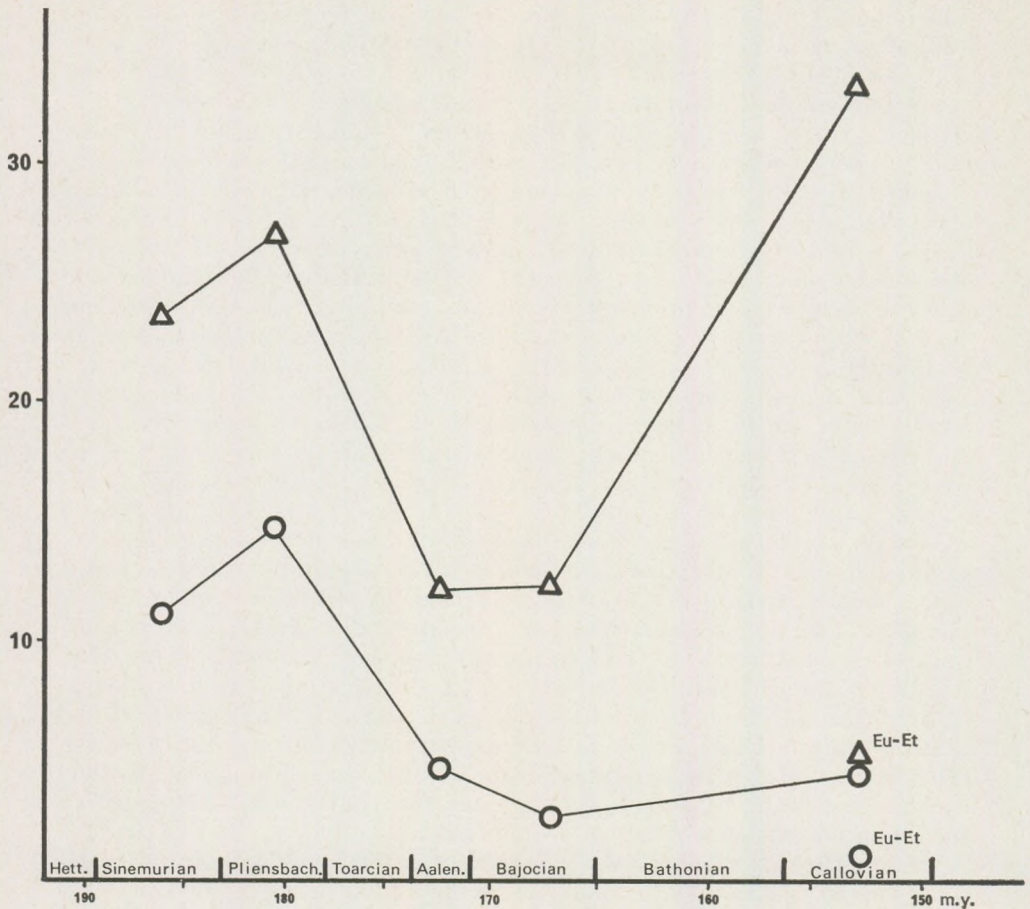


Fig. 11. Changes in similarity between the European and the Mediterranean brachiopod provinces from the Sinemurian to the Callovian. Triangles: Simpson-coefficient values; Circles: Jaccard-coefficient values; Eu-Et: coefficient values of similarity between the European and Ethiopian provinces

shelves. The sediments of the continent-ward sides of these shelves can be found now in stable European (or African) areas, with characteristic European (or Ethiopian) brachiopods. Controversial is the former geographical position of the Mediterranean province.

AGER (1967) regarded the Mediterranean province as a "bathyal" province, which means a habitat of the Mediterranean brachiopods on the outer, or deeply-sunken part of the European shelf. On the other hand, this view should be revised, because the bottom of the Mediterranean Jurassic sea was rather disintegrated, thus cannot be regarded as generally bathyal (GALÁCZ and VÖRÖS, 1972; BERNOULLI and JENKYN, 1974). The crinoidal and "Hierlatz" limestones, which yield the most abundant Me-

diterranean brachiopod faunas, were derived just from the current-swept shallow-water ridges rising above the deeper-water basins (VÖRÖS, 1975).

AGER, in his later work (1971) pointed out that in the views of researchers about the factors controlling the geographical distribution of brachiopods, three "schools" can be distinguished; those are based on 1. barriers, 2. depth-control, 3. bottom types, AGER emphasized that he was attached to the believers of the bottom-types, and that the distribution of brachiopods is environmentally controlled. According to my views, one cannot originate the Mediterranean provinciality from the differences of the sea bottom types. Nearly the same Mediterranean brachiopods do occur in relatively deep-water carbonate mud, in shallower-water calcareous sands and in extremely shallow, Bahama-type carbonates, i.e. in all Mediterranean sedimentary rocks. Within the parautochthonous sedimentary cover-series of the NW Carpathian core mountains and in the Križna nappe, there are Pliensbachian successions with dark to black limestones and rich in terrigenous clastics, which are lithologically very similar to the contemporaneous series of the European shelf, and these also yield Mediterranean brachiopods.

HALLAM (1971, 1972), on the basis of studies on bethonic groups beside brachiopods, concluded that faunal provinces may originate on continuous shelves without barriers too, as a result of certain factors (e.g. temperature, nutrient-supply, environmental stability). This model can be applied reasonably well to the interpretation of the differences between the Ethiopian and European provinces, because these were found on an originally continuous shelf several thousand kilometres long, and with established migrational faunal connections (AGER and WALLEY, 1977). On the other hand, this cannot be applied in the case of the European - Mediterranean provinciality, because here neither the continuous shelf-area, nor the direct faunal connection can be evidenced.

GÉCZY (1972) was the first to formulate a theory explaining the differentiation of the Jurassic ammonite provinces by intervening wide oceanic regions. This "barrierist" view was followed in a hypothesis (VÖRÖS, 1977), in which the habitat of the Mediterranean-type Jurassic brachiopods was outlined as a submarine ridge (microcontinent) of continental basement somewhere in the open Tethys, far off the European and African shelves. This isolated microcontinent might have produced favourable conditions for the origin of a brachiopod province, even in the sense of AGER (1971). The brachiopods of this initially especially shallow-water ridge were unable to invade the surrounding ocean floor several thousand metres in depth and in this sense, their distribution and differentiation was environmentally controlled. Being sessile organisms, they had no faunal connections with the European shelf, because their larvae could not reach there. According to RUDWICK (1970), the planktonic period of the larvae of articulate brachiopods is very short, only some hours, or occasionally some days. Within this short interval, even for a 100 to 200 km travel one should suppose such rapid ocean currents which are impossible to assume for the Tethys, a westerly closed ocean in the Jurassic of temperate climate. What remained

were the driftwood and floating algae, which might have contributed to the dispersal of adult forms, but these made possible only actual, sporadic connections. The reduced nutrient-supply suggested by HALLAM (1971) as characteristic in the Mediterranean, is consistent with this explanation (i.e. with the removal from the continental nutrient sources). The Mediterranean brachiopods show many phylogenetically archaic features, e.g. the predominance of the superfamily Dimerellacea (AGER et al., 1972), brachidium support (VÖRÖS, 1978). These features can be explained by supposing that in the oceanic microcontinent (submarine ridges) the environment was more stable than that on the European and African shelves, favouring the endurance or re-appearance of archaic characters.

Conclusively: the European-Ethiopian provinciality is a result of spatially continuous variation in the environmental conditions along a shelf area of several thousand kilometres, while the European – Mediterranean provinciality was caused by deep-sea and oceanic barriers.

Paleogeographic position of the Jurassic brachiopod provinces of the western Tethys

The maps in Figs. 12, 13 and 14 show a possible paleogeographical pattern — as a very rough sketch. The maps are based on data from the work of DEWEY et al. (1973) for the position and Jurassic movement of the continents, and from the book of HALLAM (1975) for the shore-lines (islands disregarded). The shape and position of the microcontinent within the Tethys is drawn arbitrarily, thus may arise further discussions and considerations, while its extent is so large to embrace at least its present-known fragments, i.e. the Periadriatic region, the Austroalpine units, the northern part of the intra-Carpathian region, the Rif-Betic mass and some other fragments lying along the Pontian-Crimean-Caucasian range. This reconstruction leaves the Anatolian and Iranian microcontinent out of considerations; these were probably out of the maps' area in the Jurassic. The symbols marking the composition of the brachiopod faunas are — except some cases — placed into their plate-tectonically re-arranged sites. Because of difficulties in the faunistical and tectonical interpretation, these paleogeographic maps do not show some faunas in the Saharan Atlas, Anatolia and the Carpathians and the Caucasus (7 data).

Combined Sinemurian and Pliensbachian data are shown in Fig. 12. The European faunas are arranged within the European epicontinental sea; those which were near to the outer shelf margin show some Mediterranean influence. Marked Mediterranean influence is shown by the Calabrian and West-Sicilian Sinemurian faunas on the northern end of the Mediterranean microcontinent. There are no evaluable data on the Gondwanian shelf.

Distributional pattern of the early Middle Jurassic (Aalenian and Bajocian) is illustrated in Fig. 13. The Atlantic lies partially open, and this oceanic belt probably connected the western end of the Atlantic to the proto-Pacific, making deep-circulations possible. The opening Atlantic

Sinemurian + Pliensbachian

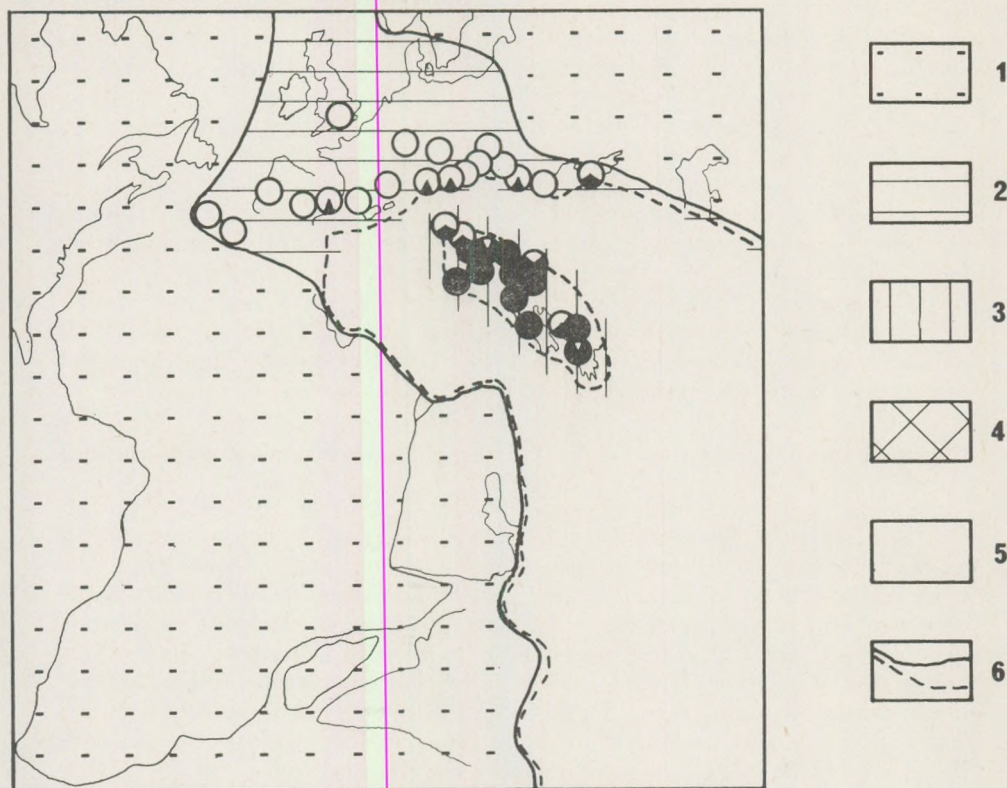


Fig. 12. Palaeogeographical distribution of Sinemurian and Pliensbachian brachiopod faunas. Legend: 1. Land; 2–4. shelf and epicontinental seas (2. European province, 3. Mediterranean province, 4. Ethiopian province); 5. oceanic Tethys; 6. shore-line and shelf-edge. For legend to the faunistical symbols, see Figs 2. and 8. Position of continents after Dewey et al. (1973), shore lines after Hallam (1975)

disconnected the European and African shelves, leaving the Moroccan and Oranian mesetas of the Central Atlas at the European side (the present interpretation expects so, because the brachiopod faunas give such evidences). The connections between the European and Mediterranean provinces fell to minimal. In the Gondwanian epicontinental sea, many endemic, "Ethiopian" elements occur, associated with European species.

During Callovian times (Fig. 14.) the Atlantic got wider, and the Eurasian and Gondwanian epicontinental seas overflowed vast areas. The life conditions of the Mediterranean brachiopods seemed to become unfavourable; relatively rich faunas are known only from the Northern Alps and the Carpathians. Greater part of the European province is rather uniform, but some faunas near the shelf margin (e.g. Crimea, Villány,

Aalenian + Bajocian

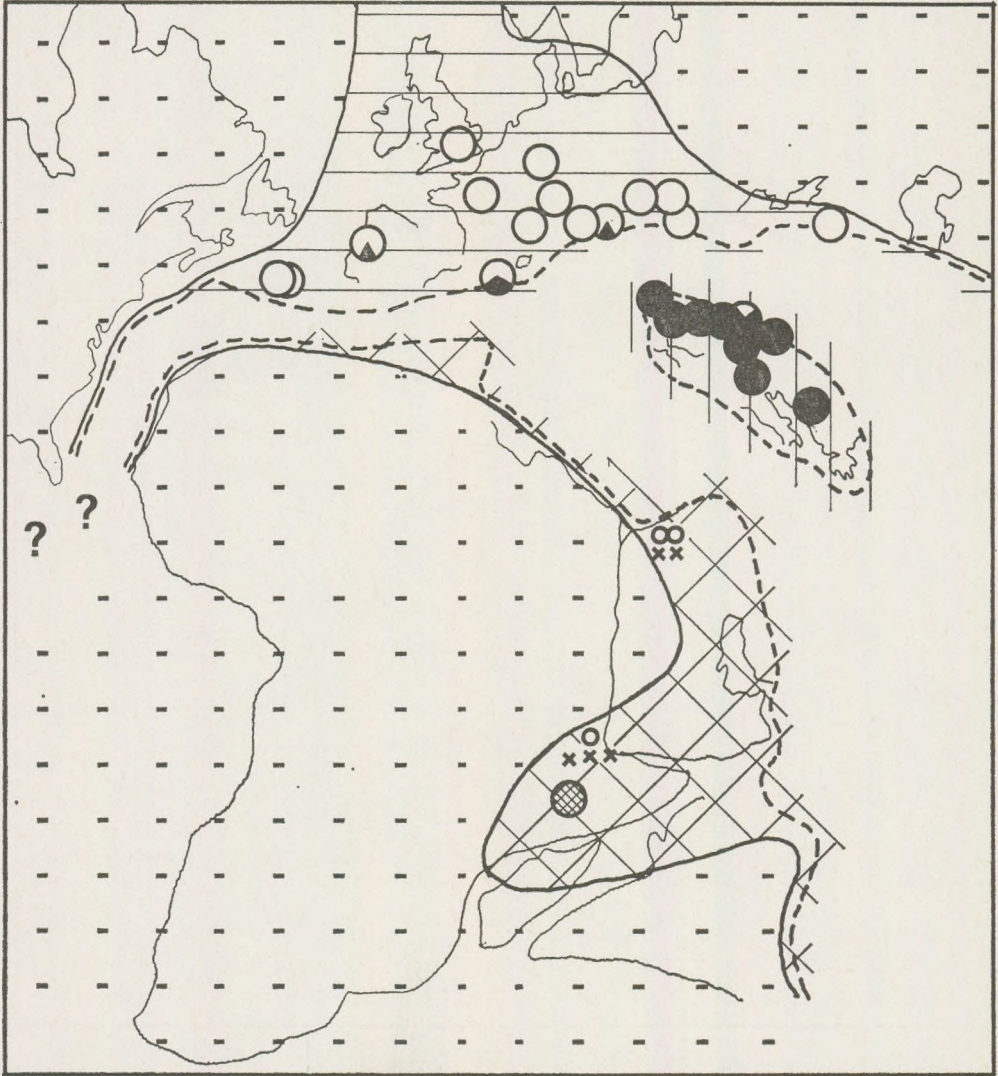


Fig. 13. Palaeogeographical distribution of Aalenian and Bajocian brachiopod faunas.
Legend: same as in Fig. 12

Provence) show marked Mediterranean influence. It was probably caused by the reinforced circulation which promoted the dispersal, and also by the fact that in the Callovian, with the continent-ward moving of the shore-lines, the environmental circumstances became more pelagic on the

Callovian

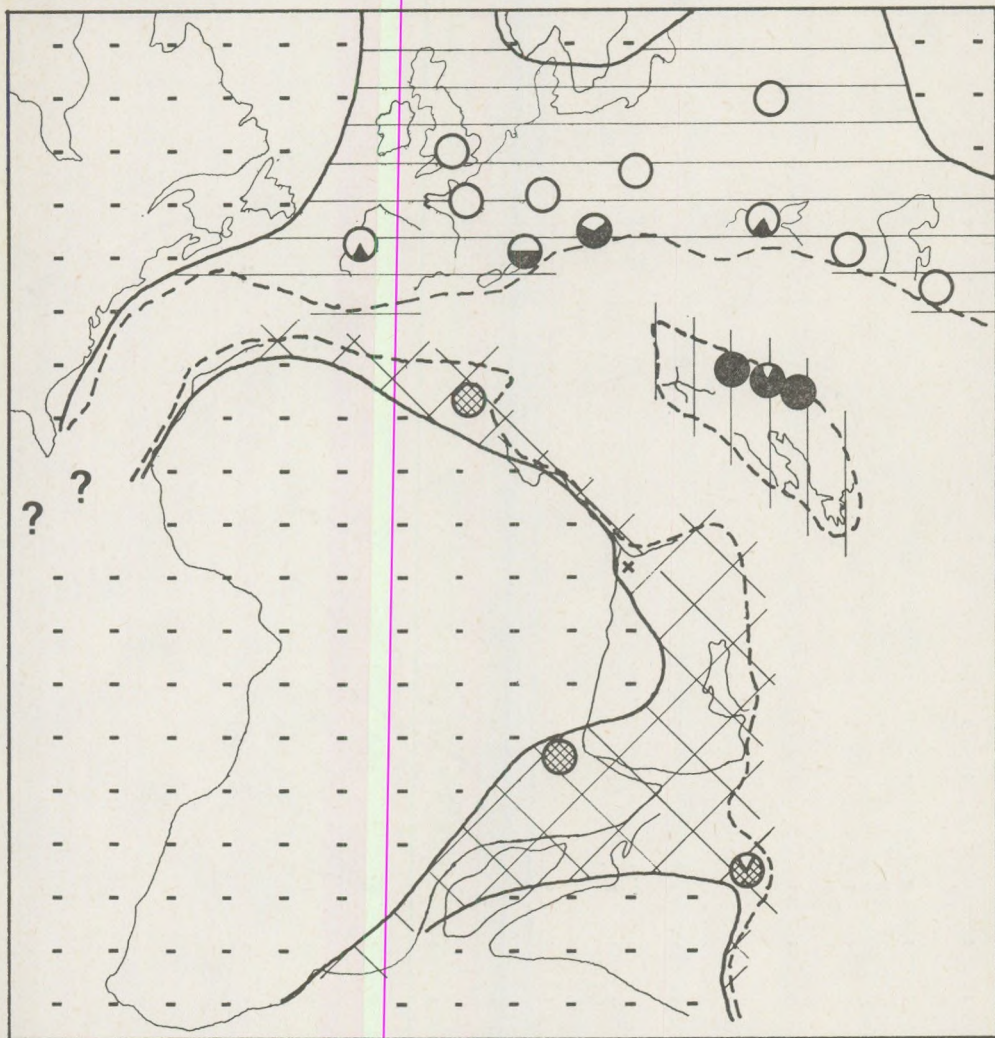


Fig. 14. Palaeogeographical distribution of Callovian brachiopod faunas. Legend: same as in Fig. 12

European shelf margins (appearance of Paleotrix-bearing and radiolarian rock facies). The Gondwana shelves are characterized by the Ethiopian province from Tunisia to India, with still remaining migrational connections with the European province. Connection between the Mediterranean and Ethiopian provinces cannot be proved.

* * *

In the Jurassic three brachiopod provinces were formed within the western Tethys. Their differentiation and individualization became possible partly by the adaptational possibilities in growing epicontinental sea areas, and partly by the isolation connected to widening oceanic barriers. At the same time, this was the last flourishing of the Brachiopoda phylum, which was ended by the closure of the Tethyan ocean in the Late Cretaceous.

REFERENCES

- AGER, D. V. (1967): Some Mesozoic brachiopods in the Tethys region. Syst. Assoc. Publ., No. 7. (Aspects of Tethyan biogeography), pp. 135–151.
- AGER, D. V. (1971): Space and time in brachiopod history. In: Middlemiss, F. A., Rawson, P. F., Newall, G. (Eds): Faunal provinces in space and time. Geol. J., No. 4., 95–110.
- AGER, D. V. (1973): Mesozoic Brachiopoda. In: Hallam, A. (Ed.): Atlas of palaeobiogeography. Elsevier., 431–436.
- AGER, D. V., CHILDS, A., PEARSON, D. A. B. (1972): The evolution of the Mesozoic Rhynchonellida. Geobios, 5., 157–235.
- AGER, D. V., WALLEY, C. D. (1977): Mesozoic brachiopod migrations and opening of the North Atlantic. Palaeogeogr., Palaeoclimatol., Palaeoecol., 21., 2., 85–99.
- BERNOULLI, D., JENKYN, H. C. (1974): Alpine, Mediterranean and Central Atlantic Mesozoic facies in relation to the early evolution of the Tethys. In: Dott, R. H., Shaver, R. H. (Eds): Modern and ancient geosynclinal sedimentation. SEPM Spec. Publ. No. 19., 129–160.
- CAMPBELL, C. A., VALENTINE, J. W. (1977): Comparability of modern and ancient marine faunal provinces. Paleobiology, 3., 1., 49–57.
- CHEETHAM, A. H., HAZEL, J. E. (1969): Binary (presence-absence) similarity coefficients. J. Paleont., 43., 5., 1138–1136.
- DELANCE, J.-H. (1972): Problèmes posés par la variation géographique des espèces, leurs implications stratigraphiques. Exemples pris chez les Brachiopodes jurassiques. Mém. B.R.G.M., No. 77., 69–75.
- DEWEY, J. F., PITMAN, W. C., RYAN, W. B. F., BONNIN, J. (1973): Plate tectonics and the evolution of the Alpine system. Geol. Soc. Amer. Bull., 84., 3137–3180.
- DIAZ-ROMERO, V. (1931): Contributo allo studio della fauna giurese della Danalia centrale. Palaeontogr. Ital., 31. (1929–30), 1–61.
- DOUVILLÉ, H. (1916): Les terrains Secondaires dans le Massif du Moghara à l'est de l'isthme de Suez. Mém. Acad. Sci. Fr., Paris, (2), 54.
- FLAMAND, G. M. B. (1911): Recherches géologiques et géographiques sur le Haut-Pays de l'Oranie et sur le Sahara (Algérie et territoires du sud). Thèses Fac. Sci. Univ. Lyon, No. 47.
- GALÁCZ A., VÖRÖS A. (1972): Jurassic history of the Bakony-Mountains and interpretation of principal lithological phenomena — Földt. Közl., 102, 2, pp. 122–135.
- GÉCZY B. (1972): A jura faunaprovinciák kialakulása és a mediterrán lemeztektonika. MTA X. Oszt. Közl., 5., 297–311.
- GÉCZY B. (1974): Lemeztektonika és paleontológia. Литовая тектоника и палеонтология — Földtani Kutatás, 17, 3, pp. 17–21.
- HALLAM, A. (1971): Provinciality in Jurassic faunas in relation to facies and palaeogeography. In: Middlemiss F. A., Rawson, P. F., Newall, G. (Eds): Faunal provinces in space and time. Geol. J., No. 4., 129–152.
- HALLAM, A. (1972): Diversity and density characteristics of Pliensbachian-Toarcian molluscan and brachiopod faunas of the North Atlantic margins. Lethaia, 5., 389–412.
- HALLAM, A. (1975): Jurassic environments. Cambridge, 269 p.
- JEKELIUS E. (1915): Die mesozoischen Faunen der Berge von Brassó. I–II. M. Kir. Földt. Int. Évk. 23. pp. 25–135.
- KILLAN, W. (1889): Études paléontologiques sur les terrains secondaires et tertiaires de l'Andalousie. Mém. Acad. Sci. Inst. Nat. France, 30., 2., 651–739.
- KRENKEL, E. (1915): Die Kellowayfauna von Popilani in Westrußland. Palaeontographica, 61.
- LANQUINE, A. (1929): Le Lias et le Jurassique des Chaines Provençales. I. Le Lias et le Jurassique inférieur. Bull. Serv. Carte Géol. Fr., 32., No. 173., 385 p.
- MAHEL, M. (1953): Geologie des Gebirges Stratenská Hornatina. Geol. Práce (Bratislava), 48 b., 176 p.
- MUIR-WOOD, H. M. (1926): Jurassic brachiopoda from the Jordan Valley. Ann. Mag. Nat. Hist. London, (9), 15. 181–192.
- ROUSSELLE, L. (1975): Distribution verticale des rhynchonelles dans le Domérien et le Toarcien en Espagne (Chaîne Celtibérique Orientale, Catalogne Méridionale), au Maroc (Préfrif, Moyen Atlas, Région d'Oujda) et en Algérie Occidentale. Bull. Soc. géol. Fr., (7), 17., 878–885.
- RUDWICK, M. J. S. (1970): Living and fossil Brachiopods. London, 199 p.
- STOLL, E. (1934): Die Brachiopoden und Mollusken der pommerschen Doggergeschiebe. Abh. geol. pal. Inst. Greifsw. 13., 1–62.
- TROEDSSON, G. (1951): On the Högnas Series of Sweden (Rhaeto-Lias). Lunds Univ. Arsskr., N. F., Avd. 2., 47. 268 p.
- TURCULET, I. (1971): Cercetări geologice asupra depozitelor jurasice și eocretacee din cuveta Rarău-Breaza. Inst. Geol., Stud. tehn. econ., (J), No. 10., 141 p.
- VÖRÖS A. (1975): Bathymetric distribution of some Mediterranean Lower Jurassic brachiopods (Bakony Mountains, Hungary). Ann. Univ. Sci. Budapest., Sec. Geol., 17. (1973), 279–286.
- VÖRÖS A. (1977): Provinciality of the Mediterranean Lower Jurassic brachiopod fauna: causes and plate-tectonic implications. Palaeogeogr., Palaeoclimatol., Palaeoecol., 21., 1., 1–16.
- VÖRÖS A. (1978): Viallithyris gen. n. (Terebratulida, Brachiopoda) from the Mediterranean Lower Jurassic. Ann. Hist.-nat. Mus. Nat. Hung., 70., 61–63.

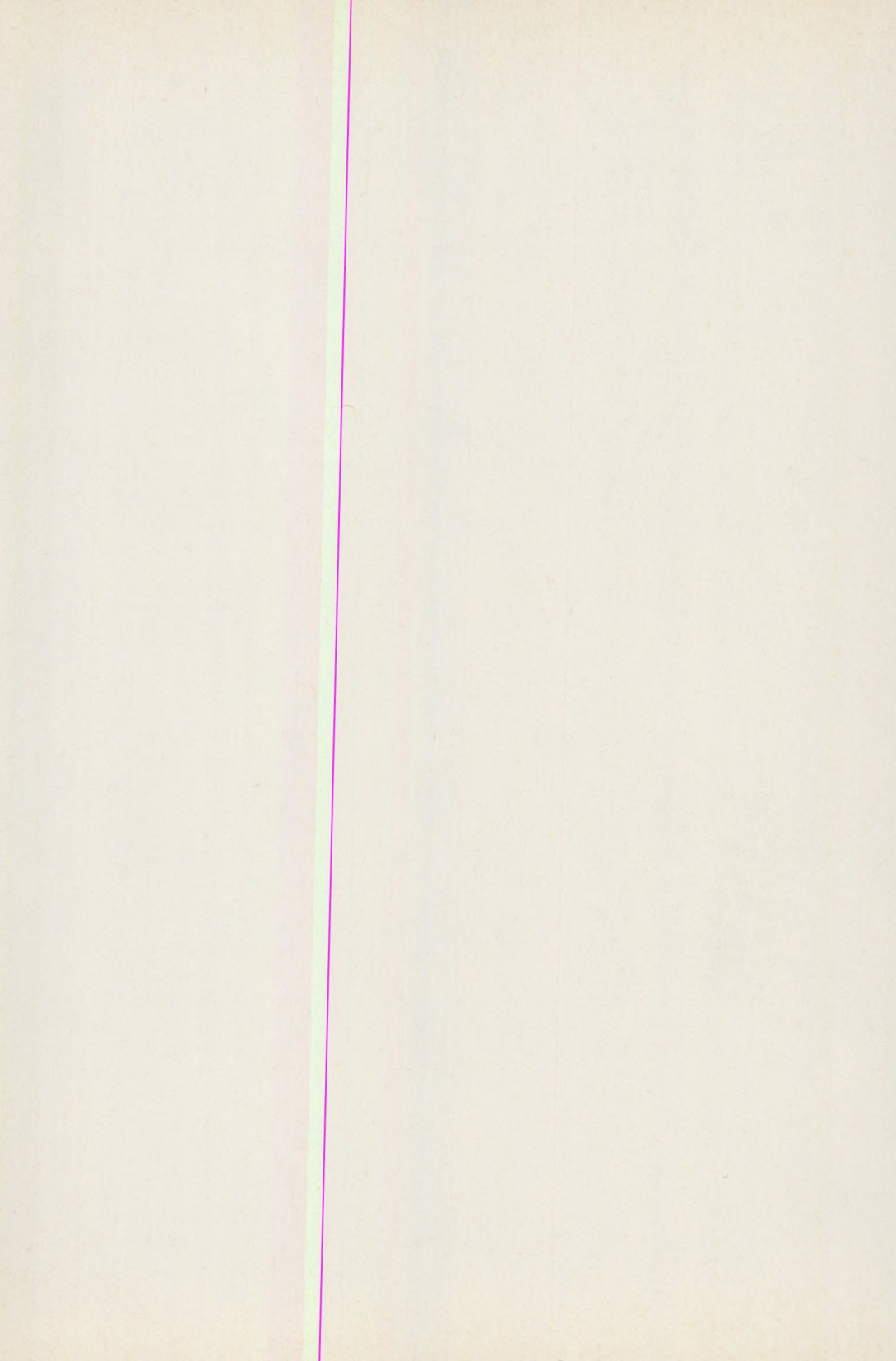
REFERENCES CITED IN THE FAUNISTICAL TABLES

- AGER, D. V. (1956): The geographical distribution of brachiopods in the British Middle Lias. *Quart. J. Geol. Soc. London*, 112., 157—187.
- AGER, D. V. (1959): Lower Jurassic brachiopods from Turkey. *J. Paleontol.*, 33., 6., 1018—1028.
- AGER, D. V. (1956—1967): A monograph of the British Liassic Rhynchonellidae. *Palaeontogr. Soc. London*, 1—172.
- AGER, D. V., CALLOMON, J. H. (1971): On the Liassic age of the "Bathonian" of Villány (Baranya). *Ann. Univ. Sci. Budapest., Sec. Geol.*, 14., 5—16.
- ARCELIN, F., ROCHÉ, P. (1936): Les brachiopodes bajociens du Monsard. *Trav. Lab. géol. Fac. Sci. Lyon*, 30., 1—107.
- БАБАНОВА, Л. И. (1964): Новые данные о юрских брахиоподах. *Палеонт. Журн.* 1964, 1. pp. 63—70.
- BITTNER, A. (1895): Ueber die Gattung *Rhynchonellina* Gemm. *Jb. k. k. geol. Reichsanst.*, 44., 547—572.
- BIZET, P. (1894): Note sur les limites du terrain Callovien dans le Nord-Ouest de la France. *Bull. Soc. Géol. Normandie*, 16. (1892—93), 79—119.
- BÖCKH J. (1874): Die geologischen Verhältnisse des südlichen Teiles des Bakony. II. *M. Kir. Földt. Int. Évk.*, 3, pp. 1—180.
- BÖSE, E. (1898): Die mittelliasische Brachiopodenfauna der östlichen Nordalpen. *Nebst einem Anhang über die Fauna des unteren Dogger in bayerischen Innthal.* *Palaeontographica*, 44., 145—236.
- BÖSE, E., FINKELSTERN, H. (1892): Die mitteljurassischen Brachiopoden-Schichten bei Castel Tesino im östlichen Südtirol. *Zeitschr. deutsch. geol. Ges.*, 44., 2., 265—302.
- BÖSE, E., SCHLOSSER, M. (1900): Über die mittelliasische Brachiopodenfauna von Südtirol. *Palaeontographica*, 46., 175—212.
- BRANCO, W. (1879): Der untere Dogger Deutsch-Lothringens. *Abh. geol. Spez. karte Elsass-Lothr.*, 2., 1., 1—160.
- CANAVARI, M. (1879): Sui fossili del Lias inferiore nell'Appennino centrale. *Atti Soc. Tosc. Nat.*, 4., 2., 141—172.
- CANAVARI, M. (1880): I Brachiopodi degli Strati à *Terebratula Aspasia* Mgh. nell'Appennino Centrale. *Atti R. Accad. Lincei* (3), *Mem. Cl. Sci. Fis. Mat. Nat.*, 8., 329—360.
- CANAVARI, M. (1881): Alcuni nuovi Brachiopodi degli Strati à *Terebratula Aspasia* Mgh. nell'Appennino Centrale. *Atti Soc. tosc. Sci. nat.*, *Mem.*, 5., 1., 177—188.
- CANAVARI, M. (1882): Beiträge zur Fauna des unteren Lias von Spezia. *Palaeontographica*, 29., 125—192.
- CANAVARI, M. (1883): Contribuzione III alla conoscenza dei Brachiopodi degli Strati à *Terebratula Aspasia* Mgh. nell'Appennino Centrale. *Atti Soc. tosc. Sci. nat.*, *Mem.*, 6., 1., 70—110.
- CHOFFAT, P. (1947): Description de la faune jurassique du Portugal. *Brachiopodes. Serv. Geol. Portugal*, 1—46.
- ČIRIČ, B. (1949): Brachiopodi srednjeg lijsa sa Lovčena (Crna Gora). *Glasn. prirod. Muz. Szrpszke Zemle*, (A), 2., 159—171.
- CISNEROS, D. J. DE, (1923): La fauna de los estratos de "Pygope *Aspasia*" Menegh. del Liásico medio del Rincón de Egea en el NW de la provincia de Murcia. *Trab. Mus. Nac. Cienc. nat. Madrid, Ser. Geol.*, 30., 1—55.
- COHEN, E. R. (1931): Geologie des Vorkalkan von Tetewen. *Zeitschr. Bulg. Geol. Ges.*, 3., 1., 15—96.
- COMAS-RENGIFO, M. J., GOY, A. (1975): Estratigrafía y Paleontología del Jurásico de Ribarredonda (Guadalajara). *Estud. Geol.*, 31., 3—4., 297—339.
- CONTI, S. (1954): Stratigrafia e paleontologia della Val Solda (Lago di Lugano). *Mem. Descr. Carta Geol. Ital.*, 30., 1—248.
- CONTINI, D., ROLLET, A. (1970): Sur quelques térébratules du Bajocien supérieur et du Bathonien inférieur. *Ann. Sci. Univ. Besancon*, 9. (3), 28—44.
- CORROY, G. (1932): Le Callovien de la bordure orientale du Bassin de Paris. *Mém. carte géol. dét. France*, (1932), 1—337.
- COUFFON, O. (1919): Le Callovien du Châlet, commune de Montreuil-Bellay. *Bull. Soc. Étud. Sci. Angers*, 47—49.
- ЧУМАЧЕНКО, П. (1978): Среднюрские брахиоподи от околностите на село Долни Лом, Видинско. — *Годишн. Соф. Univ., Геол. — Геогр. Фак.*, 1. Геол. (1976/1977), pp. 194—229.
- DAL PIAZ, G. (1909): Nuovo giacimento fossilifero del Lias inferiore dei Sette Comuni (Vicentino). *Mém. Soc. Paléont. Suisse*, 35. (1908), 3—10.
- DARESTE DE LA CHAVANNE, J. (1920): Fossiles liasiques de la région de Guelma. *Matér. carte. géol. Alg. (Paléont.)*, 5., 1—73.
- DARESTE DE LA CHAVANNE, J. (1930): La région d'Oudjda. *Monographie paléontologique des faunes Liasiques et Jurassiques du Maroc nord-oriental (Brachiopodes, Echinodermes, Lamellibranches et Gastropodes)*. *Notes Mém. Serv. Min. Carte géol. Maroc*, 16., 31—100.
- DAVIDSON, T. (1878): A Monograph of the British fossil Brachiopoda. Supplement to the Jurassic and Triassic species. *Palaeontogr. Soc. London*, 145—241.
- DELANCE, J.-H. (1969): Étude de quelques Brachiopodes liasiques du Nord-Est de l'Espagne. *Ann. Paléont. (Invertebr.)*, 55., 3—44.
- DEL CAMPANA, D. (1907): Fossili del Lias inferiore del Canal di Brenta. *Riv. Ital. Pal.*, 13., 123—129.
- DESIO, A., ROSSI RONCHETTI, C., INVERNIZZI, G. (1960): Il Giurassico dei dintorni di Jefren in Tripolitania. *Riv. Ital. Pal.*, 44., 1., 65—118.
- DESJONGCHAMPS, E. E. (1859a): Notes sur le terrain Callovien. Note sur le Callovien des environs d'Argentan, et des divers points du Calvados. *Bull. Soc. Linn. Normand.* 4.
- DESJONGCHAMPS, E. E. (1859b): Notes sur le terrain Callovien. Note sur les brachiopodes du Callovien de la Voulte et autres localités du département de l'Ardèche. *Bull. Soc. Linn. Normand.*, 4
- DESJONGCHAMPS, E. E. (1860): Mémoire sur les brachiopodes du Kelloway-Rock ou zone ferrugineuse du terrain Callovien dans le Nord Ouest de la France. *Mém. Soc. Linn. Normand.*, 11., 1—54.
- DE STEFANI, C. (1887): Lias inferiore ad Arieti dell'Appennino settentrionale. *Atti Soc. tosc. Sci. nat.*, *Mem.*, 8., 9—76.
- DI STEFANO, G. (1884): Ueber die Brachiopoden des Unteroolithes von Monte San Giuliano bei Trapani (Sicilien). *Jb. k. k. geol. Reichsanst.*, 34., 729—742.
- DI STEFANO, G. (1887): Sul Lias inferiore di Taormina e de'suoi dintorni. *Giorn. Soc. sci. nat. econ. Palermo*, 18. (1886), 46—184.
- DI STEFANO, G. (1892): Il Lias medio del M. San Giuliano (Erice) presso Trapani. *Atti Accad. Gioenia Sci. Nat., Catania*, (4), 3., 121—270.

- DOUVILLÉ, H. (1886): Examen des fossiles rapportés des Choas par M. Aubry. Bull. Soc. géol. Fr., (3), 14., 223—241.
- DROT, J. (1952): Espèces nouvelles de Rhynchonellidae du Lias. Bull. Soc. géol. Fr., (6), 2., 57—65.
- DUBAR, G. (1925): Études sur le Lias des Pyrénées Françaises. Mém. Soc. géol. Nord, 9., 1., 1—332.
- DUBAR, G. (1938): Études paléontologiques sur le Lias du Maroc. Brachiopodes: Rhynchonellines du Rif. Notes et Mém. Serv. Géol. Maroc, 41., 1—52.
- DUBAR, G. (1942): Études paléontologiques sur le Lias du Maroc. Brachiopodes: Térébratules et Zeilléries multiplissées. Notes et Mém. Serv. Géol. Maroc, 47., 1—103.
- DUBAR, G. (1967): Brachiopodes jurassiques du Sahara Tunisien. Ann. Paléont. (Invertébr.), 53., 1., 33—101.
- DUMORTIER, E. (1867): Études paléontologiques sur les dépôts jurassiques du bassin du Rhône. II. Lias inférieur. Paris, 1—252.
- DUMORTIER, E. (1869): Études paléontologiques sur les dépôts jurassiques du bassin du Rhone. III. Lias moyen. Paris, 1—348.
- EICHENBAUM, J. (1883): Die Brachiopoden von Smokovac bei Risano in Dalmatien. Jb. k. k. geol. Reichsanst., 33., 713—720.
- FERRARI, A., MANARA, C. (1972): Brachiopodi del Dogger inferiore di Monte Peller-Trentino. Giorn. geol. (1970), 35., 253—333.
- FINKELSTEIN, H. (1889): Ueber ein Vorkommen der Opalinus- (und Murchisonae?) Zone im westlichen Süd-Tirol. Zeitschr. deutsch. geol. Ges., 41., 40—78.
- FINKELSTEIN, H. (1889): Der Laubenstein bei Hohen-Aschau. Ein Beitrag zur Kenntniss der Brachiopodenfazies des untern alpinen Doggers. N. Jb. Min. Geol. Pal., Beilage-Bd. 6., 36—104.
- FRAUSCHER, K. (1883): Die Brachiopoden des Untersberges bei Salzburg. Jb. k. k. geol. Reichsanst., 33., 721—734.
- FRENEX, S., DROT, J., DELATRE, M. (1956): Faune de l'Aalenien de Mamers (Sarthe). I.: Lamellibranches, Brachiopodes, Bélemnites. Ann. Centr. Étud. Docum. Paléont., 16., 1—48.
- FUCINI, A. (1892): Molluschi e Brachiopodi del Lias inferiore di Longobucco (Cosenza). Bull. Soc. Malacol. Ital., 16., 9—64.
- FUCINI, A. (1893): Alcuni fossili del Lias inferiore delle Alpi Apuane e dell'Appennino di Lunigiana. Atti Soc. tosc. Sci. nat., Mem., 12., 293—309.
- FUCINI, A. (1895): Fauna dei calcari bianchi ceroidi con Phylloceras cylindricum Sow. sp. del Monte Pisano. Atti Soc. tosc. Sci. nat., Mem., 14., 125—351.
- GEMMELLARO, G. G. (1874): Sopra alcune faune giuresi e liasiche di Sicilia. Studi paleontologici. III. Sopra i fossili della zona con Terebratula aspasia Menegh. della provincia di Palermo e di Trapani. Giorn. Sci. nat. econ. Palermo, 10., 53—112.
- GEMMELLARO, G. G. (1877): Sopra alcune faune giuresi e liasiche di Sicilia. Studi paleontologici. V. Sopra alcuni fossili della zona con Posidonomya alpina Gras. di Sicilia. Giorn. Sci. nat. econ. Palermo, 12., 51—81.
- GEMMELLARO, G. G. (1878): Sopra alcune faune giuresi e liasiche di Sicilia. Studi paleontologici. VIII. Sui fossili del calcare cristallino delle Montagna del Casale e di Bellampo nella provincia di Palermo. Giorn. Sci. nat. econ. Palermo, 13., 233—434.
- GEYER, G. (1889): Über die liassischen Brachiopoden des Hierlitz bei Hallstatt. Abh. k. k. geol. Reichsanst., 15., 1—88.
- GOURION, A. (1960): Révision de certains brachiopodes liasiques de l'Ouest de l'Algérie. Publ. Serv. Carte Géol. Alg. (N.S.), 28., 61—148.
- GRECO, B. (1894): Il Lias inferiore nel circondario de Rossano Calabro. Atti Soc. tosc. Sci. nat., Mem., 13., 56—180.
- GRECO, B. (1899): Fauna della zona con Lioceras opalinum Rein. sp. di Rossano in Calabria. Palaeontogr. Ital., 4. (1898), 93—139.
- GRECO, B. (1900): Fossili oolitici del Monte Foraporta presso Lagonegro in Basilicata. Palaeontogr. Ital., V. (1899), 105—123.
- GREPPIN, E. (1900): Description des fossiles du Bajocien supérieur des environs de Bâle. Mém. Soc. Pal. Suisse, 27., 127—210.
- GROSSOURE, A. DE. (1891): Callovien de l'Ouest de la France et sur sa faune. Bull. Soc. géol. Fr., (3), 19., 255—257.
- HAAS, H. (1885): Étude monographique et critique des brachiopodes rhétiens et jurassiques des Alpes vaudoises et des contrées environnantes. I. Brachiopodes rhétiens, hettangiens et sinémuriens. Mém. Soc. Pal. Suisse, 11., 1—66.
- HAAS, H. (1889): Kritische Beiträge zur Kenntniss der jurassischen Brachiopodenfauna des Schweizerischen Jura-gebirges, und seiner angrenzenden Landestheile. I. Mém. Soc. Pal. Suisse, 16., 1—35.
- HAAS, H., PETRI, C. (1882): Die Brachiopoden der Juraformation von Elsass-Lothringen. Abh. geol. Spez.-karte Elsass-Lothr., 2., 2., 161—320.
- HAAS, O. (1912): Die Fauna des mittleren Lias von Ballino in Südtirol. I.: Brachiopoden, Lamellibranchiaten und Gastropoden. Beitr. Pal. Geol. Österr.-Ung., 25., 223—285.
- HINKELBEIN, K. (1969): El Triásico y el Jurásico de los alrededores de Abarracín. Teruel, 41., 35—75.
- IORDAN, M. (1966): Contribuții la orientarea doggerului din zona Svința. Dări de Seamă Sedint., 52., 1. (1964—65), 265—273.
- JEKELUS E. (1916): Die mesozoischen Faunen der Berge von Brassó. III—VIII. M. Kir. Földt. Int. Évk., 24., pp. 25—107.
- КАМЫЩАН, В. П.; БАБАНОВА, Л. И. (1973): Среднеюрские и позднеюрские брахиоподы Северо-западного Кавказа и Горного Крыма. — Харьков, pp. 1—175.
- KSLAZKIEWICZ, M. (1956): Jura i Kreda Bachowiec. Roczn. Pol. Tow. Geol., 24. (1954), 2—3., 1—405.
- KUNH, O. (1938): Die Fauna des Dogger der Frankenalb. (Mit Nachträgen zum übrigen Jura). Nova Acta Leopold. (N.F.), 6., 37., 125—170.
- KUNZ, B. W. L. VON (1967): Eine Fauna aus dem oberen Dogger der niederösterreichischen Kalkvorpalen. Ann. Naturhist. Mus. Wien, 71., 263—293.
- ЛАГУЗЕН, (1883): Фауна юрских образований Рязанской губернии. — Труды Геол. ком., 1, 1.
- МАКРИДИН, В. П. (1964): Брахиоподы юрских отложений Русской платформы и некоторых прилегающих к ней областей. — Москва, pp. 3—339.
- MARTELLI, A. (1906): Brachiopodi del dogger Montenegro. Boll. Soc. Geol. Ital., 25., 281—319.

- MARZLOFF, D., DARESTE DE LA CHAVANNE, J., MORET, L. (1936) Étude sur la faune du Bajocien supérieur du Mont d'Or Lyonnais (Ciret). *Trav. Lab. Géol., Fac. Sci., Lyon*, 28., 9., 56–147.
- MELÉNDEZ HEVIA, F., RAMIREZ DEL POZO, J. (1972): El Jurásico de la Serranía de Cuenca. *Bol. Geol. Min.*, 83., 4., 313–342.
- MIHAJLOVIĆ, M. (1955): Quelques espèces de Rhynchonellinae du calcaire Jurassique à Smokovac près de Risan (Boka Kotorska). — *Ann. Géol. Pénnins. Balk.*, 23, 67–73.
- МОЙСЕЕВ, А. (1934): Брахиоподы юрских отложений Крыма и Кавказа. — *Труды ВГРО*, 203, pp. 1–213.
- МОЙСЕЕВ, А. С. (1944): Юрские брахиоподы Гиссарского хребта, Кугитанга, Кугитанга, Тваркыра и Мангышлака. — *Уч. зап. ЛГУ, геол.* — *почв. наук*, 11, pp. 38–66.
- MUIR-WOOD, H. M. (1935): Jurassic Brachiopoda. In: *The Mesozoic palaeontology of British Somaliland*. London, 75–147.
- MUIR-WOOD, H. M. (1937): The Mesozoic Brachiopoda of Attock district. *Palaeont. Indica, N.S.*, 20., 6., 1–34.
- NEUMAYR, M., UHLIG, V. (1892): Über die von H. Abich im Kaukasus gesammelten Jurafossilien. *Denkschr. Akad. Wiss. Wien*, 59., 1–122.
- NOETLING, F. (1895): The fauna of the Kelloways of Mazár Drik in Baluchistan and NW frontier of India. *Palaeont. Indica*, (16), 1., 1–22.
- OPPEL, A. (1861): Ueber die Brachiopoden des unteren Lias. *Zeitschr. deutsch. geol. Ges.*, 13., 4., 529–550.
- OPPEL, A. (1861): Ueber die weissen und rothen Kalke von Vils in Tyrol. *Jahresh. Verein. vaterl. Naturk. Württemb.*, 17., 129–169.
- OPPEL, A. (1863): Ueber das Vorkommen von jurassischen Posidonomyen-Gesteinen in den Alpen. *Zeitschr. deutsch. geol. Ges.*, 15., 188–217.
- ORMÓS E. (1937): A bakonyi Kékhegy alsóliászkori brachiopoda faunája. *Közl. Debrecen. T.E. Ásv. Földt. Int.* 9., 1–45.
- PARONA, C. F. (1880): Il calcare liassico di Gozzano e i suoi fossili. *Atti R. Accad. Lincei, Mem. Cl. Sci. Fis. Mat. Nat.*, 8., 187–216.
- PARONA, C. F. (1880): I fossili degli strati a Posidonomya alpina di Camporovere nei Sette Comuni. *Atti Soc. Ital. Sci. Nat.*, 23., 244–277.
- PARONA, C. F. (1884): Sopra alcuni fossili del Lias inferiore di Carenno, Nese ed Adrara nelle Prealpi bergamasche. *Atti Soc. Ital. Sci. Nat.*, 27., 356–367.
- PARONA, C. F. (1896): Nuove osservazioni sopra la fauna e l'età degli strati con Posidonomya alpina nei Sette Comuni. *Palaeontogr. Ital.*, 1., 1–42.
- PARONA, C. F., BONARELLI, G. (1897): Sur la fauna du Callovien inférieur (Chanazien) de Savoie. *Mém. Acad. Sci. Savoie*, (4), 6., 1–35.
- PARONA, C. F., CANAVARI, E. M. (1880): Brachiopodi oolitici di alcune località dell'Italia settentrionale. *Atti Soc. tosc. Sci. nat.*, Mem., 5., 330–350.
- PETERHANS, E. (1926): Révision des brachiopodes liasiques du Grammont, des Tours d'Al, du Pissot et de Rosnière figurés dans l'ouvrage de M. H. Haas. *Mém. Soc. Vaud. Sci. Nat.*, 2., 353–384.
- PEVNY, J. (1964): Brachiopóda severnej časti Malých Karpát. *Geol. Práce, Zprávy*, 33., 157–172.
- PEVNY, J. (1969): Middle Jurassic brachiopods in the Klippen Belt of the central Váh valley. *Geol. Práce, Správy*, 50., 133–160.
- POINTINGHER, D. (1959): I brachiopodi di M. Najarda nelle Prealpi Carniche (Lias-Dogger). *Atti Ist. Veneto Sci. Lett. Art. Cl. sci. mat. nat.*, 117., 77–109.
- POZZI, R. (1960): La fauna liassica dell'Alta Valtellina (Alpi Retiche). *Riv. Ital. Pal.*, 64., 445–490.
- PREDA, A. (1967): Brachiopodele jurasice de la Roşia (Munţii Pádurea Craiului). *An. Univ. Bucureşti, Ser., ştiinţ. nat. geol. geogr.*, 16., 1., 47–71.
- PREDA, I. (1976): Contribuţii la cunoaşterea Liascului şi Doggerului din Munţii Hăghimaş (Carpaţii Orientali). *An. Muz. Ştiinţ. Nat. Piatra Neamţ, (Geol. Geogr.)*, 3., 19–41.
- ПРОЗОРОВСКАЯ, Е. Л. (1968): Юрские брахиоподы Туркмении. — *Ленинград: pp.* 1–194.
- QUENSTEDT, F. A. (1858): *Der Jura*. Tübingen, 1–842.
- QUENSTEDT, F. A. (1865–71): *Petrefactenkunde Deutschlands*. II. Brachiopoden. Leipzig, 1–748.
- RADOVANOVIĆ, S. (1888): Beiträge zur Geologie und Palaeontologie Ostserbiens. I. Die Liasablagerungen von Rogina. *Ann. géol. Pénnins. Balkan*, 1., 1–106.
- RĂILEANU, G., IORDAN, M. (1964): Studiul brachiopodelor liasice din zona Sviña. *Stud. Cerc. Geol. Geof. Geogr., Ser. geol.*, 9., 1., 3–24.
- RAMACCIONI, G. (1936): Il Lias medio di Monte Cucco nell'Appennino Centrale. *Boll. Soc. Geol. Ital.*, 55., 169–190.
- RAU, K. (1905): Die Brachiopoden des mittleren Lias Schwabens mit Ausschluss der Spiriferinen. *Geol. Pal. Abh.*, 10. (N.S. 6.), 5., 263–355.
- RENZ, C. (1932): Brachiopoden des südschweizerischen und westgriechischen Lias. *Abh. Schweiz. Pal. Ges.*, 52., 1–62.
- ROCHÉ, P. (1939): Aalénien et Bajocien du Maconnais et de quelques régions voisines. *Trav. Lab. Géol. Fac. Sci. Lyon*, 35., Mém. 29., 1–355.
- ROTHPLETZ, A. (1886): Geologische-palaeontologische Monographie der Vilser-Alpen, mit besonderer Berücksichtigung der Brachiopoden-Systematik. *Palaeontographica*, 33., 1–180.
- ROUSSELLE, L. (1965): Rhynchonellidae, Terebratulidae et Zeilleridae du Dogger Marocain (Moyen-Atlas septentrional, Hauts-Plateaux, Haut-Atlas). *Notes et Mém. Serv. Géol. Maroc*, 187., 1–168.
- RUGGIERO, E. (1964): Fauna a Rhynchonellina delle "Carboniere" (Abruzzo). *Boll. Soc. Nat. Napoli*, 73., 37–53.
- SACCHI VIALI, G. (1964): Revisione della fauna di Saltrio. V. I Gasteropodi. I Cefalopodi Dibranchiati. I Briozoi. I Brachiopodi. Gli Echinodermi. I Vertebrati. *Atti. Ist. Geol. Univ. Pavia*, 15., 1–23.
- SEIFERT, I. (1963): Die Brachiopoden des oberen Dogger der Schwäbischen Alb. *Palaeontographica (A)*, 121., 4–6., 156–203.
- SIBLIK, M. (1964): K nálezu liasových brachiopodu v horní časti Belanské doliny. *Geol. Práce, Zprávy*, 31., 157–181.
- SIBLIK, M. (1965): Some new Liassic Brachiopods. *Geol. Sborn.*, 16., 1., 73–82.
- SIBLIK, M. (1966): Ramenozočí Kosteleckého Bradla. *Geol. Práce, Zprávy*, 35., 137–157.
- SIBLIK, M. (1967): Tetrarhynchinae a Cyclothyridinae slovenského doméru. *Geol. Práce, Zprávy*, 41., 11–25.

- SIBLIK, M. (1968): Rhynchonellinae a Cirpinae (Brachiopoda) slovenského doméru. Geol. Práce, Správy, 46., 21—36.
- SIMIONESCU, I. (1899): Studii geologice și paleontologice din Carpații Sudici. III. Fauna Calloviana din Valea Lupului (Rucar). Acad. Rom. Publ. fond. V. Adamachi, 3., 189—230.
- SUCIC-PROTIC, Z. (1969): Mesozoic Brachiopoda of Yugoslavia. I. Middle Liassic Brachiopoda of the Yugoslav Carpatho-Balkanids (1). Univ. Belgrade Monogr., 1., 1—214.
- SUCIC-PROTIC, Z. (1971): Mesozoic Brachiopoda of Yugoslavia. Middle Liassic Brachiopoda of the Yugoslav Carpatho-Balkanids (2). Univ. Belgrade Monogr., 5., 1—150.
- SZAJNOCHA, L. (1879): Die Brachiopoden-Fauna der Oolithe von Balin bei Krakau. Denkschr. Akad. Wiss. Wien, 41., 2., 197—240.
- TADDEI RUGGIERO, E. (1966): I brachiopodi aaleniani di Monte Zari (Sardegna sudoccidentale). Boll. Soc. Nat. Napoli, 75., 293—315.
- TRAUTH, F. (1909): Die Grestener Schichten der österreichischen Voralpen und ihre Fauna. Beitr. Pal. Österr. Ung., 22., 1—142.
- UHLIG, V. (1880): Über die liassischen Brachiopodenfauna von Sospirolo bei Belluno. Sitz.-ber. Akad. Wiss. Wien, 80. (1879), 1., 259—310.
- UHLIG, V. (1881): Ueber die Fauna des rothen Kellowaykalkes der penninischen Klippe Babierzówka bei Neumarkt in Westgalizien. Jb. k. k. geol. Reichsanst., 31., 381—422.
- VACEK, M. (1886): Ueber die Fauna der Oolithe von Cap San Vigilio verbunden mit einer Studie über die obere Liasgrenze. Abh. k. k. geol. Reichsanst., 12., 3., 57—212.
- VADÁSZ E. (1935): A Mecsekhegység. Das Mecsek-Gebirge. Magy. Tájék Földt. Lefrása, 1., 1—180.
- VIGH G. (1943): Die geologischen und paläontologischen Verhältnisse im nordwestlichen Teil des Gerecse-Gebirges. Földt. Közl., 73., 301—329, 537—550.
- VÖRÖS A. (1970): A kericséri (Bakony hg.) pliensbachi brachiopoda fauna vizsgálata. The Pliensbachian Brachiopod fauna of Kericsér (Bakony Mountains, Hungary). — Ősl. Viták, 14, pp. 61—76.
- WEIR, J. (1929): Jurassic fossils from Jubaland, East Africa, collected by V. G. Glenday. Monogr. Geol. Dept. Hunterian Mus. Glasgow Univ., 3., 1—63.
- ZITTEL, K. A. (1869): Geologische Beobachtungen aus den Central-Appenninen. Benecke's Geognost. Pal. Beitr., 2., 2., 91—177.



КОЛИЧЕСТВЕННОЕ ИССЛЕДОВАНИЕ ПРОЦЕССА УТОНЬЩЕНИЯ ЗЕМНОЙ КОРЫ В ОБЛАСТЯХ С ВЫСОКИМ ТЕПЛОВЫМ ПОТОКОМ В ПРИМЕНЕНИИ К ПАННОНСКОМУ БАСЕЙНУ

by

L. BODRI

Department of Geophysics, Eötvös University, Budapest

(Received: 15th March, 1982)

ABSTRACT

The results of this study can be considered as a quantitative evidence in favour of the hypothesis according to which the small thickness of the crust observed in areas of high positive heat flow anomalies, and also the strong correlation between crustal thickness and surface heat flow, is the consequence of a past transition of material of the lower crust into garnet granulite. The thinning of the crust (known also as subcrustal erosion) should have proceeded by formation of blocks of the heavy garnet granulite material and subsequent sinking of these blocks into the upper mantle. The $p-T$ conditions necessary for subcrustal erosion have been calculated and certain phenomena accompanying the process of crustal thinning have also been investigated.

Введение

Ряд исследований корреляции между тепловым потоком и толщиной коры указывает на существование определенной отрицательной корреляции, когда более высокие тепловые потоки соответствуют более тонкой коре, а низкие потоки наблюдаются в районах с толстой или очень толстой корой (СЕРМАК, 1979). В общем, корреляционная связь между этими двумя величинами не очень тесна и однозначна. Это вызвано по всей вероятности тем, что граница Мохо, скорее всего, по природе преимущественно химическая, и термические факторы в нормальных условиях не играли существенной роли в ее образовании.

Тем не менее существует ряд районов, где наблюдается почти функциональная зависимость между величиной теплового потока и мощностью коры. Эти районы все без исключения области молодой тектонической активности и осадконакопления с поверхностным тепловым потоком по крайней мере вдвое выше среднемирового и значительно утоньшенной корой. В Европе примером таких структур могут служить, например, Рейнский грабен и Паннонский бассейн, или область Тирренского моря. Так, в Карпатском регионе мощность коры постепенно возрастает от Паннонского бассейна (25–27 км) к Внешним Карпатам и Предкарпатскому прогибу, где достигает максимального значения (55–56 км). Тепловой поток в этом направлении уменьшается от 80–110 до 35–45 мвт/м². Корреляционный коэффициент между тепловым потоком и мощностью коры для Паннонского бассейна по расчетам Бодри (1976, 1981а) составля-

ет 72%, и поверхностный тепловой поток Q может быть получен из толщины коры h по следующей формуле:

$$Q = 85.0 + 9.5(26.0 - h). \quad (1)$$

В формуле (1) толщина коры h берется в км, тепловой поток Q — в мвт/м². Как видим из формулы (1), средняя толщина коры Паннонского бассейна составляет 26 км, то есть она примерно на 10 км утоньшена по сравнению с нормальной, а средний тепловой поток на 40–45 мвт/м² выше среднеконтинентального.

Аналогичную картину показывает зона Рейнского грабена с толщиной коры 24 км и средним тепловым потоком 100 мвт/м² (GIESE ET AL., 1973; СЕРМАК, 1979). Что касается строения коры в этих районах, то его характерной чертой, особенно ярко проявляющейся в Паннонском бассейне, является то, что понижение ее толщины целиком обусловлено утоньшением слоя нижней коры. Так, в Паннонском бассейне, где глубина залегания поверхности Мохо составляет 24–29 км, нижняя кора на 5–10 км тоньше, чем в нормальных областях. При этом толщина слоя верхней коры обычная или даже несколько увеличена (СОЛЛОУБ и др., 1978).

В данной работе приводится ряд доказательств в пользу того, что причиной утоньшения коры (подкорковая эрозия) и сильной корреляции этого утоньшения с температурой в областях молодой тектонической активности мог являться фазовый переход габбро — гранатовый гранулит — эклогит и сопутствующие этому переходу процессы. В качестве иллюстрации действия предполагаемого механизма автор использовал Паннонский бассейн.

Фазовый переход габбро-эклогит в районах с повышенным потоком

Как уже упоминалось выше, тепловой поток Паннонского бассейна стабилен и имеет значения 80–110 мвт/м², что более чем вдвое превышает 45 мвт/м² — среднее значение для докембрийских платформ. Столь же высоки и глубинные температуры, полученные автором при экстраполяции вниз теплового потока с использованием сведений о строении коры бассейна и экспериментальных данных по определению теплопроводности и радиоактивной генерации тепла в различных породах. Согласно расчетам автора, на подошве гранитного слоя аномалия температуры составляет 300–350К, а на границе Мохо температура на 500К выше тех 300–400 °С, до которых она нагрета в областях с нормальным потоком. Температура в нижней коре Паннонского бассейна изменяется от 600 до 750 °С при давлении 40–60 МПа. Зависимость давления от глубины здесь и в дальнейшем бралась для модели 1066А (GILBERT and DZIEWONSKI, 1975).

Как показали эксперименты ВРАСЕ (1972), TULLIS and YUND (1977) при указанных p – T условиях в коре осуществляется пластический тип разрушения. Трещины в породе не возникают, деформации идут за счет дислокаций. Закрытие трещин в нижней коре делает этот слой «сухим».

Как видно из рис. 1, составленного на основании фазовых диаграмм RINGWOOD and GREEN (1969) и ИТО и КЕННЕДИ (1972), «сухие» фазовые переходы осуществимы только при температурах, соответствующих поверхностным тепловым потокам не ниже 60 мвт/м^2 и только в фазах гранатового гранулита — базальта. Сухая нижняя кора Паннонского бассейна при имеющихся температурах будет находиться в поле стабильности базальта или в зоне переходной к гранатовому гранулиту. Не исключено, впрочем, что часть материала в менее прогретых областях находится в фазе низкоплотностного гранатового гранулита. Этот вывод частично подтверждается сейсмическими измерениями, которые дают для нижней коры некоторых районов Венгрии скорости продольных волн $v_p = 7,1-7,3 \text{ км/сек}$, характерные скорее не для базальта, а для гранатового гранулита с небольшим содержанием граната и плотностью $\rho = 3100-3200 \text{ кг/м}^3$ (Пошгай, 1977). Иногда в нижних частях коры

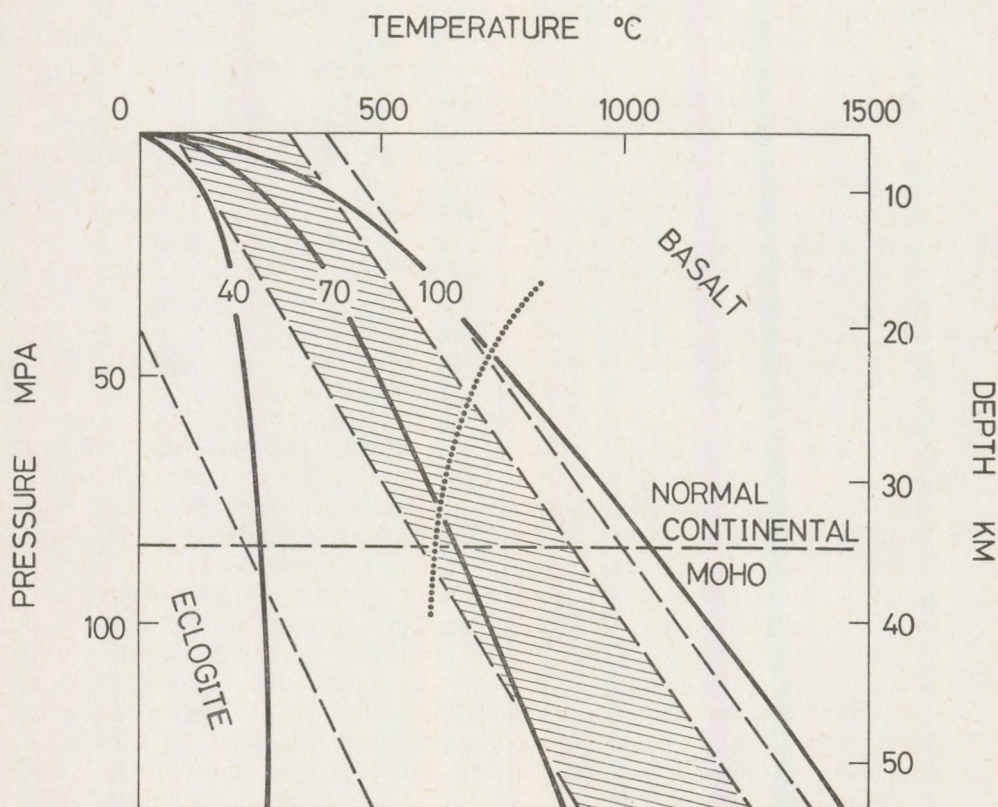


Рис. 1. Поля стабильности эклогита, гранатового гранулита и габбро и геотермические градиенты при различных значениях поверхностного теплового потока. Заштрихованный район — область стабильности гранатового гранулита, точечная линия — граница зоны пластического типа разрушения пород (плавное течение)

наблюдаются еще более высокие скорости $v_p = 7,5 - 7,6$ км/сек, что может соответствовать гранатовому гранулисту с плотностью $\rho = 3300$ кг/м³.

Каковы были условия для фазового перехода в прошлом? Это зависит от того, как развивалась Паннонская тепловая аномалия. Возникновение бассейна связано с активными тектоническими процессами, происходившими в этом районе в третичном периоде. Предполагается, что образование бассейна явилось результатом одного или нескольких процессов субдукции, имевших место в Паннонском регионе одновременно или с некоторым временным сдвигом по отношению друг к другу. Погружение в мантию одной или нескольких литосферных плит индуцировало вторичную конвекцию со всеми явлениями, обычно сопровождающими этот процесс: возникновение тепловой аномалии, вулканизм, утоньшение литосферы и т.п. Ряд геолого-геофизических данных позволяет заключить, что активный период развития, связанный с усиленным массопереносом в мантии, закончился для бассейна не позже начала плиоцена. То есть настоящее состояние аномалии является результатом кондуктивного охлаждения из некоторого состояния максимальной прогретости, в котором находился бассейн в момент прекращения конвективных движений. Эта фаза развития аномалии, в основном, ясна. Расчеты остывания различных аномалий применительно к условиям Паннонского бассейна, представленные в работе Водри (1981b), показали, что остывание идет довольно медленно, требуется несколько десятков млн. лет, чтобы снизить поверхностный тепловой поток хотя бы на одну треть первоначального значения. Таким образом, современное термальное состояние молодых структур, подобных Паннонскому бассейну, можно считать практически идентичным тому, которое они имели в момент прекращения вынужденной конвекции в мантии.

Менее ясен процесс образования тепловой аномалии. Предположим, что к моменту начала вынужденной конвекции кора и литосфера под Паннонским бассейном имели нормальную толщину. В процессе конвекции к подошве литосферы поступают в результате крупномасштабного массопереноса и/или образуются прямо у подошвы литосферы из-за действия механизма вязкого трения большие массы легкого нагретого материала, который будет прогревать материал литосферы. Процесс прогрева литосферы может происходить чисто кондуктивным путем из-за ее большой вязкости, которая препятствует образованию в ней конвективных течений. Либо как указано в работе Водри and Водри (1978), некоторая часть литосферы может вовлекаться в конвективные движения, поскольку ее вязкость может существенно снизить совместное влияние температуры и высоких напряжений. В этом случае процесс прогрева будет более быстрым и интенсивным. Прогрев литосферы затрагивает, конечно, и нижние части коры, нагревание которых происходит, по всей вероятности, кондуктивно. Учет влияния на вязкость эффектов нелинейной реологии довольно труден, поэтому в данной работе автор ограничился расчетом чисто кондуктивного разогревания литосферы в случае, когда ее подошва разогрета до 1400 °С (пиролитовый ликвидус). Толщина литосферы принималась равной 80 км. Значения

теплофизических параметров брались такие же, как в работе Водри (1981а).

Как видим из рис. 2, представляющего результаты этих расчетов, даже при медленном кондуктивном разогреве через 10–15 млн. лет после начала разогрева материал нижней коры (глубина 30–40 км, давление 70–100 МПа) становится сухим и оказывается в поле стабильности гранатового гранулиты. Процесс разогрева будет более быстрым, а достигнутые температуры более высокими, в случае наличия конвективных течений не только в астеносфере, но и в нижних слоях литосферы.

Наряду с простой возможностью осуществления фазового перехода, важнейшим моментом этого процесса является время, которое он зани-

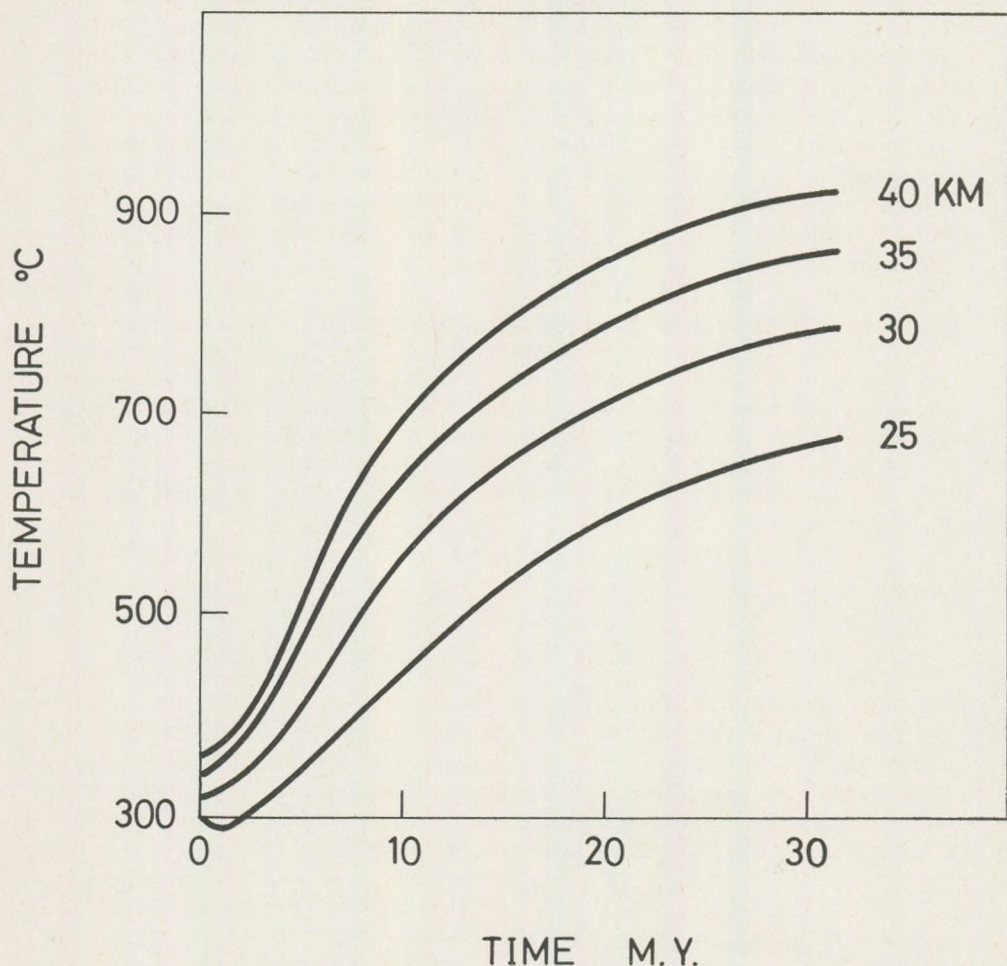


Рис. 2. Изменение температуры 80-км-вой литосферы со временем, когда ее подошва нагрета до 1400 °C

мает. Обобщая ряд предположений и скудные данные, имеющиеся по этому вопросу, Артюшков (1979) полагает, что переход чрезвычайно медлен при температурах 300–500 °С. Его характерное время в таких условиях > 1 млрд. лет. С ростом температуры скорость перехода резко увеличивается, примерно на порядок величины на каждые 100К. При температуре ~ 800 °С характерное время перехода снижается до ~ 1 млн. лет. Сравнивая эти данные с рис. 1 находим, что температуры 700–800 °С, необходимые для того, чтобы фазовый переход произошел в геологически приемлемое время, достигаются при давлении не ниже 60–70 МПа, что соответствует глубине 25–30 км. Таким образом уровень ~ 25 км следует считать верхней границей слоя, способного к переходу в гранатовый гранулит за сравнительно короткое время. Обобщая вышесказанное, можно считать установленным, что при температурах, соответствующим интервалу поверхностного теплового потока 65–85 мвт/м², начиная с глубины 25 км, возможно утяжеление нижнего слоя коры, то есть материал нижней коры может находиться в фазе гранатового гранулита с плотностью ~ 3280–3360 кг/м³. При потоках больших 85 мвт/м² стабильным оказывается базальт с плотностью ~ 3000–3100 кг/м³, а при потоках меньших 65 мвт/м² нижняя кора перестает быть сухой, и стабильной формой, видимо, становится такой же низкоплотный амфиболит (Вотт, 1971).

Условия отрыва и погружения гранатового гранулита в мантию

Таким образом, в интервале температур 700–1000 °С в нижнем слое коры может развиваться быстрый с геологической точки зрения переход его материала в гранатовый гранулит. Рассматривая изменение плотности нижней коры при фазовом переходе (RINGWOOD and GREEN, 1969; Ито и Кеннеди, 1972) и рассчитывая плотность верхней мантии ρ по формуле

$$\rho = \rho_0 (1 + \alpha T), \quad (2)$$

где $\alpha = 3 \cdot 10^{-5}$ град⁻¹ коэффициент теплового расширения,

T — температура,

$\rho_0 = 3350$ кг/м³ плотность при нормальных условиях, легко оценить,

что вновь образующийся гранатовый гранулит во всем указанном интервале температур будет плотнее, чем подстилающая его верхняя мантия, что создает условия для отрыва от коры блоков гранатового гранулита и погружения их в мантию. Типичное значение разности плотностей в интервале температур 700–1000 °С составляет $\Delta\rho = 100$ –200 кг/м³. Рассчитывая вязкость η нагретого вещества по формуле

$$\eta = 10 \times T \exp [(50350 + 1.13p)/T], \quad (3)$$

где p — давление в МПа,

T — температура в градусах Кельвина, легко получить, что в интервале температур 800–1200 °С вязкость вещества изменяется от 10^{23} до

10^{19} Пас. Как было отмечено в работах Воды and Воды (1978, 1979), в процессах с характеристическими временами $\sim 10^4 - 10^6$ лет материал такой вязкости будет вести себя подобно ньютоновской жидкости. Материал с большей вязкостью — как аморфное твердое тело. То есть с точки зрения механики сплошной среды процесс утоньшения нижнего слоя коры происходит как движение друг относительно друга двух несмешивающихся вязких жидкостей: слоя гранатового гранулита и подстилающей его мантии. Этот процесс может быть описан уравнениями Навье-Стокса с использованием предположения о несжимаемости вещества. Область вычислений изображена на рис. 3.

Предположим, что имеются малые возмущения границы Мохо ($z=0$), расположенные в начальный момент хаотически. Хаотически расположенные начальные возмущения могут быть разложены в гармонический ряд, и поскольку уравнения движения линейны, то они могут быть решены для каждой гармоники отдельно. При постоянных по каждому слою плотности и вязкости решение уравнений движения может быть найдено в аналитической форме для начального этапа развития гармонического возмущения, когда его амплитуда $a \ll h_1$. В данной работе автор

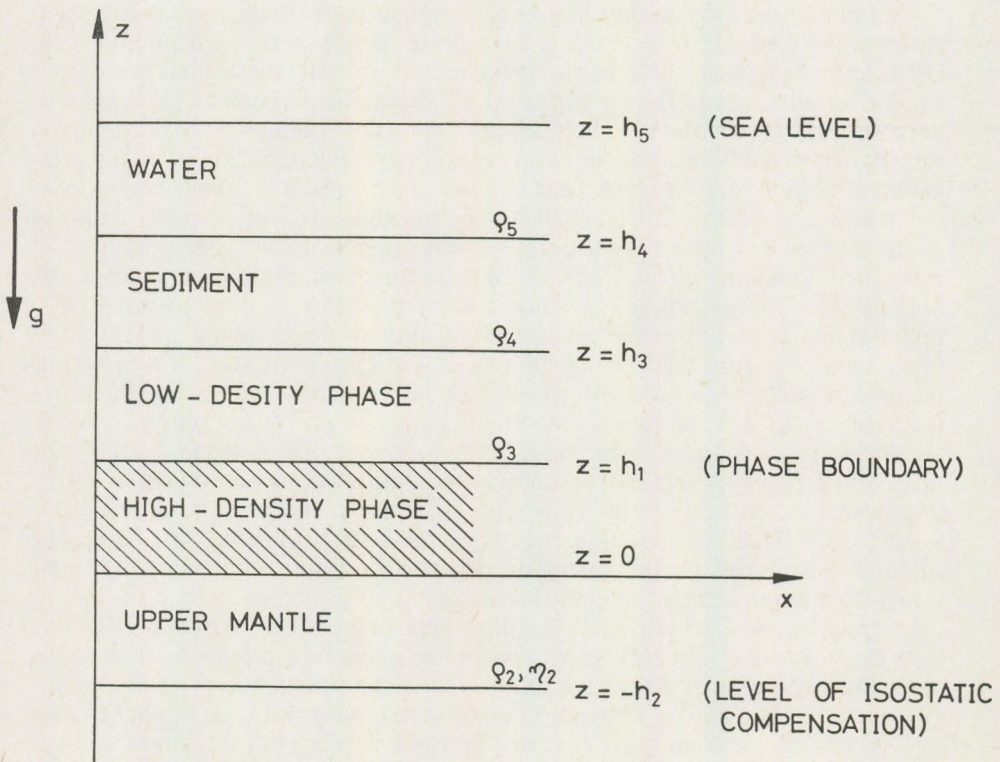


Рис. 3. Схема вычислительного района

воспользовался общим решением Артыушников (1971), упростив его для случая, когда уровень $z = h_1$ представляет собой твердую стенку и $h_2 \gg h_1$, $\eta_2 \ll \eta_1$. Функция тока для одной из гармоник возмущения при этих предположениях представлена на рис. 4. Возмущение границы имеет вид $a \cos kx$, где k — волновое число. Изменение амплитуды этого возмущения со временем будет происходить по следующему закону:

$$\begin{aligned} a &= a_0 \exp(\gamma t) \\ \gamma &= E \frac{\sinh \alpha \cosh \alpha - \alpha}{\alpha (\cosh^2 \alpha + \alpha^2)} \\ E &= \frac{(\rho_1 - \rho_2) h_1 g}{2\eta_1}, \end{aligned} \quad (4)$$

где t — время,

a_0 — начальная амплитуда возмущения,

g — ускорение силы тяжести,

$\alpha = kh_1$, $k = 2\pi/l$, l — длина волны возмущения.

Для нашего случая, когда $\rho_1 > \rho_2$, коэффициент γ всегда положителен, то есть даже малые возмущения всех длин волн будут увеличиваться, когда они развиваются в более тяжелой по сравнению с подстилающей ее вязкой жидкости. Таким образом, разрыв плотности вида, изображенного на рис. 3, абсолютно неустойчив даже по отношению к бесконечно малым возмущениям, что должно привести к распаду указанного разрыва. Как будет протекать этот процесс? Функция γ имеет максимум, равный $3,2 E$, при $\alpha = 2,1$ ($l = 3,0h_1$), быстро убывает и в сторону длинноволновых, и в сторону коротковолновых возмущений. Это приводит к тому, что первоначально хаотически возмущенная граница скачка плотностей уже на начальной стадии своего распада трансформируется в правильное гармоническое возмущение, включающее лишь длины волн близкие к $3h_1$. Заметим, что величина α_{\max} и следовательно длина волны результирующего возмущения границы Мохо мало чувствительна к отношению η_2/η_1 . Так, замена условия $\eta_2 \ll \eta_1$ на $\eta_2 = \eta_1$ передвигает α_{\max} лишь на 0,2 в сторону длинных волн и делает максимум несколько более пологим. Время существенного изменения амплитуды возмущения имеет порядок $1/\gamma$. При $\Delta\rho = 100$ кг/м³, $g = 10$ м/сек², $\alpha = 2,1$, $h_1 = 10$ км, $\eta_1 = 10^{19} - 10^{20}$ Пас, это время имеет порядок 0,01–0,1 млн. лет, то есть с геологической точки зрения процесс трансформации произвольной границы в гармоническую должен быть довольно быстрым.

Труднее описать процесс дальнейшей эволюции разрыва. Множитель $\exp(\gamma t)$ в формуле (4) быстро растет со временем, допуская неограниченный рост амплитуды возмущения. Однако выражение (4) для амплитуды пригодно лишь в течение промежутков времени $\sim 1/\gamma$, когда сама амплитуда достаточно мала. Это же время следует считать характерным временем существования замкнутой картины течений, изображенной на рис. 4. Дальнейший количественный анализ картины движений не пред-

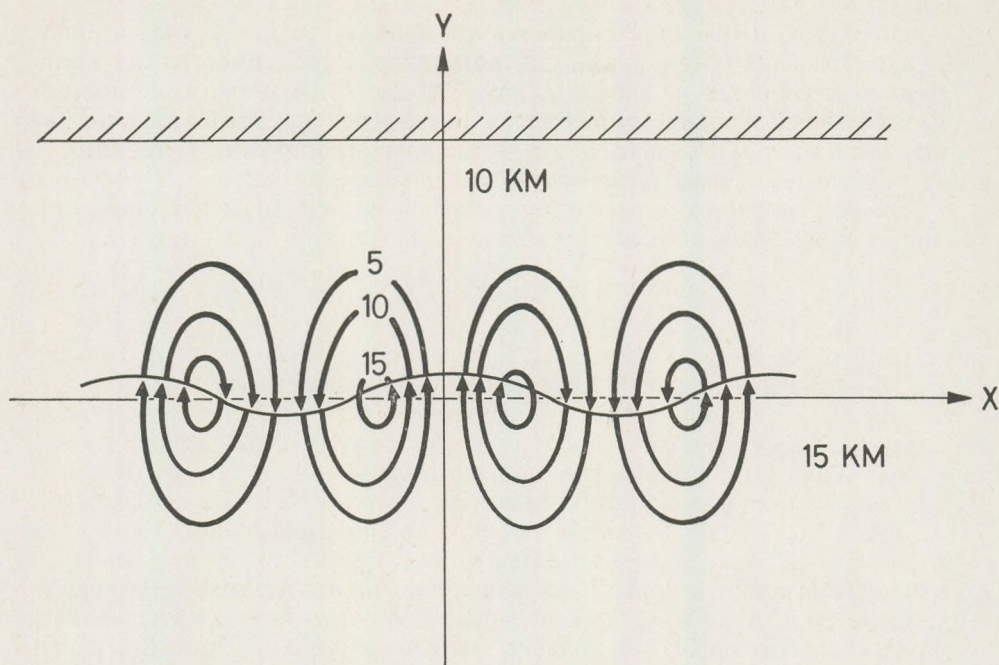


Рис. 4. Функция тока в единицах $\text{м}^2/\text{сек}$ в начальной стадии развития возмущения на границе Мохо ($\alpha=5$, $h_1=10$ км, $\eta_1=10^{19}$ Пас)

ставляется возможным, поскольку в системе действуют одновременно два диссипативных механизма: теплопроводность и диффузия. Последний довольно неопределен для настоящей задачи. Картина же движений зависит от взаимного влияния этих процессов друг на друга и к тому же сильно осложняется перекрестными кинетическими процессами. Можно лишь предполагать, что дальнейшее опускание тяжелого вещества может осуществляться либо как непрерывное стекание его по каналам, образовавшихся в местах максимальных возмущений границы, либо как отрыв и погружение тяжелых вязких капель гранатового гранулита в более легкую и менее вязкую жидкость. Ряд соображений качественного характера заставляет считать более вероятным второе предположение. Основными параметрами подобия в данной задаче являются температурное и диффузионное числа Рэлея, знак которых определяется соответственно характерной для задачи разностью температур и концентрации тяжелой компоненты на границах изучаемого слоя. В нашем случае первое из этих чисел положительно, а второе отрицательно. В работе Мясникова и Фадеева (1980) на основании анализа данных по лабораторному моделированию конвекции в бинарных смесях была составлена качественная диаграмма реализации различных типов конвекции в зависимости от значений чисел Рэлея. Указанные авторы делают вывод, что режим течения, связанный с образованием удлиненных структур

типа струй или «пальцев», является устойчивым лишь в случае отрицательности обоих чисел Рэлея. Он соответствует состоянию, когда внизу расположено более холодное и легкое вещество. В данном же случае, видимо, более устойчивым будет режим разделения, связанный с погружением в мантию отдельных капель тяжелого гранатового гранулит.

Легко оценить допустимый интервал размеров капель. В системах с большой вязкостью скорость опускания уже оторвавшейся капли при допущении $\eta_1 \gg \eta_2$ в первом приближении равна

$$v = \frac{2(\rho_1 - \rho_2)gR^2}{3\eta_2} \quad (5)$$

где R — радиус капли. На рис. 5 изображено изменение скорости v в зависимости от температуры и радиуса опускающихся капель, когда вязкость рассчитывается по формуле (3). Если считать приемлемыми скорости опускания не ниже 0,1 см/год, то легко видеть, что погружение нижней части коры в мантию может осуществляться при температуре не менее 900 °С. Поскольку само образование гранатового гранулита возможно в интервале температур 700–1100 °С, то вообще процесс утоньшения нижней коры (подкорковая эрозия) может идти в интервале температур 900–1100 °С, при этом радиус гранат-гранулитовых капель, опускающихся в мантию, должен быть не менее 2–3 км, то есть по порядку сравнимым с толщиной слоя, испытавшего фазовый переход. Следует отметить, что максимальное напряжение сдвига при $l = 3h_1$ для картины течений, изображенной на рис. 4, достигается на глубине около 4 км. На той же глубине происходит смена скорости движения тяжелого материала с преимущественно вертикальных на преимущественно горизонтальные.

После прекращения конвекции в мантии, когда перестает действовать и механизм дополнительного к радиоактивному разогрева ее вещества, условия для процесса подкорковой эрозии быстро исчезают. Как показали расчеты Водвг (1981b), снижение температуры с 1100° до 900 °С на глубинах до 35 км происходит за время от 1 до 5 млн. лет. Поскольку современная температура границы Мохо даже в наиболее прогретых областях Паннонского бассейна не превышает 900 °С, то следует признать, что в настоящее время дальнейшего утоньшения коры под бассейном не происходит.

И наконец несколько слов об энергии, которая выделяется при погружении тяжелых включений в мантию. Она имеет порядок $(\rho_1 - \rho_2)gVh_1$, где V — объем погрузившегося материала, что составляет 10^{11} дж/м² на единицу площади Паннонского бассейна. Это значение на три порядка ниже, чем энергия, выделенная дополнительным источником нагрева, связанным с конвективным массопереносом в активный период развития Паннонской тепловой аномалии. Даже если вся выделившаяся при опускании включений энергия расходовалась на нагревание материала мантии, то дополнительное повышение температуры составило бы не более 10К.

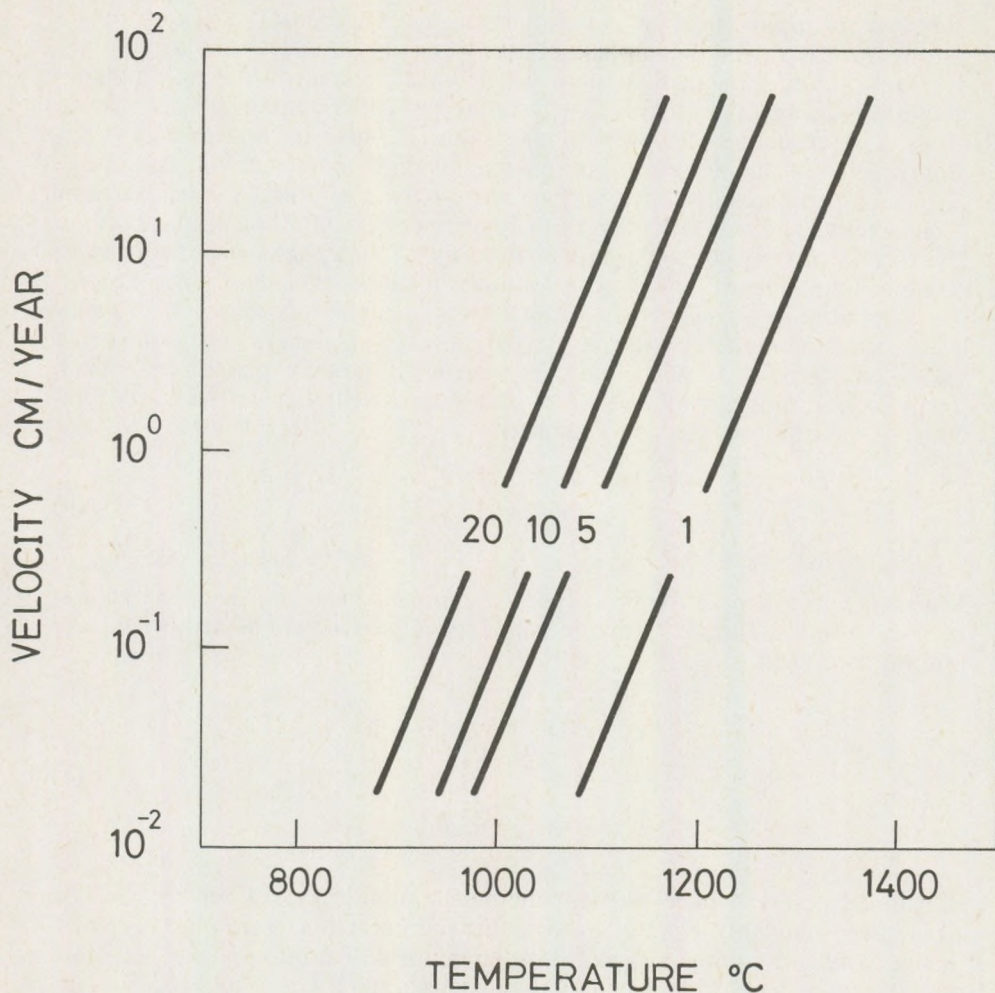


Рис. 5. Изменение скорости погружения в мантию 1, 5, 10 и 20 км-вых гранат-гранулитовых включений

Образование депрессии при фазовом переходе в нижней коре

Утяжеление слоя нижней коры в результате превращения части его в гранатовый гранулит приводит к нарушению изостатического равновесия района. При восстановлении изостазии происходит погружение территории, под которой произошел фазовый переход. Подробное рассмотрение процесса этого погружения далеко выходит за рамки настоящей работы (см. например, O'CONNELL and WASSERBURG, 1972). Оценим лишь максимальную глубину депрессии, которая может образоваться,

когда территория, в коре которой произошел фазовый переход, вновь достигнет изостатического равновесия.

Опускание района будущего бассейна обусловлено двумя одновременно идущими процессами. Увеличение плотности приводит к сжатию коры и образованию депрессии такой же глубины на поверхности. Заполнение этой депрессии осадками увеличивает нагрузку на литосферу сопровождается ее изостатическим погружением. Рис. 3 представляет собой схему строения коры и верхней мантии после образования бассейна. Пусть $H = h_2 + h_5$ общая толщина литосферы до уровня изостатической компенсации. Перед началом осадконакопления, очевидно, $H = h_3^0 + h_2^0$, где величины с индексом «0» относятся к начальному моменту. Равновесие устанавливается, когда нагрузка, создаваемая совокупностью слоев на глубине компенсации, в конечный момент равна начальной нагрузке на этой глубине. То есть для определения максимальной глубины депрессии имеется два уравнения:

$$H = (h_5 - h_4) + (h_4 - h_3) + (h_3 - h_1) + h_1 + h_2 = h_3^0 + h_2^0 \quad (6)$$

$$\rho_5 (h_5 - h_4) + \rho_4 (h_4 - h_3) + \rho_3 (h_3 - h_1) + \rho_1 \cdot h_1 + \rho_2 \cdot h_2 = \rho_3 \cdot h_3^0 + \rho_2 \cdot h_2^0.$$

Учитывая при этом, что при простом сжатии вещества в слое его нагрузка на нижележащие слои не меняется, в результате решения уравнений (6) получаем

$$h_4 - h_3 = \frac{\rho_2}{\rho_2 - \rho_4} (h_3^0 - h_3) \quad (7)$$

$$h_3^0 - h_3 = \frac{\rho_1 - \rho_3}{\rho_3} h_1.$$

В формулах (7) первое выражение представляет собой максимальную толщину осадочного слоя образовавшегося бассейна, а второе — сокращение мощности коры в результате ее сжатия. Таким образом, глубина получающегося осадочного бассейна оказывается в $\rho_2/(\rho_2 - \rho_4)$ раз больше уменьшения толщины коры. Для случая $\rho_2 = 3350 \text{ кг/м}^3$, $\rho_4 = 2550 \text{ кг/м}^3$, $\rho_3 = 3000 \text{ кг/м}^3$, $\rho_1 = 3200 - 3300 \text{ кг/м}^3$, когда в гранатовый гранулит перешел слой толщиной 10–15 км, толщина осадочного слоя оказывается равной 3–6 км. Эти цифры хорошо совпадают с толщиной осадочного слоя Паннонского бассейна, которая в среднем составляет 3–3,5 км, местами доходя до 5 км.

Каково время восстановления изостази? Зависимость характерной скорости восстановления изостази от характерного горизонтального размера области нескомпенсированной нагрузки изучалась Артюшковым (1979), который пришел к выводу, что в тектонически активных областях, где литосфера утоньшена, а вязкость астеносферы ниже, чем в спокойных областях, при характерном горизонтальном размере нагрузки $\sim 50 \text{ км}$, равновесие восстанавливается очень быстро, за время

порядка десятков или сотен лет. Для Паннонского бассейна, поперечник которого составляет около 400 км, это время заведомо меньше времени, характеризующего процесс подкоровой эрозии ($\sim 10^5 - 10^6$ лет) или характерного времени развития тектонических процессов ($\sim 10^7$ лет).

Заключение

Таким образом, в сильно прогретых областях тектонической активности, где существуют другие источники разогрева материала верхних слоев Земли, помимо радиоактивного нагрева, при поверхностных тепловых потоках 80–100 мвт/м² на глубинах не меньших 20–25 км может осуществляться относительно быстрый переход вещества нижней коры в гранатовый гранулит. Выше 20–25 км переход невозможен, поскольку температуры на этих глубинах слишком низки для того, чтобы этот переход совершился достаточно быстро. Поскольку гранатовый гранулит на всем $p-T$ интервале своего существования тяжелее подстилающей его мантии, то создаются условия для утоньшения коры посредством механизма, называемого подкоровой эрозией. Процесс подкоровой эрозии состоит в отрыве от нижнего слоя коры сравнительно крупных (не менее 2–3 км в поперечнике) блоков или вязких капель гранатового гранулита и погружении их в мантию со скоростью ~ 1 см/год. Энергия, выделяющаяся при таком погружении, незначительна. Подкоровая эрозия происходит в интервале температур 900–1100 °С, полностью зависит от температуры и регулируется двумя факторами. С одной стороны при относительно низких температурах вязкость подстилающей кору мантии может быть слишком высока для того, чтобы даже будучи плотнее ее, гранатовый гранулит мог оторваться от коры и утонуть в мантии. В случае сильно нагретого материала фазовый переход может не дать существенного увеличения плотности.

Утяжеление нижнего слоя коры приводит к опусканию территории, под которой произошел фазовый переход, в результате изостатического выравнивания. То есть области утоньшенной коры должны ассоциироваться с депрессиями на поверхности, глубина которых составляет около половины толщины слоя, испытавшего фазовый переход.

ЛИТЕРАТУРА

- АРТЮШКОВ, Е. В. (1971): Convective instability in geotectonics. — *J. Geophys. Res.*, 76: 1397–1415.
- АРТЮШКОВ, Е. В. (1979): Геодинамика. — Наука, Москва, 327 стр.
- BODRI, L. (1976): Mélyégi hőáram és mélyhőmérsékletek a Pannon medencében. — Budapest, 80 о., manuscript, in Hungarian.
- BODRI, L. (1981a): Geothermal model of the earth's crust in the Pannonian basin. — *Tectonophysics*, 72: 61–73.
- BODRI, L. (1981b): Three-dimensional modelling of deep temperature and heat flow anomalies with applications to geothermics of the Pannonian basin. — *Tectonophysics*, 79: 225–236.
- BODRI, L., BODRI, B. (1978): Numerical investigation of tectonic flow in island-arc areas. — *Tectonophysics*, 50: 163–175.
- BODRI, L., BODRI, B. (1979): Flow, stress and temperature in island-arc areas. — *Geophys. Astrophys. Fluid Dynamics*, 13: 95–105.
- БОТТ, М. Н. П. (1971): The Interior of the Earth. — Edward Arnold (Publishers) Ltd., London, 316 pp.
- BRACE, W. F. (1972): Laboratory studies of stick-slip and their application to earthquakes. — *Tectonophysics*, 14: 189–200.
- ČERMÁK, V. (1979): Heat flow map of Europe. — In: V. Čermák and L. Rybach (Editors), *Terrestrial Heat Flow in Europe*. Springer, Berlin–Heidelberg–New York, pp. 3–40.

- GIESE, P., MORELLI, C., and STEINMETZ, L. (1973): Main features of crustal structure in Western and Southern Europe based on data of explosion seismology. — *Tectonophysics*, 20: 367–379.
- GILBERT, F., DZIEWONSKI, A. M. (1975): An application of normal mode theory to the retrieval of structural parameters and source mechanisms from seismic spectra. — *Phil. Trans. R. astr. Soc.*, 278, A: 187–269.
- ИТО, К., КЕННЕДИ, Дж. К. (1972): Экспериментальное изучение перехода базальт-гранатовый гранулит-эклогит. — *Геохимия*, 27, No. 4: 415–427.
- МЯСНИКОВ, В. П., ФАДЕЕВ, В. Е. (1980): Модели эволюции Земли и планет земной группы. — В: А. П. Капица (Редактор), Серия «Физика Земли», т. 5, ВИНТИ, Москва, 232 стр.
- O'CONNELL, R. J., WASSERBURG, G. J. (1972): Dynamics of submergence and uplift of sedimentary basin underlain by a phase-change boundary. — *Revs. Geophys. Space Phys.*, 10: 335–368.
- ПОШГАЙ, К. (1977): Сейсмические отражающие границы и распределение скоростей в земной коре и мантии. — В: Соллогуб, В. Б. и Чекунов, А. В. (Редакторы), Строение земной коры и верхней мантии по данным сейсмических исследований. Наукова Думка, Киев, 272 стр.
- СОЛЛОГУБ, В. Б., ГУТЕРХ, А., ПРОСЕН, Д. (1978): Строение земной коры и верхней мантии Центральной и Восточной Европы. — Наукова Думка, Киев, 286 стр.
- RINGWOOD, A. E., GREEN, D. H. (1969): Phase transitions. — In: Pembroke J. Hart (Editor), *The Earth's Crust and Upper Mantle*; AGU Geophysical Monograph Series, Washington, 736 pp.
- TULLIS, J., YUND, R. A. (1977): Experimental deformation of dry Westerly granite. — *J. Geophys. Res.*, 82: 5705–5718.

К ВОПРОСУ О ВЫЧИЛЕНИИ ПРИЛИВНОГО ПОТЕНЦИАЛА НА ЛУНЕ

by

B. BODRI

Department of Geophysics, Eötvös University, Budapest

(Received: 15th March, 1982)

ABSTRACT

An algorithm designed for calculating different components of the tidal gravity field on the Moon with an accuracy of 0.05%, is presented. The results of some numerical examples obtained by this algorithm are discussed. It is shown that the difference between the corresponding values calculated by present algorithm and by that of Harrison (1963) reaches about 5% in the tidal potential and some 20–30% in the derivatives of this potential by the angle-coordinates. The necessity of calculating lunar tides with a very high accuracy is motivated partly by peculiar features of its internal structure and partly by recent achievements of lunar gravimetry.

Введение

Явление приливов легко описать в нескольких словах. Вследствие воздействия движущихся относительно некоторой планеты небесных тел, на ней возникают периодические изменения гравитационного поля. Зная положение приливообразующих светил относительно этой планеты, предполагаемой абсолютно твердой, можно аналитически описать их приливный гравитационный потенциал, как в точках самой планеты, так и в окружающем ее пространстве. Это так называемое *основное* приливное поле. Кроме того, под действием приливных сил планета деформируется, из-за чего в небольших пределах изменяются как координаты ее точек относительно своего первоначального положения, так и распределение плотности вещества в ее недрах. Оба эффекта приводят к тому, что к основному приливному полю, соответствующему абсолютно твердой планете, добавляется малое приливное гравитационное поле, обусловленное ее деформацией. Величина приливных деформаций зависит от упругих свойств планеты и от распределения плотности в ее недрах. Эффектом следующего порядка малости является влияние на гравитационное поле планеты ее неупругости. Из-за неупругости вещества недр планеты должно существовать так называемое запаздывание в ней приливов, то есть несовпадение фаз максимума или минимума прилива, наблюдаемого на реальной планете и рассчитанного для абсолютно упругой. Таким образом, наблюдение амплитуды реальных приливов на какой-нибудь планете и сравнение их с рассчитанными для абсолютно твердой планеты дало бы информацию о ее плотности и упругих свойствах, а по запазды-

ванию приливов, в принципе, можно было бы судить о неупругих свойствах.

В случае Земли на приливы было впервые обращено внимание именно как на новый метод исследования ее физических свойств. Первые попытки использовать измерение приливных деформаций Земли для получения дополнительной информации о ее внутреннем строении имеют уже почти столетнюю давность. В последней четверти 19 века появились классические работы по теории приливов Кельвина и Дарвина, а уже в 1890 году Ребер-Пашвиц в Потсдаме установил первый прибор, и до настоящего времени остающийся одним из основных приборов для изучения земных приливов, — горизонтальный маятник. Уже к концу 19 века четыре станции: Потсдам, Страсбург, Тенериф и Николаев, оснащенные приборами Ребер-Пашвица, доказали существование периодических приливных уклонений отвеса. Несколько позже, в 1913 году, Швейдаром был установлен бифилярный гравиметр, позволявший наблюдать лунно-солнечные эффекты в изменении силы тяжести. В продолжение более полувека различные виды наблюдений подтвердили взгляды Кельвина и других теоретиков приливов и вместе с данными сейсмологии и движениями полюса сделали возможным более детальное исследование внутреннего строения Земли.

Наряду с этим все возрастающая точность измерений в экспериментальных науках привела к обнаружению эффекта земных приливов во многих явлениях, к которым они на первый взгляд кажутся совершенно непричастными. В действительности каждый прибор, установленный на земной коре, испытывает воздействие деформаций Земли, и при достаточной чувствительности его показания являются систематически возмущенными и должны быть соответственно исправлены, прежде чем они станут пригодными для интерпретации. Базой для вычисления необходимых поправок за влияние земных приливов также является основное приливное поле.

Последние десять лет, подобно началу нашего века для науки о земных приливах, являются революционным временем для гравиметрии Луны. Безусловно, общие принципы, характеризующие приливы, остаются для Луны такими же, как для Земли, однако имеются и существенные специфические различия. В главной задаче: исследовании внутреннего строения Луны с помощью приливов, — этим различием является тот факт, что влияние упругости Луны на приливы примерно на порядок меньше, чем для Земли, что требует соответствующего повышения как экспериментальной точности, так и точности вычисления компонент основного прилива, соответствующего абсолютно твердой Луне, поскольку, как уже было замечено, именно основное приливное поле служит эталоном для сравнения при выделении упругих эффектов. Повышение точности вычисления основного приливного поля потребовалось также и в связи с тем, что гравитационное поле используется для расчета полета ракет и искусственных спутников и в инерциальной навигации. И наконец, фундаментальным фактом, открытым в семидесятых годах в процессе проведения лунного сейсмического эксперимента, было обна-

ружение приливной периодичности в активности лунотрясений. К настоящему времени уже установлено, что приливы играют основную роль в генерации лунотрясений. Хотя характер конкретного механизма этого влияния до сих пор не ясен, важность изучения приливов на Луне не подлежит сомнению.

Настоящая статья посвящена одному из основных вопросов теории приливов — аналитическому описанию приливного гравитационного потенциала для абсолютно твердой Луны. Первая попытка такого рода была сделана в работе НАВКИСОН (1963), однако в связи с успехами более чем десятилетнего активного гравиметрического изучения Луны к точности расчета основного приливного потенциала стали предъявляться гораздо более высокие требования, чем те, которым удовлетворяет работа Харрисона. В данной работе выводятся более точные выражения для основного приливного поля.

Приливообразующий потенциал на Луне

Известно, что приливный потенциал в некоторой точке P Луны (см. рис. 1) возникает как разность гравитационных воздействий приливообразующего светила на эту точку и на центр масс Луны. Пусть M — масса приливообразующего тела, находящегося в точке E , R' — расстояние рассматриваемой точки до приливообразующего тела, R — расстояние от этого тела до центра масс Луны O , a — расстояние от центра масс Луны до рассматриваемой точки P , z — зенитное расстояние приливообразующего тела в этой точке. Приливный потенциал в этих величинах выражается с помощью известного разложения в ряд по зональным сферическим гармоникам (см., например, ВАЙТЕЛЬС, 1957):

$$W(P) = \frac{GM}{R} \sum_{n=2}^{\infty} \left(\frac{a}{R}\right)^n P_n(\cos z), \quad (1)$$

где n — порядок сферической гармоники,
 G — гравитационная постоянная.

Отношение $(a/R)^n$ быстро убывает с ростом степени n . Так для Земли $a_{\oplus}/R_{\oplus} \approx 5 \times 10^{-3}$, а для Солнца $a_{\odot}/R_{\odot} \approx 10^{-5}$, то есть каждый последующий член разложения (1) меньше предыдущего для Земли более чем на два порядка, а для Солнца почти на пять порядков. Поэтому обычно при расчете потенциала от Земли, если требуется точность около 1%, то третьей гармоникой можно пренебречь. Для солнечного потенциала необходимо учитывать лишь вторую гармонику. Легко также показать, что отношение главного члена приливного потенциала от Солнца $(W_{\odot})_2$ к такому же земному члену $(W_{\oplus})_2$ составляет

$$\frac{(W_{\odot})_2}{(W_{\oplus})_2} = \frac{M_{\odot}}{M_{\oplus}} \left(\frac{a_{\oplus}}{a_{\odot}}\right) \approx 6 \times 10^{-3},$$

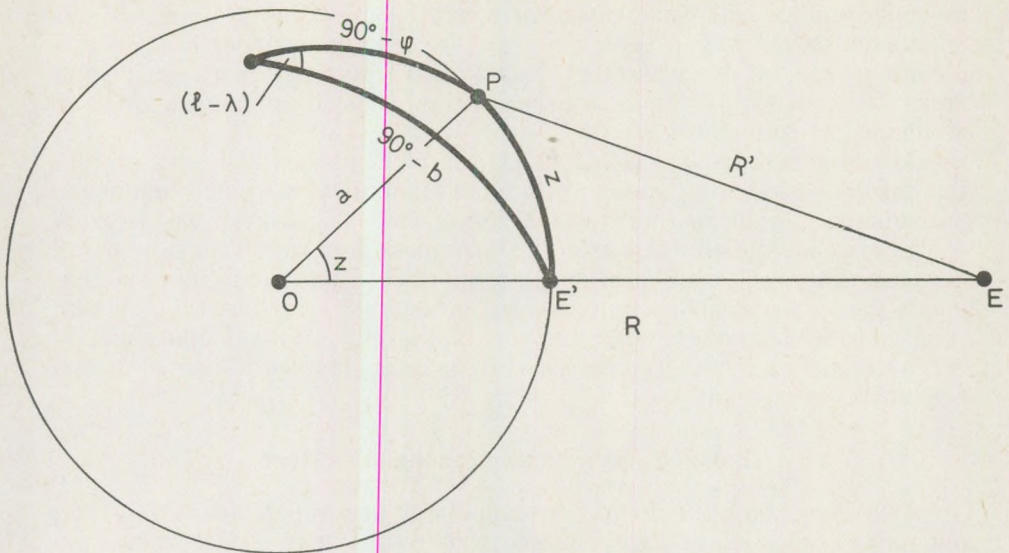


Рис. 1. Геометрические соотношения при определении приливного потенциала в точке P.

то есть максимальный солнечный прилив более чем в сто раз меньше земного. Поэтому часто в расчетах пренебрегают и приливным гравитационным потенциалом Солнца.

Для наблюдателя, находящегося на поверхности Луны, зенитное расстояние z возмущающего тела удобнее выразить через селенографические координаты точки наблюдения (φ, λ) и селеноцентрические экваториальные координаты (b, l) приливообразующего небесного тела. Из параллактического треугольника $E'PN$ на рис. 1, где N — северный полюс Луны, с помощью формул сферической тригонометрии легко получить:

$$\cos z = \sin \varphi \sin b + \cos \varphi \cos b \cos (l - \lambda). \quad (2)$$

Подставив (2) и (1) и используя теорему сложения сферических функций, главный член выражения (1) можно привести к следующему виду:

$$W_2(P) = \frac{1}{12} \frac{GMa^2}{R^3} [12 P_{20}(\sin \varphi) P_{20}(\sin b) + \quad (3)$$

$$+ P_{22}(\sin \varphi) P_{22}(\sin b) \cos 2(l - \lambda) + 4P_{21}(\sin \varphi) P_{21}(\sin b) \cos(l - \lambda)],$$

то есть представить главную гармонику приливного потенциала в виде суммы трех слагаемых, соответствующих трем типам сферических функций второго порядка: зональной, секториальной и тессеральной. Разделение земного прилива соответственно трем типам сферических функ-

ций и их геометрическая интерпретация впервые было проведено Лапласом.

На Луне главная зональная волна с периодом 27,555 суток (средний аномалистический месяц) вызвана эксцентриситетом лунной орбиты. Она зависит только от широты места наблюдения, симметрична относительно лунного экватора и обращается в ноль на параллелях $\varphi = \pm 35^\circ, 26'$. Кроме того, поскольку наблюдаются заметные вариации лунного эксцентриситета (0,0432—0,0666), возникающие из-за солнечных возмущений лунной орбиты, то на основную волну накладываются модуляции с периодом около 206 дней, вызванные периодическими значительными изменениями расстояния от Земли до Луны.

Главную секториальную волну вызывает оптическая либрация Луны по долготе, происходящая также с периодом 27,555 суток. Эта либрация возникает в результате того, что Луна, двигаясь по эллиптической орбите с переменной угловой скоростью, вращается равномерно вокруг своей оси. Разница в скоростях вращения и обращения приводит к колебаниям лунного лимба вдоль экватора с максимальной амплитудой $\pm 8^\circ$. Нулевыми линиями для этого типа приливов являются меридианы, расположенные на расстоянии $\pm 45^\circ$ от меридиана возмущающего тела. Эти меридианы делят сферу на четыре сектора, в которых прилив поочередно принимает положительные и отрицательные значения. Приливная картина симметрична относительно меридиана приливообразующего тела. Максимальный прилив возникает на экваторе при нулевой широте возмущающего тела.

Главную тессеральную волну с периодом 27,212 дней (драконический месяц) вызывает оптическая либрация Луны по широте. Либрация по широте связана с тем фактом, что ось вращения Луны не перпендикулярна к плоскости ее орбиты и наклон оси остается постоянным. Таким образом, в течение месяца Луна часть времени наклонена к Земле своим северным полюсом, а часть — южным, в результате чего смещения объектов лунного лимба по широте в селенографических координатах могут достигать $\pm 6^\circ, 68'$. Тессеральная волна обращается в ноль на экваторе и на меридиане, отстоящем на 90° от меридиана возмущающего светила, относительно которого она симметрична. Знак прилива в областях, на которые нулевые линии делят сферу, меняется в соответствии с изменением знака широты приливообразующего тела b . Амплитуда прилива максимальна на широтах $\pm 45^\circ$ при максимальной широте возмущающего тела.

Как видим, картина приливного потенциала на Луне существенно отличается от земной. Периоды изменения основных лунных приливных волн равны или очень близки, все зональные, тессеральные и секториальные члены относятся к идентичным долгопериодическим волнам, которые производят приливы примерно одинаковой амплитуды, хотя конкретный вклад каждой из волн в общий прилив существенно зависит от места наблюдения на поверхности Луны. Общее распределение приливного потенциала поэтому очень сложно, а отдельные члены не могут быть выделены с помощью гармонического анализа наблюдений, в отличие

от случая значительно отличающихся по частоте земных приливных волн. Поэтому для лунных приливов выгоднее для каждой точки пользоваться прямым вычислением по формулам (1), (2), в которых переменными являются лишь три величины: R , b и l . Эти величины вычисляются с помощью тригонометрических рядов пяти аргументов:

$$\begin{aligned} s &= 270.43659^{\circ} + 481267.89057^{\circ} T + 0.00198^{\circ} T^2 + 0.000002^{\circ} T^3, \\ p &= 334.32956^{\circ} + 4069.03403^{\circ} T - 0.01032^{\circ} T^2 - 0.00001^{\circ} T^3, \\ h &= 279.69668^{\circ} + 36000.76892^{\circ} T + 0.00030^{\circ} T^2, \\ N &= 259.18328^{\circ} - 1934.14201^{\circ} T + 0.00208^{\circ} T^2 + 0.000002^{\circ} T^3, \\ p_s &= 281.22083^{\circ} + 1.71902^{\circ} T + 0.00045^{\circ} T^2 + 0.000003^{\circ} T^3. \end{aligned} \quad (4)$$

В формулах (4) T — время в юлианских столетиях, s — средняя долгота Луны, измеряемая от даты среднего равноденствия, p — средняя долгота лунного перигея, N — средняя долгота восходящего узла лунной орбиты, h — средняя долгота Солнца, p_s — средняя долгота солнечного перигея. Все величины, так же, как s , измеряются от даты среднего равноденствия.

Брауном в начале нашего века (Brown, 1919) были составлены таблицы по которым до настоящего времени вычисляются эфемериды Луны. Во второй половине нашего века эти таблицы были лишь несколько усовершенствованы с помощью быстродействующих электронно-вычислительных машин. При этом были устранены некоторые несовершенства таблиц Брауна, что позволило значительно повысить точность определения лунных эфемерид. Формулы для вычисления координат Луны, представленные ниже, приведены в обзоре Монтсуласа (1971).

Так, величина R^{-1} в единицах среднего расстояния между центрами Земли и Луны R_0 может быть представлена в форме:

$$\begin{aligned} R_0/R &= 1 + 10^{-6} [54\,501 \cos(s-p) + 8249 \cos 2(s-h) + 2970 \cos 2(s-p) + \\ &+ 1025 \cos(s+p-2h) + 902 \cos(3s-2h-p) + \\ &+ 560 \cos(2s-3h+p_s) + 422 \cos(s-3h+p+p_s) + \\ &+ 337 \cos(s-p-h+p_s) - 286 \cos(s-h) - 277 \cos(s+h-p-p_s) - \\ &- 208 \cos(s+p) + 182 \cos 3(s-p) + 176 \cos(3s-4h+p) - \\ &- 117 \cos(h-p_s) + 109 \cos 2(s+p-2h) - 89 \cos 2(h-p) - \\ &- 88 \cos(2s-p_s-h) + 83 \cos(4s-2p-2h) + 76 \cos 4(s-h) + \\ &+ 67 \cos(3s-3h-p+p_s) - 66 \cos(s+p-h-p_s) + \dots]. \end{aligned} \quad (5)$$

В разложении (5) автор ограничился только основными членами, отбрасывая гармоники, амплитуды которых не превышают 5×10^{-5} . На основании формулы (5) легко могут быть получены разложения для $(R_0/R)^3$ и $(R_0/R)^4$, входящие в гармоники второго и третьего порядка.

Эти формулы из-за их громоздкости в данной работе не приводятся. Заметим лишь, что первую из этих величин нужно знать с той же точностью, что и R_0/R , во второй же достаточно оставить лишь члены, превышающие 1×10^{-3} .

Аналогично выглядят формулы для селеноцентрической широты и долготы Луны, в которых были удержаны лишь члены с амплитудой не менее 1×10^{-4} радиана:

$$\begin{aligned}
 -b = 10^{-4} [& 895 \sin(s-N) + 49 \sin(2s-p-N) - 48 \sin(p-N) - \\
 & - 30 \sin(s-2h+N) + 10 \sin(2s-2h+p-N) + \\
 & + 8 \sin(-2s+3p-2p_s+N) + 6 \sin(3s-2h-N) + \\
 & + 3 \sin(3s-2p-N) + 2 \sin(2s-p-2h+N) - \\
 & - 2 \sin(-s+2p-N) + \sin(s-3h+p_s+N) + \\
 & + \sin(-s+2p-2h+N) + \sin(4s-p-2h-N) - \\
 & - \sin(s-h-p_s+N)],
 \end{aligned} \tag{6}$$

$$\begin{aligned}
 l = 10^{-4} [& 1098 \sin(s-p) + 222 \sin(s-2h+p) + 115 \sin 2(s-h) + \\
 & + 37 \sin 2(s-p) + 32 \sin(-h+p_s) - 20 \sin 2(s-N) + \\
 & + 10 \sin 2(-h+p) + 10 \sin(s+p-3h+p_s) + 9 \sin(3s-p-2h) + \\
 & + 8 \sin(2s-3h+p_s) + 7 \sin(s-h-p+p_s) - 6 \sin(s-h) + \\
 & + 5 \sin(-s+p-h+p_s) + 2 \sin 3(s-p) + 3 \sin 2(N-h) - \\
 & - 2 \sin(3s-p-2N) + 2 \sin(3s+p-4h) - 2 \sin(s+p-2N) + \\
 & + \sin(2s+2p-4h) - \sin(s-h+p-p_s) - \sin(2s+h-3p_s) - \\
 & - \sin(-h+p) + \sin(s-p_s) + \sin(3s-p-3h+p_s) + \\
 & + \sin(4s-2p-2h) + \sin 4(s-h) + \sin(-s-2h+3p)].
 \end{aligned} \tag{7}$$

И наконец, поскольку зенитное расстояние Земли в каждой точке Луны изменяется всего в пределах нескольких градусов относительно некоторого нулевого направления, соответствующего среднему зенитному расстоянию Земли \bar{z} в данной точке поверхности Луны

$$\cos \bar{z} = \cos \varphi \cos \lambda,$$

и углы b и l малы, то целесообразно представить приливообразующий потенциал в виде некоторой постоянной части, зависящей только от положения точки наблюдения на поверхности Луны, и переменной, выраженной в виде ряда по степеням b и l :

$$\begin{aligned}
 P_2(\cos z) = & P_2(\cos \bar{z}) + b \left(\frac{3}{2} \sin 2\varphi \cos \lambda \right) + l \left(\frac{3}{2} \cos^2 \varphi \sin 2\lambda \right) + \\
 & + \frac{3b^2}{2} (1 - \cos^2 z - \cos^2 \varphi) - \frac{3l^2}{2} \cos^2 \varphi \cos 2\lambda + \frac{3bl}{2} \sin 2\varphi \sin \lambda - \\
 & - b^3 \sin 2\varphi \cos \lambda - l^3 \cos^2 \varphi \sin 2\lambda - \frac{3b^2 l}{2} \cos^2 \varphi \sin 2\lambda - \frac{3bl^2}{4} \sin 2\varphi \cos \lambda.
 \end{aligned} \tag{8}$$

Заметим, что тот факт, что в приливном потенциале на Луне присутствует значительная постоянная часть, также существенно отличает его от потенциала на Земле. Выражение (8) представляет собой ряд функций $P_2(\cos z)$, в котором были удержаны только третьи степени аргументов. Аналогично находится разложение для члена $(5/2 \cos^2 z - 3/2 \cos z)$ — третьей гармоники приливного потенциала. В этом разложении, которое не приводится здесь с целью экономии места, достаточно удержать лишь вторые степени величин b и l .

Таким образом, потенциал от Земли полностью определен. В приливном потенциале от Солнца, как уже упоминалось выше, достаточно учесть лишь вторую гармонику. Вид формул для вычисления расстояния Солнце—Луна и селеноцентрических широты и долготы Солнца, много проще формул (5)—(7). Они также не приводятся в данной работе, поскольку с достаточной точностью даны в статье HARRISON (1963).

Исследование точности вычисления основного приливного поля

Земно-солнечный приливный потенциал на поверхности Луны, вычисленный на основании вышеописанного алгоритма, представлен на рис. 2. Как видно из рис. 2, приливный потенциал в центре диска Луны колеблется около постоянного значения $21 \text{ м}^2/\text{сек}^2$ с амплитудой примерно $3 \text{ м}^2/\text{сек}^2$, то есть максимальное изменение потенциала в центре диска Луны составляет $6-7 \text{ м}^2/\text{сек}^2$. Однако для сравнения с лунно-солнечным приливом на Земле лучше брать обычно измеряемые в приливной практике величины изменения ускорения силы тяжести

$$\Delta g = -\frac{\partial W}{\partial a}$$

и уклонение отвеса

$$e_\varphi = \frac{1}{ag} \frac{\partial W}{\partial \varphi}, \quad e_\lambda = -\frac{1}{ag \cos \varphi} \frac{\partial W}{\partial \lambda}, \quad (9)$$

где g — ускорение силы тяжести. Пользуясь формулами (9) и алгоритмом вычисления приливного потенциала, легко рассчитать, что для твердой Луны максимальная постоянная часть приливного ускорения силы тяжести составляет $2,5 \text{ мГал}$ и изменяется с амплитудой около 1 мГал . Уклонение же отвеса по каждой из компонент изменяется более чем на $0'',5$ около постоянного значения $2'',3$. Для сравнения отметим, что на Земле переменная часть ускорения силы тяжести составляет примерно $0,24 \text{ мГал}$, а уклонений отвеса $0'',05$. Поскольку точность лучших современных гравиметров равна примерно $0,015 \text{ мГал}$, а горизонтальных маятников $0,010 \text{ мсек}$ (Мельников, 1978), легко видеть, что амплитуда изменения даже наименее точно измеряемого клинометрического прилива для Луны на четыре-пять порядков превышает точность приборов.

Из-за большей точности в вычислении земных членов приливный потенциал, приведенный на рис. 2, отличается от рассчитанного по алгоритму Харрисона в среднем на 5% . Абсолютная точность вычисления

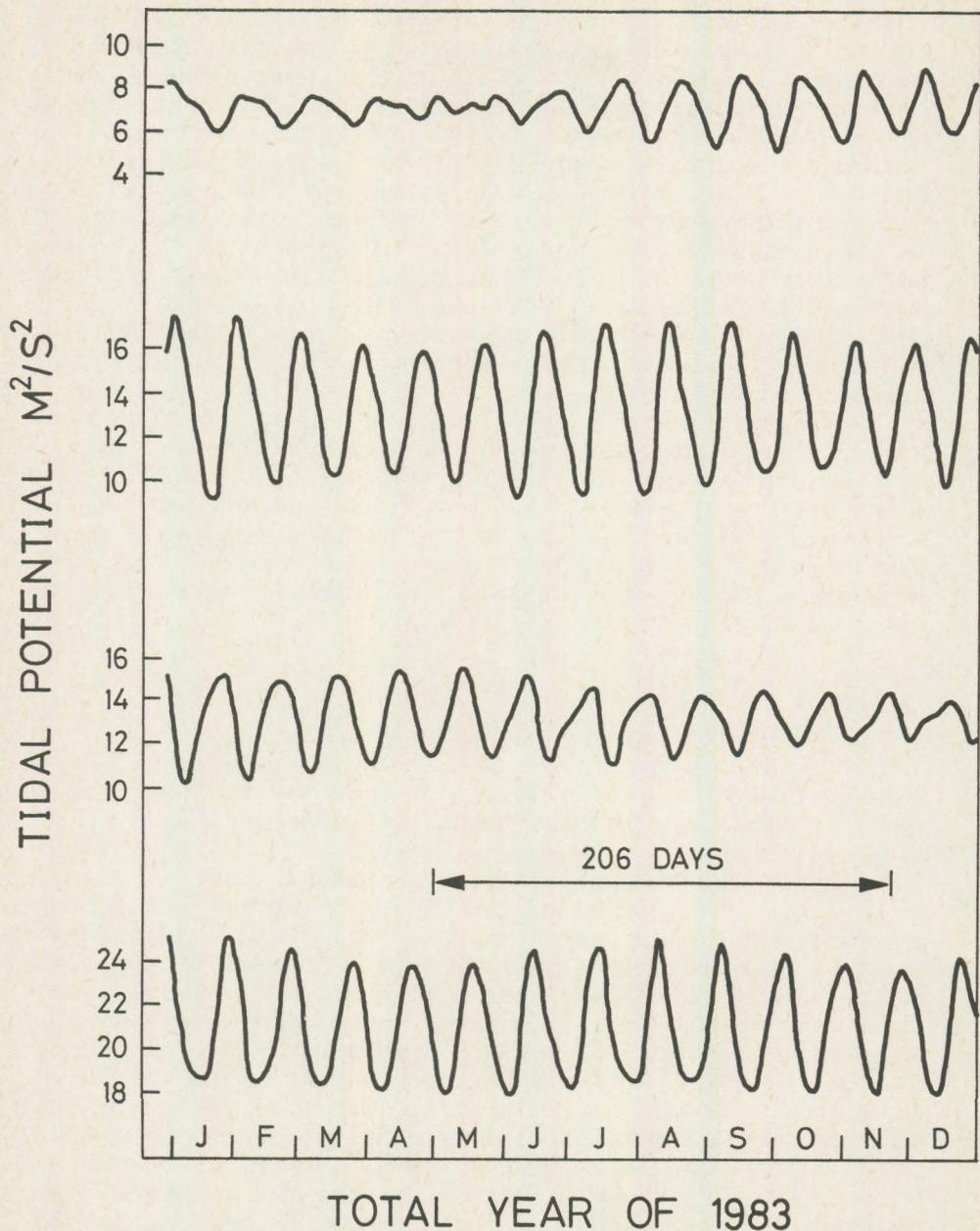


Рис. 2. Приливный потенциал на поверхности Луны в 1983 г.

ускорения силы тяжести по этому алгоритму не превышает $\pm 0,01$ мГал, что уже сравнимо с точностью измерений, то есть при интерпретации измерений с использованием основного поля в качестве эталона может существенно снизить точность интерпретации. Алгоритм, предложенный в настоящей работе, позволяет вычислять приливные изменения силы тяжести с точностью не ниже $\pm 0,0005$ мГал. Поскольку влияние упругости Луны составляет лишь 1–3% от основного поля, то задавшись целью регистрировать этот эффект с относительной точностью хотя бы 10%, необходимо силу тяжести измерять с точностью 1–3 мкГал, а отклонение отвеса с точностью до тысячных долей угловой секунды. По крайней мере такая же точность необходима и в вычислении основного поля. Для сравнения напомним, что эффект, обусловленный упругими свойствами Земли, в изменениях силы тяжести составляет 20%, а в изменениях отклонений отвеса 30%.

Еще более существенны различия между алгоритмом Харрисона и предложенным в настоящей работе в производных потенциала по угловым координатам. Эти отклонения достигают в среднем 20–30%, что в свою очередь вносит такую же ошибку в вычисление приливных напряжений и смещений в Луне. Поскольку приливные напряжения являются либо непосредственной причиной лунотрясений, либо их спусковым механизмом, то не вызывает сомнений необходимость высокой точности их вычисления.

Заключение

Изучение гравитационного поля Луны началось с запусков искусственных спутников Луны. Обращает на себя внимание различие исторической последовательности применения различных методов определения гравитационного поля Луны и Земли. Для Земли спутниковые методы начали использоваться уже тогда, когда ее гравитационное поле в общем было изучено с помощью гравиметров и маятниковых приборов. Каждый из методов, спутниковый и гравиметрический, имеет свои преимущества и недостатки. Первый из них позволяет более надежно определять гармоники низких порядков в гравитационном поле, а второй — высоких порядков. Определения силы тяжести непосредственно на поверхности Луны только начинаются. В настоящее время известно только четыре измерения силы тяжести с помощью гравиметров, установленный на Аполлоне—11, —12, —14 и —17, совершивших мягкую посадку на Луну. Измерения силы тяжести вдоль профиля на лунной поверхности были произведены специальным гравиметром, установленным на луноходе, доставленным на Луну кораблем Аполлон—17. Делом ближайшего будущего является установка на Луне гравиметров непрерывной регистрации и градиентометров, установленных на ИСЛ и позволяющих изучать высокочастотную часть гравитационного поля. Теоретическое изучение гравитационного поля Луны, одному из аспектов которого посвящена настоящая работа, будет необходимо как при планировании будущих экспериментов, так и при интерпретации их результатов.

ЛИТЕРАТУРА

- BARTELS, J. (1957): Gezeitenkrafte, Encyclopedia of Physics, 48 Geophysics, 2. — Springer Verlag, Berlin, pp. 734—774.
- BROWN, E. W (1919): Tables of the Motion of the Moon. — Yale Univ. Press, New Haven, Connecticut, 114 pp.
- HARRISON, J. C. (1963): An analysis of the lunar tides. — J. Geophys. Res., 68: 4269—4280.
- MELCHIOR, P. (1978): The Tides of the Planet Earth. — Pergamon Press, Oxford, 609 pp.
- МОУТСУЛАС, М. Д. (1973): Либрации Луны. — В книге: «Физика и астрономия Луны», ред. З. Копал, изд. «Мир», Москва, стр. 36—70.

CLIMATOLOGICAL FACTORS IN REGULATING THE WATER-LEVEL OF LAKE VELENCE

by

F. RÁKÓCZI

Department of Meteorology, Eötvös University, Budapest

K. KORIS

Department of Water Management, Technical University, Budapest

(Received: 15th March, 1982)

РЕЗЮМЕ

В работе дается отчет о проблеме регулирования уровня воды в озере Веленце. Прогнозируются величины, необходимые для решения уравнения водного баланса $\Delta W = P + I - E$. Установление необходимых для прогнозирования функций плотности производится на основании информации о месячных суммах исследуемых элементов.

Introduction

Lake Velence is situated not far from the capital of Hungary. The total area of its water-surface is 24.9 sq.km, of which 10.3 sq.km is free, the remaining 14.6 sq.km being covered by reed. The volume of its water is 36.1×10^6 c.m with an average depth of 1.45 m at a 140 cm water-level at Agárd. The optimal values for the above data are: 25.28 sq.km, 10.30 sq.km, 14.98 sq.km, 41.16×10^6 cóm and 1.62 m, respectively, with 160 cm water-level at Agárd.

To obtain the optimal water-surface, two reservoirs have been built for regulating the water-level of the lake, because the great importance of the small lake as a resort area is further emphasized by its vicinity to the capital.

1. The method of regulation

For the regulation of the water-level of the lake, a stochastic model has been developed on the basis of Bayes' theorem. According to the simple water-household equation

$$\Delta W = P + I - E \quad (1.1)$$

where ΔW is the natural change of water resources; P is the monthly amount of precipitation and E represent the value of monthly evaporation and I is the monthly inflow. The solution of this equation requires the knowledge of some climatological parameters. ΔW and P have a stochastic character, nevertheless, they can be measured or sometimes estimated from the reports of the observation network. I and E are of a stochastic character too, but their values cannot be measured. They must be estimated

from the data obtained from the climatological network. P is measured directly.

For the regulation of the water-level there is a system of sluices, and the question is how to use them for the optimization of the water-level. In order to develop a suitable method, we had to take into consideration both the hydrological and the climatological factors.

Using to Bayes' method, a loss-function was introduced and this function was minimalized. For this purpose we estimated the $f(\Delta W)$ density function and the other density functions — $f(P)$, $f(I)$ and $f(E)$, too. Bayes' theorem requires the forecast of density functions, for which a method is proposed in this paper. The theoretical basis for the forecasting is the information theory introduced by SHANNON (1948).

2. The estimation of potential evaporation

For the estimation of potential evaporation a modified form of the aerodynamical method was used. This method requires the knowledge of the air temperatures and the temperatures of the water-surface as well as the values of wind-speed and of moisture.

The brief description of the method is the following:

Let us design specific humidity by q . In this case, for the evaporation E we can write:

$$E = -\rho K \frac{\partial q}{\partial z}. \quad (2.1)$$

According to the theory of turbulent diffusion

$$K = k u_* z \quad (2.2)$$

and so we obtain

$$E = -\rho k u_* z \frac{\partial q}{\partial z}. \quad (2.3)$$

We can write eq. (2.3) in the form

$$E = -\rho k u_* \frac{\partial q}{\partial (\ln z)}, \quad (2.4)$$

too. Then introducing the quantities

$$\Gamma = -\frac{1}{g_f - q} \frac{\partial q}{\partial (\ln z)} \quad (2.5)$$

and

$$u_* = \frac{k \bar{u}}{\ln(z/z_0)}, \quad (2.6)$$

as well as

$$k_1 = \frac{k}{\ln(z/z_0)} \quad (2.7)$$

we obtain from (2.4)

$$E = \rho k k_1 \bar{u} \Gamma (q_f - q) . \quad (2.8)$$

From the definition of specific humidity it can be written

$$q = 0.623 \frac{\varepsilon}{E} . \quad (2.9)$$

By using constants $\rho = 1.29$ (kg m^{-3}), $k = 0.4$ (KÁRMÁN'S constant), $k_1 = 0.059$ and $\Gamma = 0.148$ (MONTGOMERY-coefficient), we obtain a working-formula for the estimation of the potential evaporation of water-surface:

$$E = 9.8 \times 10^{-4} (\varepsilon_f - \varepsilon) u \quad [\text{cm h}^{-1}] , \quad (2.10)$$

where ε is the vapour pressure in mbar and \bar{u} denotes the wind-speed (in m s^{-1}).

We used the above formula for the estimation of the monthly amount of potential evaporation by using the monthly average of climatological data. For the estimation, the period from 1900 to 1970 was used. The monthly amounts of potential evaporation were calculated for every month and, after it, the empirical density functions of potential evaporation were determined. The data on the yearly variation of potential evaporations are listed in TABLE I.

TABLE I.

Yearly variation of potential evaporation of Lake Velence
(in mm)

	J	F	M	A	M	J
Average	9.3	13.9	34.2	66.1	105.8	133.1
Maximum	16.5	34.2	62.9	116.2	162.3	203.0
Minimum	3.3	2.1	8.5	28.6	45.7	60.9
	J	A	S	O	N	D
Average	179.4	128.8	74.3	34.8	14.9	9.5
Maximum	288.9	268.7	143.4	72.3	34.6	32.6
Minimum	58.3	38.5	31.0	18.9	5.9	2.9

According to the data on TABLE I, the amount of the potential evaporation has a maximum value in July and a minimum one is January. The difference between the maximum and minimum values within each month is considerable, thus the stochastic character of evaporation is very strong. This fact is confirmed by the values of standard deviations, too.

3. The monthly amount of precipitation in the area of Lake Velence

In this paper the precipitation field of the area of Lake Velence is characterised by the territorial average of the monthly amounts of precipitation. For this purpose we used the time series of precipitation stations. The yearly variation of precipitation is presented in TABLE II.

TABLE II.

Yearly variation of monthly amounts of precipitation (in mm)					
J	F	M	A	M	J
36.3	37.5	41.3	48.2	65.0	50.0
J	A	S	O	N	D
59.9	47.4	51.6	53.0	62.0	50.0

The monthly amounts of precipitation have two maxima, one in May and another one in November. This type of yearly variation of precipitation is characteristic for this part of Hungary.

The normal deviations of values are considerably characterised by the quotient σ/m , where σ denotes the standard deviation and m represents the mean values. The values of σ/m are listed in TABLE III.

TABLE III.

Yearly variation of σ/m					
J	F	M	A	M	J
0.494	0.694	0.647	0.525	0.479	0.840
J	A	S	O	N	D
0.689	0.732	0.629	0.767	0.670	0.462

On the basis of the data in TABLE III. the σ/m quotient has a maximum in June and a minimum in December. The character of the yearly variation of σ/m is more complicated than in the case of monthly amount of precipitation. It means that the nature of precipitation cannot be characterised by the monthly amount of precipitation alone, therefore the density functions of precipitation must also be taken into consideration for our purposes. These functions have also been calculated and a logarithmical type of the distributions has been found for the precipitation.

4. The information-quantity

To carry out our programme, namely, to regulate the water-level of Lake Velence, it is necessary to forecast the quantities in (1.1). By the expression "forecast" in this paper we mean a statistical prediction.

The theoretical basis for forecasts is information theory. This theory has been used in some cases for solving meteorological problems by Rákóczy (1972).

According to this theory, the degree of relationship between two events can be measured by the information-quantity.

Let us denote one of the events by X and the other one by Y . In this case the statistical entropy of event X is defined by

$$H(X) = - \sum_{i=1}^n p_i \log p_i \quad (4.1)$$

and the statistical entropy of even Y is expressed by

$$H(Y) = - \sum_{j=1}^m w_j \log w_j \quad (4.2)$$

where p_i denotes the probability of event X_i , and w_j is the same for the event Y_j .

(4.1) and (4.2) measure the uncertainty of the events. If the probabilities for the event X_1, X_2, \dots, X_n and Y_1, Y_2, \dots, Y_m are the same, $H(X)$ and $H(Y)$ respectively have maximum values. In other words, $H(X)$ has a maximum, if for every primary event $p_i = 1/n$ in the event field of X . If $p(X_i) = 1$ and $p(X_j) = 0$ when $i \neq j$, then $H(X) = 0$, because the uncertainty of the event in this case is zero. The same is valid for $H(Y)$, too.

We can use the concept of conditional entropy $H_x(Y)$, too. This quantity gives information about Y if we know the realization of event X . Events X and Y are independent if $H_x(Y) = H(Y)$, i.e. in the case of the knowledge of event X gives no information for the event Y . If $H_x(Y) = 0$, it implies that knowing X we know everything about event Y too. Therefore, it is possible to measure our knowledge quantitatively by the difference between $H(Y)$ and $H_x(Y)$:

$$I(X, Y) = H(Y) - H_x(Y). \quad (4.3)$$

In information theory the quantity $I(X, Y)$ is called quantity of information. This quantity is a measure of the degree of relationship between events X and Y , quantitatively. This particularity of the quantity of information was used in this work for searching for the predictors.

To find the predictors, we determined the internal relationship between the monthly amounts of precipitation on the basis of the information theory. The whole sample of precipitation was divided into three parts with equal probabilities. The contingency levels are given in TABLE IV for the precipitations and in TABLE V for the potential evaporations.

TABLE IV.

Contingency values of precipitation

	A ₂	A ₂	A ₃
J	28.58	28.58 - 44.02	44.02
F	26.31	26.31 - 48.69	48.69
M	29.80	29.80 - 52.80	52.80
A	37.31	37.31 - 59.09	59.09
M	51.61	51.61 - 78.39	78.39
J	31.93	31.93 - 68.07	68.07
J	40.04	40.04 - 73.76	73.76
A	32.47	32.47 - 62.33	62.33
S	37.63	37.63 - 65.57	65.57
O	35.50	35.50 - 70.50	70.50
N	44.12	44.12 - 79.88	79.88
D	40.04	40.04 - 59.96	59.96

TABLE V.

Contingency values of potential evaporation

	B ₁	B ₂	B ₃
J	8.01	8.01 - 10.59	10.59
F	11.10	11.10 - 16.70	16.70
M	28.32	28.32 - 40.08	40.08
A	57.86	57.86 - 74.34	74.34
M	94.78	94.78 - 116.98	116.98
J	117.09	117.09 - 149.11	149.11
J	156.39	156.39 - 202.41	202.41
A	107.75	107.75 - 149.85	149.85
S	62.98	62.98 - 85.62	85.62
O	29.52	29.52 - 40.08	40.08
N	11.58	11.58 - 18.22	18.22
D	7.05	7.05 - 11.95	11.95

After having calculated the contingency levels, one can determine the contingency tables for the precipitation as well as for the potential evaporation. With the help of such tables $H(X)$ and $H(Y)$ can be calculated from month to month from the marginal distributions. In the same way, from the two dimensional distribution the value of $H(X, Y)$ can also be determined for

$$H(X, Y) = H(X) + H_x(Y) \quad (4.4)$$

and $I(X, Y)$ is defined by (4.3). By substituting (4.3) into (4.4) we obtain

$$I(X, Y) = H(X) + H(Y) - H(X, Y). \quad (4.5)$$

Therefore, on the basis of the contingency tables the values of $I(X, Y)$ can be calculated. The results of our calculations are listed in TABLE VI. for precipitation and in TABLE VII. for potential evaporation.

TABLE VI.

	I.	II.	III.	IV.	V.	VI.	VII.	VIII.	IX.	X.	XI.	XII.
I.	—	0.0849	.0169	.1149	.0889	.0504	.0305	.0300	.0287	.0344	.0332	.1351
II.			.0396	.0623	.0080	.0643	0.811	.0210	.0803	.0492	.0436	.0112
III.				0.453	.0253	.0023	.0601	0.818	.0402	.1521	.0500	.0310
IV.					.0359	.0261	.0509	.0510	.1666	0.407	.0198	.0248
VI.						.0710	.0172	.0483	.0151	.0372	.0343	.0985
VII.							0.351	.0191	.0552	.0209	.0559	.0095
VIII.								.0304	.1108	.0515	.0751	.0679
IX.									.0501	.0421	.0627	.0148
X.										.1540	.0273	.0431
XI.											.0094	.0322
												.0319

The data in TABLE VI. represent the measure of the degree of relationship between the months. E.g. the value 0.0504 in the first line of column 6 indicated that there is a moderate relationship between the amount of precipitation in January and June.

TABLE VII.

	I.	II.	III.	IV.	V.	VI.	VII.	VIII.	IX.	X.	XI.	XII.
XII.	.0408	.0493	.0226	.0703	.0404	.0780	.1048	.0551	.0131	.0096	.0539	
XI.	.0521	.0929	.0448	.0221	.0222	.0418	.0186	.0029	.0345	.0388		
X.	.0278	.0185	.0429	.0867	.0805	.0303	.0155	.0427	.0434			
IX.	.0019	.0146	.0255	.0754	.0157	.0328	.0493	.0848				
VIII.	.0727	.0675	.0545	0.366	.1074	.0237	.0201					
VII.	.0289	.0263	.0473	.0826	.0857	.0476						
VI.	.0097	.0210	.0483	.0292	.0611							
V.	.0035	.0699	.0318	.0072								
IV.	.0324	.0273	.0193									
III.	.0216	.0336										
II.	.0116											

TABLE VII. has a similar construction. The monthly amounts of precipitation and the monthly amounts of evaporation providing the greatest informations will be the predictors for precipitation and evaporation, respectively, for the reference months. For the predictor and predictant physical values are the same, because we use the internal relationship between them.

5. The forecast ing procedure

In TABLES V and V the values of A_k and B_2 ($1 \leq k \leq 12$), the quantities giving the limit of terciles of the amount of precipitation and of potential evaporation are listed. It is known that the intervals $x < A_k$, $A_k \leq x \leq B_k$ and $x > B_k$ we have the same number of sample elements.

In the process of estimation we do not make any effort to give the values of the elements of sample, but we give the probability of the events $x < A_k$, $A_k \leq x \leq B_k$, $x > B_k$.

The essence of this procedure is the following.

1. We denote by i_1, i_2, \dots, i_r the subscripts of the month of the predictor and by k the subscript of the month of the predictant.
2. We determine in which interval of $(-\infty, A_i)$, (A_i, B_i) , (B_i, ∞) the actual data of the i -th month will occur.
3. After this we select the data from a time series in which the values of i_1, i_2, \dots, i_r will occur one after the other in the same interval.
4. On the basis of the data for the given years we calculate the conditional probabilities of the event approaching them in their relative frequencies.

This procedure gives a distribution function of the precipitation and of potential evaporation and these functions have been incorporated into the present regulation programme of the sluices of Lake Velence.

REFERENCES

- GÖTZ, G., RÁKÓCZI, F. (1981): A dinamikus meteorológia alapjai. — Tankönyvkiadó, Budapest. (In Hungarian)
- HALTNER, G. J., MARTIN, F. L. (1957): Dynamical and Physical Meteorology. — McGraw Hill. Co.
- KORIS, K., NAGY, B. (1978): Regulation model of the Lake Velence reservoir system. — Journ. of Hydr. Sci. Vol No. 1.
- RÁKÓCZI, F. (1976): Budapest hőmérsékleti sorának információ tartalma. — Időjárás 80, 2. 86–92. (In Hungarian)

The list of symbols:

A_1, A_2, A_3	
B_1, B_2, B_3	— confidence levels
E	— monthly amount of evaporation
$H(X), H(Y)$	— statistical entropy
$H(X, Y)$	— entropy of two events
I	— monthly amount of inflow
$I(X, Y)$	— quantity of information
K	— turbulent diffusion coefficient
k	— Kármán's constant
P	— monthly amount of precipitation
p	— air pressure
p_i	— probability of event X_i
q, q_f	— specific humidity
\bar{u}	— wind-speed
u_*	— friction speed
w_j	— probability of event Y_j
W	— variation of water level
Γ	— Montgomery's potential-function
ε, \bar{E}	— vapour pressures
ρ	— density of air

UNTERSUCHUNG DER WIRBELGLEICHUNGEN BEI BODENREIBUNG

von

F. RÁKÓCZI

Lehrstuhl der Meteorologie Eötvös Loránd Universität, Budapest

(Eingegangen am 15. 3. 1982)

SUMMARY

The investigations of this paper are based on the equation of atmospherical motion with respect of friction. After the decompose of the pressure force into two parts there is deduced the vorticity equation with respect of friction and baroclinity. The discussion of this equation presents the result that the potential vorticity law can not be valid in currents with friction.

* * *

Die Wirkung der Bodenreibung auf die atmosphärischen Bewegungen untersuchten schon GULDBERG und MOHN (1876). Durch das von ihnen aufgestellte einfache Modell kann man sehr anschaulich die Tatsache erklären, dass in Falle einer Strömung mit Reibung der Windvektor und die Isobaren einen Winkel einschliessen und somit besitzt die Strömung eine auf die Isobare senkrechte Komponente. Das führt in Falle von anizobaren Massenströmung und damit bei Zyklonen zur Auffüllung, und im Falle von Antizyklonen zum Abbau.

Die einfache Konzeption von GULDBERG und MOHN, insbesondere die Vorstellung, dass die Reibung entgegengesetzte Richtung mit dem Windvektor und mit diesem direkt proportional ist, wurde von den Messungen nicht bestätigt. SANDSTRÖM (1910, 1911) zeigte, dass der Windvektor und die Reibungskraft den auf der 1. *Abbildung* zu erkennenden Winkel schliessen.

SANDSTRÖM fand auf statistischem Wege, dass der Durchschnittswert des Winkels über dem Lande 38° beträgt. Die durch $-k \vec{v}$ zu beschreibende Reibungskraft ist in diesem Fall aufspaltbar auf eine Komponente, die senkrecht auf die Windrichtung ist, und eine die parallel zu ihr ist. Natürlich führen die Luftquanten auf Wirkung der Reibungskraft, der Druckgradientkraft und der Ablenkungskraft der Erdrotation eine beschleunigende Bewegung aus, und so ist die Bewegungsgleichung im rechtwinkligen geradelinigen Koordinaten-System die folgende Art aufzuschreiben

$$\frac{du}{dt} - mv + nu = -\frac{1}{\rho} \frac{\partial p}{\partial x}, \quad (1)$$

$$\frac{dv}{dt} + mu + nv = -\frac{1}{\rho} \frac{\partial p}{\partial y}, \quad (2)$$

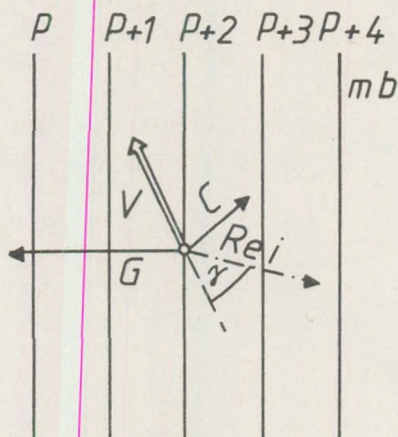


Abb. 1. Kräfteverteilung beim geradlinigen Wind mit Reibung

wobei x, y sind die Koordinaten, u und v sind die Windkomponenten, m und n sind Koeffizienten, ρ ist die Dichte, p ist der Luftdruck und t ist die Zeit.

Entsprechend der Abbildung 1. ist

$$m = f + k \sin \gamma, \quad (3)$$

$$n = k \cos \gamma, \quad (4)$$

also n drückt die Komponente der Reibungskraft aus, welche der Windrichtung entgegengesetzt ist, und $k \sin \gamma$ hingegen diejenige, welche senkrecht auf die Windrichtung ist.

Auf der Grundlage von Messungen ist über den Meeren $k = 2 \times 10^{-5} s^{-1}$ und über die Lande ist $k = 12 \times 10^{-5} s^{-1}$, ANDERKÓ (1902) hat auf der Grundlage statistischer Untersuchungen, die aus der Analyse synoptischer Karte stammen, für die Meere den $k = 1,8 \cdot 10^{-5} s^{-1}$ Wert gefunden.

Suttcliffe (1936) fand für das Land den $k = 6 \times 10^{-4} s^{-1}$ Wert. ROSSBY und MONTGOMERY (1935) zeigen den Wert $k = 3 \times 10^{-4} s^{-1}$ auf.

In diesem Zusammenhang weisen wir darauf hin, dass die Abweichungen der k Werten daraus stammen, dass bei den aus den synoptischen Karten stammenden Werten von Winkel (α) der Isodaren und des Windvektors ausgegangen wurde, und die Forscher mit der Formel $k = f \operatorname{tg} \alpha$ rechneten. Die Werte in der $10^{-4} s^{-1}$ Größenordnung hingegen wurden aus den bodennahen Windprofilen und in Bezug auf verschiedenen Rauigkeitsparameter abgeleitet.

Das bedeutet, dass wir im Falle von Bewegungssystemen mit synoptischen Skalen die durch Anderkó errechneten Werte benutzen können, weil diese (1) und (2) in Betracht ziehen, also auf der 1. Abbildung zu sehenden Kräfteverhältnissen entsprechen.

Die Werte von TAYLOR, ROSSBY und MONTGOMERY sind für solche atmosphärischen Räume: erdnahe Grenzschichten gültig, wo die $(1/\rho)$

$(\partial\tau/\partial z)$ Schubspannungskraft die vorherrschende Kraft ist, und wodurch ein mit der Höhe abnehmendes aber richtunghaltendes Strömungssystem hervorgerufen ist.

Wir sehen also, dass wir bei Kenntnis der numerischen Werte von k ohne weiteres m und n bestimmen können.

Mit dem Ziel, die gestellte Aufgabe zu lösen, betrachten wir die Gasgleichungen

$$p = \varrho RT, \tag{5}$$

wobei die üblichen Bezeichnungen benutzt werden. Wenn wir (5) differenzieren nach x und y , erhalten wir

$$\frac{\partial p}{\partial x} = RT \frac{\partial \varrho}{\partial x} + R \varrho \frac{\partial T}{\partial x} \tag{6}$$

und

$$\frac{\partial p}{\partial y} = RT \frac{\partial \varrho}{\partial y} + R \varrho \frac{\partial T}{\partial y}. \tag{7}$$

Setzen wir jetzt (6) in (1) ein und (7) in (2). So erhalten wir die folgenden Gleichungen.

$$\frac{du}{dt} - mv + nu = -RT \left(\frac{1}{\varrho} \frac{\partial \varrho}{\partial x} + \frac{1}{T} \frac{\partial T}{\partial x} \right), \tag{8}$$

$$\frac{dv}{dt} + mu + nv = -RT \left(\frac{1}{\varrho} \frac{\partial \varrho}{\partial y} + \frac{1}{T} \frac{\partial T}{\partial y} \right). \tag{9}$$

Jetzt differenzieren wir (8) nach y und (9) nach x und wir erhalten

$$\begin{aligned} \frac{\partial}{\partial y} \left(\frac{du}{dt} \right) - m \frac{\partial v}{\partial y} - v \frac{\partial m}{\partial y} + n \frac{\partial u}{\partial y} &= -R \frac{\partial T}{\partial y} \left(\frac{1}{\varrho} \frac{\partial \varrho}{\partial x} + \frac{1}{T} \frac{\partial T}{\partial x} \right) - \\ &- RT \left(-\frac{1}{\varrho^2} \frac{\partial \varrho}{\partial x} \frac{\partial \varrho}{\partial y} + \frac{1}{\varrho} \frac{\partial^2 \varrho}{\partial x \partial y} - \frac{1}{T^2} \frac{\partial T}{\partial x} \frac{\partial T}{\partial y} + \frac{1}{T} \frac{\partial^2 T}{\partial x \partial y} \right), \end{aligned} \tag{10}$$

$$\begin{aligned} \frac{\partial}{\partial x} \left(\frac{dv}{dt} \right) + m \frac{\partial u}{\partial x} + n \frac{\partial v}{\partial x} &= -R \frac{\partial T}{\partial x} \left(\frac{1}{\varrho} \frac{\partial \varrho}{\partial y} + \frac{1}{T} \frac{\partial T}{\partial y} \right) - \\ &- RT \left(-\frac{1}{\varrho^2} \frac{\partial \varrho}{\partial y} \frac{\partial \varrho}{\partial x} + \frac{1}{\varrho} \frac{\partial^2 \varrho}{\partial y \partial x} - \frac{1}{T^2} \frac{\partial T}{\partial y} \frac{\partial T}{\partial x} + \frac{1}{T} \frac{\partial^2 T}{\partial y \partial x} \right). \end{aligned} \tag{11}$$

Danach führen wir die sich anbietenden Zusammenfassungen in (10) und (11) durch, und subtrahieren (10) von (11); erhalten wir als Ergebnis

den Ausdruck

$$\begin{aligned} & \frac{d}{dt} \left(\frac{\partial v}{\partial x} - \frac{\partial u}{\partial y} \right) + \left(\frac{\partial u}{\partial x} + \frac{\partial v}{\partial y} \right) \left(\frac{\partial v}{\partial x} - \frac{\partial u}{\partial y} \right) + \frac{\partial w}{\partial x} \frac{\partial v}{\partial z} - \frac{\partial w}{\partial y} \frac{\partial u}{\partial z} + \\ & + m \left(\frac{\partial u}{\partial x} + \frac{\partial v}{\partial y} \right) + \beta v + n \left(\frac{\partial v}{\partial x} - \frac{\partial u}{\partial y} \right) = \frac{R}{\varrho} \left(\frac{\partial \varrho}{\partial x} \frac{\partial T}{\partial y} - \frac{\partial \varrho}{\partial y} \frac{\partial T}{\partial x} \right). \end{aligned} \quad (12)$$

Wir definieren

$$\frac{\partial v}{\partial x} - \frac{\partial u}{\partial y} = \zeta \quad (13)$$

und

$$\frac{\partial u}{\partial x} + \frac{\partial v}{\partial y} = \nabla_h \vec{v} \quad (14)$$

und betrachten die (3) und (4) Gleichung. Dann erhalten wir

$$\begin{aligned} & \frac{d}{dt} (\zeta + f) + k \zeta \cos \gamma + (\zeta + f) \nabla_h \vec{v} + \vec{k} \cdot \nabla_h w \times \frac{\partial \vec{v}_h}{\partial z} + k \sin \gamma \nabla_h \cdot \vec{v} = \\ & = \frac{R}{\varrho} J(\varrho, T) \end{aligned} \quad (15)$$

wobei

$$J(\varrho, T) = \begin{vmatrix} \frac{\partial \varrho}{\partial x} & \frac{\partial \varrho}{\partial y} \\ \frac{\partial T}{\partial x} & \frac{\partial T}{\partial y} \end{vmatrix} \quad (16)$$

die Jakobi Determinante der Dichte und der Temperatur ist.

Unter Berücksichtigung der (16) und (12) können wir schreiben, dass

$$\begin{aligned} & \frac{d}{dt} (\zeta + f) + (\zeta + f) \nabla_h \cdot \vec{v} + \vec{k} \cdot \nabla w x \frac{\partial \vec{v}}{\partial v} + k \zeta \cos \gamma = \\ & = -k \sin \gamma \nabla_h \cdot \vec{v} + \frac{R}{\varrho} \nabla_h \varrho x \nabla_h T. \end{aligned} \quad (17)$$

In (17) steht auf der linken Seite die Summe der zeitlichen Veränderung der absoluten Vorticity und des Produktes der relativen Vorticity und des Reibungsfaktors. Hier finden wir auch den Vertikalschwenkungsterm.

Auf der rechten Seite finden wir zwei Terme: der eine Term drückt die Divergenz aus, der andere gibt die Effekte der Baroklinität, also er enthält den solenoidalen Effekt. (17) ist eine solche Form der Wirbelgleichung,

welche die Reibungswirkung enthält, und ausserdem enthält sie auch den Effekt der Baroklinität, der die thermische Kraft ausdrückt. Die Reibung hat auf zwei Glieder von (17) einen Einfluss. Einmal auf der linken Seite als Faktor von ζ , auf der anderen Seite hingegen als Faktor von

$\nabla_h \cdot \nabla$. Wir können sehen, das die Reibung keinen Einfluss auf die Baroklinität ausübt, das ist aber auch natürlich, da dieser Faktor eine Folge von thermischen Effekte ist, die sich durch Ein- und Ausströmung von Wärme bilden.

Der $(1/\rho) (\nabla_h \rho \times \nabla_h T)$ Term unterscheidet sich dann von Null, wenn das untersuchte Bewegungssystem eine thermale Assymetrie ausweist. Im Falle, dass $\nabla_h T = 0$ und $\nabla_h \rho = 0$ ist, ist auch der zweite Summand von (17) gleich Null. Das bedeutet: bei der Inkompressibilität der Flüssigkeit, oder bei barotropen Atmosphäre brauchen wir mit den zweiten Summanden der rechten Seite nicht zu rechnen. In baroklinen Atmosphäre aber bedeutet dieser Term einen positiven Beitrag, wenn $(\nabla_h \rho \times \nabla_h T)$ ein positives Vorzeichen besitzt, und negativen Beitrag in umgekehrten Falle.

Als Vektroprodukt ist

$$|\nabla_h \rho \times \nabla_h T| = |\nabla_h \rho| |\nabla_h T| \sin \varepsilon \tag{18}$$

das Vorzeichen des Produktes wird also vom Winkel ε der beiden Vektoren bestimmt.

Wenn ε zwischen 0 und π fällt, dann ist das Vorzeichen von $(\nabla_h \rho \times \nabla_h T)$ positiv, und negativ im Interwall von π bis 2π . Die räumliche Anordnung der Gradienten der Dichte und der Temperatur zeigen wir in der 2. *Abbildung*.

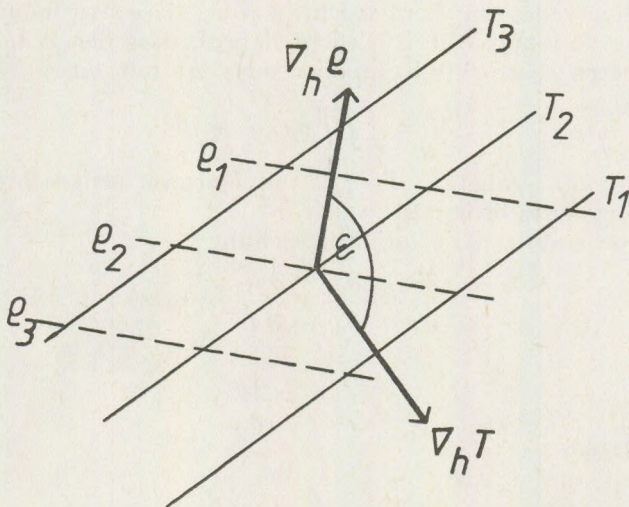


Abb. 2. Der Winkel ε zwischen $\nabla_h \rho$ und $\nabla_h T$.

Beweisen wir noch, dass die Zahl der Solenoide die im (ϱ, T) Diagramm auftauchen übereinstimmt mit dem Flächenintegral des oben definierten solenoiden Vektor. Es ist nämlich

$$\oint \varrho dT = \oint \varrho \nabla_h T d\vec{r} = \int_A (\nabla_h \varrho \times \nabla_h T) dA \quad (19)$$

wobei wir die Stoke-Regel benutzen. In (19) bedeutet \vec{r} den Ortsvektor und A eine Fläche.

Hieraus folgt

$$\oint \varrho dT = \int_A (\nabla_h \varrho \times \nabla_h T) dA. \quad (20)$$

(20) zwingt, dass die zeitliche Veränderung der Vorticity durch die Baroklinität zur Geltung kommt. Diese Wirkung kann man mit der Dichte der Solenoiden messen, die durch die im (ϱ, T) System auftretenden Isothermen und isopiknischen Linien gebildet werden. Bei durchschnittlichen Verhältnissen ist die Grössenordnung der überprüften Faktor $3,5 \cdot 10^{-10} s^{-2}$. Demgegenüber ist die Grössenordnung des Termes, welcher die Divergenz enthält, über Meeren $1,06 \cdot 10^{-9} s^{-2}$ und über dem Land $1,8 \cdot 10^{-9} s^{-2}$. Wir sehen also, dass der solenoide Term, die Wirkung der Baroklinität nicht vernachlässigt werden kann, da ja der Divergenzterm bloss das fünffache des baroklinischen Termes über Land, und bloss das dreifache dieses Termes über Meer ist. Wenn wir noch überdenken, dass wir gerade durch die Baroklinität die diabatische Einflüsse berücksichtigen können, kommen wir zu dem Schluss, dass wir diesen Term nicht vernachlässigen dürfen beim Studium der Entwicklung des Bewegungssystems mit synoptischer Skala.

Der Divergenzterm berücksichtigt die Massenverteilung und die Wirkung der Reibung. Mit Rücksicht darauf, dass der Windvektor eine auf die Isobaren senkrechte Komponente besitzt, tritt ein

$$M = \iiint \varrho v_n dx dz dt. \quad (21)$$

Massenstrom auf, wobei v_n die auf die Isobaren senkrechte Geschwindigkeitskomponente bedeutet.

Entsprechend der Kontinuitätsgleichung

$$\frac{\partial u}{\partial x} + \frac{\partial v}{\partial y} + \frac{\partial w}{\partial z} = 0 \quad (22)$$

können wir

$$\nabla_h \cdot \vec{v} = -\frac{\partial w}{\partial z} \quad (23)$$

schreiben. Daher ist

$$w = -\int_0^z \nabla_h \cdot \vec{v} dz. \quad (24)$$

Der Divergenzterm ist also proportional zur Vertikalgeschwindigkeit. Benutzen wir (24) definieren eine

$$m = \iiint w \varrho \, dx \, dr \, dt \tag{25}$$

Grösse. Diese Grösse gibt den Massentransport an, die aus der geordneten Vertikalbewegung stammt. Nach der Gleichung (21) and (25) man kann das Verhältnis

$$F = \frac{M}{m} \cong 1 \tag{26}$$

als Kriterium für Auffüllen oder das Entleeren benutzen. Wenn $F > 1$ ist – im zyklonalen Falle tritt ein Auffüllen auf, beim antizyklonalen Fall ein Entleeren. $F > 1$ ist also ein Kriterium des Abbaus und $F < 1$ das Kriterium des Entstehens; $F = 1$ bedeutet stationere Verhältnisse.

Über (17) können wir abschliessend sagen, dass diese Gleichung beschreibt die zeitliche Veränderung der Vorticity unter Berücksichtigung der Reibung, der Divergenz und die Wirkung der Baroklinität.

Aus Rotorbildung der Bewegungsgleichung folgt

$$\nabla x \left[\frac{d\vec{v}}{dt} + 2\vec{\Omega} x \vec{V} \right] = \nabla \times \frac{\partial \vec{v}}{\partial t} + \nabla \times ([\nabla x \vec{v}] \times \vec{v}) + \nabla \times (2\vec{\Omega} x \vec{v}) \tag{27}$$

und daher

$$\iint_{\sigma} \left\{ \frac{\partial \zeta}{\partial t} + \text{rot}_z ([\text{rot } \vec{v} + 2\vec{\Omega}] \times \vec{v}) \right\} d\sigma = \frac{d}{dt} \iint \eta \, d\sigma$$

können wir schreiben, dass

$$\begin{aligned} \frac{d}{dt} \iint_{\sigma} \eta \, d\sigma &= -k \cos \gamma \iint_{\sigma} \zeta \, d\sigma - k \sin \gamma \iint_{\sigma} \nabla_h \cdot \vec{v} \, d\sigma + \\ &+ \iint_{\sigma} \frac{R}{\varrho} (\nabla_h \varrho \times \nabla_h T) \, d\sigma \end{aligned} \tag{28}$$

wobei $\eta = \zeta + f$.

In barokliner Atmosphäre mit Reibung hängt also die zeitliche Veränderung der absoluten Vorticity von Produkt des Reibungsfaktors mit dem Divergenz und der Summe des Richtungseffektes und von baroklinischen Faktor ab.

Der stationäre Fall kann so auftreten, wenn die rechte Seite von (28) verschwindet; das heisst die Summe der untersuchten Wirkung ist gleich Null. Das müssen wir auf jeden Fall als Spezialkraft betrachten, da die komplizierten orografischen Verhältnisse, die Wärmehaushaltunterschiede,

die inhomogene Bewölkung, die Veränderlichkeit von stark stochastischen Charakter bekommt. Das bedeutet dass es in der Atmosphäre kaum zu

$$\frac{\zeta + f}{\delta z} = \text{Konstant} \quad (29)$$

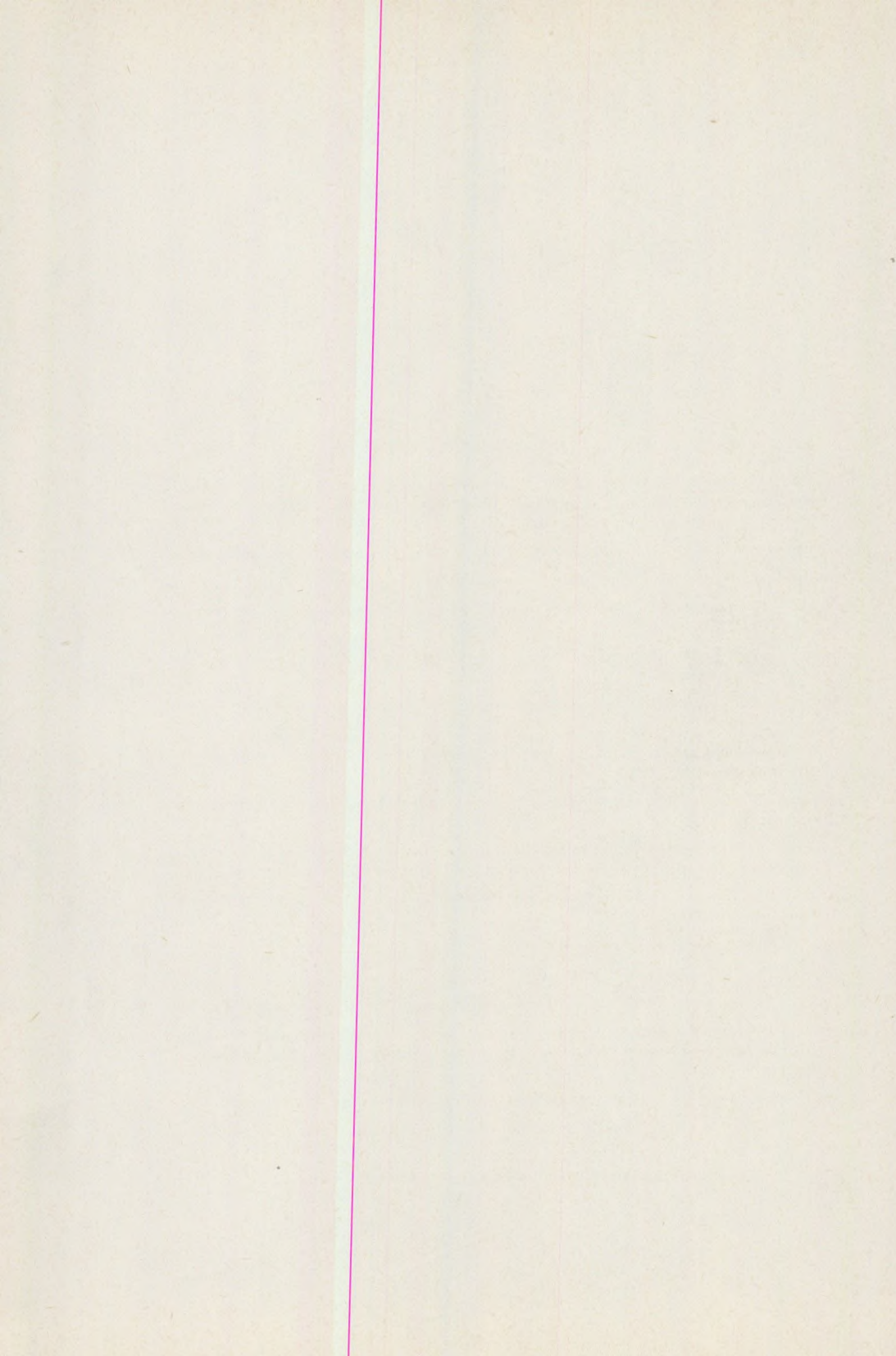
kommen kann, was der Satz der Erhaltung der potenziellen Vorticity ist und in der Praxis — in der Modellen der numerischen Wettervorhersagen — oft benutzt wird, es ist hingegen viel wahrscheinlicher, dass der in (28) beschriebene Vorgang näher zur Wirklichkeit steht. An Hand der Gleichung (28) kann man auch erklären dass über Lande Druck-Systeme eher dissipieren als über den Meeren. Das wird durch zwei Gründe auch erklärt. Zum einen ist der k Faktor in (28) auf der rechten Seite steht für Landgebiete um eine Größenordnung grösser, als für Meere, zum anderen treten im Term der Baroklinität wegen der komplizierenden optischthermodynamischen Wirkungen komplizierende Wärmequellen und Wärmesenken auf. In Wirklichkeit lösen sich nach den synoptischen Erfahrungen die sich vom Platz bewegenden barische Systemen auf, sobald sie über das Land kommen.

LITERATUR

- ANDERKÓ, A. (1902): Adalék az időprognózis elméletéhez. — Budapest.
 BERNHARDT, K. (1971): Die Vertikalbewegungen in quasigeotriptischen Windfeld der Bodenreibungsschicht. — Zeitschr. für Met. Band 22. A 1—5. 39—45.
 BERNHARDT, K. (1975): Some Characteristics of the Dynamic Air-Surface Interaction in Central Europe. — Zeitschrift für Met. B. 25. H 2. 63—68.
 DOBSON, G. M. B. (1914): Pilot Balloon Ascents at Central Flying School Upavon during Year 1913. — Quart. J. Roy. Met. Soc. 40. 123—135.
 HESSELBERG, TH., SVERDRUP, U. U. (1915): Die Reibung in der Atmosphäre. — Veröff. Geophys. Inst. Univ. Leipzig, 9 2. H. 10. 241—309.
 RÁKÓCZI, F. (1976): Az örvényességi és balanszegenlet súrlódásos áramlás esetén. — Időjárás 80. 3. 169—171.
 ROSSEY, C. G., MONTGOMERY, R. B. (1935): The layer of frictional Influence in Wind and Ocean Currents. — Pap. Phys. Ocean. Met. Mass. Inst. Techn. and Woods Hole Ocean Inst. 3, Nr. 3. 1—101.
 SANDSTRÖM, J. W. (1910): Über die Beziehung zwischen Luftdruck und Wind. — Kong. Svenska Vetensk. Akad. Handl 45, Nr. 10.
 SANDSTRÖM, J. W. (1911): On the Relation between Atmospheric Pressure and Wind. — Bull. Mc Weath. Obs. 3, 5. 275—303.
 SUTCLIFFE, R. G. (1936): Surface Resistance in Atmospheric Flow. — Quart. J. Met. Soc. 62, 3—14.
 TAYLOR, G. I. (1916): Skin-Friction of the Wind on the Earth's Surface. — Proc. Roy. Soc. A 92, 196—199.

INDEX

IMREH, J.; MÉSZÁROS, N.; MIHÁLKA, ST.; BERNER, ZS.: Geochemische Untersuchungen einiger eozäner und oligozäner Kalksteine aus dem Siebenbürgischen Becken (Rumänien)	3
MINDSZENTY, A.; BÉRCI, J.: Contribution to the problem of weathering of diasporites	39
WEISZBURG, T.; LOVAS, GY. A.: On the crystal structure of mátrait	47
DÓDONY, I.; WEISZBURG, T.: The structure of a "wad" sample from Dognacea (Rumania)	53
DÓDONY, I.; BALOG, A.: Mineralogical study on waterite and other related minerals of thermal water origin	63
ÖRKÉNYI-BONDOR, L.: Formulas for the determination of Euler angles of plagioclases	73
MILANOVSKY, YE, YE.: Kinematics of tectonic movements and volcanism of the Mediterranean geosynclinal belt and its "frame" at the orogenic period of the Alpine "cycle"	79
JANSSEN, A. W.: Late Oligocene molluscs from a sand-pit near Máriahalom (Hungary), a provisional study	109
FÁY-TÁTRAY, M.: Contribution to the lithology of the reworked clastic dolomite complex of the southern Gerecse Forelands (Transdanubia, Hungary)	151
GALÁCZ, A.: Ammonites and stratigraphy of the Bathonian at Ófalu, eastern Mecsek Mountains (S. Hungary)	167
GÉCZY, B.: The Jurassic ammonites of Villány	189
MONOSTORI, M.: The problem of extinction	199
VÖRÖS, A.: Lower and Middle Jurassic brachiopod provinces in the western Tethys	207
БОДРИ, Л.: Количественное исследование процесса утоньшения земной коры в областях с высоким тепловым потоком в применении Паннонскому бассейну	235
БОДРИ, Б.: К вопросу о вычислении приливного потенциала на Луне	249
RÁKÓCZI, F.; KORIS, K.: Climatological factors in regulating water-level of Lake Velence	261
RÁKÓCZI, F.: Untersuchung der Wirbelgleichungen bei Bodenreibung	269



A kiadásért felelős az Eötvös Loránd Tudományegyetem rektora — A kézirat nyomdába érkezett:

1983. május — Megjelent 1984. szeptember — Terjedelem: 23,3 (A/5) ív —

Példányszám: 650 — Készült monószedéssel, íves magasnyomással,

az MSZ 5602-59 és az MSZ 5602-55 szabvány szerint

83.456. Állami Nyomda, Budapest

Felelős vezető: Mihalek Sándor igazgató

ISSN 0365 — 0634